

Geologic Analysis of Naturally Fractured Reservoirs

Geologic Analysis of Naturally Fractured Reservoirs

SECOND EDITION


By R.A. Nelson
BP Amoco
Houston, TX

G | P
P |  **Gulf Professional Publishing**
an imprint of Butterworth-Heinemann

Boston Oxford Auckland Johannesburg Melbourne New Delhi


Gulf Professional Publishing is an imprint of Butterworth–Heinemann.


Copyright © 2001 by Butterworth–Heinemann

 A member of the Reed Elsevier group

All rights reserved.

No part of this publication may be reproduced, stored in a retrieval system, or transmitted in any form or by any means, electronic, mechanical, photocopying, recording, or otherwise, without the prior written permission of the publisher.

 Recognizing the importance of preserving what has been written, Butterworth–Heinemann prints its books on acid-free paper whenever possible.

 Butterworth–Heinemann supports the efforts of American Forests and the Global ReLeaf program in its campaign for the betterment of trees, forests, and our environment.

Library of Congress Cataloging-in-Publication Data

Nelson, Ronald A.

Geologic analysis of naturally fractured reservoirs / by R.A. Nelson.—2nd ed.
p. cm.

Includes bibliographical references and index.

ISBN 0-88415-317-7 (alk. Paper)

1. Rocks—Fracture. 2. Rocks, Sedimentary. 3. Hydrocarbon reservoirs. I. Title.

QE431.6.P5 N45 2001
553.2'8—dc21

2001017058

British Library Cataloguing-in-Publication Data

A catalogue record for this book is available from the British Library.

The publisher offers special discounts on bulk orders of this book.

For information, please contact:

Manager of Special Sales
Butterworth–Heinemann
225 Wildwood Avenue
Woburn, MA 01801–2041
Tel: 781-904-2500
Fax: 781-904-2620

For information on all Gulf Professional Publishing publications available, contact our World Wide Web home page at: <http://www.gulfpp.com>

10 9 8 7 6 5 4 3 2 1

Printed in the United States of America

*To my colleagues Roberto Aguilera, Mel Friedman,
and Dave Stearns, and to my friends in the industry
who have taught me so much over the years.*

Contents

Acknowledgments	xi
Foreword	xiii
Preface	xvii
Notation	xix
1. Evaluating Fractured Reservoirs: Introduction	1
Avoid Fracture Denial, 1	
Problems, 2	
Definitions, 3	
The Evaluation Sequence, 4	
Basic Types of Evaluation, 4	
Early Exploration Evaluations, 5	
Evaluations of Economic Potential, 5	
Evaluations for Recovery Planning and Modeling, 6	
General Sequence of Study, 7	
Fracture System Origin, 7	
Generic Classification, 9	
Geologic Classification, 10	
Fractured Properties Affecting Reservoir Performance, 32	
Introduction, 32	
Fracture Morphology, 37	
Fracture Width and Permeability, 64	
Fracture Spacing, 79	
Fracture and Matrix Porosity Communication, 82	
Introduction, 82	

- Basics of Fracture and Matrix Porosity, 83
- Cross-Flow in a Two-Porosity System, 95
- Examples of Cross-Flow in Thin Section, 96
- Inhibited Cross-Flow, 96
- Estimation of Porosity Interaction, 100

2. Reservoir Management 101

- Classification of Fractured Reservoirs, 101
 - Reservoir Types, 101
- Positive Reservoir Attributes, 107
- Potential Problems, 109
- Strategies of Fractured Reservoir Management, 110
 - Reservoir Description, 113
- Thoughts on Risk Analysis in Fractured Reservoirs, 123

3. Detecting and Predicting Fracture Occurrence and Intensity 125

- Detection, 125
 - Direct Detection, 125
 - Indirect Detection, 127
 - Application of Direct and Indirect Techniques, 135
- Prediction of Subsurface Fracture Spacing, 135
 - Composition, 137
 - Porosity, 137
 - Grain Size, 141
 - Bed Thickness, 141
 - Structural Position, 146
- Summary, 150
 - Picking Well Locations and Well Paths in Folded Fractured Reservoirs, 152
 - Fracture Intensity, 153
 - Well Trajectory, 160

4. Analysis of Anisotropic Reservoirs 163

Stylolites, 163

Stylolites and Their Contribution to Reservoir Anisotropy, 165

Effect of Stylolite Zones on Porosity and Permeability, 172

Stylolites as an Indicator of Mechanical Properties, 173

Development of Permeability Tensors for Anisotropic Reservoirs, 185

Crossbedding, 186

Fractures, 189

Other Factors, 193

Permeability Tensors for Crossbedding and Fractures, 198

Relative Effect of Rock Parameters, 202

Permeability Anisotropy and Stylolites, 204

Combined Tensors, 206

Statistical Data in Reservoir Modeling, 207

Reservoir Domains or Compartments, 207

Averaging Techniques in Three Dimensions, 212

Three-Dimensional Correlation of Reservoir

Properties in Fractured Reservoirs, 215

Statistical Characterization of Block Sizes, 217

Stimulation in Fractured Reservoirs, 217

5. Analysis Procedures in Fractured Reservoirs 223

Screening Tools in Defining a Fractured Reservoir, 223

Data Types and Constraints as a Function of

When the Fractured Reservoir is Discovered, 226

Core and Outcrop Analysis, 229

Fracture Stratigraphy and the Interrelation of Deformation,
Petrology, and Petrophysics, 229

Determining Natural Versus Induced Fractures, 230

Data Acquisition, 239

Coring in Fractured Reservoirs, 240

Useful Checklists, 246

Data Presentation, 248

Pressure and Production Analysis for
Quantifying Fracture System Properties, 251
 Logging Techniques, 251
 Well Testing, 251

Numerical Modeling in Geology, 252

Appendix A: List of Documented Fractured Reservoirs	255
Appendix B: Procedures Checklist	277
Appendix C: Averaging Techniques	279
Glossary	281
Conversion Factors	285
References	287
Index	323

Acknowledgments

I wish to acknowledge the support and guidance of my colleagues David W. Stearns, Roberto Aguilera, and Melvin Friedman that made this second edition possible. I also acknowledge the management of BP Amoco and the former Amoco Production Co. without whose encouragement and permission this manuscript would not have been published. I am grateful to the American Association of Petroleum Geologists (AAPG), the American Geophysical Union, the International Society of Rock Mechanics, the Society of Petroleum Engineers, and the Canadian Society of Petroleum Engineers for permission to draw material from their publications. Lastly, I thank all of those attendees of the fractured reservoir courses that I have taught over the years who have truly taught me the art and practice of fractured reservoir analysis.

Foreword

Fractures are a universal element in sedimentary rock layers, so much that they are virtually omnipresent in outcrops of sedimentary rocks. Think of all the outcrops of sedimentary rocks that you have ever seen and try to recall a layer that was completely unfractured, with the possible exception of extremely ductile rock, such as salt or certain shales, you will not be able to recall any unfractured rocks simply because they do not exist. Further, it has been demonstrated over and over again that the vast majority of fractures observed in outcrop are not solely the result of surface conditions. In other words, the fractures seen in outcrop also exist in the subsurface. Therefore, it follows that hydrocarbon reservoirs in sedimentary rock all contain fractures and most of them are fractured enough to be treated as fractured reservoirs.

Though the geological fractures necessary to conclude that fractures are common in the subsurface have been known for at least the last half century, the practice of treating reservoirs as fractured rock masses has been extremely slow in becoming a standard industry practice. Why is this so? Probably the greatest contributor to the widespread reluctance to face the reality of fractured reservoirs is because fractured reservoirs are extremely complex and therefore, much more difficult to deal with than are unfractured reservoirs. The complexity comes from the vast number of both dependent and independent variables that dictate final reservoir response. Consider for a minute just a few of the obvious, straightforward reservoir variables, and their interactions, that must be included in a reservoir analysis. Calculating reservoir storage depends on knowing both matrix and fracture porosities. Fracture permeability, matrix permeability, and especially their interaction, all contribute to the behavior of a given reservoir. Fracture geometry, fracture spacing, fracture surface area, and fracture opening all combine with fracture morphology and pore space distribution to create true reservoir permeability and/or permeability anisotropy. Fluid pressure decline with time changes the value of some variables but not the value of others. Therefore, initial calculations do not apply throughout the life of the reservoir and some parameters must be recalculated at several intervals during the life of the reservoir.

Anyone who has dealt with fractured reservoirs realizes that these variables are only a few of the numerous variables that have to be evaluated and properly combined in order to predict reservoir performance. Is there any doubt, then, that reservoir complexity is a major contributor to the reluctance even to attempt systematic treatment of reservoirs as fractured rock masses?

Another factor that is a deterrent to doing systematic fractured reservoir analysis is that almost all fractured reservoirs respond in a manner unique to that specific reservoir. That is, despite the existence of a good, working fractured reservoir classification, each fractured reservoir responds in its own distinctive way. As a consequence, applying general rules of thumb to specific fractured reservoirs can be dangerously misleading.

Both the complexity and individuality of fractured reservoirs, then, strongly argue for the need for a reference book that deals in a practical way with proven methods of dealing with fractured reservoirs. This book serves that function. In the first edition of this book, Ron Nelson shortened the effort it took someone new to get into reservoir analysis. He did this by going beyond his lucid academic discussion of the important geologic and engineering factors that must be considered in fractured reservoir analysis. In addition to technical details, he also used his vast experience to discuss how to organize, collect, and deal with fractured reservoir data while at the same time staying within the practical limits demanded by most corporations. His coverage in 1985 was complete for the state of the art that existed at that time. However, the influence that the first edition had on industry is no better demonstrated than by the fact that since 1985 the industry-wide level of sophistication in treating fractured reservoirs has accelerated enormously. In addition, since the publication of the first edition, Nelson has undertaken the organization and presentation of numerous American Association of Petroleum Geology (AAPG) fractured reservoir workshops all over the world.

These activities not only permitted him the opportunity to promulgate the ideas expressed in the first edition, they also permitted him the opportunity to listen to others concerning their needs relative to dealing with fractured reservoirs. Now in the updated second edition, Nelson has extended the first edition by coupling his own research and experience with the wide exposure he received from listening to the problems of other geoscientists during the last 15 years of giving annual AAPG seminars.

The second edition not only still includes the cardinal aspects of fractured reservoirs that were contained in the first edition, but it also incorporates what is new in 15 years of progress in treating fractured reservoirs. In addition to the rudiments of the first edition, Nelson has included six entirely new sections, which range from “how to avoid fracture denial” to “positive reservoir attributes” to “screening tools in defining a fractured

reservoir.” Also, in the second edition new advances in directional drilling are integrated into fractured reservoir treatment.

I was fortunate enough to participate personally with Nelson in 10 or 12 of the AAPG fractured reservoir seminars, and there is no doubt that the most frequent request for data not presented in these seminars was to include a summary of fractured reservoir case histories. Nelson has remedied this request by including a totally new appendix in the second edition in which he presents historic production charts for 25 fractured reservoirs on which he has personally worked.

Another new feature included in the second edition will aid in solving a frequent communication problem. It is not unusual for the person(s) with the most technical background in fractured reservoirs to present a highly shortened version of a proposed project to people with much less technical background. To aid in this task, a companion website is also offered with the second edition so that any table or illustration in the book can be downloaded and projected as part of a communication effort.

Just as the first edition was, the new edition is equally indispensable as a shelf reference for any person working with fractured reservoirs, even those who own a first edition.

David W. Stearns
University of Oklahoma

Preface

Much has happened in the field of fractured reservoir analysis since the publication of the first edition of this text in 1985. Many more reservoirs have been identified as being fracture-controlled and great strides have been made in the integration of the work and approaches of the many disciplines needed to work successfully with these reservoirs. Indeed, from exploration through blow-down, the effective management of these reservoirs requires the application of multi-disciplinary approaches more than virtually any other type of petroleum reservoir.

In this second edition, I have tried to retain the emphasis on rock data approaches to the study of these reservoirs while adding more material on their production histories and characteristics. In addition, practical checklists have been added to help determine if you are dealing with a fractured reservoir or not as well as procedures for how to approach the study of fractured reservoirs depending on when in its history we “discover” that it is fractured. I believe that the material included in this second edition will allow us to move away from the historical “fracture denial” that our reservoir workers have suffered from for many years.

An addition has been made to this edition in the form of companion website (<http://www.bh.com/companions/0884153177>). This site includes .pdf files of the slides that I have used in the various AAPG fractured reservoir courses that I have taught over the last 20 years. These include many more illustrations than are used in the text and can be used by the purchaser as training resource material.

Notation

a, b, n	= various constants
A	= cross-sectional area
B_1	= plug permeability parallel to bedding
B_2	= plug permeability 45° to bedding
B_3	= plug permeability 90° to bedding
B_{11}, B_{12}, B_{33}	= maximum, intermediate, and minimum principal bedding permeability tensor components
B_{ij}	= bedding permeability tensor
B'_{ij}	= rotated bedding permeability tensor
d	= average constitutive grain diameter of the rock
D	= average fracture spacing (average distance between parallel fractures)
e	= fracture width
E	= Young's elastic modulus
F_1	= plug permeability parallel to fracture
F_2	= plug permeability 45° to fracture
F_3	= plug permeability 90° to fracture
F_{11}, F_{22}, F_{33}	= maximum, intermediate, and minimum principal fracture permeability tensor components
F_{ij}	= fracture permeability tensor
F'_{ij}	= rotated fracture permeability tensor
g	= acceleration of gravity
h	= hydraulic head
k	= intrinsic permeability
\bar{k}	= mean permeability
k_f	= fracture permeability
k_{fr}	= total permeability (rock plus fracture system)
k_r	= rock or matrix permeability
K	= hydraulic conductivity
k_{11}, k_{22}, k_{33}	= maximum, intermediate, and minimum principal permeability tensor components
k_{H90}	= horizontal 90° from maximum horizontal whole-core permeability

k_{Hmax}	= maximum horizontal whole-core permeability
k_v	= vertical intrinsic whole-core permeability
l	= length
M_{ij}	= matrix permeability
M'_{ij}	= rotated matrix permeability tensor
N	= dimensionless coefficient characteristic of the medium
NB	= permeability plug with no visible bedding
NF	= permeability plug with no visible fractures
P	= fluid pressure
P_p	= pore or formation pressure
Q	= flow rate
R	= a randomly taken permeability plug
S_{11}, S_{22}, S_{33}	= maximum, intermediate, and minimum total principal stresses
S_{ij}	= stylolite permeability tensor
S'_{ij}	= rotated stylolite permeability tensor
S_v	= total vertical stress ($s_v + P_p$)
S_h	= total horizontal stress ($S_h + P_p$)
V_B	= bulk volume
V_p	= pore volume
α, β	= angles between fracture planes and pressure gradient
ϵ	= strain component
γ	= Poisson's ratio
μ	= viscosity
ρ	= density
σ	= stress
σ_1	= maximum principal effective stress component
σ_2	= intermediate effective principal stress component
σ_3	= minimum principal effective stress component
σ_h	= horizontal effective stress component
σ_{mean}	= mean stress
σ_v	= vertical effective stress component
ϕ	= porosity
ϕ_f	= fracture porosity (pore volume to total volume)
ϕ_r	= matrix or rock porosity (pore volume to total volume)

1

Evaluating Fractured Reservoirs: Introduction

AVOID FRACTURE DENIAL

Fractured reservoirs make up a large and increasing percentage of the world's hydrocarbon reserves. In BP Amoco alone, current and future fields in various types of fractured reservoirs are estimated to account for some 21 billion barrels of oil equivalent (BBOE). However, in spite of the importance of fractured reservoirs, we in the industry tend to deny the presence of fractures in our reservoirs. This fracture denial is probably due to our desire to avoid complication in our technical work and reduction of cycle times in our exploration and production (E&P) efforts. Indeed, fractured reservoirs are more complicated than matrix reservoirs, and they do require more time and money to be evaluated correctly. The tendency is to ignore the presence and effect of natural fractures for as long in the field history as possible. The problems with this denial or avoidance include: 1) often irreparable loss of recovery factor; 2) primary recovery patterns that are inappropriate for secondary recovery; 3) inefficient capital expenditure during development; 4) drilling of unnecessary in-fill wells; and 5) improper assessment of economic opportunities.

It is important to determine the effect of natural fractures in our reservoirs as early as possible so that our evaluations and planning can be done correctly from day one. *Fracture denial* does nothing positive for our exploration and development activities and can only lead to poorer technical and economic performance.

Remember: *Finding fractures is not enough.*

Fractured reservoirs are very complicated and difficult to evaluate. Effective evaluation, prediction, and planning in these reservoirs require an early recognition of the role of the natural fracture system and a systematic approach to the gathering and analysis of pertinent data. However, care should always be taken to make sure that the degree of analysis and evaluation is commensurate with the particular problem being addressed. It is easy to get lost in detail and data acquisition, and lose sight of the economic questions.

Problems

Interest in natural fracture studies in surface and subsurface formations has increased dramatically in the past years. This has been brought about by greater industry knowledge of the effect of fractures on subsurface fluid flow and by a significant and ever increasing percentage of oil and gas discoveries where natural fractures play a significant role in production. Fractured reservoirs possess many inherent obstacles to proper analysis due to difficulties in prediction, evaluation, and characterization, but possess very positive attributes as well. Several obstacles stem from:

1. A general lack of in-depth quantitative approaches to description and characterization of highly anisotropic reservoirs.
2. Failure of geologists and engineers to recognize fractures and/or the regularity of their distribution.
3. Over-simplistic approaches in the description of fracture distributions and morphologies.
4. The need for a deterministic solution to modeling fluid flow in fractured porous media, while understanding that our data limitations force us toward stochastic solutions, at best.

These obstacles are compounded by the improper use or nonuse of the many techniques available to detect natural subsurface fractures. While most of these techniques do work, seldom are they significant by themselves, and often they may even cloud the real issues of evaluation. Remember: *Finding fractures is not enough.*

Detecting subsurface fractures or predicting their occurrence is indeed only the first, most basic step in fully evaluating a fractured reservoir. The key to economically producing these reservoirs lies in:

1. Evaluating recoverable reserves as a function of well costs.
2. Predicting optimum well locations and well performance with time under a variety of potential completion and development scenarios.

3. Obtaining sufficient rock and fracture data to make these calculations possible.

In general, this book will emphasize techniques addressing the last two key issues. The book will show the breadth of rock data and production data that can be used in evaluating fractured reservoirs. These data are required to address all of these issues at various times during the history of the field. Therefore, this material should be considered the database necessary to make the major economic and engineering decisions at various decision points from exploration, to production, to harvest. While some of this data is not fully used until later times during field history, much of the static (versus dynamic) data can only be obtained early, in working life with the field.

Definitions

The word “fracture” has been defined in various ways. Some definitions are purely descriptive (Dennis, 1967) while others are mechanical (Ranalli and Gale, 1976). The range in definitions generally reflects the different interests of the authors. Because this book addresses the effect naturally occurring fractures have on reservoir rock, the definition will be restricted here to a reservoir context.

A *reservoir fracture* is a naturally occurring macroscopic planar discontinuity in rock due to deformation or physical diagenesis. If related to brittle failure, it was probably initially open, but may have been subsequently altered or mineralized. If related to more ductile failure, it may exist as a band of highly deformed country rock. As a result, natural reservoir fractures may have either a positive or negative effect on fluid flow within the rock. This broad definition allows this text to address fluid flow anisotropy created by numerous features regardless of any mechanical differences in their generation and propagation (extension versus shear, mode 1 versus mode 2, fracture versus microfault, etc.). This definition also makes it possible to treat effects of various fracture morphologies on fluid flow. For example, one can look at the effect of highly permeable open fractures on reservoir behavior, but can also consider the strong anisotropy in rock permeability created by low-permeability deformed fractures.

The definition of a reservoir fracture is a broad one, and the definition of a “fractured reservoir” even more so. Because natural fracture systems can have a variety of effects on reservoir performance in primary, secondary, and tertiary recovery, and because these effects must often be predicted long before they are evidenced in production data, an operational definition of a fractured reservoir becomes a necessity. A *fractured reservoir* is defined as a reservoir in which naturally occurring fractures either have, or are

predicted to have, a significant effect on reservoir fluid flow either in the form of increased reservoir permeability and/or reserves or increased permeability anisotropy. The qualifier, or “are *predicted* to have a significant effect,” is important operationally because the data necessary to quantify a fractured reservoir must be collected very early in the life of a reservoir. We must often, therefore, predict the “significant effect” and *treat* the formation as a fractured reservoir prior to true substantiation by production history.

THE EVALUATION SEQUENCE

The remainder of this chapter presents the critical attributes that must be evaluated to quantify fractured reservoirs in a logical, workable sequence: origin, properties, fracture/matrix interaction, reservoir typing and, eventually, well placement and completion.

BASIC TYPES OF EVALUATION

Exploration and production cannot be separated from evaluation in fractured reservoirs. It is of paramount importance to know what we are looking for and what we have found in terms of reservoir properties. There are three basic types of evaluation to be addressed in fractured reservoir analysis (Nelson, 1982). They are listed in order of increasing complexity, amount of data, and time to completion:

1. Early exploration evaluations to determine or predict gross reservoir quality.
2. Evaluations of economic potential (reserves, flow rates, etc.).
3. Evaluations for recovery planning and detailed reservoir modeling.

These are distinctly different types of evaluation, requiring various amounts of both qualitative and quantitative data. They were performed in the past at different times within the history of a field or prospect. Today, however, work cycles in the industry are much more compressed, forcing us to address some of the more detailed modeling aspects early in the “prospect phase.”

Early Exploration Evaluations

Economically, the most frequent and often most critical fracture evaluation is that performed early in the exploration phase of a hydrocarbon play. The purpose is to better define the properties of interest and to determine or predict the gross reservoir quality of a discovery. These evaluations only deal with a general knowledge of the structure and stratigraphic sequence (petrophysical and mechanical attributes), log suites that are not designed specifically for natural fracture evaluation, and minimal core and well-test data. Evaluations performed at this time are qualitative at best, and are probably more like speculations than true evaluations.

However, these evaluations often will “make or break” a play in its drilling infancy. For example, cores from an early well cutting into the Cambrian section in Amal Field in Libya would have shown a permeable fracture system with no significant rock matrix contribution to reservoir flow or storage (fractured reservoir Type 1, see Chapter 2). Because we are always skeptical of such reservoirs, extreme caution would have been advised, including the possibility of abandoning the play. However, knowledge that the fracture system present is fold-related (tectonic in origin) and *should*, therefore, be developed over the entire 100,000 acres of structural closure, and that the entire quartzite package, which is 800 ft. thick, and *should* fracture as a unit, would have allowed workers to predict the enormous potential of this discovery (1,044 million barrels of oil [MMBO]).

The early exploration evaluation data most often used are:

1. General geological/geophysical data on structural forms.
2. A good lithologic description of the stratigraphic section.
3. Mechanical data on the particular rocks of interest or on similar lithologies.
4. Matrix properties from logs or as interpreted from nearby areas.
5. Drill stem test (DST) or initial potential (IP) flow rates.
6. Core analysis (standard or whole core).
7. Borehole imaging logs.
8. In situ stress data.

Evaluations of Economic Potential

After it has been proven that fractures are an integral portion of the total reservoir quality and more quantitative data are available, evaluations of

economic potential are made. The purpose is to estimate reserves and flow rates to more accurately determine the potential worth of the reservoir.

Estimates of fracture spacing and width become more important as well as knowledge of fracture-matrix porosity interaction. Also important are laboratory estimates of relative flow within fractures and matrix at simulated depth.

In addition to early exploration data, other information should include:

1. Extended time pressure tests.
2. 3-D whole-core permeability analyses (oriented if possible), borehole imaging logs.
3. Laboratory data on matrix and fracture properties under simulated depth and depletion conditions.
4. Estimations of fracture/matrix interaction.

Evaluations for Recovery Planning and Modeling

During full development of a major field, several depletion schemes must be evaluated to optimize recovery and/or economic factors. An important tool is reservoir modeling: using computer-assisted mathematical models to investigate compositional behavior and relative flow rates under changing reservoir pressure and temperature conditions. In creating such models for fractured reservoirs, the most detailed quantitative fracture analyses are required. These involve not only statistical analyses of fracture properties and patterns, but also detailed knowledge of 3-D distributions of fractures within the reservoir. This requires a foot-by-foot description and documentation of numerous cores and or image logs. Such in-depth analyses are costly and time consuming, and are deemed appropriate in only the larger, complicated reservoirs.

The types of data most often used in recovery planning evaluations are:

1. Detailed structure maps covering several horizons above and below the producing formation.
2. Detailed core descriptions including lithology, mineralogy, textures, and a foot-by-foot documentation of fracture occurrence, orientation, and morphology.
3. Interpreted borehole imagery logs in all wells, especially those that are uncored.
4. 3-D whole-core analyses with at least one oriented core in the field.
5. Mechanical data derived from core samples of interest.

6. Long-term flow tests and multiple well tests.
7. Estimation of initial *in situ* stress state in the reservoir.
8. Laboratory data on both matrix and fracture properties under simulated depth and depletion conditions.
9. Laboratory data on fracture/matrix interaction.

GENERAL SEQUENCE OF STUDY

The order of investigation in fractured reservoirs is important in that study can be suspended at any time if the reservoir quality appears to be poor. If, for example, the fracture network initially detected was interpreted, because of the origin, to be of limited aerial extent, further evaluation and data generation may be considered unnecessary. The next three sections discuss the first three phases of this evaluation sequence. The fourth (Classification of Reservoir Type) and fifth (Optimum Locations and Paths) phases will be discussed in later chapters.

FRACTURE SYSTEM ORIGIN

The origin of the fracture system is postulated from data on fracture dip, morphology, strike (if available), relative abundance, and the angular relationships between fracture sets. These data can be obtained from full-diameter core (oriented or conventional), borehole imaging log output, or other less oriented logging tools, and applied to empirical models of fracture generation. Available fracture models range from tectonic to others of primarily diagenetic origin (Stearns and Friedman, 1972; and Nelson, 1979). It is only by a proper fit of fracture data to one of these genetic models that any effective extrapolation or interpolation of fracture distribution can be made.

The interpretation of fracture system origin involves a combined geological/rock mechanics approach to the problem. It is assumed that natural fracture patterns depict the local state of stress at the time of fracturing, and that subsurface rocks fracture in a manner qualitatively similar to equivalent rocks in laboratory tests performed at analogous environmental conditions. Natural fracture patterns are interpreted in light of laboratory-derived fracture patterns (Handin and Hager, 1957) and in terms of postulated

paleo-stress fields and strain distributions at the time of fracturing. In general, any physical or mathematical model of deformation that depicts stress or strain fields can, by various levels of extrapolation, be used as a fracture distribution model (Hafner, 1951; Odé, 1957; and Lorenz and others, 1993).

A genetic classification scheme for natural fracture systems, which is an expansion of that found in Stearns and Friedman (1972), permits separation of complicated natural fracture systems into superimposed components of different origin. Such partitioning can make delineation of structure (Friedman, 1969; and Friedman and Stearns, 1971) and prediction of increased fracture-related reservoir quality (McCaleb and Willingham, 1967; and Stearns and Friedman, 1972) from fracture data more tractable. Stearns and Friedman (1972) classify fractures into those observed in laboratory experiments and those observed in outcrop and subsurface settings. Their classification scheme, together with modifications suggested by this book, forms a useful basis for fracture models (Table 1–1). The major modification to Stearns' and Friedman's scheme is the addition of two categories of naturally occurring fractures: contractional fractures and surface-related fractures. A minor modification to the experimental fracture classification is the addition of a category similar to extension fractures in morphology and orientation, but having a different stress state at generation and rock strength: tension fractures.

Table 1–1
Experimental and Natural Fracture Classification

Experimental Fracture Classification

1. Shear fractures
2. Extension fractures
3. Tensile fractures

Naturally Occurring Fracture Classification

1. Tectonic fractures (due to surface forces)
 2. Regional fractures (due to surface forces or body forces)
 3. Contractional fractures (due to body forces)
 4. Surface-related fractures (due to body forces)
-

Generic Classification

Three fracture types are observed to form at consistent and predictable angles to the three principal stress directions during laboratory compression, extension, and tensile tests. All brittle fracture in rock must conform to one of these basic fracture types: shear, extension, and tension fractures.

Shear Fractures

Shear fractures have a sense of displacement parallel to the fracture plane. They form at some acute angle to the maximum compressive principal stress direction (σ_1) and at an obtuse angle to the minimum compressive stress direction (σ_3) within the rock sample. Potentially, two shear fracture orientations can develop in every laboratory fracture experiment, one on either side of, and oriented at the same angle to, σ_1 . In laboratory experiments, these fractures form parallel to σ_2 and at an obtuse angle to σ_3 (Figure 1-1). Shear fractures form when all three principal stresses are compressive (compressive stresses are considered positive for this work). The acute angle between shear fractures is called the conjugate angle and is dependent primarily on:

1. The mechanical properties of the material.
2. The absolute magnitude of the minimum principal stress (σ_3).
3. The magnitude of the intermediate principal stress (σ_2) relative to both the maximum (σ_1) and minimum (σ_3) principal stresses (as σ_2 approaches σ_1 the angle between σ_1 and the fracture plane decreases).

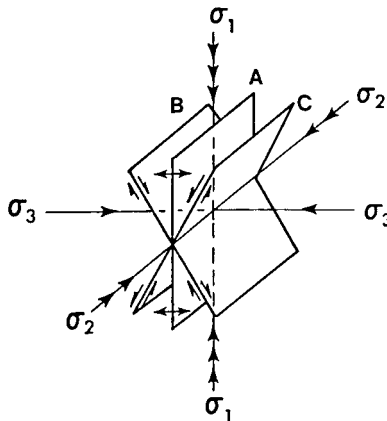


Figure 1-1. Potential fracture planes developed in laboratory compression tests. Extension fractures (A) and shear fractures (B and C) are shown.

Extension Fractures

Extension fractures have a sense of displacement perpendicular to and away from the fracture plane. They form parallel to σ_1 and σ_2 and perpendicular to σ_3 (Figure 1–1). These fractures also form when all three principal stresses are compressive. In laboratory fracture experiments, extension fractures can and often do form synchronously with shear fractures.

Tension Fractures

Tension fractures also have a sense of displacement perpendicular to and away from the fracture plane and form parallel to σ_1 and σ_2 . In terms of orientation of σ_1 and sense of displacement, these fractures resemble extension fractures. However, to form a tension fracture, at least one principal stress (σ_3) must be negative (tensile). To form an extension fracture, all three principal stresses must be positive (compressive). The distinction between the two is important because rocks have a much lower (10 to 50 times lower) fracture strength in tension tests than they do in extension tests. This becomes important in mathematical prediction of subsurface fracturing. Also, it is likely that true tensile fractures only occur in near subsurface environment, while extension fractures can occur in all low mean stress subsurface conditions. In general, I will call extension fractures those that are parallel to σ_1 and perpendicular to σ_3 when σ_3 is compressive (positive) or when its sign is unknown; tensile fractures will be referred to only when evidence suggests σ_3 is negative.

Geologic Classification

The genetic natural fracture classification presented in Stearns and Friedman (1972) and expanded here is built on two fundamental assumptions:

1. Natural fracture patterns (conjugate shear and extension or tensile fractures) faithfully depict the local state of stress at the time of fracturing.
2. Subsurface rocks fracture in a manner qualitatively similar to equivalent rocks in laboratory tests performed at analogous environmental conditions.

Thus, we assume that natural fracture patterns reflect the same geometry with respect to applied loads as do fractures generated in laboratory exper-

iments. If these assumptions are correct, then naturally occurring fractures can be classified on the basis of the origin of their causative forces as determined from laboratory data and fracture system geometry (Table 1–1). Therefore, this classification relies heavily on the previously presented experimental or generic fracture classification.

There are two schools of thought on the best means to observe and describe complex natural fracture systems in outcrop. One assumes that fracture data must be handled statistically to be meaningful. Thus, by combining large amounts of data from many outcrops together and searching for preferred orientations, it is believed that objectivity in interpretation can be obtained (Currie and Reik, 1977). While this combining of data is necessary at some stage of a fracture study, I believe this approach to be inefficient due to the great loss of interpretive precision when data are lumped together prior to interpretation. For example, an orientation plot containing 10,000 fracture measurements from many places on a fold will display gross trends in the data but will not allow description of subtle changes in orientation and inferred stress states from outcrop to outcrop.

A second approach involves the interpretation of individual outcrop data with respect to the mode of origin prior to statistical treatment (Stearns and Friedman, 1972). These interpreted data sets can then be added together sequentially to arrive at a combined description. The combined data set will have more statistical meaning and is also more easily interpreted for stress analysis due to prior interpretation of the statistically less significant individual data sets.

This approach to fracture interpretation necessitates the use of a genetic natural fracture classification such as that used in this book. Determining the origin of loads that caused fracturing at the outcrop scale increases the precision of structural interpretation on all scales. This can be accomplished because fractures form in a consistent geometry with respect to the three principal stress directions, thus delineating the paleo-stress field at the time of fracture (compare figures 1–1 and 1–2).

The geologic classification described below has important ramifications to pervasiveness, or the degree to which the fracture system is developed over multiple scales of size. For example, tectonic fractures related to folding are pervasive because the same fracture types and orientations are seen from aerial photographs of the outcrop, to hand samples from the outcrop, to thin sections taken from the outcrop or core. On the other hand, regional fractures are nonpervasive because they can usually be seen on only a limited number of scales, i.e., down to outcrop scale only. A generalization of the pervasiveness of the various geological classifications is given in Table 1–2.

Table 1-2
Scales of Natural Fracture Development
for the Geologic Classification

Orders of Magnitude in Size Spanned

Tectonic Fractures	9-10 Orders
Regional Fractures	5
Contractional Fractures	2
Surface-Related Fractures	4-5



Figure 1-2a Probable conjugate shear fractures in outcrop from Trinidad, courtesy of S. Serra and D.B. Felio.



Figure 1-2b Conjugate fold-related fractures expressed on a bedding plane in carbonate rocks in the Western Wyoming Thrust Belt. Field of view is about 3 ft. Photo courtesy of S. Serra.

Tectonic Fractures

Tectonic fractures are those whose origin can, on the basis of orientation, distribution, and morphology, be attributed to or associated with a local tectonic event. They are formed by the application of surface forces. This author has observed that the majority of tectonic fractures in outcrop tend to be shear fractures. However, locally I have seen examples of folds in compressive environments where the deformation is dominated by extension fractures. Tectonic fractures form in networks with specific spatial relationships to folds and faults.

Fault-Related Fracture Systems

Fault planes are, by definition, planes of shear motion. The majority of fractures developed in the vicinity of faults are shear fractures parallel to the fault, shear fractures conjugate to the fault, or extension fractures bisecting the acute angle between these two shear directions (the zone of fault slip or gouge is complex, and has its own internal deformation morphology). These three orientations (Figure 1–3) correspond to the three potential fracture directions during laboratory fracture experiments (Figure 1–1) and are developed relative to the local state of stress causing the fault. The fault is a result of the same stress field that caused the fractures. The fracture swarm predates the through-going fault and acts as a process zone conditioning the rock mass for the eventual fault offset. There are cases where large-scale slip did not occur, leaving only the precursive fracture swarm. In these cases, the orientation of the swarm itself, as well as the internal fracture orientations are needed to ascribe a fault-related origin. Several authors have noted and documented the fault-fracture relationship: Stearns (1964), Yamaguchi (1965), Norris (1966), Stearns (1968a, 1968b, 1972), Skehan (1968), Friedman (1969, 1975), Tchalenko and Ambraseys (1970), Stearns and Friedman (1972), and Freund (1974).

Because of the relationship between faulting and fracturing, it is possible to determine the direction of the principal stresses or loads at the time of formation. Also, knowing the orientation of a fault plane and the fractures associated with it, the sense of movement of the fault can be determined (Figure 1–4). The relationship of fractures to faults exists on all scales. Indeed, Friedman (1969) was able to use the orientation of microscopic fractures from oriented cores in the Saticoy Field of California to determine the orientation and dip of a nearby fault. An outcrop example of fractures associated with a normal fault in the Sinai in Egypt is shown in Figure 1–5.

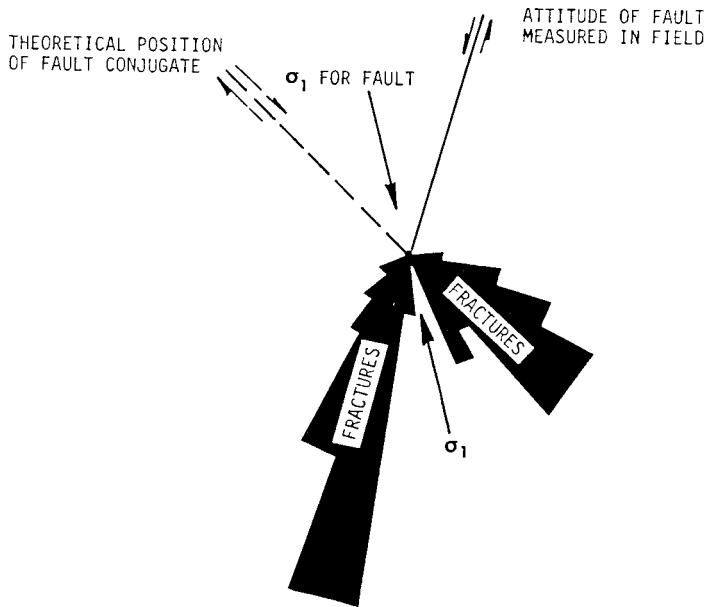


Figure 1-3 Rose diagram of shear fractures associated with normal default. After Stearns (1968b).

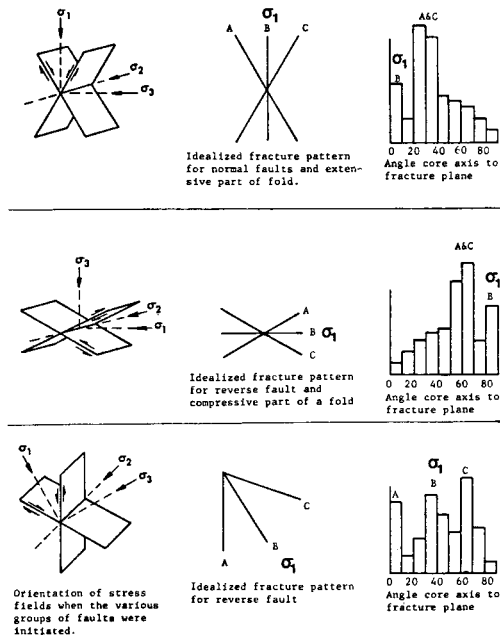


Figure 1-4 Relationships between stress states, the fault and fracture orientations derived from those stress states, and the resultant dip histograms subsequently obtained from core analyses. After Price (1966) and Friedman (1969), courtesy of Pergamon Press, Ltd., and the American Association of Petroleum Geologists (AAPG).



Figure 1–5 A normal fault in the Miocene clastic section of the Gulf of Suez. The fault is down to the right (west) and occurs on the Sinai side of the Gulf. The width of the outcrop is about 100 ft. Note the conjugate shear and extension fractures in the footwall (left side) of the fault. These predated the fault displacement and are related to the same stress state that caused the fault.

While, under ideal conditions, it is now possible to determine the orientation and sense of displacement of a nearby fault by the analysis of fractures, it is difficult to determine the proximity of the fault (Skehan, 1968; Pohn, 1981; Shepherd and others, 1982). The intensity of fracturing associated with faulting appears to be a function of lithology, distance from fault plane, amount of displacement along the fault, total strain in the rock mass, depth of burial, and possibly the type of fault (thrust, growth, etc.). Which of these parameters will dominate fracture intensity varies from fault to fault.

There are other less frequent fracture orientations associated with faulting of various scales. One group of grain-sized fractures occurs at acute angles to the fault plane and is called microscopic feather fractures (Friedman and Logan, 1970). Conrad (1974) relates these to displacement along the fault and the normal stress across the fault plane. While these feather fractures are important in determining a faulting origin and in microscopic examination of fault planes for the sense of shear motion, their importance in macroscopic fracture production of hydrocarbons is probably minimal.

Other fractures associated with faults occur within the slip zone itself. These reflect complex and changing stress and strain states inherent in the slip zone or mylonite zone itself. A description of these can be found in Higgs (1981).

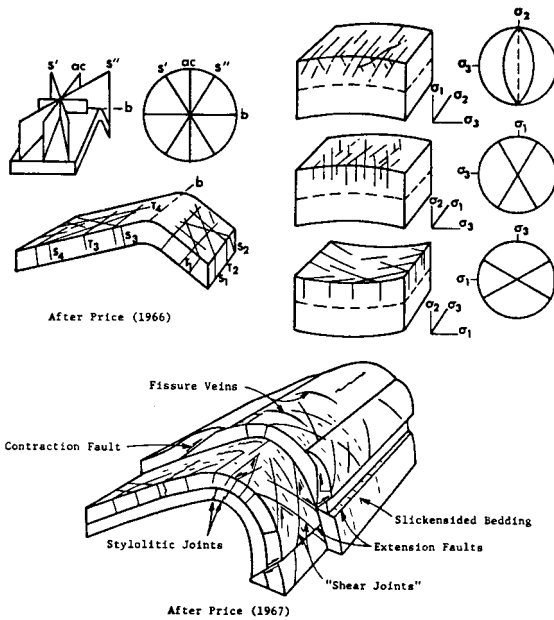


Figure 1-6 Typical fold-related fracture orientation diagrams depicting a portion of the total fracture geometry on folds. After Price (1966) and Price (1967), courtesy of Pergamon Press Ltd. and the National Research Council of Canada.

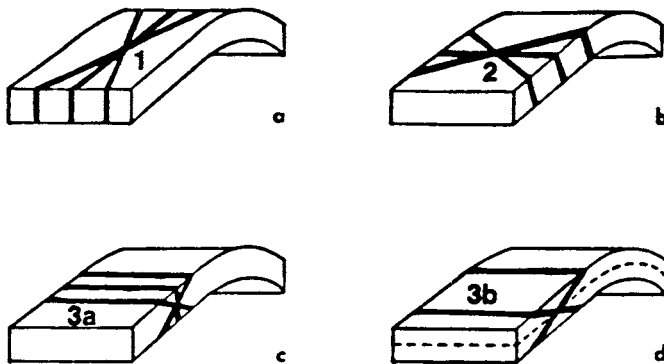


Figure 1-7a A generalization of dominant fold-related fracture sets according to Stearns (1968b).

Fold-Related Fracture Systems

The stress and strain history during the initiation and growth of a fold in rock is very complex. Therefore, the fracture patterns that develop within the fold are also complex. A significant amount of literature has been pub-

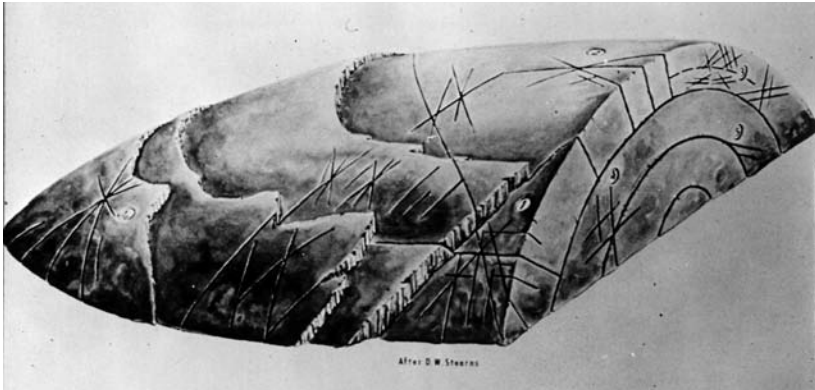


Figure 1-7b A block diagram showing the geometry of the major conjugate fracture patterns observed on folds in rock (Stearns, personal communication).

lished describing the orientation of fractures on folds: Martin (1963), Stearns (1964, 1968a, 1968b), Muecke and Charlesworth (1966), Price (1966), Roberts (1966), Nickelson and Hough (1967, 1969), Norris (1966), Price (1967), Charlesworth (1968), Parker (1942, 1969), Arndt and others (1969), Burger and Thompson (1969, 1970), Friedman and Stearns (1971), Stearns and Friedman (1972), McQuillan (1973, 1974), and Reik and Currie (1974). The majority of these papers describe only portions of the total fracture geometry (Figure 1-6). Stearns (1964, 1968a, 1968b) presents the most useful description of the total fracture geometry of folds (Figures 1-7a and 1-7b, and Table 1-3).

While the position and intensity of these fracture sets varies with fold shape and origin, most sets are observed on all folds that are studied in detail. These orientations are seen in a well-exposed fold flank in carbonate rocks in the thrust belt of western Canada in Alberta in Figure 1-8. In this figure, you can see all of the geometric elements of the total fracture system displayed on the bedding surface, and you can see that the individual elements are unequally developed in terms of their position and intensity. Indeed, core taken from multiple spots on the flank of the fold shown in Figure 1-8 would show different elements in the total pattern and different fracture intensities. At a large scale (the entire flank) most or all of the elements of the total fracture pattern of the fold would be expressed on a strike histogram or pole plot of all fractures. However, not all elements will be expressed at every point on the fold. In other folds, the distribution of orientations tends to be more regular (Figure 1-9). The difference is that each fold has uniqueness in its strain pattern during folding. The distribution of various elements of the fold-related fracture geometry that are utilized on the structure during deformation will vary. An example of this variation in



Figure 1–8 Tectonic fold-related fractures expressed on the bedding surfaces of a fold in the Western Canadian Thrust Belt in the wilderness area near Grand Cache, Alberta. This is the back limb of a leading-edge fold verging into the photograph. The outcrop pictured is about 300 ft. across.



Figure 1–9 Tectonic fold-related fractures expressed on the bedding surface of Black Canyon Anticline in the Rocky Mountains Foreland near Rawlins, Wyoming. Dip of the Permian Phosphoria limestone is toward the viewer. The field of view is about 20 ft.

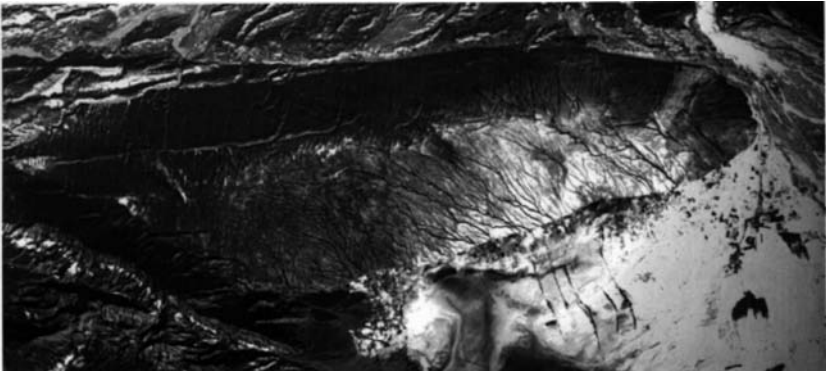


Figure 1–10 Tectonic fold-related fractures expressed on the bedding surface on a fold in northern Pakistan. Fractures are expressed on a satellite image of carbonate beds. The field of view is about 50 mi. left to right. Photo courtesy of S. Serra.



Figure 1–11 Type 3 fold-related tectonic fractures expressed in cross section of a chalk anticline along the western coast of Denmark. The field of view of the photo is about 10 ft. left to right.

carbonate folds in Iran can be found in Gholipour (1994). Similar variations are often seen at different scales such as on the satellite image of a fold in Pakistan in Figure 1–10.

The outcrop examples of the fracture patterns shown so far on folds have looked at those elements that have conjugate expression on the bedding plane. A distribution of Type 3 fracture sets expressed in an outcrop cross section of a fold in chalk in Denmark is given in Figure 1–11.

Table 1–3
Fracture Geometry of Folds

Type Set	σ_1	σ_2	σ_3
I	parallel to dip direction parallel to bedding	perpendicular to bedding	parallel to bedding
II	perpendicular to dip direction parallel to bedding	perpendicular to bedding	parallel to bedding
III	(a) perpendicular to bedding	parallel to bedding strike	parallel to dip direction
	(b) parallel to dip direction	parallel to bedding strike	perpendicular to bedding
IV	parallel to bedding	parallel to bedding strike	perpendicular to bedding
V	at an angle to bedding plane (dihedral angle)	parallel to bedding strike	at an angle to bedding plane (90° – dihedral angle)

I associated with bending in strike section

II associated with bending dip section

III associated with bending in cross-section: a. extensional, b. compressional

IV associated with fold-related thrusting

V associated with bedding plan slip

Fractures associated with domes have been briefly investigated by Nakagawa (1971) and Nelson (1975). It is concluded that the distribution of fractures on structural domes is analogous to that on folds. In essence, domes may be treated as equidimensional anticlines that plunge in all directions. As such, several of the Stearns fracture sets, which are defined with respect to the strike and dip of the beds, become coincident on domes.

Other Tectonic Fracture Systems

Fractures associated with other tectonic features such as piercement and impact structures can be predicted by determining the principal stress directions at failure. For example, the fracture system generated during impact should resemble that developed during the fracture below an indenter or point load, as in hardness testing, or during the deformation experienced below the tooth of a rotary drill bit. If a model can be made for the forces involved in the formation of a simple geological structure, a prediction of the stress directions and resultant fracture orientations can be made. This prediction involves the use of structural mechanics and experimentally de-

terminated relationships between potential fracture directions and the applied loads. More detailed discussion of fracture prediction will be covered later.

Regional Fractures

Regional fractures are those that are developed over large areas of the earth's crust with relatively little change in orientation, show no evidence of offset across the fracture plane, and are always perpendicular to major bedding surfaces (Stearns, 1968a, 1968b, 1972; and Nelson and Stearns, 1977). Regional fractures differ from tectonic fractures in that they are developed in a consistent and simple geometry, have a relatively large spacing, and are developed over an extremely large area crosscutting local structures. These fracture systems have (1) orientation variations of only 15–20° over 80 mi.; (2) fracture spacings ranging from just under 1 ft. to over 20 ft.; and (3) consistent development in areas as large as the entire Michigan and Uinta Basins and one-fourth of the Colorado Plateau. These fractures have also been called “systematic joints” by Price (1959, 1966, 1974), Hodgson (1961a), and Ziony (1966); “regional joints” by Babcock (1973, 1974a, 1974b); and simply “joints” by numerous authors, including Kelley and Clinton (1960). The descriptive terms of Hodgson (1961a) are the most commonly used. He describes the longer and more through-going fracture set as the “systematic” set (usually 90° Azimuth [AZ] from the first) and the shorter more discontinuous fracture set as the “nonsystematic” set. Because the nonsystematic set often abuts or terminates against the systematic set, they are considered

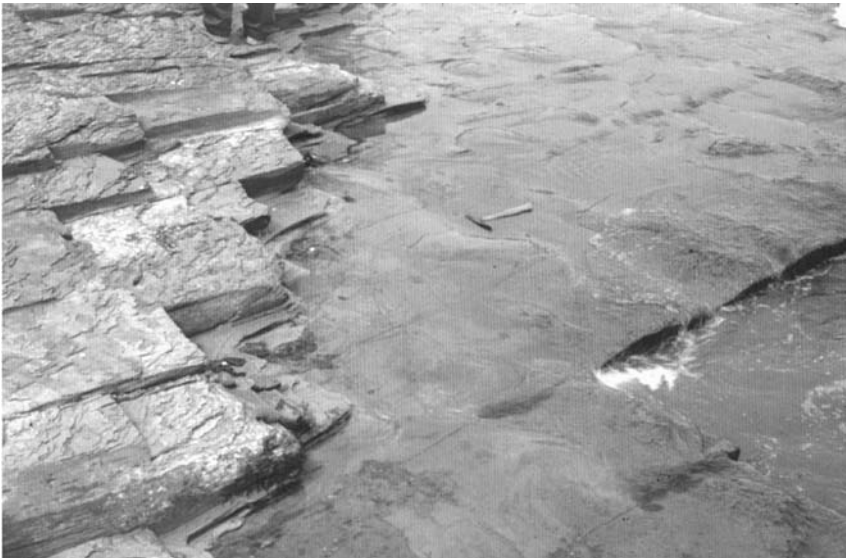


Figure 1–12 Orthogonal regional fractures in Devonian Antrim shale, Michigan Basin.

to have formed sometime after the systematic set. However, the time delay may have been milliseconds or many years.

Regional fractures in the stratigraphic section generally parallel cleat directions in coal beds in an area, with the face cleat corresponding to the systematic regional fracture set and the butt cleat corresponding to the nonsystematic regional fracture set. This correspondence and parallelism has been documented in Szwilski (1984), and Tremain and Whitehead (1990). Cleat in coals differs from regional fractures in the sedimentary units surrounding it only in its fracture intensity. Coals contract substantially as they thermally mature and increase in grade or rank. This component of shrinkage is in addition to whatever contraction is responsible for regional fracture development, thus giving the coals similar patterns but greater fracture intensity. An important aspect of this correspondence between regional fractures and cleat is the body of observational data available for coals. While regional fracture directions have not been mapped and published for many areas of the earth, cleat directions have. Cleat directions are important in coal mining because they affect extraction and tunneling. As a result, cleat directions have been recorded for hundreds if not thousands of years throughout the world. If you wish to understand the regional fracture directions in an area, the coal literature for that area is a good place to start.

Regional fractures (Figure 1–12) are commonly developed in orthogonal sets (Price, 1959, 1966; Stearns, 1968a; and Holst, 1982) and often change strike slightly from formation to formation (Stearns, 1968b; Nelson and Stearns, 1977). Price (1974) suggests that the two orthogonal orientations parallel the long and short axes of the basin in which they form and are due to the loading and unloading history of the rock. Supporting studies have been reported in Narr and Currie (1982) and Das Gupta and Currie (1983).

From a detailed study of fractures in the south-central Colorado Plateau, regional fractures appear to be extension fractures with the maximum principal stress acting in the vertical direction, Figure 1–13 (Nelson, 1975). Along these lines, regional fracture trends have been used by Engelder and Geiser (1980) to map paleostress fields on a regional scale. The origin of regional fractures is obscure. Many theories have been proposed, ranging from plate tectonics to earth tides (fatigue); however, none have proven conclusive. At present, they are considered to be due to the application of external or surface forces. They are probably developed with respect to vertical earth movements, but their distribution indicates that the scale of this movement is much larger in areal extent than anything we see in local structures.

One proposal of regional fracture origin that has gained support in the last 10 years is that of Lorenz et al. (1993). In their model, regional fractures are thought to be related to tectonic loading at the basin edges, in much the same way as proposed by Engelder and Geiser (1980). Lateral



Figure 1–13 Regional fractures in Jurassic Navajo sandstone, Lake Powell, in southeastern Utah. Local strength anisotropies may cause the development of one dominant orientation rather than the typical orthogonal pattern.

basin compression such as in the intermountain basins of the U.S. Rockies (Piceance Basin, for example) are thought to create extension fractures within the adjoining basin. It is postulated that these fractures owe their orientation to the compression or shortening directions of the belt at the basin edge and on the belt's geometric variation. Variations in the shape of the indenter or compressing block are envisioned to give variations in the strike of the resulting regional fractures within the basin. A convincing argument can be made for this idea. However, several features of regional fractures worldwide do not fit this model:

1. The intensity of regional fracture systems do not vary dramatically from the active basin margin to the basin center; they should decrease noticeably in intensity toward the basin center.
2. There are many basins that have well-developed regional fractures that have no structural belts at their edges to cause the fracturing; the Michigan Basin for example.

As an alternate hypothesis, regional fractures are seen as part of the normal basin compaction process. The fractures are an artifact of the loss of vertical dimension of the sediments, and the pattern and azimuth of the extension fractures are imparted by the geometry of the basin itself. Price (1966) contends that the two perpendicular orientations of most regional fracture sets are rotated to basin shape. As most basins are elliptical to some degree he rightly pointed out that one orientation of the orthogonal pattern parallels the long axis of the basin and the other parallel the short axes of the sedimentary basin. For the foreland basins of Engelder and Geiser



Figure 1–14 Shrinkage cracks due to desiccation in a 3 ft.-deep mud pan in the western Sinai of Egypt. Note the plumose texture along the fracture surfaces indicating a mode 1 extension or tension opening. Also note that in the flat center of the pan, the fractures display a polygonal pattern. While on the dipping edge of the pan, the fractures display a systematic/nonsystematic orthogonal pattern with the systematic direction down the dip (radial to the basin shape) and the nonsystematic direction in the strike direction (tangential to the basin shape). A pen is shown for scale.

(1980) and the intermountain basins of Lorenz et al. (1993), this would mean that one direction would be in the strike direction locally in the basin and one in the dip direction.

One analogy can be drawn from an evaporating mud pan in the western Sinai of Egypt. Figure 1–14 shows a mud pan with about 1 m of relief from its top edge to the bottom of the evaporating pan. The clay was saturated with water when this pan began as a small water pool. Upon drying, the clay desiccated and contracted upon the loss of water. In the center of the pan, contraction created tension fractures with a polygonal pattern or distribution on the surface. The center of the pan was flat and contracted equally in all azimuths. However, as seen in Figure 1–14, at the edges of the pan where the clay surface experiences dip (toward the center of the pan), the polygonal pattern of tension fractures gives way to an orthogonal pattern; two fracture directions perpendicular to the surface with one in the local dip directions and one in the local strike direction. These orientations keep this geometric relationship around the pan with one pointing down-dip to the center of the pan and the other following contours on the surface. In addition, using the regional fracture terms of systematic (first formed and through-going), and nonsystematic (second formed and discontinuous), the fractures in the down-dip direction are always the systematic set and the fractures in the strike direction are always the nonsystematic set. This is the same geometry as that found in Engelde and Geiser (1980), further substantiated in McColloch et al. (1974). Because in foreland basins and intermountain basins the basin shape is controlled by the deformation at the edges, the fractures have the same relationship with structural blocks at the edge as they do with the local basin geometry. It is only when you see the fractures in the mud pan or in the circular untectonized Michigan Basin (Holst and Foote, 1981) that it can be seen to be a basin geometry control rather than a basin edge control. In this model, the regional fractures and body forces can be due to normal compaction within a subsiding basin (Figure 1–15). The rocks lose vertical dimension and a small amount of resultant lateral dimension as well (a small negative Poisson's Ratio, like a cork, when compacting and dewatering). In this way, the forces that cause the fractures are body forces rather than surface forces with the orientations of the fracture pattern the result of basin geometry and pre-existing in situ stress.

Whatever the origin, there appear to be several factors that control the orientation of these fractures. In several areas of the Colorado Plateau, there appears to be a sub-parallelism between fault and fracture orientations in the crystalline basement and the regional fracture pattern in the overlying sedimentary rocks (Hodgson, 1961a, 1961b; Case and Joesting, 1972; Nelson, 1975). In some way, the regional stress system could have displaced existing fractures in the crystalline basement, which, in turn, could

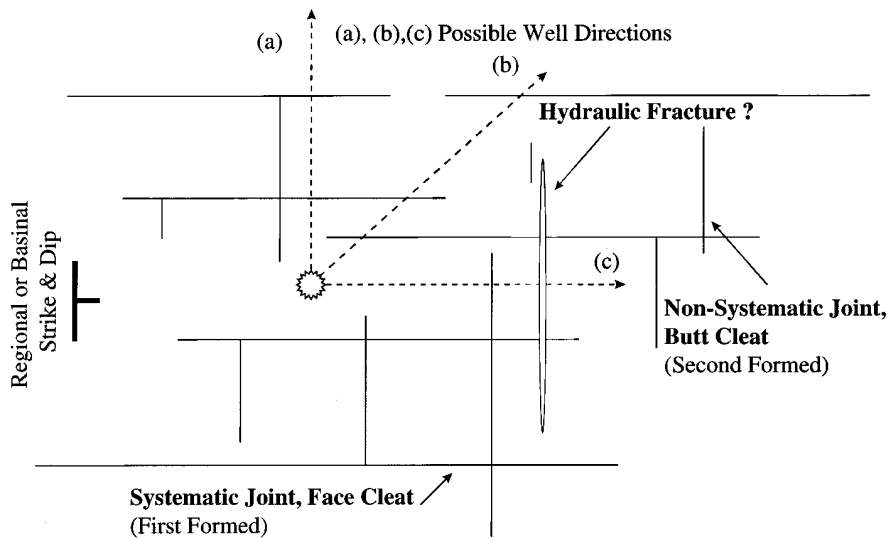


Figure 1-15 Schematic diagram showing the concept that regional orthogonal fractures are oriented with respect to the basin shape in which they formed. Also shown are possible horizontal drilling directions that could be used to optimize fracture permeability in the wellbore.

have extended and fractured the overlying sediments (Nelson, 1975). Evidence against this upward inheritance is, however, presented in Harper (1966) and Roberts (1976).

On a smaller scale, it is possible to cause a shift in regional fracture orientation of ± 20 degrees by strength anisotropies within and between formations (Nelson and Stearns, 1977). Such strength anisotropies can result from primary sedimentary fabrics such as crossbedding or preferred grain orientation. Locally on the Colorado Plateau, primary rock anisotropy is often great enough to inhibit the development of one of the regional fractures in the normal orthogonal set (Nelson and Stearns, 1977), leaving only one dominant fracture trend (Figure 1-8). Similar anisotropic control of fracture orientations brought about by sedimentary fabric in tectonic fractures is found in Winsor (1979).

Regional fracture systems produce hydrocarbons in numerous fields including Big Sandy and Altamont-Blue Bell. Regional fracture systems are second in importance only to tectonic fractures in hydrocarbon production. Excellent fractured reservoirs occur when later tectonic fracture systems are superimposed over a strong regional system. This relative importance of regional fractures will probably increase as large stratigraphic traps (off structure) become more prevalent.

Contractional Fractures

This class is a collection of tension or extension fractures associated with a general bulk volume reduction throughout the rock. These fractures are the result of:

- Desiccation
- Syneresis
- Thermal gradients
- Mineral phase changes

The importance of these volume reduction-related features to hydrocarbon production has long been overlooked. Because these fractures are initiated by internal forces to the body (body forces) rather than external forces (surface forces), their distribution is not necessarily restricted to local geologic structures as in tectonic. Herein lies their great value to production. Under the right depositional and diagenetic circumstances, contractional fractures can occur throughout the reservoir independently of the trapping mechanism. These fractures do produce hydrocarbons and are especially important in gas production in the Chase and Council Grove sections of the Panoma Field in Kansas and Oklahoma.

Desiccation Fractures (Mud Cracks)

In the contractional class, mud cracks are the most familiar to geologists, but they may also have the least economic significance. This fracture system is known to be due to shrinkage upon loss of water in subaerial drying. These tensile fractures are generally steeply dipping (with respect to bedding), wedge-shaped fractures often filled with later deposited material. The fracture system forms cusped-shaped polygons of several nested sizes (Figure 1–16). Desiccation fractures are generally developed in clay-rich sediments (Netoff, 1971; and Kahle and Floyd, 1971). These fractures are important in reconstructing depositional environments because they indicate subaerial drying. However, because they are restricted to thin topographic exposure surfaces or unconformity surfaces, they are probably of minimal importance to direct hydrocarbon production.

Syneresis Fractures

Syneresis is a chemical process that brings about bulk volume reduction within sediments by subaqueous or subsurface dewatering. This can involve dewatering and volume reduction of clay, or of a gel or colloidal suspension. Either or both of these processes can occur in sediments of varying grain size and sorting.



Figure 1–16 Desiccation cracks in mud. From Nelson (1979), courtesy of AAPG.

Syneresis, unlike desiccation, can generate either tension or extension fractures. Several papers that discuss syneresis and the fractures it produces are White (1961), Burst (1965), Picard (1966, 1969), and Donovan and Foster (1972). Syneresis fractures are referred to in this text as “chicken-wire fractures” because of the three-dimensional polygonal network of fractures developed within the sediment (Figure 1–17). Because syneresis fractures are initiated by internal body forces, they tend to be closely and regularly spaced, and are often isotropically distributed in three dimensions (equal spacing in all directions). Associated fracture permeability also tends, therefore, to be isotropically distributed. While desiccation fractures are restricted primarily to shaly or clay-rich sediments, syneresis fractures have been observed in shales, siltstones, limestones, dolomites, and fine- to coarse-grained sandstones (Picard, 1966, 1969; and Netoff, 1971). Desiccation and syneresis have been separated as distinct processes in this discussion. But in reality, a gradation between the two probably exists. What is important is that these two end-member processes produce fracture systems of distinctly different properties (Figure 1–18). Of these two, syneresis is far more important to hydrocarbon production because it occurs in greater volumes and types of rocks, and because the fracture system interconnects in three dimensions.

Thermal Contractional Fractures

For the purposes of this study, macroscopic thermally induced fractures are those caused by contraction of hot rock as it cools. Depending on the

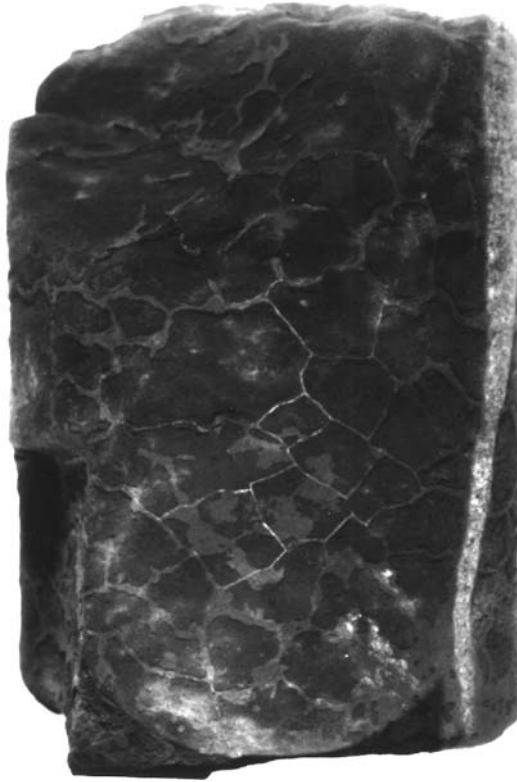


Figure 1–17 Contractional (chickenwire) fractures in core from 2,568 ft., Amoco Myler Gas Unit No. 2, Stanton County, Kansas. From Nelson (1979), courtesy of AAPG.

PROCESS	DESICCATION ←————→ SYNAERESIS	
TYPE	MECHANICAL	CHEMICAL
ENVIRONMENT	SUBAERIAL	SUBAERIAL, SUB-AQUEOUS OR SUBSURFACE
FRACTURE PATTERN	2-D POLYGONAL	3-D POLYGONAL
MATERIAL	CLAY-RICH SEDIMENTS	CLAY-RICH SEDIMENTS OR COLLOIDS (SILICA)

Figure 1–18 Contrasting characteristics of desiccation and syneresis.

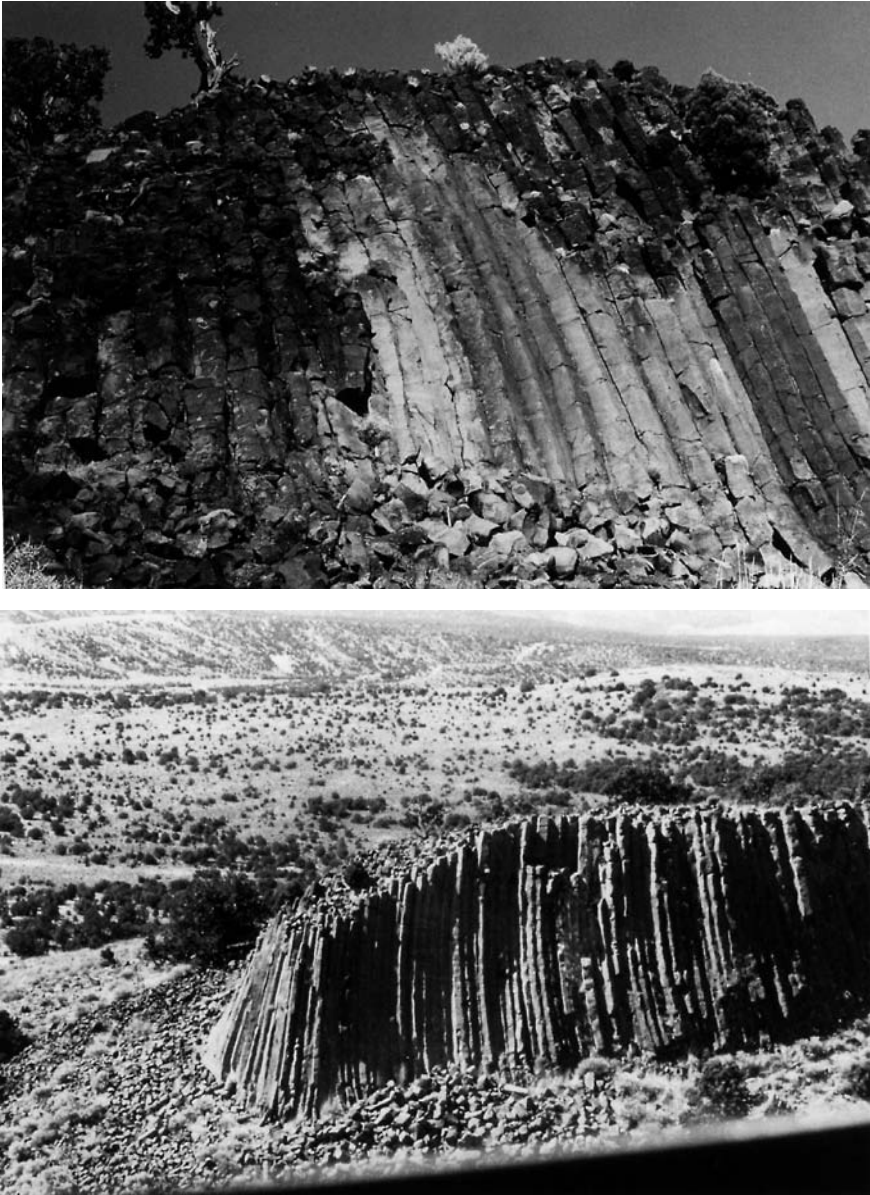


Figure 1–19 Columnar jointing in basalt northwest of Great Salt Lake, Utah.

depth of burial, these can be either extension or tension fractures and their generation is usually dependent on the existence of a thermal gradient across the material (Thirumalai, 1970). The classic example of natural thermally induced fractures is columnar jointing (Figure 1–19) in fine-grained igneous rocks (Peck and Minakami, 1968; DeGraff and Aydin, 1986).

In the subsurface, both overburden-derived and thermally-derived stresses are superimposed. In this way, tensile stresses derived from heating are often cancelled out by larger compressive stresses derived from overburden pressure. As such, true thermal fracturing at depth in the subsurface is probably rare relative to fracture patterns of other origin.

In most cases, the effects of temperature are evidenced by an alteration of the mechanical properties and rheologic behavior of rocks rather than by true thermally induced fracturing. True thermal fracturing may be of use in hard-rock mining and wellbore fracturing, but is considered of minimal importance in petroleum production in all but igneous rocks, such as oil production from the tertiary basalt flows at West Rozel Field, Salt Lake, Utah. In this field, sustained flow of oil and water of up to 1,000 barrels per day (bbl/day) was achieved from this form of contractional fractures.

Mineral Phase Change Fractures

This fracture system is composed of extension or tension fractures of often-irregular geometry related to volume reduction due to mineral phase change in the carbonate and clay constituents of sedimentary rocks. The chemical change from calcite to dolomite, for example, involves a change in molar volume of about 13 percent. Phase change from montmorillonite to illite involves a similar type of volumetric change. Under proper conditions, such phase change shrinkage could cause chickenwire fracturing, especially if superimposed over other contractional processes. A possible fracture pattern of this type has been reported in a porous dolomitized reef (Lang, 1964).

Surface-Related Fractures

This diverse class includes fractures developed during unloading, release of stored stress and strain, creation of free surfaces or unsupported boundaries, and weathering in general. Surface-related fractures are often developed due to the application of body forces. They have not proven to be important in hydrocarbon production to date in other than weathering surfaces (Karst), but it is important to know their origin with respect to other fracture types present in core or outcrop.

Unloading fractures are often found in quarrying operations. As rock material is removed from the quarry, rock bursts are common. This is due to the release of load or constraint in one direction. The rock relaxes and spalls, or fractures, on a plane parallel to the newly developed free surface. These fractures are often irregular in shape and follow topography in many eroded areas. Such fractures are often called sheeting in erosional terrains

(Price, 1966). Similar unloading fractures are frequently found in subsurface cores. These disk-shaped or cusp-shaped fractures are especially prevalent in shales and rocks that show evidence of substantial pressure solution (Figure 1–20).

Another type of fracture in this group is derived from the creation of a free or unsupported surface. These fractures can be either extension or tension and are often observed paralleling high canyon walls (Figure 1–21). A planar loss of support and gravitational forces acting on the unsupported material cause failure or spalling parallel to the strike of the free surface. Such fractures are similar in morphology and orientation to unloading fractures, but are primarily generated by gravitational forces, and are often associated with and initiate large-scale slumping.

The term “weathering fracture” describes fractures that *relate to the diverse processes* of mechanical and chemical weathering (e.g., freezethaw cycles, small-scale collapse and subsidence, mineral alteration, and diagenesis) and mass-wasting. A weathering fracture should not be confused with the control of weathering or erosion by pre-existing fractures and residual stresses in outcrop. In these cases, fractures preferentially erode, causing the parallelism between free surfaces and fracture planes. Weathering fractures are probably of minimal importance to direct hydrocarbon production except possibly for such production as from the Precambrian granite wash in Kansas and the buried granite hills in China, and various solution-enlarged weathering fractures associated with karsting in carbonates. Such solution-related fracture porosity may be quite important in unconformity-related carbonate reservoirs.

FRACTURE PROPERTIES AFFECTING RESERVOIR PERFORMANCE

Once the origin of a fracture system has been determined in a reservoir, the sequence of study suggests that the petrophysical properties of the rock-fracture system must be addressed next. This involves characterization of the fracture system in terms of physical morphology, distribution, and estimation of the reservoir properties (porosity, permeability, etc.) resulting from the fracture system characteristics.

Introduction

Fractures are present in all rock formations; subsurface or outcrop. The physical character of these fractures is dictated by their mode of origin, the

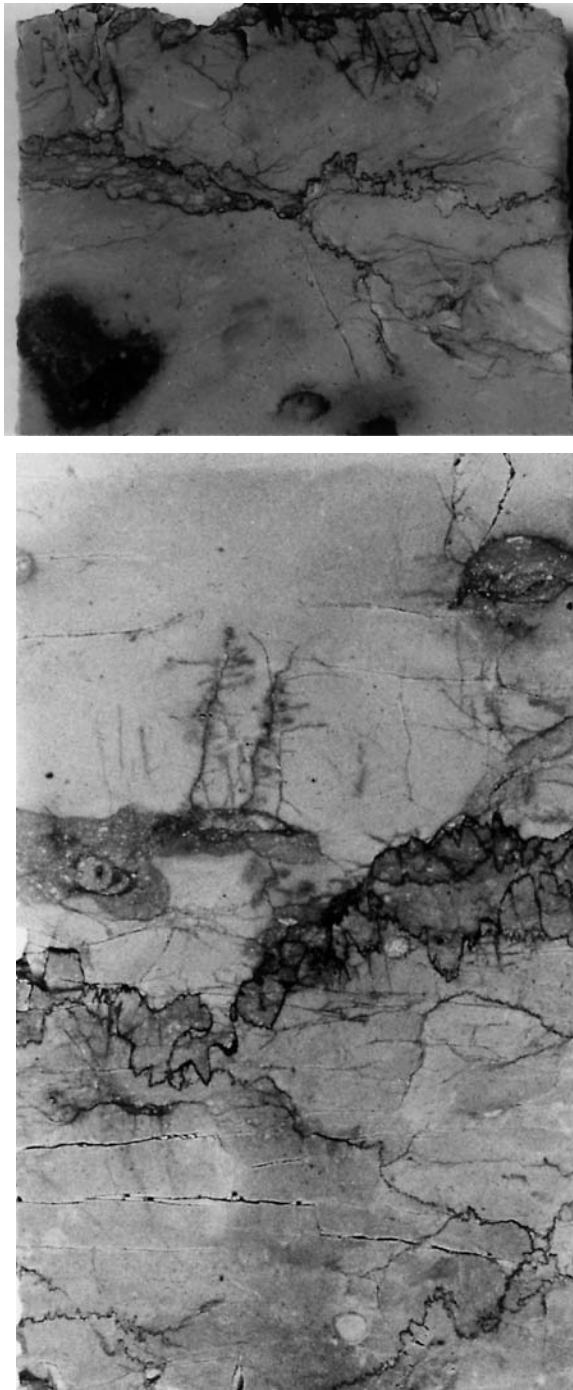


Figure 1–20 Unloading fractures in proximity to a stylolite zone in Yamama Limestone, Darius Field, Persian Gulf. From Nelson (1979), courtesy of AAPG.



Figure 1–21 Fractures (shown by arrows and numbers) associated with free, unsupported surfaces in Navajo sandstone at Lake Powell, southeastern Utah. From Nelson (1979), courtesy of AAPG.

mechanical properties of the host rock, and subsurface diagenesis. These factors combine to develop a feature that can either increase or decrease reservoir porosity and permeability. While always present in some large scale, it is only when fractures occur in sufficient spacing or length that their effect on fluid flow becomes important. To accurately assess this effect, either positive or negative, it is important to know the fluid flow properties of individual representative fractures and how many of these fractures of a given orientation exist in a given reservoir volume.

Therefore, in addition to the normal petrophysical determinations made on the rock matrix (rock in which the fracture resides), it is also necessary to determine the reservoir properties of the fracture network (either advantageous or detrimental to fluid flow) and how it changes with depth and reservoir depletion, which tends to mechanically close the fractures.

The four petrophysical determinations most useful in evaluation are, in order of increasing difficulty of calculation:

1. Fracture permeability
2. Fracture porosity
3. Fluid saturations within the fractures
4. The recovery factor expected from the fracture system

The data most useful in these determinations are derived either from analysis of whole-core samples or from single or multiple well testing. Data derived from various well logs are often used but in my experience are less accurate and less appropriate than whole-core and well-test data in such studies. This differs from the experience of Aguilera (1980), who claims that little useful data can be derived from core analysis. Wholecore samples are useful in fracture evaluation for two reasons:

1. They sample a relatively large volume of rock and thus potentially sample more regularly-spaced reservoir fractures than plug analysis; and
2. Standard permeability analyses can be performed in three dimensions on these samples (vertical, maximum horizontal, and horizontal 90 degrees to maximum horizontal permeability).

Such permeability analyses not only allow for calculation of the absolute permeability of a fracture or fractures at surface conditions, but also adequately depict the permeability anisotropy developed due to the presence of the fracture(s).

In addition, correlative fractured and unfractured plugs taken from the whole-core samples can be subjected to tests that measure the variation in fracture and matrix properties under simulated burial conditions. This is done in confining pressure tests or under a variety of mixed loading conditions to simulate subsurface conditions. Determinations of fracture permeability under confining pressure are very important because open fractures are generally higher in absolute permeability than the matrix, but the fractures are much more compressible and, therefore, reduce in permeability and porosity much more rapidly than the matrix with the application of force (Jones, 1975; Nelson and Handin, 1977; and Nelson, 1981b).

Whole-core samples can also be used as material for selected mercury injection and fluid saturation or relative permeability tests, which sample both fractured and unfractured material. The difference between the two companion (fractured and unfractured) samples can be considered a crude measure of fracture width distribution in the mercury injection tests (fracture width analogous to pore throat size) and variations in fluid saturation and relative permeability between the matrix and fractures in the fluid saturation tests.

Core analysis is used to determine reservoir quality and performance by summing together the individual small-scale elements of the reservoir. Well testing, on the other hand, is used to determine the bulk response of a relatively large volume of the reservoir and is a summary of the relative contribution of all its individual parts. A complete, accurate evaluation includes both small-scale and large-scale determinations of porosity, 3-D permeability, etc. However, early in exploration, sophisticated well-test data, especially multiple well interference test data, may be unavailable and more emphasis must be placed on smaller-scale whole-core analyses. The useful well tests are pressure transient analysis, pressure pulse testing, and interference testing. These techniques are described in detail in Aguilera (1980) and van Golf-Racht (1982).

Log analysis has been used successfully to delineate fracture occurrence and distribution in the wellbore. The quantification of the subsurface reservoir properties such as porosity and permeability of fracture systems by well logs is, however, much more difficult. Quantitative measurement of subsurface fracture porosity and fracture permeability by well logs gives highly variable and inaccurate results, especially when not tied closely to core from the specific fractured zones of interest. A complete listing of well log techniques is given in Aguilera (1995).

Fracture Morphology

An important factor that dictates fracture porosity and permeability is the morphology of the fracture planes. This morphology can be observed in core and outcrop and inferred from some well logs. There are four basic types of natural fracture plane morphology:

1. Open fractures
2. Deformed fractures
 - a. Gouge-filled fractures
 - b. Slickensided fractures
3. Mineral-filled fractures
4. Vuggy fractures

Open Fractures

Open fractures, as the name implies, possess no deformational or diagenetic material filling the width between the walls of the fracture. Such fractures are potentially open conduits to fluid flow. The permeability of open fractures is a function of the initial fracture width, the *in situ* effective stress component normal to the fracture plane, and the roughness and contact area of the fracture walls. Initial fracture width, roughness, and contact area are functions of the grain size distribution of the host material because the number and height of asperities along the surface dictating these parameters must be made up of multiples of the smallest basic rock units—grains. In general, open fractures greatly increase reservoir permeability parallel to the fracture plane. Because the fracture is only the width of one pore, it will have little or no effect on fluid flow perpendicular to the fracture plane (Figure 1–22).

Fractures open to fluid flow are often evidenced in outcrop by an oxidation staining or liesegang banding parallel to the fractures (Figure 1–23). These features indicate groundwater motion along the fracture planes. Examples of open fractures in outcrop and thin section are depicted in figures 1–24 and 1–25. Open fractures show little associated deformation in thin section and scanning electron microscope (SEM) photographs.

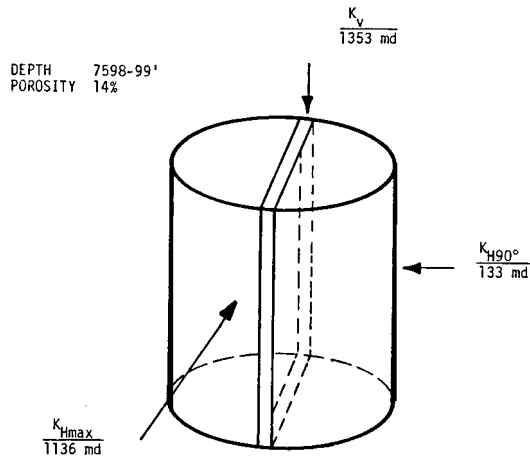


Figure 1-22 Example of 3-D whole-core permeability associated with an open fracture.

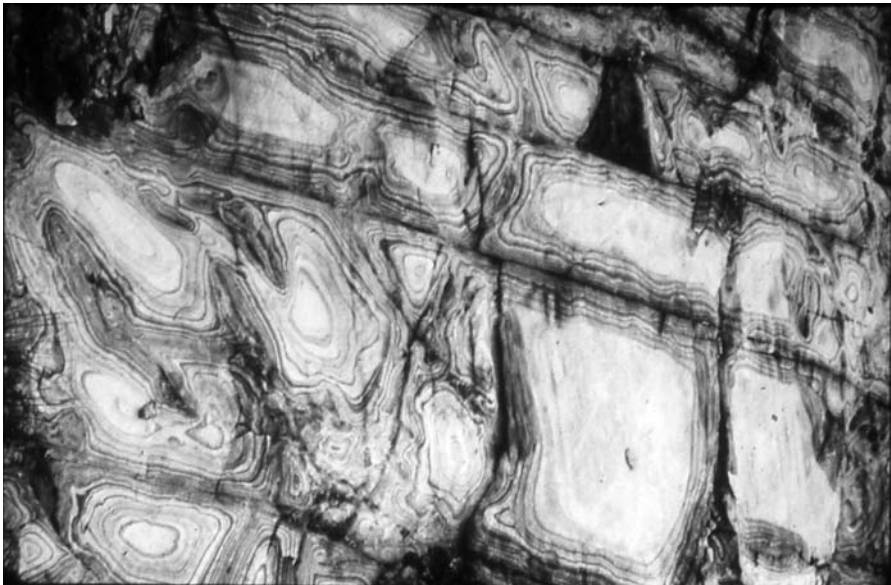


Figure 1-23 Natural fractures with liesegang banding in eolian Triassic/Jurassic Aztec Sandstone, Valley of Fire State Park, Nevada. The banding is iron oxide staining associated with ground water flow and exchange of iron between the sandstone and fractures. This geometry may be analogous to pressure isopotential lines in a subsurface reservoir that is being produced.



Figure 1–24 Open fractures in outcrop, Triassic Wingate sandstone, Lake Powell, southeastern Utah.

Deformed Fractures

Deformed fractures are ones that either formed as a relative ductile shear zone or were initially open and subsequently physically altered by later tectonic shear motions. This morphology creates strong anisotropy within the reservoir that is considered two end-member fracture morphologies within the deformed fracture category: gouge-filled (deformation bands) and slickensided. Intermediate mixtures of the two are possible and do occur in the subsurface.

Gouge-Filled Fractures (Deformation Bands)

Gouge is defined as the finely abraded material occurring between the walls of a fracture as a result of grinding or frictional sliding motion. Displacement of rock masses along the fracture plane causes cataclasis or granulation of the grains in contact across the fracture. This granulation or cataclastic zone can be several grain diameters wide, and it reduces the porosity, grain size, sorting, and therefore, the permeability of the fracture zone. In some instances, secondary mineralization on the freshly broken mineral surfaces further reduces the porosity and intrinsic permeability. In addition, the fine-grained deformed material possesses high-water saturation that can drastically reduce the relative permeability to hydrocarbons.

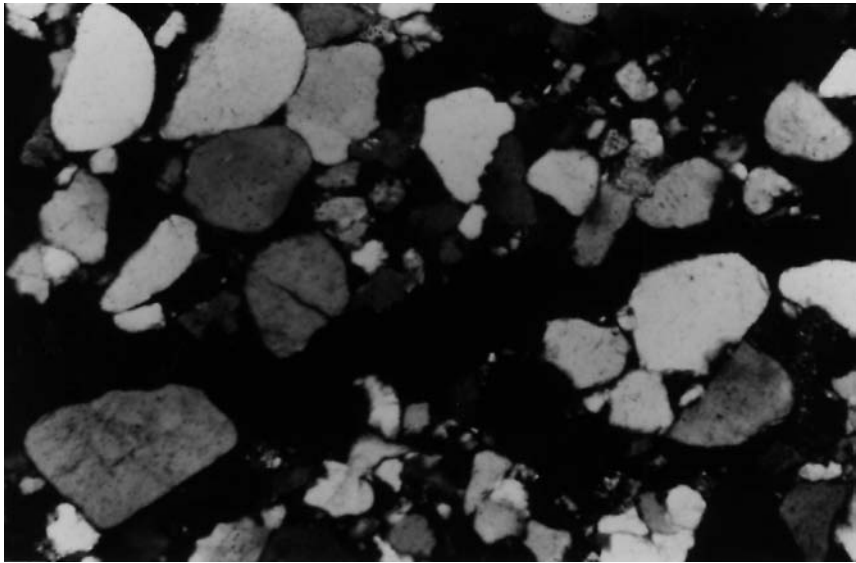
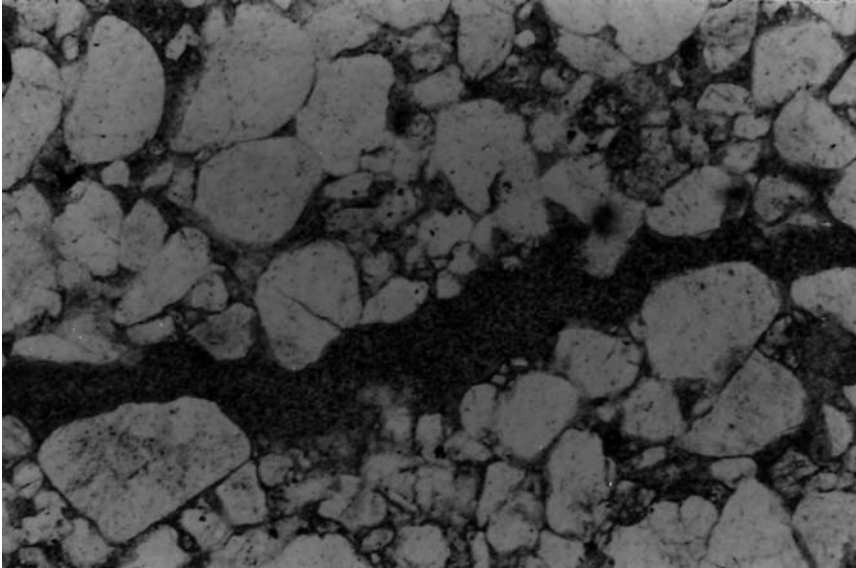


Figure 1–25 Open fracture in thin section in plane (above) and polarized (below) light. Rock is Nugget sandstone. (Magnification 140x).

In controlled laboratory experiments, it appears that the width of the gouge zone within a rock increases with the amount of shear displacement (Engelder, 1973; and Jamison and Stearns, 1982). Because the fracture is long and narrow, reduction in permeability occurs primarily perpendicular to the fracture or gouge zone (Figure 1-26).

Rock ductility and sliding friction developed across the fracture are of prime importance in the formation of gouge and, as will be discussed later, slickensides. The two vary with composition and texture of the rock. In general, sliding friction (not to be confused with *internal* friction) along a fracture plane is relatively low if we consider brittle rock in contact with brittle rock across the fracture plane, and relatively high if we consider two ductile rocks in contact across the fracture plane (Logan and others, 1972). The lowest relative sliding friction is developed with unlike rocks in contact across the sliding surface. A great deal of work has been done on gouge development in both field and laboratory observations (Stearns, 1968a; Brock, 1973; Engelder, 1973; Aydin, 1977; Pittman, 1981; and Jamison and Stearns, 1982).

Gouge-filled fractures are often the easiest of the fracture morphologies to observe in core or outcrop, because gouge material is usually more resistant to weathering and abrasion than the unfractured rock. It usually shows up as light colored, raised linear features in sandstone (Figures 1-27a and b, 1-28, and 1-29). While most prevalent in porous sandstones (porosi-

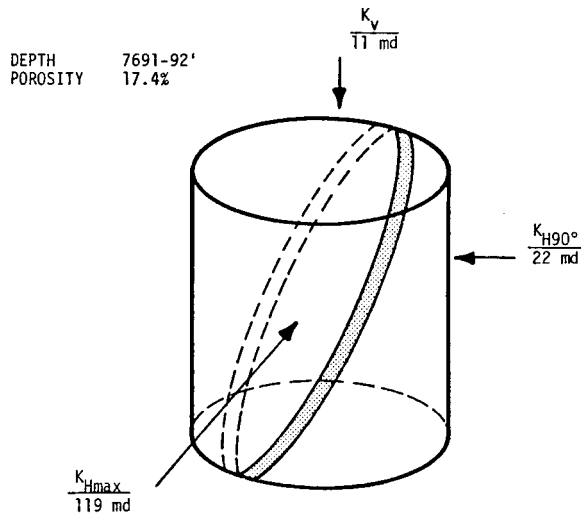


Figure 1-26 Example of 3-D whole-core permeability associated with a gouge-filled fracture.



Figure 1–27a A gouge-filled fracture or deformation band in Jurassic Nugget Sandstone for a well in the Western Wyoming Thrust Belt. This is a whole-core sample approximately 4 in. diameter. Photo courtesy of B. Ward.



Figure 1–27b Tectonic gouge-filled fractures or deformation bands in Silurian Oil Creek Sandstone of the Simpson Group in southern Oklahoma (lens cap for scale).

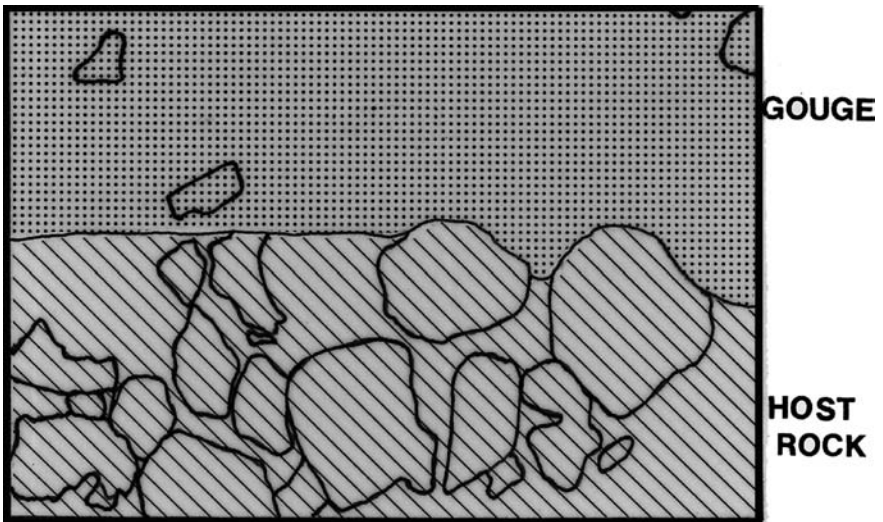
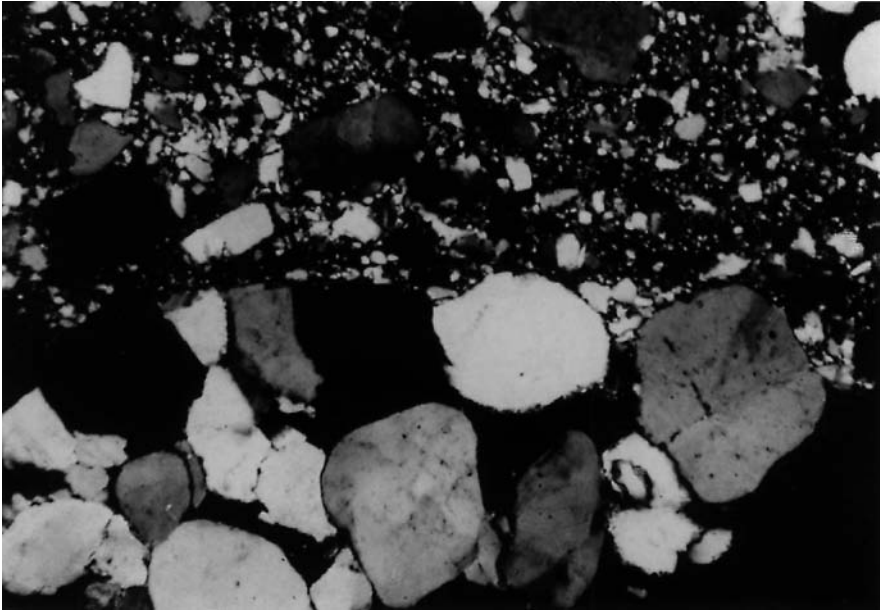


Figure 1–28 Gouge-filled fracture in thin section, polarized light. Shown is the gouge/country rock contact. Sample is Nugget sandstone from 10,171 feet, American Quasar 3-1, Summit County, Utah. (Magnification 56x.)

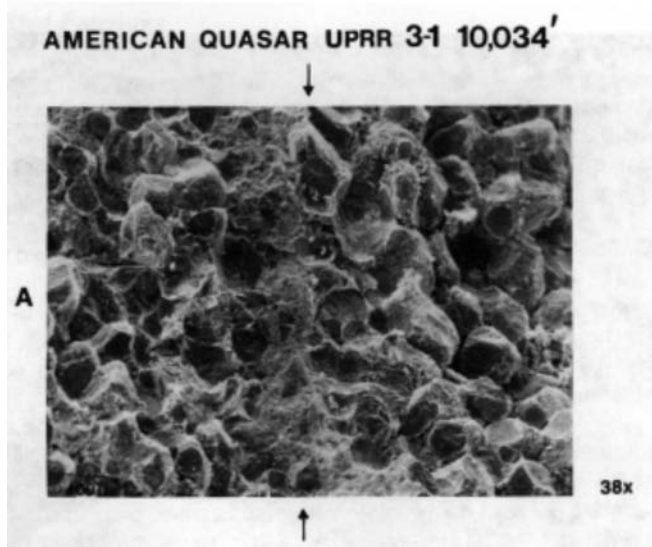


Figure 1-29 Sandstone gouge on SEM photomicrographs of Nugget sandstone.

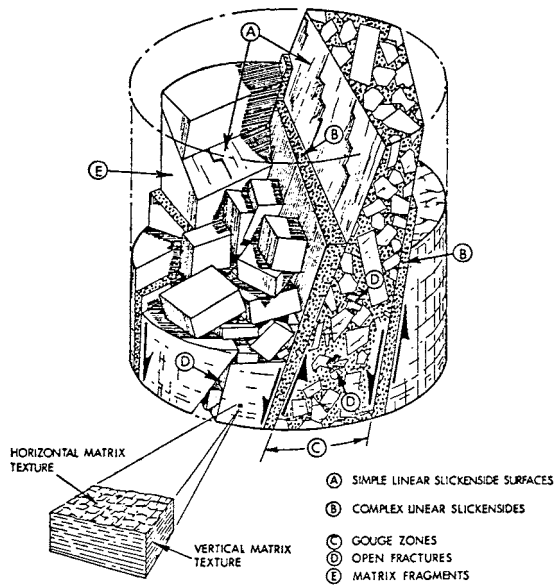


Figure 1-30 Gouge textures in shale. Drawing courtesy of H.H. Hinch.

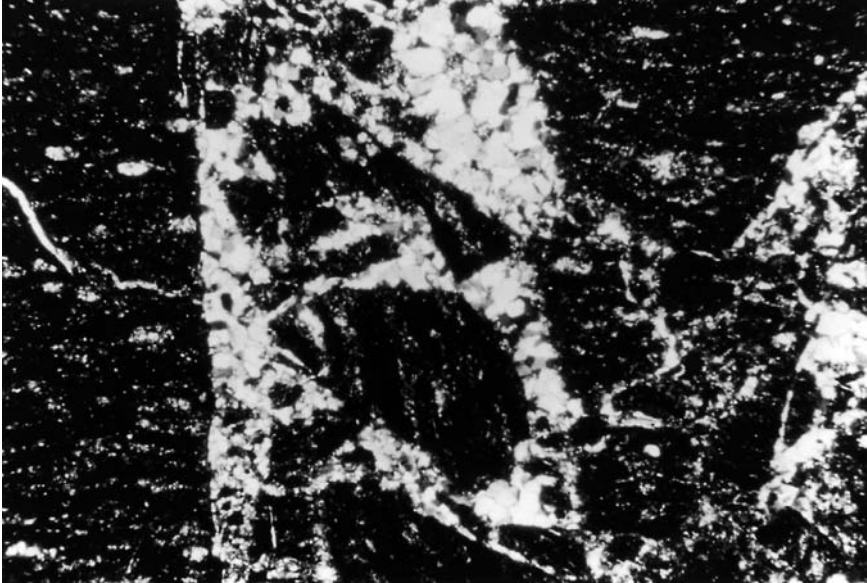
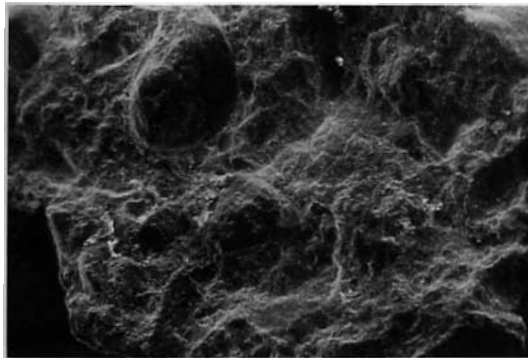
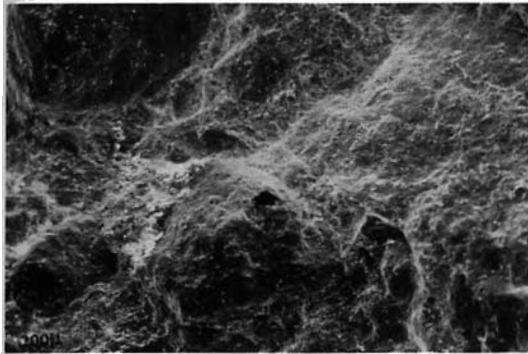


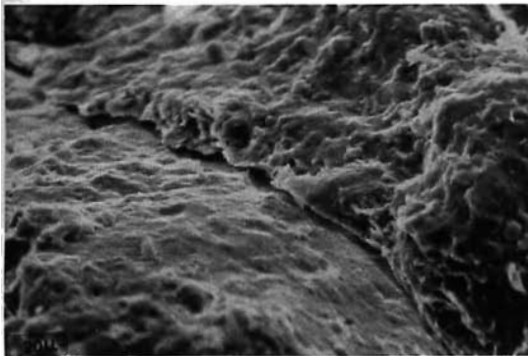
Figure 1–31 Gouge in thin section in plane (above) and polarized (below) light. Sample is Devonian Woodford shale.



33x



65x



650x

Figure 1–32 Gouge material in shale on SEM photomicrographs.



Figure 1-33 Limestone gouge in an outcrop sample from Deer Creek Thrust, Nevada.

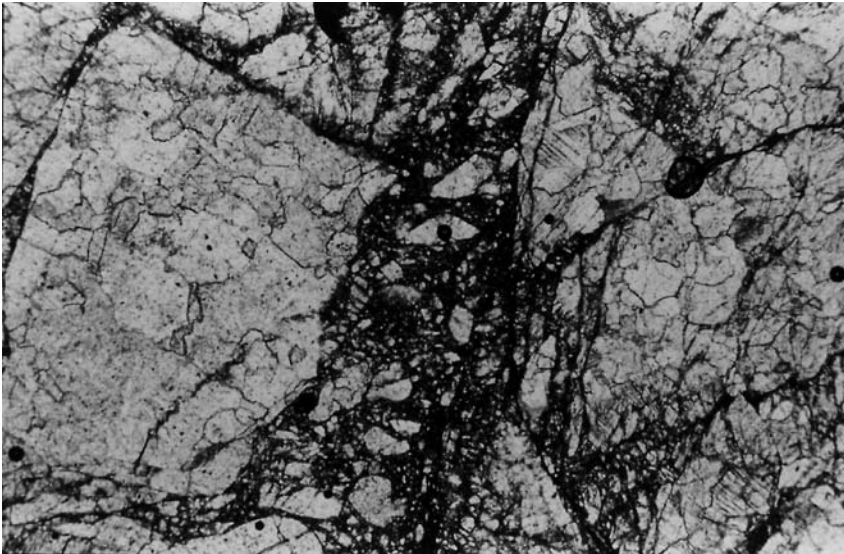
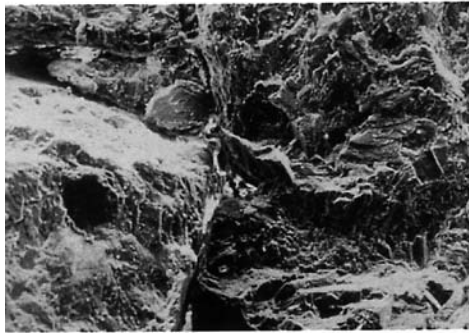


Figure 1-34 Limestone gouge in thin section (plane light) from an outcrop sample of the Deer Creek Thrust, Nevada. (Magnification 40x).

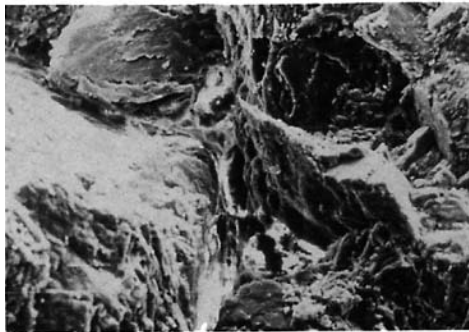
ties above 15 percent), gouge development also occurs in shales (Figures 1-30, 1-31, and 1-32) and in limestones (Figures 1-33, 1-34, and 1-35). The deformation band or gouge-filled morphology is probably a primary feature, forming with the earliest shear motions of the fracture.



33x



130x



325x

Figure 1–35 Limestone gouge on SEM photomicrographs from an outcrop sample of the Deer Creek Thrust, Nevada.

Slickensided Fractures

A slickenside is a polished or striated surface that results from frictional sliding along a fracture or fault plane. Slickenside development involves either pulverization and cataclasis of the host rock, or the creation of glass by

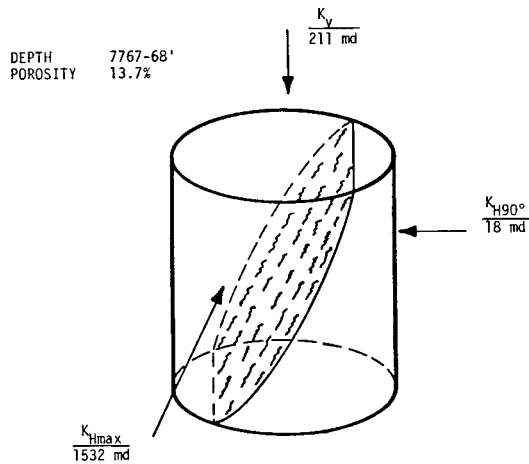


Figure 1–36 Example of 3-D whole-core permeability associated with a slickensided fracture.

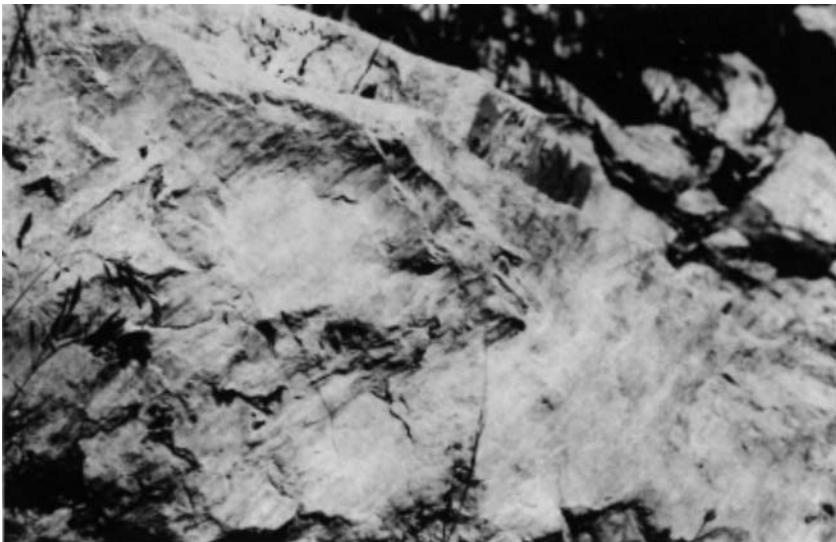


Figure 1–37 Slickensided fracture in Nugget sandstone outcrop, Big Elk Anticline, northwest of Alpine, Wyoming. Photo width is about 3 ft. of outcrop.

grain melting. The result of this deformation is a reduction in permeability, at least in the direction perpendicular to the slip surface. However, some permeability increase may occur parallel to the slip surface due to mismatch of the smooth fracture walls. In contrast to gouge, the deformation zone in slickenside development is generally only one or two grain diameters away from the fracture plane (Figure 1–36).

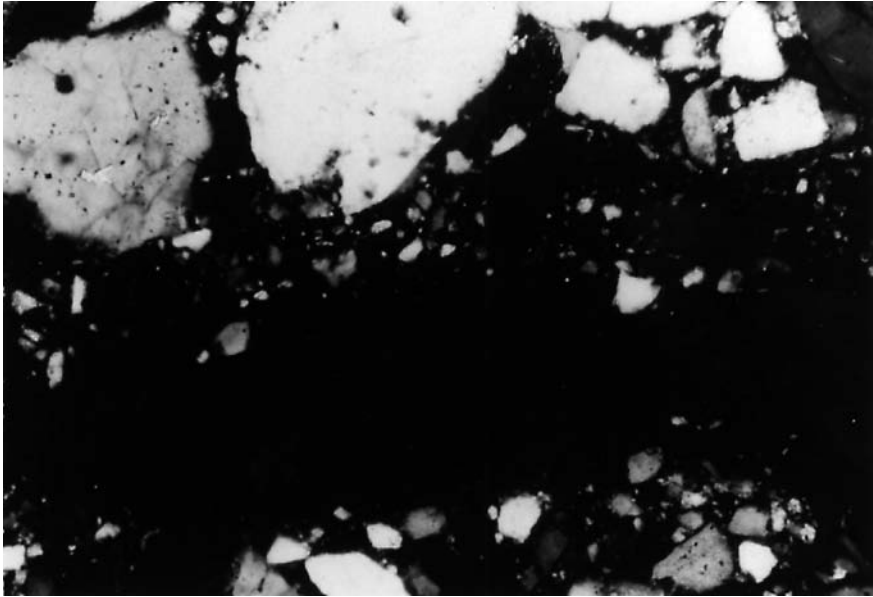
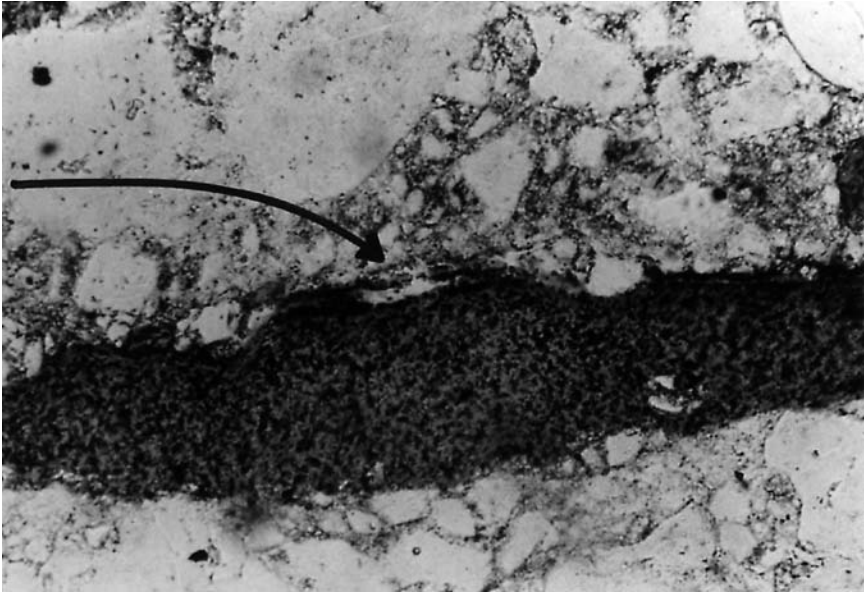


Figure 1–38 Slickensided fracture in thin section in plane (above) and polarized (below) light. Sample is from Nugget sandstone core, 7,613 ft., Champlin 224 Well, Uinta County, Wyoming. (Magnification 126x.)

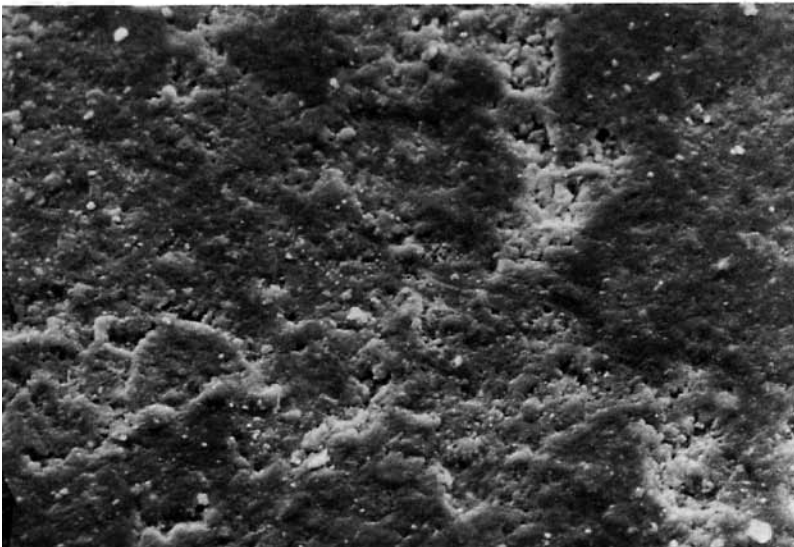
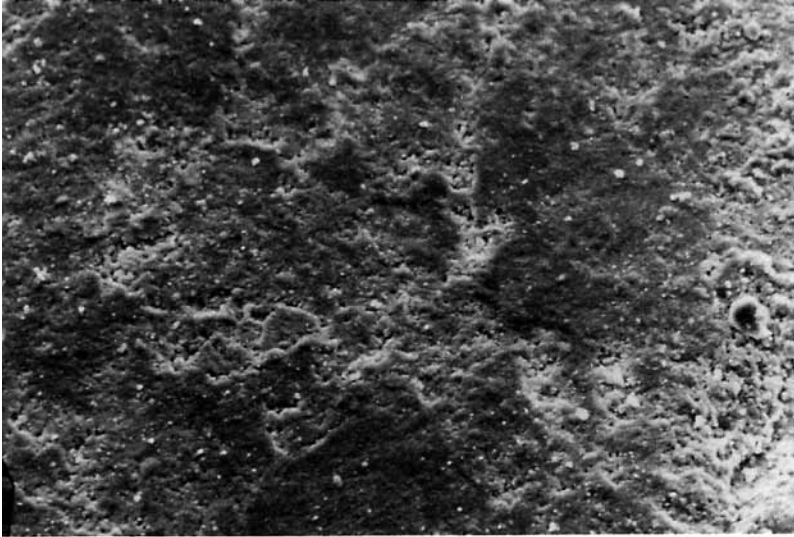


Figure 1–39 Slickensided fracture surface on SEM photomicrographs (500x and 1,000x). Sample is from Nugget sandstone core, Uinta County, Wyoming.



Figure 1-40 Slickensided fracture in a limestone outcrop sample from the Deer Creek Thrust, Nevada.

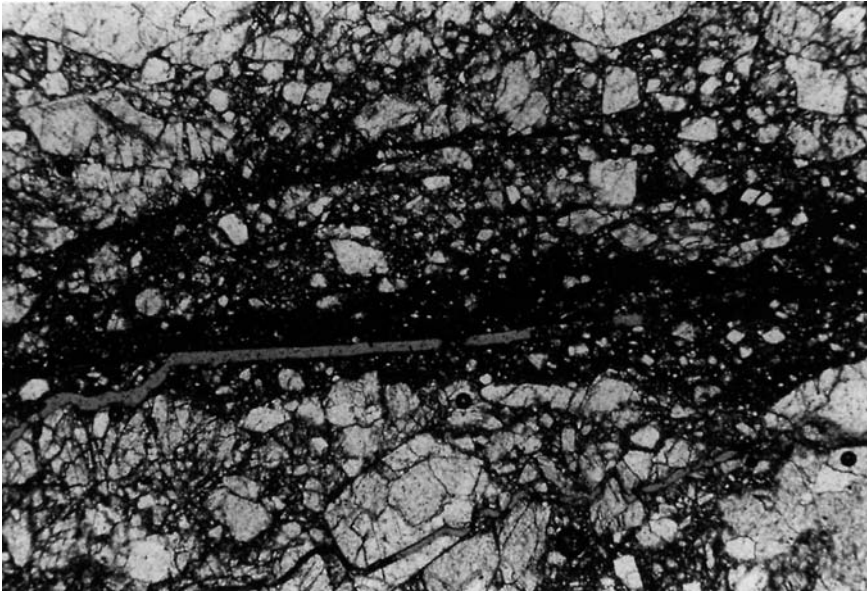


Figure 1-41 Slickensided fracture in a limestone in thin section (plane light). Sample is from outcrops along the Deer Creek Thrust, Nevada. (Magnification 40x).

In the literature, these fractures are most often described in sandstones (Figures 1-37, 1-38, and 1-39) and especially limestones (Figures 1-40, 1-41, and 1-42), but they have been found with increasing regularity in shales (Figures 1-43, 1-44, and 1-45), as shales are being examined more often for source rock and reservoir potential.

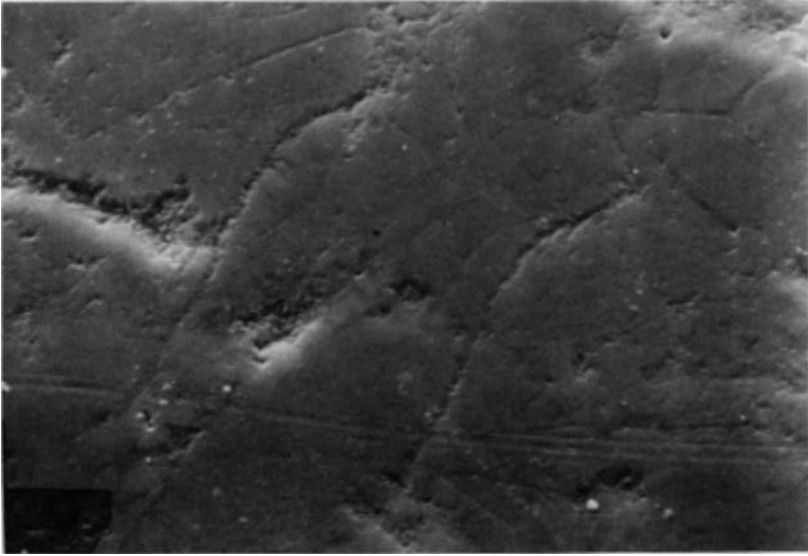


Figure 1–42 Slickensided fracture in limestone on SEM photomicrograph. Sample is from outcrop along the Deer Creek Thrust, Nevada.



Figure 1–43 Slickensided fracture in shale. Sample is from Devonian Second White Specks, Alberta, Canada.

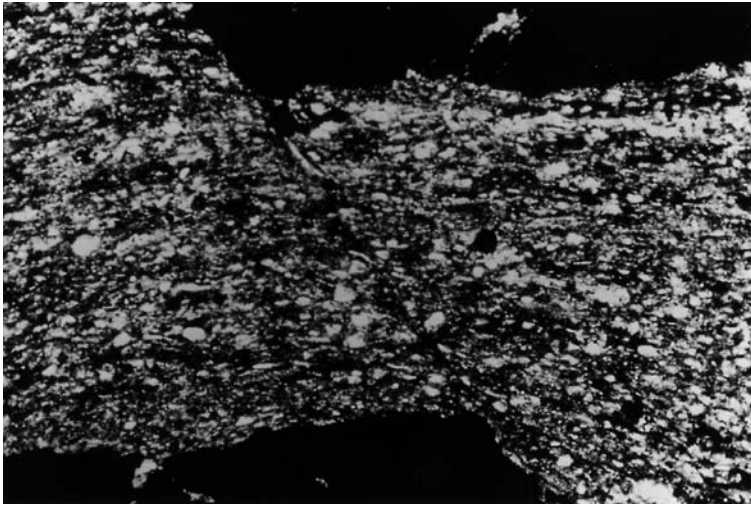


Figure 1-44 Slickensided fracture in shale in thin section (polarized light). (Magnification 242x).

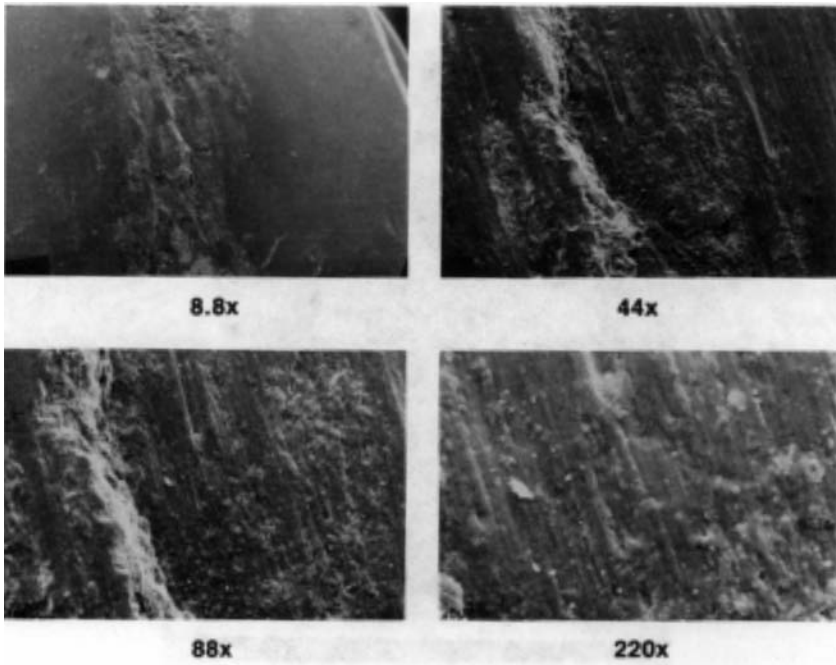


Figure 1-45 Slickensided fracture in shale on SEM photomicrographs.

Slickensides are prominent in relatively low-porosity sandstones and carbonates of various properties. These rocks are usually somewhat stronger or more brittle than analogous rocks that develop gouge, environmental conditions being equal. Also, rocks that contain significant amounts

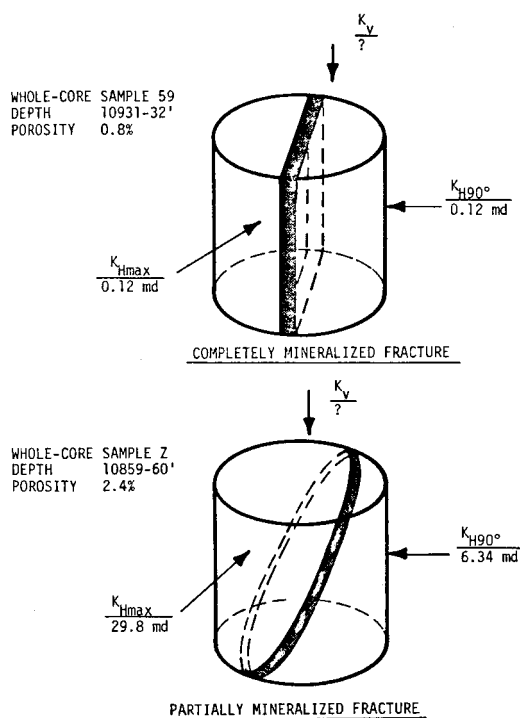


Figure 1-46 Example of 3-D whole-core permeability associated with mineralized fractures.

of material not subject to granulation or cataclasis, such as clay, gypsum, and calcite fill, will tend to form slickensides in preference to gouge even though they are not strong, brittle materials.

Occasional glass development can be seen in thin sections along the sliding surface (Figure 1-38). This glass is the result of quartz grain melting during frictional sliding along the fracture surface. Laboratory experiments indicate at least 1200°C can be developed along sliding surfaces in sandstone (Teufel, 1976). Such pools of glass are impervious to fluid flow. If sufficient glass is created by continued displacement, permeability perpendicular to the fracture plane will be drastically reduced. The slickenside morphology can either form as a primary feature of the fracture surface or as an effect of rejuvenation of slip at a later event.

Combined Gouge-Filled and Slickensided Fractures

One type of fracture morphology in porous sandstones being observed with more frequency involves a combination of gouge and slickensides. This morphology is frequently observed in Jurassic Nugget Sandstone cores from the Western Wyoming Thrust Belt. The morphology consists of a thick



Figure 1–47 Incompletely mineralized fracture in Silurian Tuscarora Sandstone on SEM photomicrograph from the Amoco No. 1 Texas-Gulf Well, Centre County, Pennsylvania. Photo courtesy of R.E. Larese.

gouge zone with discrete striated or slickensided surfaces occurring either totally within the gouge or at the boundary or contact between the gouge and country rock.

The slickenside development appears to post-date the gouge formation and indicates a progressive change in the mechanical properties of the gouge-filling and its relation to the host or country rock. As the compactive process of gouge formation proceeds, the material becomes finegrained, indurated, brittle material with a pronounced fabric. With increasing gouge width, the material begins to act as a separate mechanical entity within the rock mass. As further deformation occurs, the gouge itself fractures, and due to its now lower ductility, forms slickensided fractures rather than additional gouge. Also, as the gouge material grows in thickness and changes its properties drastically from that of the host rock, slip and slickensides often occur at the gouge/host contact. Initiation of slip at this contact indicates a relatively low coefficient of sliding friction at this surface due to a large ductility contrast.

The importance of the combined gouge-filled and slickensided morphology lies in the differing reservoir properties of the two individual features. Slickensided fractures have some porosity and permeability parallel to the plane, while gouge has little to none. The presence of the combined morphology often displays some fracture porosity and permeability on the scale

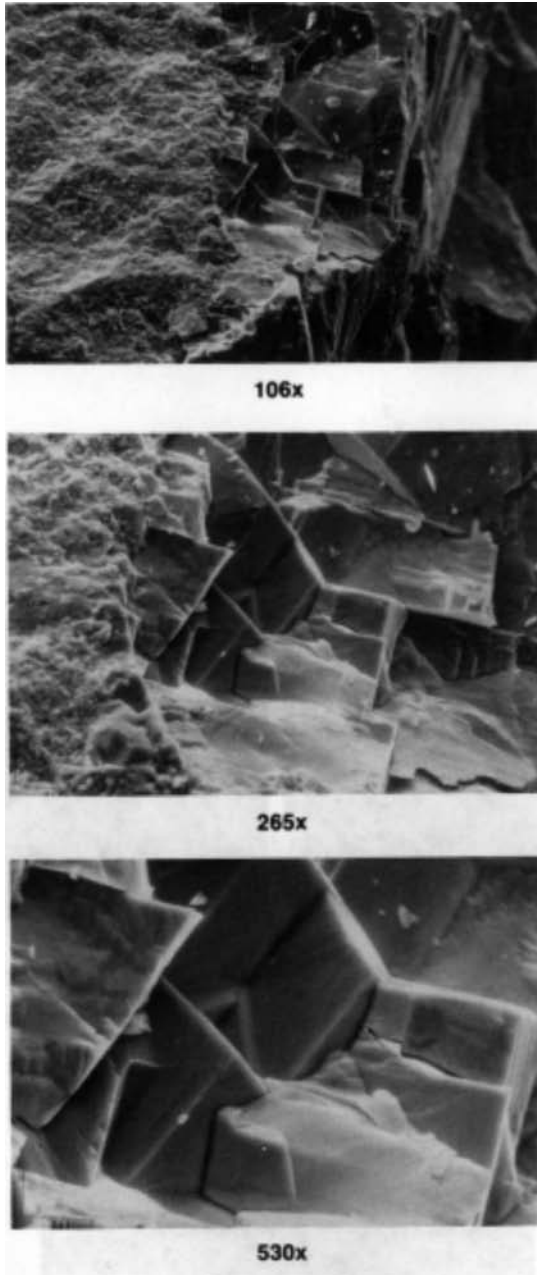


Figure 1–48 Completely mineralized fracture in shale on three magnifications of SEM photomicrographs. Sample is Devonian Second White Specks, Alberta, Canada.

of whole-core analyses, but the effect on reservoir flow as a whole is probably minimal because the slickensided fracture is often encased with low-permeability gouge. Therefore, core analyses involving this combined morphology with the fractures intersecting the core surface could be misleading.

Mineral-Filled Fractures

As the name implies, these fractures are those that have been filled or “choked-off” by secondary or diagenetic mineralization. Quite often this secondary cementing material is quartz, carbonate, or both. Mineral filling may or may not be complete, of course. Its effect on permeability depends on the completeness of filling and diagenetic history of the material. Usually, filled fractures are permeability barriers, but incomplete filling of a fracture in the form of either vug development or intergranular porosity can give some measurable increase in permeability to the reservoir (Figure 1–46).

Mineral-filled fractures are extremely common. Mineral filling is the nemesis of flow prediction and quantification in fractured reservoirs. While the presence, width, and intensity of natural fracture systems can be predicted to some degree, mineral filling and the completeness of filling cannot. The presence of complete mineral filling can kill an otherwise scientifically sound exploration play. Fortunately, mineral filling is often incomplete or has undergone some degree of dissolution, making reservoir permeability acceptable for production. Mineralized fractures occur frequently in sandstone, shale, and limestone (Figures 1–47, 1–48, and 1–49).

Completely Filled Fractures

Complete mineral filling in a fracture system imparts no positive reservoir attributes to the rock in which it resides. There are, however, some analyses that can be performed on these fractures that are relevant to an in-depth reservoir study. First, if the fractures are filled with a mineral phase significantly different in acoustic properties from the matrix, recognition on the acoustic televiewer may be easier and facilitate fracture recognition and orientation. This allows for better determination of and intensity of the fracture system. This may in turn allow for the prediction of a fractured reservoir nearby where the fractures are not completely filled.

Other uses of completely filled fractures lie in documenting diagenesis. The fracture fill often records deformation and cementation events that occurred after the fracture was formed. Evidence for these events can be found in the form of twinning and translation of the filling crystals, multiple cementation sequences, and fluid inclusions. These occurrences can be quite

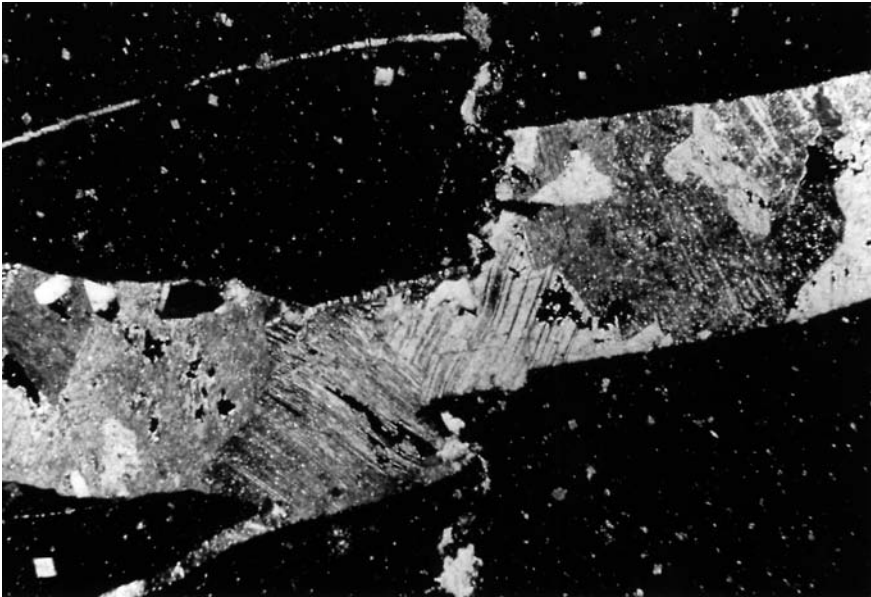


Figure 1–49 Completely mineralized fracture in thin section (polarized light). Sample is Devonian carbonate from outcrops near Nahanni Butte N.W.T., Canada. (Magnification 83x.)

useful in unraveling the depth, alteration, and fluid migration history of the rock after fracturing took place (Narr and Currie, 1982; and Tillman, 1983).

Incompletely Filled Fractures

In incompletely filled fractures, some measurable pore space exists within the filling material. This pore space may be primary to the fracture or secondary in nature. Frequently, secondary porosity development in fracture fill is the result of calcite dissolution.

Incomplete mineral fill in fractures can be very important and in some cases actually creates the *total* reservoir quality. The Tuscarora Sandstone (Figure 1–47) is an example of such a reservoir. In this rock the matrix porosity is about 0.5 percent. The dissolution/fracture porosity is about 1 percent. This dissolution/fracture porosity is the result of a complex diagenetic history of the fracture fill. After fracturing, four periods of mineralization took place in fractures of one tectonic fracture set. The sequence was:

1. Early chlorite coating the fracture walls
2. Euhedral quartz mineralization
3. Calcite mineralization
4. Sulfide mineralization (mostly pyrite, chalcopyrite, and galena)

Subsequent to this, a period of calcite dissolution took place forming the present day secondary porosity along the fracture fill that represents the essential porosity and permeability within the reservoir. Initial flow rates from this discovery well were estimated at 48 million cubic feet per day (MMcfd).

Vuggy Fractures

Vuggy fractures are not so much a true fracture morphology as they are a matrix alteration surrounding the fracture (Figure 1–50). Vuggy fractures form when fluids enter a low-permeability rock along fracture planes. If the fluid is in disequilibrium with the rock matrix, dissolution may occur. Vugs develop along and adjacent to the fractures and are more or less restricted to a narrow zone surrounding the fracture “channel.” This produces vuggy porosity intimately associated with fractures. Such vuggy fractures are often associated with unconformities in carbonates and the development of karst. Similar morphologies have also been observed in fine-grained cherts, like the Caballos Novaculite and in the hydrothermally altered granites at Bach Ho Field in offshore Vietnam. Vuggy fractures are very important in many of the largest carbonate reservoirs in the world, such as the Middle Eastern Asmari fields. Secondary porosity associated with these fractures can be quite large compared to more normal fracture porosity values (Weber and Bakker, 1981). In addition, due to the spherical to oblate shape of the vugs, this fracture-associated porosity will be relatively incompressible during reservoir drawdown.



Figure 1–50 Vuggy fracture in carbonate core. Courtesy of B.J. Ward, Jr. (Magnification 1.5x.)

Morphology/Permeability Summary

It can be seen from the preceding sections that the morphology of a fracture can influence the directional permeability of the rock mass around it. In general, an open fracture will dramatically increase reservoir permeability parallel to the fracture plane. However, because the fracture may be only one matrix pore or so wide, reservoir permeability across the open fracture will be identical to normal matrix permeability in that direction. A gouge-filled fracture will drastically reduce reservoir permeability across the fracture. Due to the relatively small cross-sectional area of the fill, however, permeability will be close to (or slightly less than) normal matrix permeability parallel to the fracture fill.

A slickensided fracture creates perhaps the largest permeability anisotropy of all the fracture morphologies because it increases permeability parallel to the fracture and decreases it across the fracture. The deformation along the walls of the fracture decreases reservoir permeability, as in gouge, across the fracture. However, due to the mismatch of smooth sliding surfaces, continuous interconnected pore space occurs along the fracture, which increases reservoir permeability parallel to the fracture. Vuggy fractures without diagenetic alteration of the vug walls should, as in open fractures, increase reservoir permeability parallel to the fracture and have little permeability effect across the fracture. Mixtures of the various morphologies can give unusual directional permeability effects and must be treated individually, often with 3-D whole-core data.

Relationship Between Fracture Morphology and Rock Strength and Ductility

In lieu of direct observation of fracture morphology in the subsurface, some predictability of morphology can be gained through the use of rock mechanics principles and laboratory mechanical testing.

There are many parameters that must affect fracture and fault plane morphology in the subsurface (depth, strain rate, stress level, rock composition, and texture). These combined factors control the strength and brittleness or ductility of rocks in the subsurface. It appears that fracture plane morphology is directly related to the strength and ductility of the rock materials involved. This discussion will be restricted to faults and fractures with like rock in contact across the plane, thus eliminating the problem of low sliding friction of unlike rocks in contact (Logan and others, 1972). It is possible that the potential transition from open to slickensided to gouge-filled fractures accompanies a reduction in strength and/or an increase in ductil-

ity in any one rock (fracture mineralization is, on the other hand, considered to be unrelated to the mechanical properties of the rocks involved). Two examples of a rock mechanics approach to defining and predicting fracture morphology using Nugget sandstones and a Devonian shale will be discussed next.

Nugget Sandstone

An example of the correlation between morphology and rock properties is shown in the Nugget sandstone from the Ryckman Creek Field. Observation of core from the Amoco Ryckman Creek WI Unit No. 6, Unita County, Wyoming, showed that certain zones in the Nugget sandstone contained only slickensided fractures while other zones contained only gouge-filled fractures. This distribution is observed to varying degrees in other Nugget cores, for example the Champlin 224 Amoco A. These zones display no significant differences in composition or environment of deposition, but do display an overall difference in porosity. In general, zones possessing gouge have relatively higher porosity while zones possessing slickensides have relatively lower porosity. It was postulated that this porosity difference caused a difference in strength and ductility of the rocks in these two zones. Such a strength and ductility variation could in turn be the cause of the observed difference in fracture morphology. To test this hypothesis, two zones of distinct fracture morphology were sampled in the Nugget sandstone core from Ryckman Creek WI Unit No. 6. The samples were unfractured pieces of rock taken from within zones that had fractures that were either all slickensided or all gouge-filled. The samples were then subjected to triaxial compression tests at 10,000 pounds per square inch (psi) (690 bars) confining pressure to simulate a possible depth of burial for the corresponding natural deformation.

The sample representing the slickensided zone whole core sample designation (IG) turned out to be 48 percent stronger in ultimate strength at 10,000 psi confining pressure than the sample representing the gouge-filled fracture zone (LS—Figure 1–51). In addition, sample designation (LS) was more ductile at this confining pressure than sample IG. This greater ductility of the gouge-zone sample is evidenced in the higher brittle-ductile transition of the slickenside-zone sample. The slickenside zone sample became ductile at about 45,000 psi (3,100 bars) confining pressure while the gouge zone sample became ductile at about 20,000 psi (1,380 bars).

These results support the hypothesis that within a constant lithology rock unit, weaker more ductile zones tend to develop more gouge-filled shear fractures than relatively stronger, more brittle zones, which tend to develop more slickensided fracture planes. In the Nugget sandstone from this core, the change in strength and ductility relevant to fracture morphology differ-

ences is dependent on porosity variations—higher porosity yields gouge-filled fractures and lower porosity yields slickensided fractures. These few tests cannot prove this relationship, but certainly do substantiate the original hypothesis of strength and ductility control of fracture morphology based on core observation.

Devonian Shale

A zonation of fracture morphology similar to that shown in the Nugget sandstone of Ryckman Creek is observed in a Devonian shale core from the Appalachian Basin (Columbia Gas Well No. 2-338, Wise County, West Virginia). In this core, which cuts the Pine Mountain Thrust Fault, open and slickensided tectonic fractures occur in discrete zones. By applying the same postulated relationship between fracture morphology and rock response in deformation (strength and ductility) it was assumed that the open fracture zones would be stronger and relatively more brittle than the slickensided zone rock. A few tests similar to the Nugget sandstone tests were performed on unfractured samples of each zone at 5,000 psi (345 bars) con-

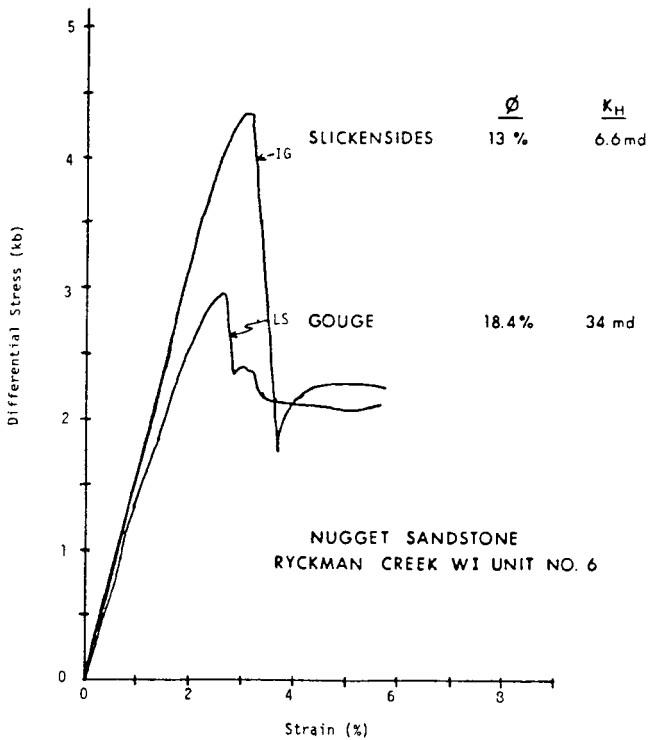


Figure 1-51 Stress-strain curves for samples deformed in triaxial compression tests at 690 bars pressure and ambient temperature and pore pressure.

fining pressure. Results of these tests do confirm the hypothesis in the form and relative position of the curves but do not show a quantitative difference great enough to be reported here.

In conclusion, these few tests cannot be considered proof of fracture morphology control by the mechanical properties of the rocks involved. However, they do confirm the postulated relationship that the samples were intended to test. While this is not statistical proof, these test results may be considered substantiation of observational or empirical conclusions.

Fracture Width and Permeability

Introduction

This section addresses the problem of quantifying the effect of natural fracture systems on reservoir quality and productivity. While exact quantification of a reservoir during exploration is very difficult, this section will discuss the determination of subsurface fracture width and permeability, and the geologic parameters necessary for an early understanding of how fractures can affect reservoir performance.

Equations for Fluid Flow

The first quantitative description of fluid flow through porous media was by Darcy (1856). In his general equation, derived for laminar, incompressible, single-phase, Newtonian flow in a continuous, homogeneous, porous material, Q , the flow rate is:

$$Q = KA \frac{dh}{dl} \quad (1-1)$$

where K = hydraulic conductivity
 A = cross-sectional area
 dh/dl = head gradient

Hubbert (1940) showed that:

$$K = k(\rho g/\mu) \quad (1-2)$$

and

$$k = Nd^2 \quad (1-3)$$

where k = intrinsic permeability
 ρ = fluid density
 g = acceleration of gravity
 μ = fluid viscosity
 N = a dimensionless coefficient characteristic of the medium
 d = average constitutive grain diameter of the rock.

The resultant dimensions of k are (length)².

It was later realized that Nd^2 could not be defined for flow along a fracture. Therefore, in an attempt to model fractures, the parallel-plate theory of flow was developed. Flow in this theory is assumed to occur between two smooth parallel plates separated by a distance, e . The basic equation as used by Huitt (1955), Lamb (1957), Snow (1965, 1968a, 1968b), and Sharp and others (1972) is:

$$\frac{Q}{A} = \frac{e^3}{12D} \frac{dh}{dl} \cdot \frac{\rho g}{\mu} \quad (1-4)$$

where D = fracture spacing, the average distance between parallel regularly spaced fractures

This equation is valid for single-phase, Newtonian, laminar flow in planar fractures with small overall changes in width e .

Each of these two quantitative relations (Equations 1-1 and 1-4) describes only a portion of the total flow through a fractured, porous rock; Darcy's equation for the intact-rock portion of the system, and the parallel-plate theory for the fractures. The next logical approach to determine the total flow was to combine these equations (Parsons, 1966):

$$k_{fr} = k_r + \frac{e^3 \cos^2 \alpha}{12D} \quad (1-5)$$

and

$$k_f = \frac{e^2}{12} \cdot \frac{\rho g}{\mu} \quad (1-6)$$

where k_{fr} = permeability of the fracture plus intact-rock system
 k_f = permeability of a fracture
 k_r = permeability of the intact-rock
 α = angle between the axis of the pressure gradient and the fracture planes

This equation assumes that flow is laminar between smooth, nonmoving, parallel plates, that fluid flow across any fracture/matrix surface does not alter the flow of either system, and that the fractures are homogeneous with respect to orientation, width, and spacing. The assumption of laminar flow in a subsurface reservoir is valid for low fluid-flow rates and low surface roughness relative to e . Increased subsurface flow velocities due to production may, however, cause turbulence. If so, much more complicated equations than those of Parsons (1966) are necessary to accurately calculate permeability. Such approaches, however, involved parameters often outside the realm of available geologic data. These will be discussed later.

Parsons' relationship (Equation 1–5) is simple but appears applicable for oil and gas movement in fractured rock. As stated in Witherspoon and Gale (1976, page 24):

Warren and Price (1961) concluded from core analysis and pressure test data that the most probable behavior of single phase flow is a heterogeneous system approaches that of an equivalent homogeneous system having a permeability equal to the geometric mean of the individual permeabilities. Parsons (1966) in studying idealized fracture systems has come to the same conclusion.

They also state that “a fractured reservoir is equivalent to a homogeneous porous medium if the dimensions of the matrix blocks are small (less than 1 m) and the matrix permeabilities are significant (greater than 0.01 millidarcies [md]).” This is further refined in Long and others (1982).

The concept of an equivalent porous media is an important one in modeling fractured reservoirs and deserves more discussion. As shown by the previous flow equations, fractured rock can be treated by various levels of complexity. In the simplest approach, the reservoir can be treated as a single porosity system with anisotropic Darcy flow (parallel plate flow if only fractures are present). More complex forms of modeling treat the fractured rock mass as a dual-porosity system, using Darcy flow for the porous matrix system and parallel plate flow for the porous fracture system. In both approaches, the continuity of the fracture system becomes important.

If at a given scale the fracture system is continuous and interconnected, it can be treated as an equivalent porous medium using either a single- or dual-porosity model. However, if the fracture system is distinctly discontinuous and noninterconnected at a given scale, it cannot be treated as an equivalent porous medium (Gale, 1982). If this is the case, the simplifying

assumptions of the equivalent porous media approach, such as symmetry of the permeability tensor, do not hold and the reservoir cannot be treated using statistical abstractions for the fracture system. The reservoir must then be modeled using discrete fractures mimicking the real size, orientation and position of the fractures present, a different task.

The question of continuous versus discrete modeling has been addressed by Long (Long and others, 1982; Long, 1983). This is an important distinction because in exploring for and engineering in subsurface fractured hydrocarbon reservoirs, we will never have sufficient fracture data to adequately apply discrete or discontinuous fracture modeling.

At best, in subsurface reservoirs we can abstract the real or predicted properties of the natural fracture system for use in a continuous, dual-porosity approach. If this equivalent porous media approach is invalid for theoretical reasons, our best-case modeling will be in error. This is why there is substantial debate in the literature about the applicability of equivalent porous media concepts to fractured reservoir modeling.

For natural subsurface reservoirs prior to production, Parsons (Equation 1–5) presents a reasonable approximation of total reservoir flow. As has been stated previously, this equation assumes that flow across the fracture/matrix surface does not alter the flow of either system. This is true for rocks of either high or near nonexistent matrix permeability. Stated another way, high matrix permeability would allow the matrix to respond individually to the overall pressure gradient rather than to the relative pressure sink of the fracture. If, on the other hand, the matrix permeability is so low as to become nonexistent, cross-flow once again becomes unimportant. In a rock of relatively low or intermediate matrix permeability, cross-flow becomes more important and Equation 1–5 becomes a poorer approximation of the total flow.

If a more accurate approximation is needed in a rock, more complex cross-flow equations such as those of Barenblatt and others (1960), Duguid (1973), Duguid and Lee (1977) and Evans (1982) should be used. Such equations are extremely complicated (Table 1–4) and difficult to work with, however. Most petroleum exploration geologists would either lack the expertise or the interest to pursue them. This, coupled with the fact that Jones (1975) has had good success with Parsons' (1966) equations in laboratory experiments on low-permeability carbonates, leads to the conclusion that Equation 1–5 is an apt semi-quantitative representation of fractured reservoir flow for use in exploration where data are often scarce.

Table 1-4
Fluid Flow In Fractured Porous Rock After
Barnblat, Zheltov, and Kochina (1960)

$$\frac{K_m}{\mu_w} \nabla^2 P_m = (C_m + \phi_m C_w) \frac{dP_m}{dt} + \frac{\omega}{\mu_w} (P_m - P_f)$$

$$\frac{K_f}{\mu_w} \nabla^2 P_f = (C_f + \phi_f C_w) \frac{dP_m}{dt} + \frac{-\omega}{\mu_w} (P_m - P_f)$$

Where: K = Permeability
 P = Pressure
 t = Time
 φ = Porosity
 C = Compressibility
 μ = Viscosity
 ω = Cross-Flow Coefficient
 (φ_m to φ_f)

Subscript m is Matrix
 f is Fracture
 w is Water

After Duguid (1973)

Continuity Eq. for Fluid in Pores

$$(1 - \phi_f) \phi_m C_w \frac{dP_m}{dt} + (1 - \phi_f) \phi_f C_w \frac{dP_f}{dt} + \frac{r}{\rho_w} + \nabla \cdot \langle \bar{v}_m \rangle = 0$$

Continuity Eq. For Fluid In Fractures

$$(1 - \phi_m) \phi_m C_w \frac{dP_m}{dt} + (1 - \phi_m) \phi_f C_w \frac{dP_f}{dt} - \frac{r}{\rho_w} + \nabla \cdot \langle v_{fm} \rangle = 0$$

Where:

$$\langle v_{fm} \rangle = \frac{K_f}{\mu_w} \left[\rho_w \frac{d \langle v_{fm} \rangle}{dt} + \nabla P_f \right], \langle \bar{v}_m \rangle = - \frac{\bar{K}_m}{M_w} \nabla^2 P_m$$

Written in Terms of

3 Components of
 Fluid Velocity in Fractures
 Pressure in Matrix
 Pressure in Fractures

Dilation of the Medium
 r = Cross-flow Term
 φ_m to φ_f

After Parsons (1966)

$$K_{fm} = K_m + \frac{e_1^3 \cos A_1}{12 D_1} + \dots + \frac{e_n^3 \cos A_n}{12 D_n}$$

$$K_f = \frac{e^2}{12} \cdot \frac{\rho_w g}{\mu_w}$$

For 1 → n
Fracture Sets

Where K = Permeability
 e = Fracture Width
 D = Fracture Spacing
 A = Angle Between Axis of Pressure Gradient and Fracture Planes
 ρ = Density
 μ = Viscosity
 g = Acc. Gravity

Subscripts:

m is Matrix
 f is Fracture
 fm is Matrix and Fracture Combined
 w is Water (Fluid)

Parsons (1966) also showed that Equation 1–5 could be expanded to incorporate multiple fracture sets:

$$k_{fr} = k_r + a \cos^2 \alpha + b \cos^2 \beta + \dots \quad (1-7)$$

where

$$a = \frac{e_1^3}{12 D_1} \text{ for Fracture Set 1}$$

and

$$b = \frac{e_2^3}{12 D_2} \text{ Fracture Set 2} \quad (1-8)$$

Each of these additional terms refers to a separate parallel fracture set of constant spacing (D_n) and opening (e_n). As in Equation 1–5, $\cos^2 \alpha$, $\cos^2 \beta$, etc., refers to the angle between each parallel fracture set and the pressure

gradient. Equation 1-7, then, can deal with a number of intersecting fracture sets, a geologically prevalent situation. In fact, this ability to deal with multiple fracture sets in a permeable matrix overshadows any imprecision that may result from using such a simple and direct equation.

The Direct Effect of Fractures on Fluid Flow

Contrary to popular belief, reservoir fractures are not always high-permeability channels, but often they act to impede or as barriers to fluid flow. The effect of individual fractures on permeability is dependent on the character and morphology of the fracture plane itself (Figure 1-52). It is often difficult to determine if natural fractures play an important role in fluid production in a given well. There are, however, several clues that can give the geologist or engineer suspicion of fracture control. All include core data. Several indicators are:

- Direct observation of oil-stained or “bleeding” fracture planes in core samples can indicate fracture control. Often, evidence of oil movement along fracture planes is prevalent (Figure 1-53).
- High flow test permeability from zones of relatively low core-derived plug permeability can indicate flow control by natural fractures. An example of this is found in Amoco Norway 2/8-10 well, Valhall Field, Norwegian North Sea. Here, a flow test permeability of greater than 100 md was recovered from a zone with corresponding atmospheric pressure plug permeability of less than 1 md, indicating fracture control of reservoir flow.
- Fluid flow control can also be revealed by three-directional wholecore permeability analysis (K_{hmax} , K_{h90° , K_v). A good example of such indication is found in the Nugget sandstone from the Champlin 224 well, Summit County, Wyoming (Figures 1-54, 1-55, and 1-56).

In a vertical versus horizontal permeability plot, most well-bedded rocks will plot below the line of equal permeability (isotropy) emphasizing preferential flow parallel to bedding. However, if substantial scatter of points exists both below and above the line of isotropy (Figure 1-54), fracture control within the reservoir should be suspected. In the same core data used in Figure 1-54, the role of fractures can be exemplified by first illustrating the effect of the bedding present. This can be done by highlighting those samples which, according to the testing laboratory report, show little or no

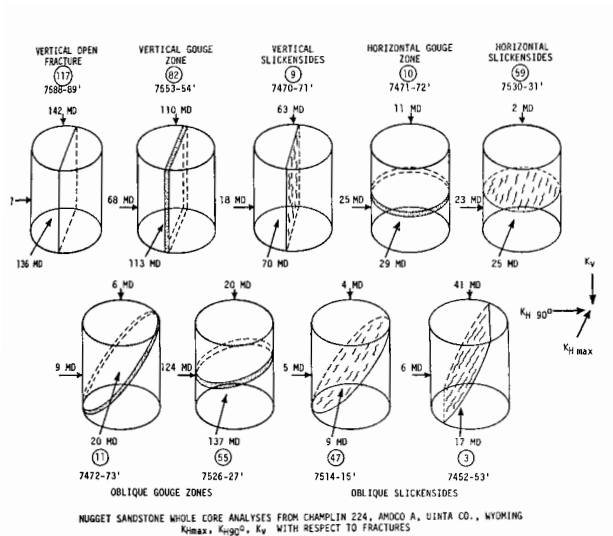


Figure 1-52 Direct effect of various fracture morphologies on whole-core permeability.

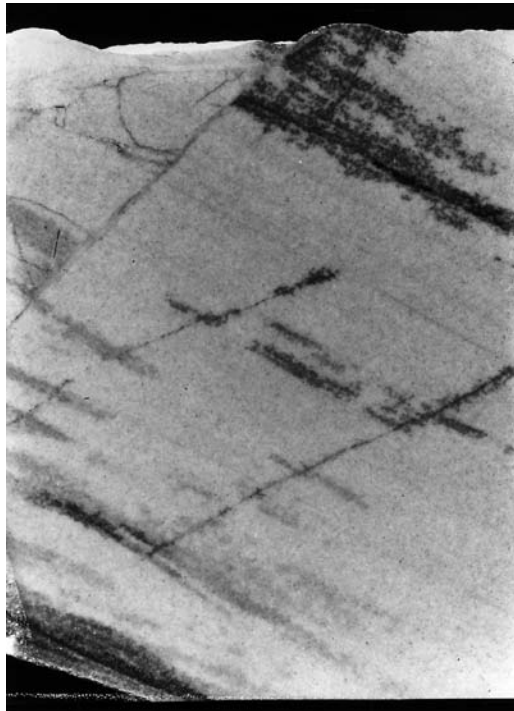


Figure 1-53 Oil staining along open fractures in Nugget sandstone core from American Quasar 3-1 UPRR, 10,159 ft. (Magnification 1.5x.)

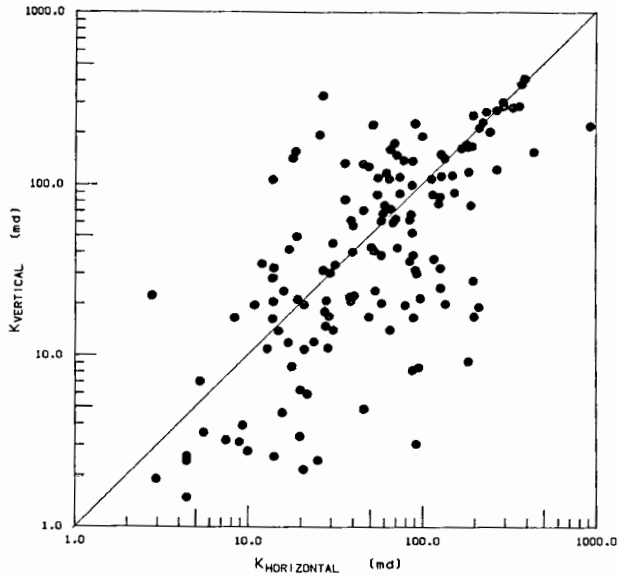


Figure 1-54 Vertical versus horizontal whole-core permeability for Nugget sandstone samples, Champlin 224 Well, Uinta County, Wyoming. Straight line indicates equal vertical and horizontal permeability.

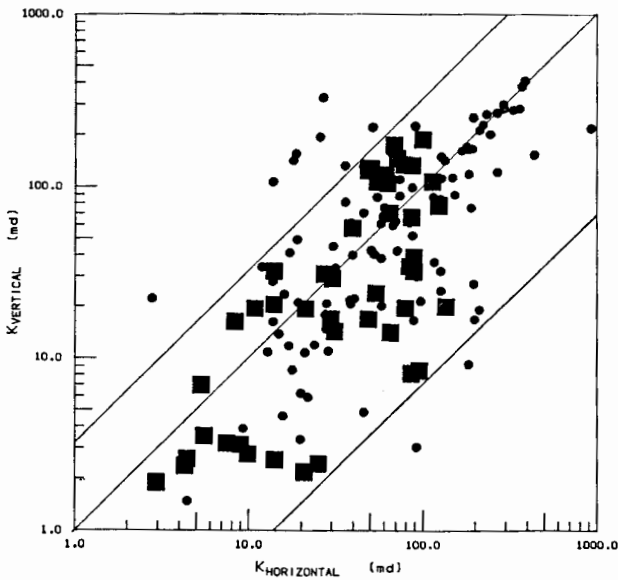


Figure 1-55 Replot of Figure 1-54 with all samples not listed as having fractures highlighted as squares.

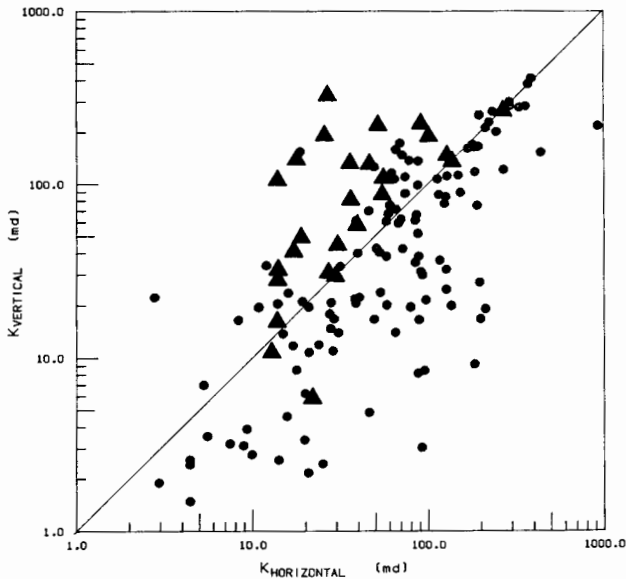


Figure 1-56 Replot of Figure 1-54 with all samples containing unambiguous vertical open and gouge-filled fractures highlighted as triangles.

visible fracturing (Figure 1-55). This diagram then gives the range of variability for nonfractured samples (all samples outside and some samples inside this field are controlled by fractures). Significant fracture variability must, then, be viewed in light of the “normal” bedding data distribution.

This core contains many fractures (gouge-filled, slickensided, and open), which are oriented oblique to bedding. The effect of these on permeability in 3-D is difficult to ascertain. Horizontal fracture effects can be obscured by bedding effects. A vertical fracture or gouge zone, however, should have a distinct effect, by moving data points above the isotropic permeability line (Figure 1-54). These effects can be illustrated by replotting the previous diagram highlighting all those samples, which have obvious and unambiguous vertical fractures or gouge zones (Figure 1-56). Both of these features would decrease horizontal permeability relative to vertical (vertical gouge decreases horizontal permeability while vertical open fractures increase the vertical permeability). Such anomalously high data points can be indicative of fracture control in a reservoir and document anisotropic permeability.

Fracture Permeability Versus Confining Pressure

In order for Equation 1-5 to simulate subsurface reservoir flow, estimation of k_r and k_f or e at depth must be made. These estimations are gener-

ally made by subjecting a nonporous, fractured laboratory rock sample to external loads (simulating depth of burial) as permeability is being measured (Summers and others, 1978; and Engelder and Scholz, 1981). For porous rocks, these tests can be run on unfractured rock (k_r) and fractured rock (k_{fr}). Fracture permeability (k_f) can then be calculated using Equations 1-5 and 1-6 (Figures 1-57 and 1-58). Once k_f and k_r are known as a function of depth, the total reservoir permeability (k_t) can be calculated for any combination of reservoir fracture systems in that rock (Equation 1-7). Usually in such tests a hydrostatic confining pressure is applied to the outside of a jacketed sample. This does not, however, simulate natural subsurface conditions where the vertical and horizontal components of burial stress are not equal ($\sigma_v \neq \sigma_h$). A detailed discussion of this point will be given later in this chapter. Theoretical analyses of fracture permeability reduction with stress have been presented in Gangi (1978) and Walsh (1981).

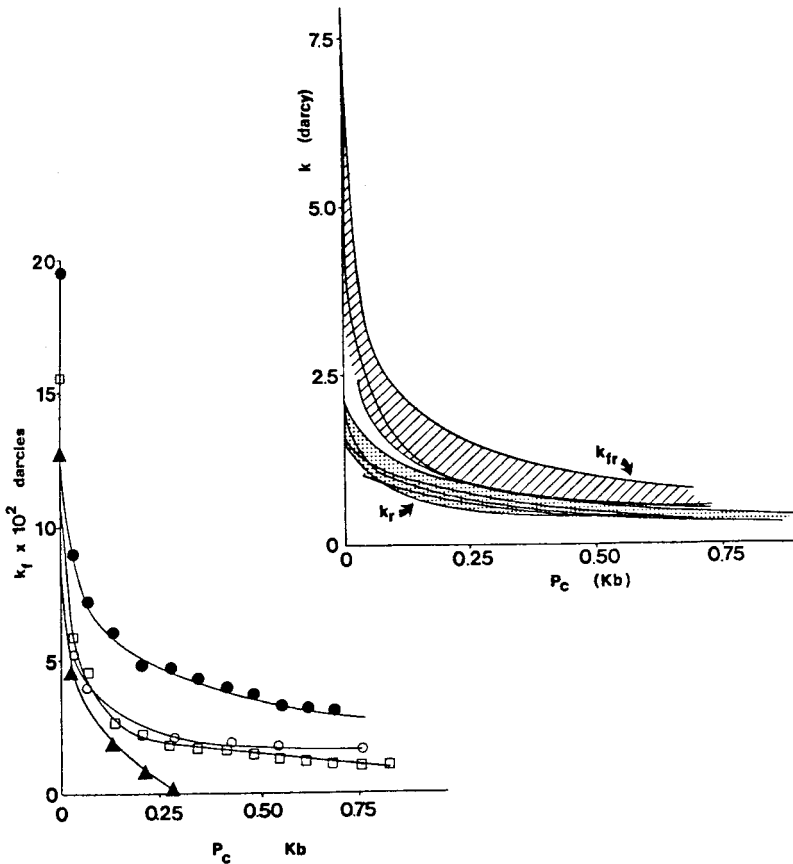


Figure 1-57 Matrix (k_r) and fracture (k_f) and total (k_{fr}) permeability versus hydrostatic confining pressure (P_c) for Jurassic Navajo sandstone samples. From Nelson (1975), courtesy of AAPG.

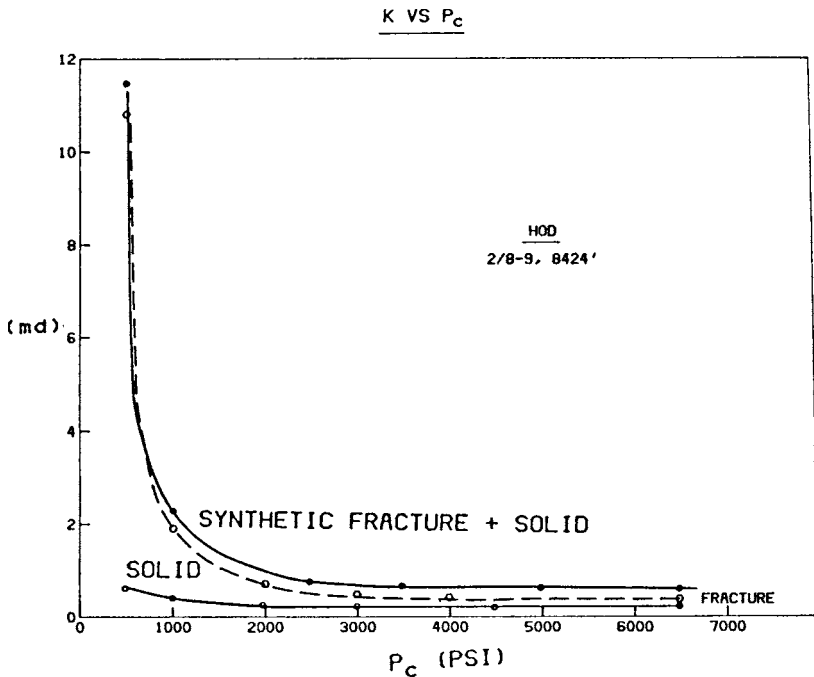


Figure 1-58 Permeability versus hydrostatic confining pressure for sample of Cretaceous North Sea chalks, Valhall Field, offshore Norway.

Fracture Width versus Confining Pressure

Subsurface fracture permeability can be approximated from laboratory data in a manner discussed in the last section or by complex testing of large in situ fractured blocks (Swolfs and others, 1981). Using the data documenting fracture permeability as a function of stress state or simulated depth from laboratory or in situ measurements, we can calculate an average effective fracture width necessary to give each permeability value from Parsons' equation (Equation 1-5). The appropriate permeability value is input to this equation along with the angle (α) between the real or artificial fracture plane and the pressure gradient, and the value for fracture spacing in the sample (D). If multiple parallel fractures are used, the average distance between fractures is input for D . If one fracture parallel to the cylinder axis is used, the assumption of an image well source from hydrology is applied (Walton, 1970), and one sample diameter is input for D .

With these input values and Equation 1-5, average effective fracture width or hydraulic aperture (e) can be approximated (Figures 1-59 and 1-60). The hydraulic aperture is somewhat different from the mechanical width, which is highly variable along the fractures. This distribution of me-

chanical width is difficult to measure on natural fractures and has been investigated as a function of stress by Sharp and others (1972). Other investigations have looked at changes in total area of contact along the fracture as a function of stress (Gale, 1982). The number derived from the fracture permeability measurement mentioned above does not directly address the mechanical width distribution or contact area, but better represents the overall hydraulic effect of its distribution in fluid flow.

In this manner, one can derive a suite of hydraulic fracture width versus stress curves representative of various lithologies or grain sizes and from them simplify prediction of fracture permeability and fracture porosity in the subsurface (see the section on "Field-Lab Determination" later in this chapter).

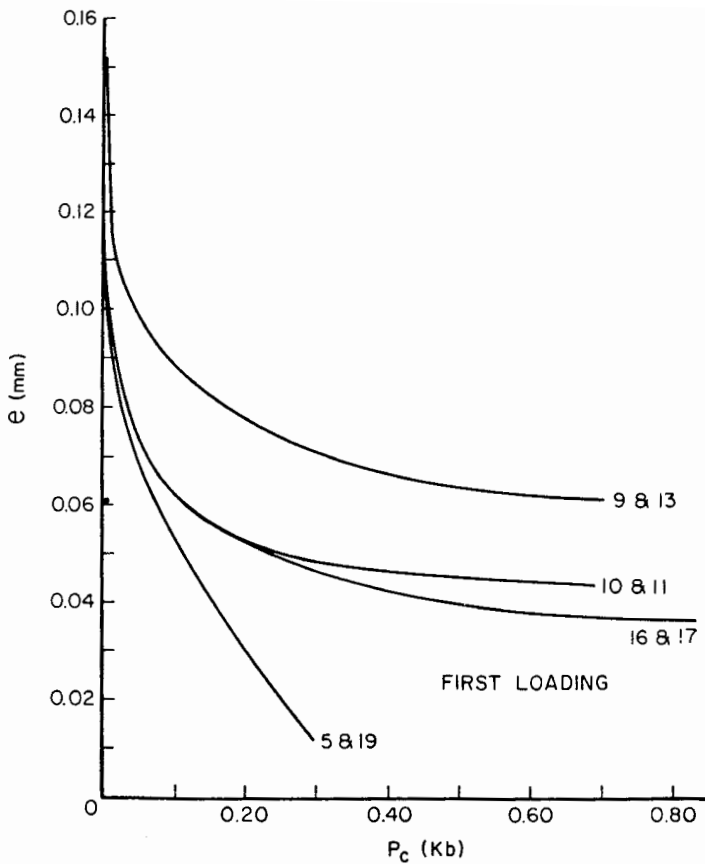


Figure 1-59 Calculate fracture width (e) versus hydrostatic confining pressure (P_c) plot for Nugget sandstone samples. From Nelson (1976), courtesy of AAPG.

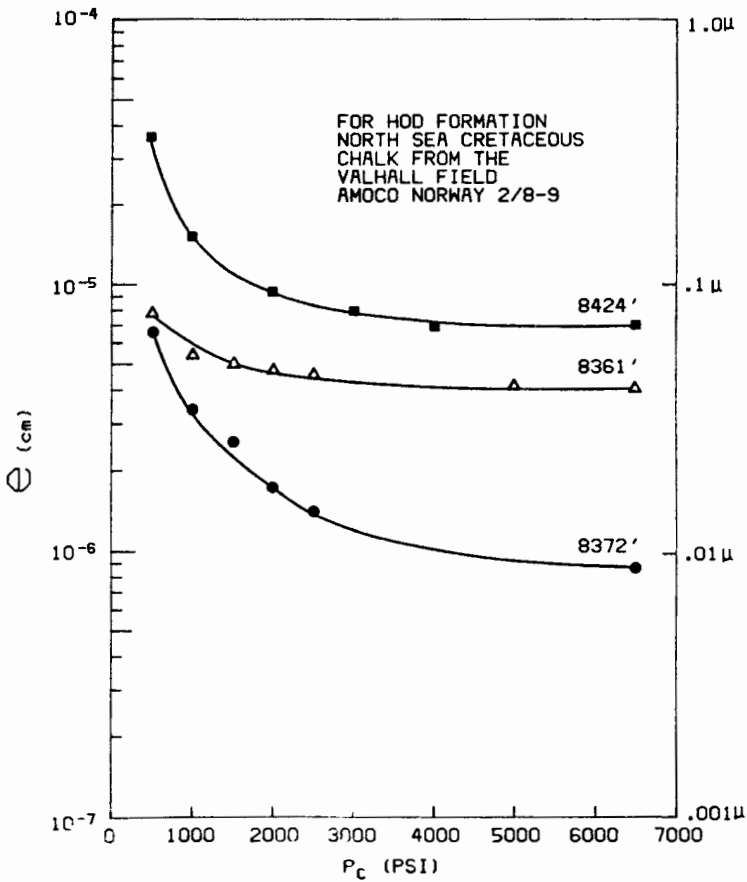


Figure 1-60 Calculated fracture width (e) versus hydrostatic confining pressure (P_c) plot for several North Sea chalk samples.

Fracture Width Distributions in Nature and Experiments

Several representative, published values for shallowly buried natural fractures indicate that their width is quite small (Table 1-5). These values range from 1.0×10^{-3} cm up to 5.0×10^{-1} cm, and span a little over one order of magnitude. As stated previously, however, these represent values for shallow depths (several hundred meters). Subsurface fracture widths at modern operating reservoir depths (5,000-20,000 ft.) are significantly smaller than this.

Natural or simulated fractures in reservoir rock subjected to external load in the laboratory indicate how these values may change at depth or during reservoir depletion. From a nonstatistically significant number of such experiments, gross values or “orders of magnitude” widths can be calculated for various rock types. Preliminary results tend to indicate a segregation by constitutive grain size of the host rock (Table 1–6).

Table 1–5
Some Published Natural Fracture Widths

Noorishad and others (1971)	3.0×10^{-1} cm
Ohnishi and Goodman (1974)	$1.3\text{--}2.5 \times 10^{-1}$ cm
Sharp and others (1972)	$1.0\text{--}5.0 \times 10^{-2}$ cm
Snow (1968a)	5.0×10^{-1} cm
Snow (1968b)	$0.5\text{--}1.5 \times 10^{-2}$ cm
van Golf-Racht (1982)	$1.0\text{--}4.0 \times 10^{-3}$ cm
Wilson and Witherspoon (1970)	2.5×10^{-2} cm (mean)

Table 1–6
Experimental Fracture Widths at 10,000 ft. (Simulated Depth)

(Number of Samples Not Statistically Significant)

Medium to Coarse Grained Sandstone	10^{-2} cm
Fine to Medium Sandstone and Crystalline Carbonates	10^{-1} cm
Siltstones	10^{-4} cm
Shales (Textural Term)	10^{-5} cm
Chalks (Compositional and Textural Term)	$10^{-1}\text{--}10^{-6}$ cm

It is evident from these low width numbers why it would be extremely difficult to detect or quantify natural fractures by standard borehole logging methods in the subsurface. Most wellbore techniques rely heavily on fracture enlargement by hole, working to allow for detection.

Natural subsurface fractures are certainly narrow and hard to measure. However, as Wilson and Witherspoon (1970) point out, the characterization problem is even more difficult because the fracture system normally has a log-normal frequency distribution with respect to fracture width (Figure 1–61). Skewed log-normal distributions of width present a problem in calculating representative values, because the mean, median, and mode values

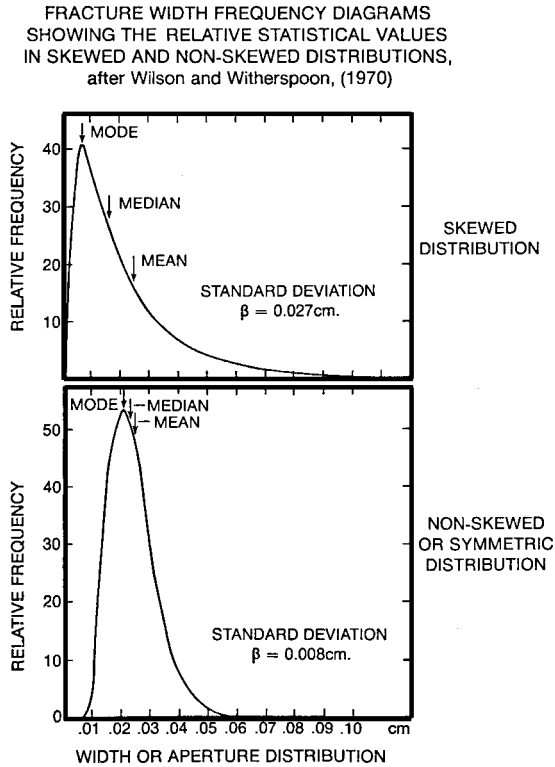


Figure 1-61 Hypothetical natural fracture frequency diagrams, after Wilson and Witherspoon (1970).

separate. Such skewed distributions are important because the few large widths present can dominate fracture system permeability due to the fact that fracture width is a cubed term in fracture permeability equations.

Fracture Spacing

Introduction

Along with fracture width, fracture spacing is the other important quantitative fracture system parameter necessary to predict fracture porosity and permeability in a reservoir. Unlike subsurface fracture width, which is difficult to observe directly, fracture spacing can be directly quantified and also does not change when the reservoir is perturbed. However, while fracture spacing can be directly observed in outcrop and mines, difficulties in quantification often arise due to the small size of our subsurface sampling methods (core and wellbore observations) with respect to the fracture spac-

ing or matrix block size (see the section on “Scale Versus Nonscale Dependency”). In addition, natural fracture systems are often of such a complicated cross-cutting fabric as to make determination of an average spacing difficult if not ill-defined.

Many parameters have been used in the literature in an attempt to quantify the abundance of fractures in a reservoir. Terms such as *fracture intensity*, *fracture density*, *fracture index*, *fracture surface area*, *fracture intersection density*, and *fracture spacing* have all been used with the exact definitions of each varying from author to author. Several usages involve volumetric terms while most are in actuality vector terms. In this text, fracture spacing is defined as the average distance between regularly spaced fractures measured perpendicular to a parallel set of fractures of a given orientation (Parsons, 1966). The terms can be applied to numerous parallel fracture sets of various orientations within the reservoir. Each spacing term will, therefore, be a vector (direction and magnitude) representing an average distance along the direction normal to the fracture planes (see the earlier section, “Equations for Fluid Flow”). This definition of fracture spacing is used here primarily because it is the format most frequently used in theoretical fracture permeability equations (e.g., Lamb, 1957).

Effect of Variation in Fracture Spacing

Variation in fracture spacing can have a dramatic effect on both fracture porosity and permeability (Figures 1–62 and 1–63). The combined effect of both fracture width and spacing on these reservoir parameters is shown in Figures 1–62 and 1–63. A good qualitative feeling for the effect of outcrop or core observations of fracture spacing at an assumed fracture width, or vice versa, can be derived from these diagrams.

Techniques for Calculating Fracture Spacing

In simple fracture networks of regular, closely spaced fractures, fracture spacing is easily calculated in core or outcrop provided the sampling area or volume is large with respect to fracture spacing. This is accomplished by counting the number of fractures encountered along a line of some given length perpendicular to the fracture set of interest, for each of the fracture sets present and dividing the length of measurement line.

In more complex fracture systems, workers have gone to similar determinations along lines in specific directions. This author has often used two perpendicular measurement directions with one parallel to bedding strike

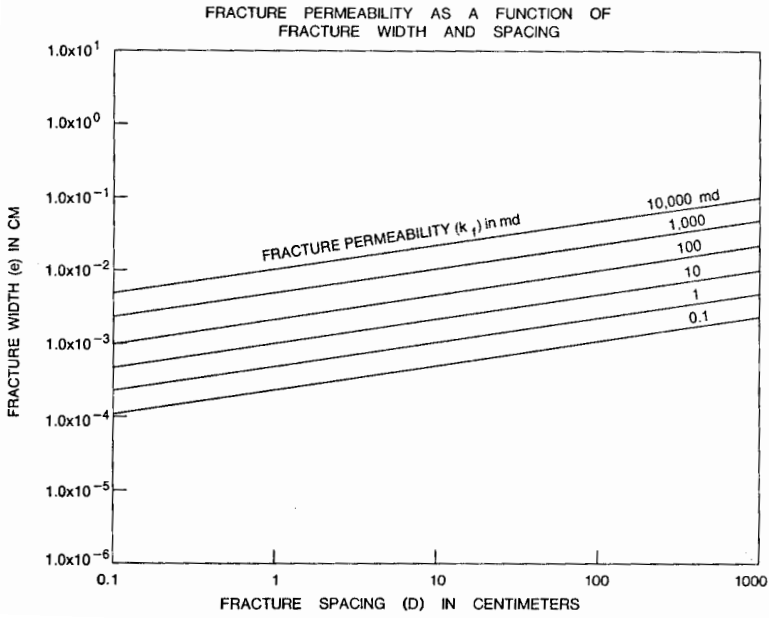


Figure 1-62 Fracture permeability as a function of fracture width and fracture spacing.

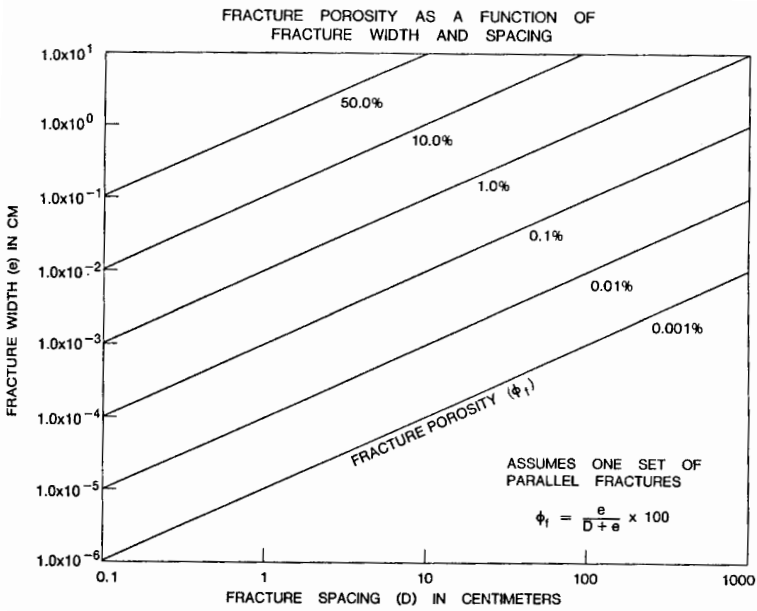


Figure 1-63 Fracture porosity as a function of fracture width and fracture spacing.

and one parallel to bedding dip. Others have tried to reconstruct the entire vector/spacing distribution (at least in a plane) by measuring along three specific directions (120° apart) and statistically manipulating the data into a full 360° distribution. Hudson and Priest (1983) present an excellent statistical technique for determining the entire 2-D array of spacing vectors present in a rock. Narr and Lerche (1984) present a statistical/geometric method for accurately depicting fracture spacing from core data.

FRACTURE AND MATRIX POROSITY COMMUNICATION

Once fracture origin and the reservoir properties of the fracture and matrix systems have been determined, fracture and matrix porosity interaction should be addressed.

Introduction

Any reservoir in which fractures play a significant role in production and storage of reserves must be treated as a two-porosity system—one system in the matrix and one in the fractures.

Reservoir interpretation that does not recognize the potential for reduced recovery because of an adverse interaction between the two porosity systems will lead to an incorrect estimation of reserves and recovery factors. These complexities in fractured reservoirs make reliable early estimations of reserves or recovery factors more complex than in conventional reservoirs. Early warning of fracture/matrix interaction problems can be gained by thin-section observation of fracture planes and by analysis of whole-core directional permeabilities selected to illustrate in a relative sense the interaction and flow rates between matrix and fractures.

In many cases, flow communication or interaction between these two systems may be good. However, in other reservoirs such communication may be inhibited by mineralization within or deformation along the fracture plane surfaces (see the earlier section on “Fracture Morphology”). For example, in a fractured reservoir where: (1) deformation is accomplished primarily by extension fracturing (as in regional fractures, Stearns and Friedman, 1972), and (2) diagenetic mineralization is minimal; fracture/matrix interaction or cross-flow is probably good. In such a system, both porosity systems can respond to the overall fluid pressure gradient as well as directly to each other.

Poor fracture/matrix porosity interaction may occur either because of deformation along, or mineralization within, the fracture. Such lack of communication may or may not be a problem in production, depending on the petrophysical properties of the two systems. For instance, poor communication between a moderately porous, permeable fracture system and a low-porosity, high-water saturation matrix would not be a problem. Such a prospect would be judged on the reservoir properties of the fracture system alone.

On the other hand, poor communication between a highly permeable fracture system and a matrix system with a large volume of potentially flowable hydrocarbons presents a significant production and evaluation problem. If the presence of an impervious lining to the fractures is not recognized, it will result in an erroneous estimate of the matrix contribution into the fracture system and then to the wellbore. The properties of a two-porosity system and some misconceptions and nonparallelisms are discussed next.

Basics of Fracture and Matrix Porosity

Fracture porosity, like matrix porosity, is the percentage of a particular void volume in a rock mass compared to its total volume. It accounts for only those voids occurring between the walls of fractures. Matrix porosity, on the other hand, accounts for all voids within a rock other than those within fractures. Thus, matrix porosity includes voids of various origin—vuggy porosity, intergranular porosity, dissolution porosity, etc. The two basic relationships used to calculate fracture porosity and matrix porosity are presented in Equations 1–10 and 1–11.

$$\phi = \left(\frac{V_p}{V_b} \right) \times 100 \quad (1-10)$$

$$\phi_f = \left(\frac{e}{D + e} \right) \times 100 \quad (1-11)$$

where ϕ_r = matrix porosity
 ϕ_f = fracture porosity
 V_p = volume of pores (other than fractures)
 V_b = bulk volume
 D = average spacing between parallel fractures
 e = average effective width of fractures

A brief analysis of these equations leads to the interesting conclusion that fracture porosity (ϕ_f) is very scale-dependent while matrix porosity (ϕ_r) as we use it is not.* For clarification of this point, consider an outcrop of rock in which we will attempt to measure fracture and matrix porosity (Figure 1-64a and b). If we assume that the fractures shown are regularly spaced and that the matrix is homogeneous, the size and position of our porosity calculation element affects ϕ_f to a much greater degree than ϕ_r .

Scale Versus Nonscale Dependency

A small element of rock (1 cm²) located between fractures (Figure 1-64a) would calculate normal ϕ_r and no ϕ_f . If this same element were positioned over a fracture (Figure 1-64b), near normal ϕ_r would be calculated while ϕ_f would be quite large. As the measurement element grows larger, ϕ_r remains nearly constant while more fractures are encountered and ϕ_f approaches a smaller but more truly representative number. This figure illustrates the fact that ϕ_f , by having a spacing term built into its calculation, is scale-dependent and as such presents a more severe sampling problem in its calculation than does matrix porosity. In fracture porosity calculations, we must use a large enough sampling element to encounter several regularly spaced fractures to get an accurate measurement. It appears that we need an area encompassing four to five regularly spaced fractures to accurately assess fracture porosity.

Porosity-Permeability Relationships

A second way that fracture porosity and matrix porosity are different is in their effect on permeability (Figure 1-65). While fracture porosity is usually slight, it is highly interconnected and does, therefore, have a much more dramatic effect on permeability than does matrix porosity. Relatively small increases in fracture porosity cause immense changes in permeability parallel to the fracture (Figure 1-63). Fracture porosity and matrix porosity thus should not be given equal significance in reservoir flow predictions.

*Matrix porosity actually is scale-dependent below the size of individual grains (unit cell equals several pores and grains), while fracture porosity is scale-dependent below the size of the fracture spacing (unit cell equals $D + e$)

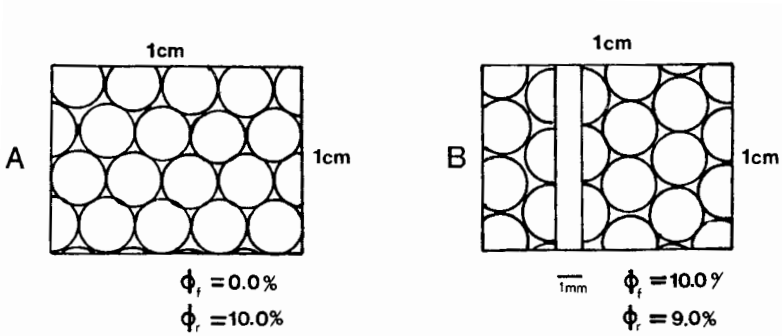
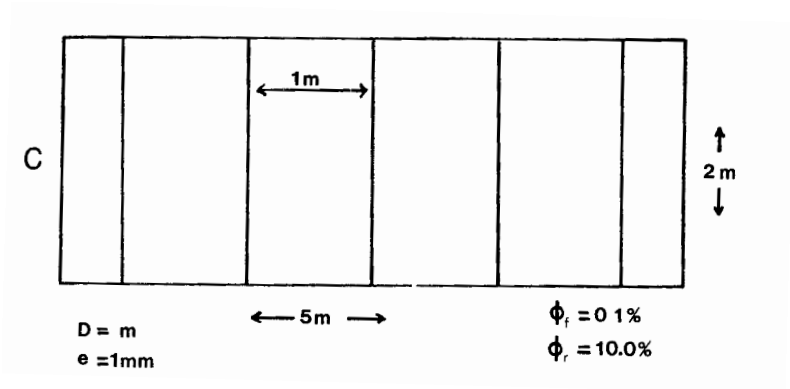


Figure 1-64a and b Fracture porosity determinations are dependent on the size and positioning of the sample, while matrix porosity determinations are not.

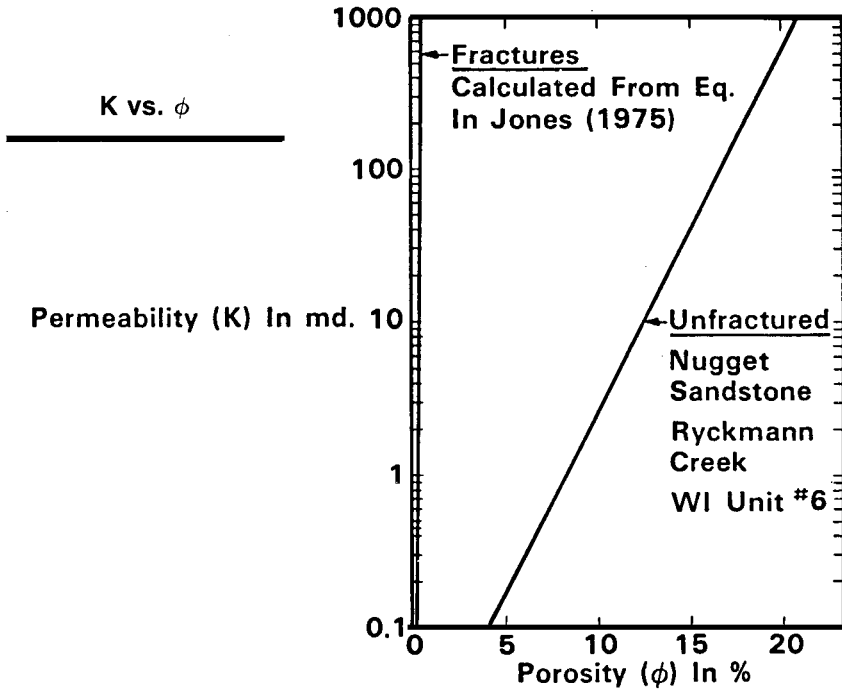


Figure 1-65 Permeability versus porosity showing the relative positions of matrix and fracture curves.

Compressibility Differences

A third way that ϕ_f and ϕ_r differ is in their compressibility. In general, fractures are much lower in porosity and much higher in permeability than the matrix in which they reside. However, as external stress increases (below the yield point) due to either increasing depth of burial or reservoir depletion, fractures compress or reduce in porosity and permeability much more readily than the matrix (Figure 1-66a and b). This difference in behavior is most dramatic in relatively brittle rocks and less dramatic in rocks with a ductile matrix, where the compressibilities of the two phases are more nearly the same.

Magnitude Differences

Fracture porosity is generally a small number compared to “normal” matrix porosity. Here are some rules-of-thumb for judging the magnitude of macroscopic fracture porosity (Table 1-7). Most good fractured reservoirs

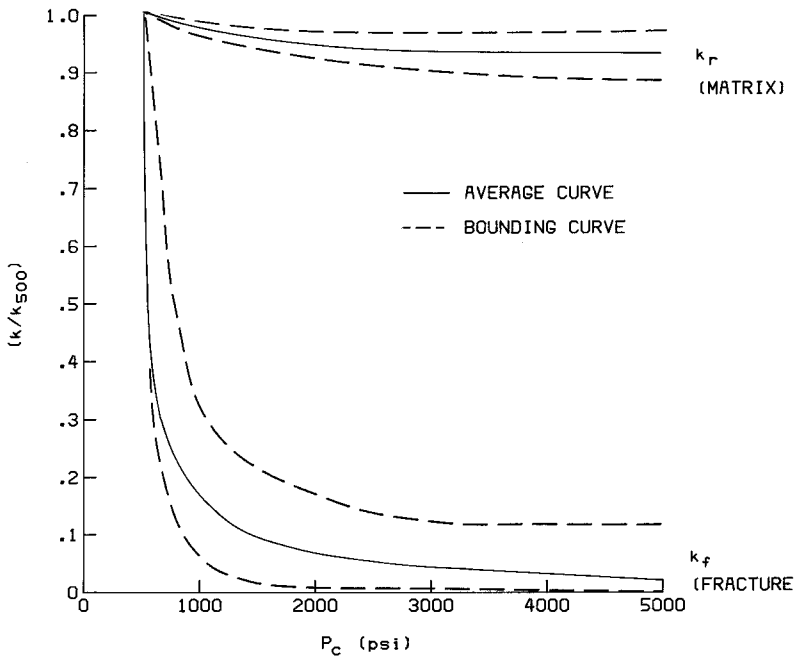
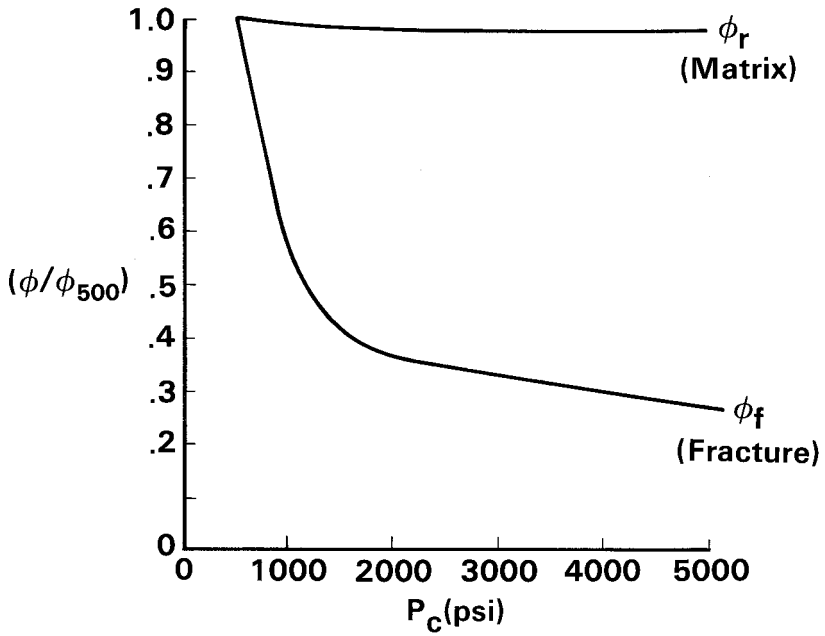


Figure 1-66 a and b Normalized porosity (ϕ/ϕ_{500}) and permeability (k/k_{500}) are shown as a function of hydrostatic confining pressure in tests on rock matrix and rock fractures.

possess less than 1 percent fracture porosity. Any large-scale subsurface fracture system of around 2 percent or greater fracture porosity has undergone dissolution along the fracture planes as in many limestones to attain sufficient void space or has unusually close fracture spacing as in some cherts. These numbers do not include grain-scale cracking, which can give larger porosities, but are usually ineffective to large-scale fluid flow. As was pointed out earlier, fracture porosity is a difficult number to calculate. Once it is calculated, however, its significance to production is still not always immediately clear.

Table 1-7
Guidelines for Fracture Porosity

Always Less Than	2%
Excluding Small Zones Less Than	1%
General Less Than	0.5%
Vuggy Fractures	O-Large

Fracture porosity is usually low but can be important in specific reservoirs with large vertical and areal extent.

Use of Fracture Volume Instead of Fracture Porosity in Evaluation

Fracture porosity is, then, a small number. However, this small porosity value can be important to production in that ϕ_f is very effective. When applied over large drainage areas and thick reservoirs, ϕ_f can amount to a large reservoir volume. In addition, it has a recovery factor generally assumed to be greater than that of the matrix, in part due to the assumed low water saturation in smooth, open fractures. The potential for substantial reservoir volume residing in fracture systems even of 1 percent fracture porosity is high, depending on reservoir thickness and drainage area (Figure 1-67). This volume can be quite large, as in some of the larger Middle East fields where drainage areas are large leading to well spacings in excess of 1,000 acres. It is probably best to not use the term “fracture porosity” in early evaluations. It could be misconstrued as “matrix porosity.” Because the two are so drastically different, it is best to calculate and use fracture-volume-obtainable-per-well rather than fracture porosity.

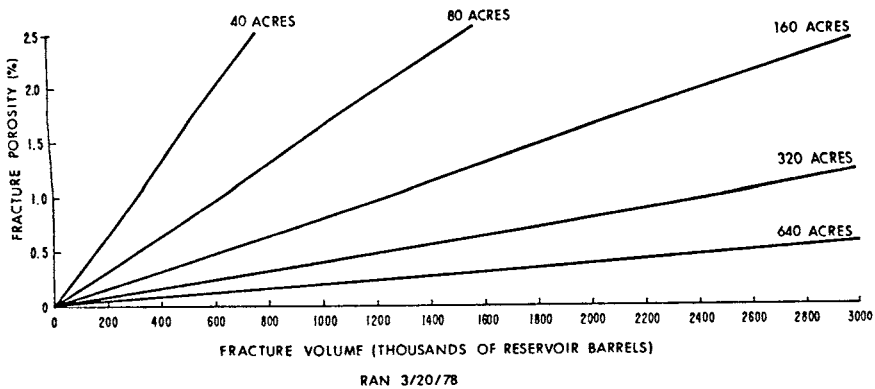


Figure 1-67 Fracture volume as a function of fracture porosity and drainage area.

The Significance of Fracture Porosity

The significance or importance of ϕ_f values in reservoir evaluation and potential production problems depends on the type of fractured reservoir encountered. In a fractured reservoir, where the fracture system provides the essential porosity and permeability to the reservoir, an early calculation of ϕ_f or fracture volume attainable per well is of paramount importance. We must have an accurate knowledge of this volume as early as possible to evaluate the reservoir properly, and this estimation must be updated continuously through the early production history with as many methods of calculation as the data permit. The significance of a ϕ_f calculation in fractured reservoirs, where the fracture system provides only permeability of various amounts to the reservoir and the matrix supplies the porosity or storage volume, is much less if not negligible. In those reservoir types, the ϕ_r , which is usually several orders of magnitude greater than ϕ_f , so overshadows the volume in the fractures as to make an accurate, early calculation of ϕ_f unimportant. What is important is to determine the reservoir type as early as possible.

Fracture Porosity Estimations

Fracture porosity is a very difficult number to calculate. Estimates can be made by:

1. Core analysis
2. k_f/ϕ_f relationship
3. Field determinations
4. Logs
5. Multiple well tests

These methods usually give slightly different values of ϕ_f because they are based on slightly different data. It is, therefore, important to use as many different methods to calculate ϕ_f as possible with the data available in order to determine the range of possible values in the reservoir.

Core Analysis

Whole core analysis samples a relatively large rock volume (3- to 5-in. diameter sample) compared to plug analysis (3/4-in. diameter sample) and, therefore, often depicts a measure of fracture porosity unattainable by standard plug analysis. Using a Tuscarora sandstone example (Table 1–8) the fracture porosity exists as incompletely mineralized, partly dissolved fractures. By subtracting the consistently low matrix porosity (taken from the average of the unfractured samples) from the whole core samples containing fractures, an estimate of fracture porosity is made. This method of calculating ϕ_f is, of course, fraught with scale and sampling problems. The fractures in this core are vertical (parallel to the core axis). The core diameter is 4 in. At any spacing of parallel fractures greater than 4 in., the sampling becomes a “hit-or-miss” problem. If fractures were spaced more than 4 in. apart, hitting one with the 4-in. core would give an anomalously high ϕ_f compared to that portion of the reservoir. Conversely, not intersecting fractures with the core would give an anomalously low fracture porosity ($\phi_f = 0$ percent). Because of these and other sampling problems, core analysis—though the most direct procedure—can often give the most misleading value for fracture porosity. However, this is often the first method available for the analysis of ϕ_f and should be performed as soon in evaluation as possible.

Fracture Porosity-Fracture Permeability Relationship

Another method used in fracture porosity calculations involves the relationship between fracture porosity and fracture permeability (Figure 1–68). In the Valhall Field in the Norwegian sector of the North Sea, a reservoir permeability of 66 md was calculated from a flow test in the same zone from which a core was taken. By standard analysis of the core, the matrix

Table 1–8
Average Porosity from Whole-Core Analysis (Arithmetic Average)

Tuscarora-Amoco #1 Texas-Gulf

Assumes < 0.5% = 0.0%

All Core	= 0.9%
Best Zone	= 1.4%
Unfractured Rock	= 0.6%
All Core ϕ_f	= 0.4%
Best Zone ϕ_f	= 0.9%
Highest ϕ_f	= 2.9%

permeability was so low (much less than 1 md) that all flow measured in the test must have been from the natural fracture system. Observation of the core material indicated a fracture spacing from this same zone of about 0.5 cm (a very intense fracture system). Therefore, by knowing the spacing of the fracture system and the total permeability of the same fracture system, fracture porosity (ϕ_f) could be approximated (Jones, 1975). By this method, a ϕ_f of 0.3 to 0.4 % was calculated for that particular portion of the reservoir.

This method of calculating fracture porosity from fracture permeability is quite elegant and should give fairly accurate values. However, the number of situations where this can be used are relatively few. Three conditions must be met:

1. A flow test permeability must have been calculated for the same zone from which a core was pulled.
2. Core analysis must show that the rock matrix (ϕ_r) contributed negligible flow to the flow test.
3. A good estimate of fracture spacing must be obtainable from the core.

If these conditions are met, the $\phi_f - k_f$ method of ϕ_f calculation can be used.

Field-Lab Determination

Because fractures are planar entities, both ϕ_f and k_f are directly dependent on the width and spacing of the fractures (e).

$$\phi_f = \left(\frac{e}{D+e} \right) \times 100 \quad (1-12)$$

$$k_f = \left(\frac{e^3}{12D} \right) \quad (1-13)$$

where D = average fracture spacing and where the fracture plane is parallel to the fluid pressure gradient

In the laboratory, we can measure the permeability of fractured and unfractured companion samples of reservoir rock under confining pressure. The permeability difference between those two curves (k versus confining pressure) at any confining pressure can be considered the effect of the fracture on flow in the samples, or fracture permeability (k_f). Once k_f is measured and an estimate of D made, these variables can be applied to Equation 1-12 and the effective width of the fractures (e) at any confining pressure can be calculated (Nelson and Handin, 1977). Once e is known for any confining pressure or simulated depth, subsurface fracture spacing data can be applied to Equation 1-12 and ϕ_f calculated (Figure 1-69).

In a study of the Paleozoic carbonate section correlative to that in the producing zone in the Whitney Canyon Field, laboratory-derived fracture width data as a function of simulated depth were combined with outcrop-derived fracture-spacing data to map fracture porosity variations in large-scale folds. This method depicted potential ϕ_f variations in exploration, such variations with structural position, and stratigraphic level could be then anticipated (Figure 1-70).

This method of ϕ_f calculation involves both field and laboratory measurements and is, therefore, quite time-consuming. Its advantage lies in the fact that structural and stratigraphic inhomogeneities in ϕ_f can be modeled and predicted. This method, however, requires that the rock section of interest outcrops in structures similar in style or form to the subsurface structure of interest. This fact may severely limit its applicability in many areas.

Logs and Log Suites

There is no direct method of calculating fracture porosity from well logs. Several log suites have been developed to detect natural fracture systems (Aguilera and van Poollen, 1977; and Aguilera, 1995), but none can calculate ϕ_f directly. Most early methods used (such as the borehole gravimeter) relied on measuring matrix porosity on one tool and total porosity on another. The difference between the two being considered fracture porosity.

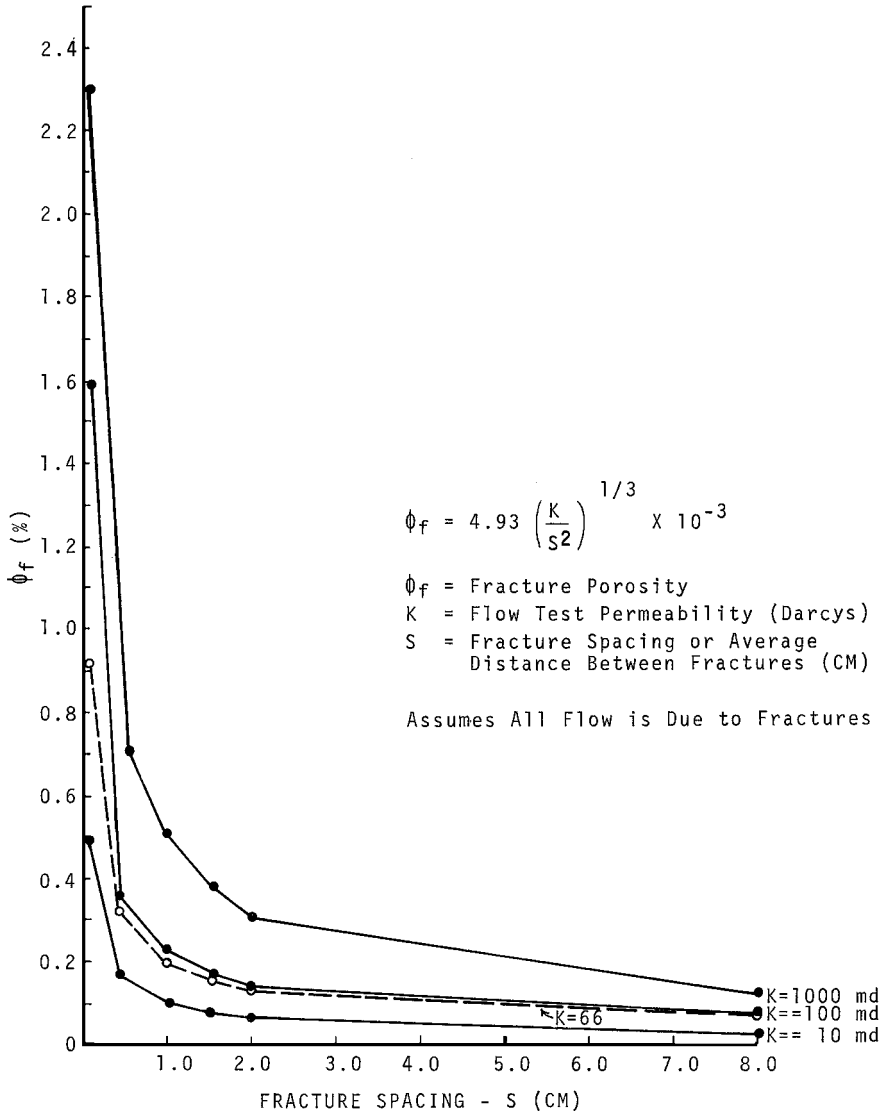


Figure 1-68 Fracture porosity as a function of fracture spacing and flow test permeability.

However, because ϕ_f is so small, calibration errors often overshadowed the true value of ϕ_f . Calculations of ϕ_f by logging methods are and should be routinely made in reservoirs where this is a relevant term; however, these values tend to overestimate fracture porosity. More modern logging ap-

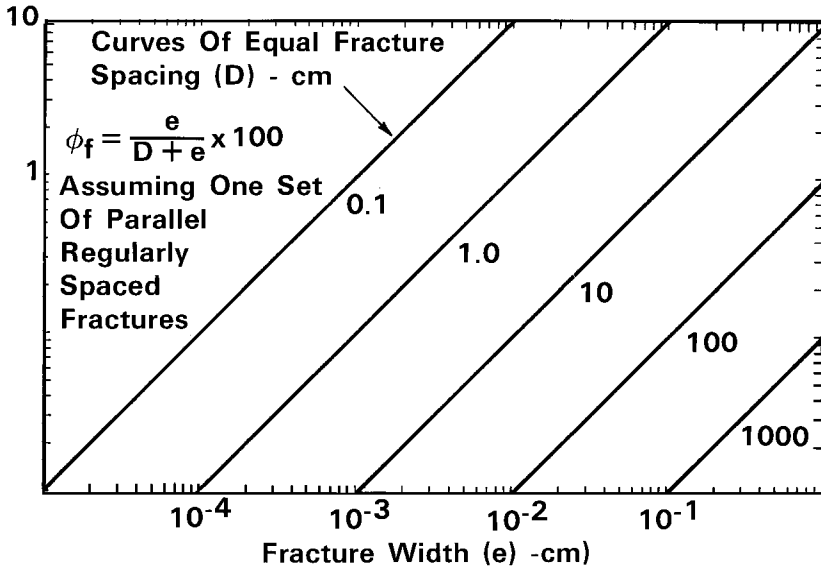


Figure 1-69 Fracture porosity as a function of fracture width and fracture spacing.

Fracture Porosity Ranges Are;
By The Station, 0.06% To 2.36%
By The Locality, 0.12% To 1.24%

Bighorn (1 Locality) = 1.23%
Darby (1 Locality) = 0.896%
Madison (4 Localities) = 0.322%

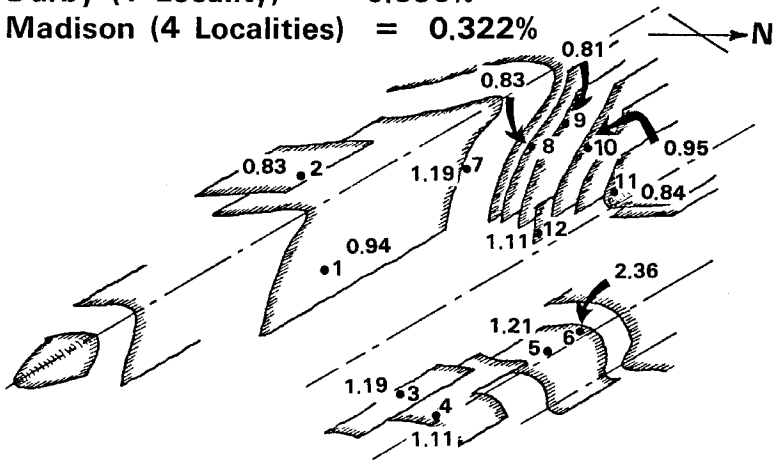


Figure 1-70 Calculated fracture porosity (%) distribution by fracture spacing measurement point or station on a surface fold in Ordovician Big Horn dolomite, western Wyoming thrust belt.

proaches to determining subsurface fracture porosity come from the electrical borehole imaging logs. This tool not only records the orientation and intensity of interpreted fractures, but will also record their apparent electrical aperture. With both integrated aperture and intensity of the recorded fractures, an estimate of fracture porosity for each fracture set can be made. The absolute values of fracture porosity using this method directly from the interpretive workstation are perhaps incorrect. However, the variation in aperture within the logged interval is accurate. If one orientation or horizon has the same fracture intensity as another, but has twice the interpreted fracture aperture as another, it has twice the fracture porosity.

Multiple Well Tests

Both single- and multiple-well testing can be used to effectively calculate ϕ_f . Pulse testing and pressure transient analyses are good methods for doing this. Because adequate discussion of these methods is beyond the background of this author, readers are referred to Aguilera (1995) and van Golf-Racht (1982).

These methods probably give the most accurate estimates of subsurface ϕ_f . However, they require close-spaced wells for testing and are usually only applicable in well-developed areas where production can be ceased in several wells long enough to perform the tests.

Cross-Flow in a Two-Porosity System

The quantitative evaluation of a natural fracture system in a fractured reservoir requires that the analyst determine three main fracture system characteristics:

1. Fracture intensity or spacing
2. Fracture plane morphology and width
3. Fracture and matrix porosity communication or interaction

The first two of these were discussed earlier. This section will discuss fracture/matrix interaction, its effect on the reservoir, and how this interaction might be evaluated early in reservoir analysis.

Several different equations have been derived to describe fluid flow in a two-porosity system (fractures and matrix). Some equations assume a fixed degree of communication or interaction between the two systems; others allow for variable interaction as a function of pressure gradients and the permeability contrast between the fractures and matrix (Table 1–4). These ap-

proaches, while valid for many simple fractured reservoirs, generally ignore the geometry and petrophysical properties of the fracture/matrix interface.

During early production, this lack of knowledge is often compensated for by adjusting recovery factors in the two-porosity systems and by assuming erroneous drainage areas. While often of limited harm in primary recovery, approximations made without a true knowledge of fracture/matrix flow interaction can become devastating in predictions of reservoir response in secondary and tertiary recovery projects. Such compensations can be disastrous in early economic evaluations when long-term investment decisions are made.

Examples of Cross-Flow in Thin Section

Uninhibited Cross-Flow

In a fractured reservoir where deformation is accomplished primarily by extension fracturing (as in the earlier section on regional fractures) and diagenetic mineralization is minimal, fracture/matrix interaction is good. In such a system, both porosity phases respond to the overall fluid pressure gradient as well as directly to each other (Figure 1-71). Such fractures are quite amenable to direct quantification by the various flow equations discussed previously.

Inhibited Cross-Flow

Producible reserve estimates for economic evaluation must include some difficult-to-determine matrix contribution. Quantification of fracture/matrix interaction is at this time quite difficult. Estimations must be made on the basis of the effect of the geometry of the fracture/matrix interface on both porosity and directional permeability. The following sections will discuss examples of porosity interaction problems related to both fracture mineralization and deformation.

Fracture Mineralization

If diagenetic mineralization within a fracture is complete, the fracture is a barrier to fluid flow and an obvious detriment to the reservoir. When mineralization is present but incomplete, the properties of the fracture/matrix interface become important. Poor fracture and matrix porosity interaction due to incomplete diagenetic mineralization is pictured in Figures 1-72 and

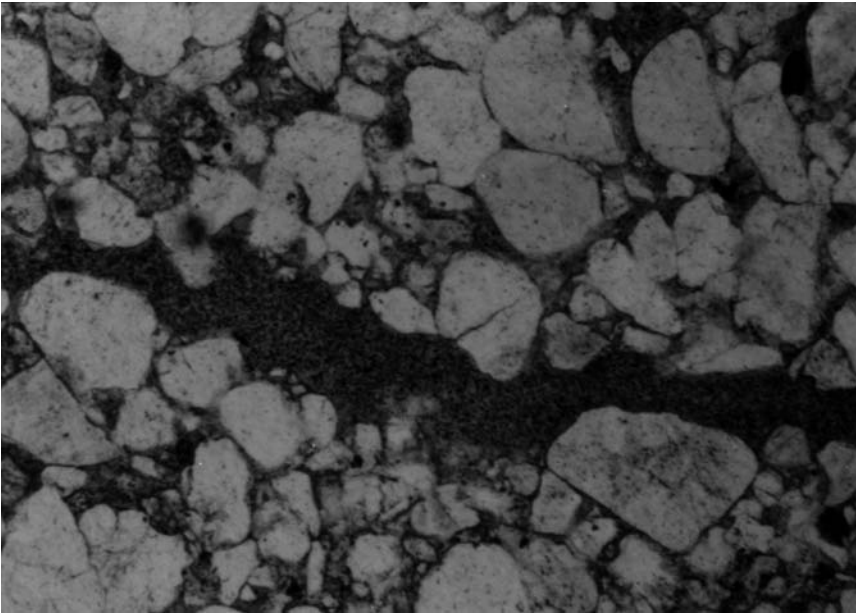
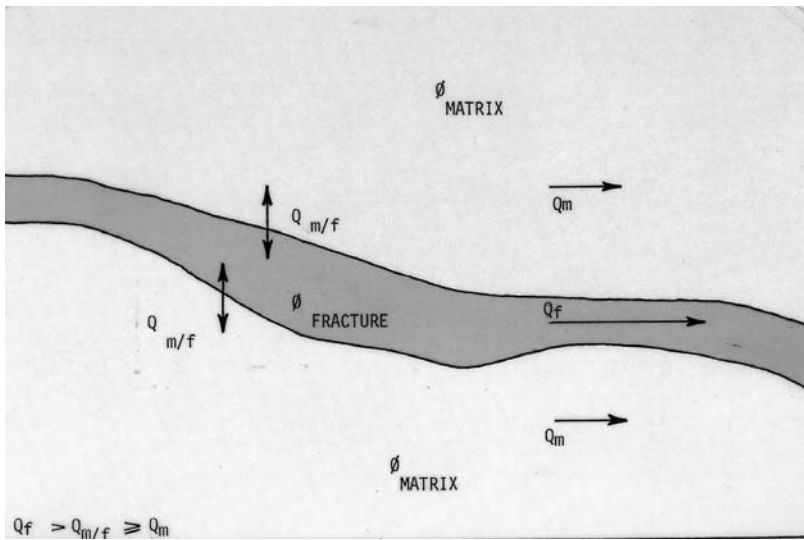


Figure 1-71 (Bottom) Photomicrograph of open fracture with good fracture and matrix porosity interaction. (Top) Schematic tracing of the two porosity systems shown on the photo (ϕ fracture and ϕ matrix). Also shown are the probable relative fluid rates (Q is a flow rate per unit area). This example is from the Champlin 224 well at 7,592 ft. depth, Pineview Field. (Magnification 140x.)

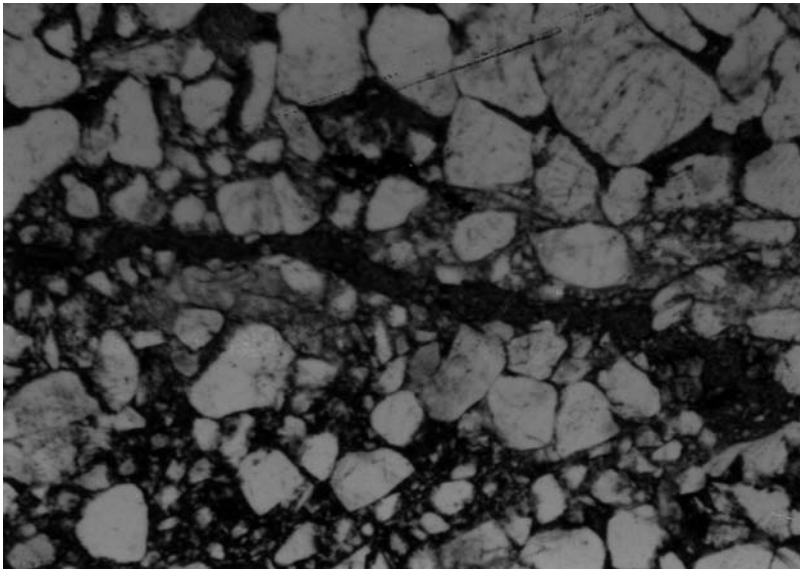
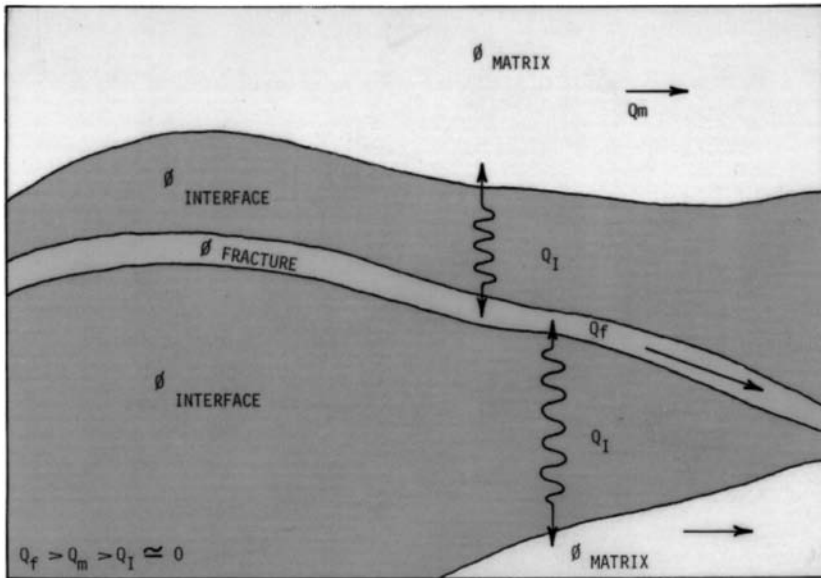


Figure 1-72 (Bottom) Photomicrograph of a rock with a very poor fracture and matrix porosity interaction. (Top) Schematic tracing of the three-porosity system shown in the photo. Also shown are relative fluid flow rates probable (Q is flow rate per unit area). From the Champlin 224 Well at 7479 ft. depth. (Magnification 140x.)

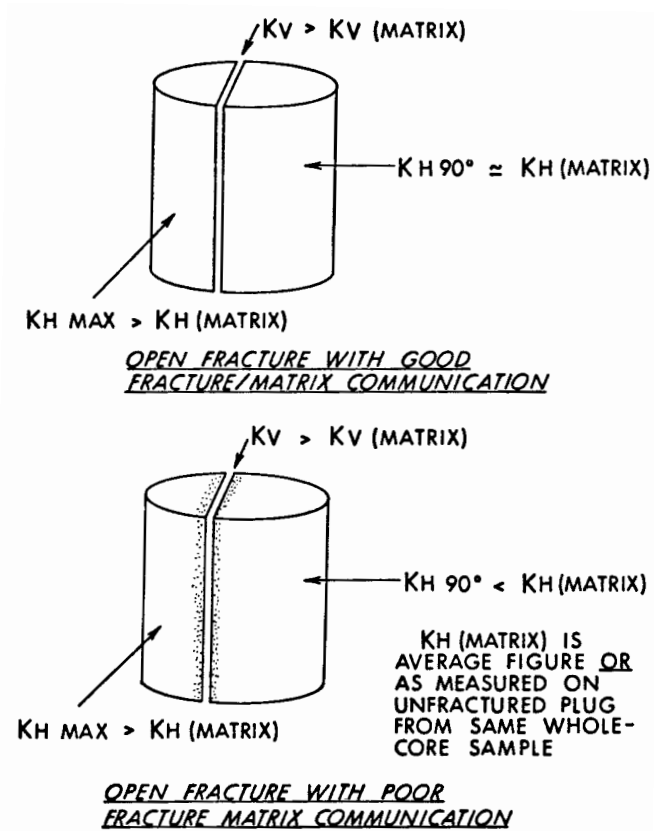


Figure 1-73 Effect of fracture and matrix interaction on whole-core permeability.

1-73. They illustrate the particularly bad problem of impervious mineral lining in fractures. In this case, large solution vugs at the center of the fracture fill are isolated from the porous matrix by a coarse lining of diagenetic mineralization. These situations make knowledge of the mineralization and solution history of paramount importance in fluid flow prediction. The presence of an impervious mineral lining can be quite damaging when we erroneously predict significant matrix contribution through the fractures to the wellbore. On the other hand, it can present little or no evaluation problem in reservoirs like the Tuscarora sandstone discoveries in central Pennsylvania in the 1980s, where matrix contribution to production is considered negligible.

Fracture Deformation

Fracture-associated deformation can significantly alter fracture/matrix interaction. Of prime importance in this alteration are slickensides and cataclasis. Both processes accomplish deformation by a crushing or breaking of host rock grains. Examples of poor fracture/matrix porosity communication due to cataclastic gouge around and slickensides along open fracture planes are shown in Figure 1–72. In general, slickenside development is less pervasive into the rock than gouge and, subsequently, affects a narrower zone of deformation. Therefore, for a constant number of fractures, slickenside formation often affects fracture/matrix interaction less drastically than cataclasis.

Estimation of Porosity Interaction

Direct determination of fracture/matrix communication is very difficult. It is as important at this point to recognize that poor communication in a reservoir exists as it is to accurately quantify it. Early recognition of poor fracture/matrix interaction allows us to be more cautious in economic evaluation of a reservoir.

The importance of thin-section observation of fracture/matrix interfaces in fractured reservoir analysis cannot be overemphasized. Such observations give direct evidence of major interaction problems as well as a chance to document the geometry of the interface itself. Porosity, grain size and shape, and sorting of the interfacing material can all be quantified and applied in estimations of fracture/matrix interaction.

In addition to thin-section measurements, estimates of communication between the two systems can sometimes be made by analyzing directional permeability data. Open or partially open fractures will generally have permeabilities much greater than the matrix rock in which they are found. Such fractures will have higher permeability parallel to the plane and “normal” matrix permeability across the fracture. In cases where poor fracture/matrix interaction exists, however, permeability perpendicular to the fracture plane is lower than that of normal or average matrix permeability, reflecting the reduced porosity and permeability of the interface or deformation zone. The reduced permeability of the zone or interface can then be used in modeling the flow distribution in the reservoir in a manner possibly similar to that of skin effects in wellbore damage.

2

Reservoir Management

After a fractured reservoir has been discovered with its initial well, early evaluations determine if the prospect will be economic to develop. This requires proper reservoir management based on (1) the knowledge of how the reservoir compares to already-developed reservoirs having similar properties, and (2) the knowledge of how the geological, engineering, and petrophysical data integrate into a coherent reservoir/depletion model. The following sections will address these aspects in detail.

CLASSIFICATION OF FRACTURED RESERVOIRS

Reservoir Types

Once the origin, continuity, and reservoir properties of the fracture system are determined, and the flow interaction between the fractures and the matrix has been investigated, the reservoir must be classified on the basis of what positive effects the fracture system provides to overall reservoir quality. The following classification has proven useful in this regard:

- Type 1:** Fractures provide the essential reservoir porosity and permeability.
- Type 2:** Fractures provide the essential reservoir permeability.
- Type 3:** Fractures assist permeability in an already producible reservoir.
- Type 4:** Fractures provide no additional porosity or permeability but create significant reservoir anisotropy (barriers).

This classification is an expansion of that proposed in Hubbert and Willis (1955). The first three types describe positive reservoir attributes of the fracture system. The fourth, while somewhat nonparallel to the others, de-

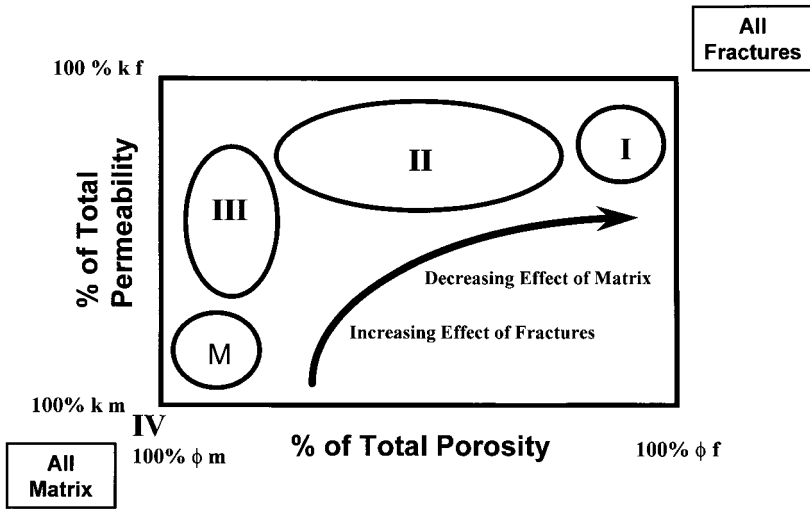


Figure 2-1 A schematic cross plot of percent reservoir porosity versus percent reservoir permeability (percent due to matrix versus percent due to fractures) for the fractured reservoir classification used by this author.

scribes those reservoirs in which fractures are important not only for the reservoir quality they impart, but for the inherent flow anisotropy and reservoir partitioning they create. A depiction of this classification in graph form is given in Figure 2-1.

The advantages of this classification are that it delineates the parameters of the fracture system, which are most important in quantifying a particular reservoir, and it allows for prediction of the types of production problems that are likely to occur.

In the first type of fractured reservoir, where the fracture system provides the essential porosity and permeability, an early calculation of fracture porosity or fracture volume attainable per well is of paramount importance. An accurate knowledge of this volume must be gained as early as possible to evaluate total reserves obtainable per well and to predict if initially high flow rates will be maintained or drop rapidly with time. In these estimations, fracture width and fracture spacing values are critical. Accurate fracture porosity calculations in fractured reservoir Types 2 through 3 are much less important because the fracture system provides only permeability—the matrix supplies any significant porosity or storage volume. In those types, the matrix pore volume (usually several orders of magnitude greater than the fracture volume) overshadows the fracture volume so much that to make an accurate, early calculation of fracture porosity is unimportant. In

these reservoirs, however, an early knowledge of fracture/matrix interaction is extremely important to determine whether the matrix porosity can be drained by the fracture system.

Similar breakdowns using this classification can be made for the other reservoir property determinations previously mentioned in Chapter 1.

Lists of Reserves by Type, and Examples of Reservoirs with Contrasting Histories

The classification scheme previously presented effectively subdivides reservoirs by size of reserves. This section will present a breakdown of reserves by fractured reservoir type. In addition, two fields will be chosen from the examples for each group to depict a relative difference in production history due to a difference in one of the parameters characteristically considered in reservoir evaluations.

A listing of reserves for several fields or groups of fields, which fall into the category of fractured reservoir Type 1, where fractures provide the essential porosity and essential permeability to the reservoir, shows that the reserves in this general reservoir type are rather low (Table 2–1). Amal is by far the largest field of this type. This field has substantial reserves due to its large thickness and very large aerial extent (100,000 acres, 800 ft. thick). The fracture porosity in this field appears to average about 1.7 percent assuming no matrix porosity in the Cambrian quartzite host rock.

Table 2–1
Examples of Fields in Which Fractures Provide the Essential Porosity and Permeability to the Reservoir

Field		Reserves
1. Amal	Libya	1700 mmbbi*
2. (5) Ellenburger Fields	Texas	107.8 (1957)
3. Edison	California	42
4. Wolf Springs	Montana	5.4
5. (8) PC Fields	Kansas	3.8
6. Big Sandy	Kentucky/West Virginia	3 TCF**

*mmbbi=million barrels of oil

**TCF=trillion cubic feet

Edison and Big Sandy fields are chosen as examples of contrasting history in this reservoir type, due to the origin and extent of the fractures (Table 2–2). The fractured reservoir of interest in Edison Field in California is the fractured Jurassic schist that constitutes basement in the area. This unit is one of nine pays within the field. The thickness of the fracture production is about 1300 ft. The fractures are tectonic in origin and are developed on a structural nose encompassing about 7,090 acres. This unit accounts for 42 MMBO or about 29 percent of the total field reserves. Matrix porosity in this unit is negligible.

Table 2–2
Examples of Contrasting History

Reservoir Type 1:

Fractures Provide the Essential Porosity and Permeability

- | | |
|---|---|
| <ul style="list-style-type: none"> • Edison (California)
Tectonic Fractures • Big Sandy (Kentucky/West Virginia)
Regional Fractures | <p>Poor History</p> <p>Good History</p> |
|---|---|

The Difference is Primarily One of Drainage Area and Fracture Type

Big Sandy Field in eastern Kentucky and western West Virginia is a fractured shale gas-producing reservoir. The producing Devonian shale units vary in thickness over the roughly 650,000 acre developed area. Reserves are estimated at about 3 trillion cubic feet of gas (TCFG). The fracture system appears unrelated to local structure and is believed to be a result of regional fractures. This field produces from shale with low effective matrix porosity, making it a Type 1 fractured reservoir.*

The difference in reserves between these two shallow, low-pressure fields is dramatic—one artifact of a difference in origin of the two fracture systems. The fractures in Edison are tectonic fractures related to the development of the structural nose or flexure. As such, the fractures are restricted to the size of the structure (7,090 acres).

The fractures at Big Sandy, however, are regional fractures and crosscut numerous structures. The area of fracture development is, therefore, very large (650,000 acres). Regional fractures will by definition be developed

* It has been pointed out, however, that gas may exist adsorbed on the small particles within the shale, which may be released and produced with time. If this is true, the field may not be a typical Type I reservoir.

over much larger areas than tectonic fractures, thus giving the potential for larger reserves in Type 1 fractured reservoirs.

A listing of reserves for several fields that fall into the Type 2 category—where fractures provide the essential permeability, and the matrix provides the essential porosity—shows that the reserves in these fields are substantially higher than the Type 1 fields (Table 2–3). This reflects the larger storage volume associated with matrix porosity (up to 20–30 percent in the matrix as opposed to up to 1–2 percent in the fractures).

Table 2–3
Examples of Fields in Which Fractures Provide
the Essential Permeability to the Reservoir

Field		Reserves
1. Agha Jari	Iran	9,500 mmbbi
2. Haft Kel	Iran	2,660
3. Rangely	Colorado	600
4. Spraberry	Texas	447
5. Altamont-Bluebell	Utah	250
6. Sooner Trend	Oklahoma	70
7. La Paz/Mara	Venezuela	800

Spraberry and Altamont-Bluebell fields are chosen as examples of contrasting production history in this reservoir type (Table 2–4). The reservoirs in these two fields are both fractured siltstones quite similar in character. The fracture systems are regional with very similar spacings. Both rocks show a tight, low-permeability matrix with moderate-to-low porosity (5–8 percent). Spraberry had an ultimate recovery of the oil in place of only 7 percent, however, while Altamont-Bluebell was much greater (possibly in the 30–40 percent range). This is due primarily to differences in initial reservoir energy.

Spraberry is an underpressured field or trend (0.33 psi/ft). Altamont-Bluebell, on the other hand, is an overpressured reservoir (0.7 and in some places up to 0.9 pounds per square inch [psi/ft]). Upon pressure drawdown there is very little pressure differential between the center of the matrix blocks and the fractures in the underpressured formation to drive the oil out. In the overpressured reservoir, however, significant pressure differential can be developed during pressure drawdown in the fractures and the oil is “forced” out of the matrix blocks into the fractures and ultimately to the wellbore. Therefore, the large difference in recovery factor between these

two fields, which are quite similar in fracture and matrix properties, is reservoir energy.

Table 2-4
Examples of Contrasting History

Reservoir Type 2:

Fractures Provide the Essential Permeability

- | | |
|--|--------------|
| • Spraberry (Texas)
Underpressured | Poor History |
| • Altamont-Blue Bell (Utah)
Overpressured | Good History |

The Difference is Primarily One of Reservoir Energy.

A listing of reserves for several Type 3 fields, where the fractures provide a permeability-assist to the reservoir in which the matrix itself is capable of significant flow, shows that these are some of the largest fields in the world (Table 2-5). Fractures here give the voluminous flow rates, which make these fields so economic (flow rates often in excess of 100,000 barrels of oil per day [BOPD]). Kirkuk and Cottonwood Creek fields are examples of this reservoir type (Table 2-6).

Table 2-5
**Examples of Fields in Which Fractures Provide
a Permeability Assist to the Reservoir**

Field		Reserves
1. Kirkuk	Iraq	15,000 mmbbi
2. Gachsaran	Iran	8,000
3. Hassi Messaoud	Algeria	6,000
4. Dukhan	Qatar	4,570
5. Cottonwood Creek	Wyoming	182
6. Lacq	France	8.8 TCF

Table 2–6
Examples of Contrasting History

Reservoir Type 3:

Fractures Provide a Permeability Assist

- | | |
|--------------------------------|--------------|
| • Cottonwood Creek (Wyoming) | Poor History |
| Late Recognition of Fractures | |
| • Kirkuk (Iraq) | Good History |
| Early Recognition of Fractures | |

One Difference is When the Fracture Systems
Were Recognized in Production Procedures.

While it is unfair to economically contrast two fields with such drastically different reserves (Kirkuk being one of the largest fields in the world), the difference in history of development of the two fields is instructive. In Kirkuk, gigantic flow rates were observed from the Asmari Limestone in the first wells drilled (100,000 BOPD with 1 to 2 pound pressure differential). The field was, therefore, recognized as a fractured reservoir immediately and was developed as such from day one. At Cottonwood Creek, however, the importance of the natural fracture system was not determined until failure of the secondary recovery project in the Phosphoria Reservoir. At that point, the field was shut in and a new secondary recovery study was made based on re-evaluation of cores and logs with natural fractures in mind. A successful secondary recovery project was then initiated, but there was a loss in ultimate recovery due to the shut-in and the failure to initially recognize the fracture contribution.

POSITIVE RESERVOIR ATTRIBUTES

Too often we look at fractured reservoirs as a bad thing: *fractures always make a simple matrix reservoir poorer and more difficult to handle*. This is not true. In fact, the first three fractured reservoir types have some inherent positive attributes due to the fracture system. Tables 2–7 through 2–9 highlight some of these positive reservoir attributes by fractured reservoir type.

Table 2-7
List of Positive Reservoir Attributes Inherent in Fractured Reservoir Type 1

Fractures Provide Essential Porosity and Permeability

1. Drainage areas per well are large
 2. Few wells needed in development (in-fill for rate acceleration only)
 3. Good correlation between well rates and well reservoirs
 4. Best wells are often early
 5. Generally high Initial Potentials (IPs)
 6. Can produce from nonstandard and nonreservoir quality rocks
-

Table 2-8
List of Positive Reservoir Attributes Inherent in Fractured Reservoir Type 2

Fractures Provide Essential Permeability

1. Can develop low permeability rocks
 2. Often higher than anticipated well rates
 3. Hydrocarbon charge often facilitated by fractures
-

Table 2-9
List of Positive Reservoir Attributes Inherent in Fractured Reservoir Type 3

Fractures Provide a Permeability Assist

1. Reserves dominated by matrix properties
 2. Reserve distribution fairly homogeneous
 3. High sustained well rates
 4. Great reservoir continuity
-

POTENTIAL PROBLEMS

Using the fractured reservoir classification scheme presented here, one can predict potential evaluation and production problems by reservoir type (Table 2–10 through 2–13). In general, problems with reservoir Type 1 revolve around delineation of the fracture system intensity and extent, as well as ultimate reservoir volume. Problems with Type 2 involve documentation of matrix and fracture interaction and optimum development patterns. In reservoir Type 3, virtually all potential problems relate to nonrecognition of the fracture system, especially during secondary development planning.

Table 2–10
Preliminary List of Problems Involved in Fractured Reservoir Type 1

Fractures Provide Essential Porosity and Permeability
<ol style="list-style-type: none"> 1. Often a rapid decline curve 2. Possible early water encroachment 3. Size and shape of drainage area is difficult to determine 4. Reserve calculations difficult to constrain 5. Many development wells add rate but not additional reserves

Table 2–11
Preliminary List of Problems Involved in Fractured Reservoir Type 2

Fractures Provide Essential Permeability
<ol style="list-style-type: none"> 1. Poor fracture and matrix porosity communication leads to poor matrix recovery and disastrous secondary recovery 2. Possible early water encroachment (production rates may need to be controlled) 3. Fracture intensity and dip critical 4. Development pattern must be tailored to the reservoir 5. Recovery factor difficult to determine and quite variable 6. Fracture closure in overpressured reservoirs may occur

Table 2–12
Preliminary List of Problems Involved in Fractured Reservoir Type 3

Fractures Provide a Permeability Assist

1. Highly anisotropic permeability
 2. Often unusual response in secondary recovery
 3. Drainage areas often highly elliptical
 4. Often interconnected reservoirs
 5. Correlation between log/core analysis and well test/performance often poor
-

Table 2–13
Preliminary List of Problems Involved in Fractured Reservoir Type 4

Fractures Create Flow Barriers

1. Reservoir compartmentalization
 2. Wells underperform compared to matrix capabilities
 3. Recovery factor highly variable across the field
 4. Permeability anisotropy opposite to other adjacent fractured reservoirs of other fracture types
-

The key to this understanding is the process of defining the fractured reservoir type and, therefore, what is to be expected from the fracture system. An example of this approach using former Amoco fractured reservoirs is shown in Figure 2–2. This historic view of the problems associated with these fields can now be used as a predictor of evaluation and development problems in new fields. We should be able to classify the type of fractured reservoir early in our evaluation and plan for the potential challenges from day one.

STRATEGIES OF FRACTURED RESERVOIR MANAGEMENT

Though many fractured reservoirs are profitably produced, very few are depleted efficiently. In general, these are very complicated reservoirs, and (especially the largest) must be studied in depth for correct evaluation and

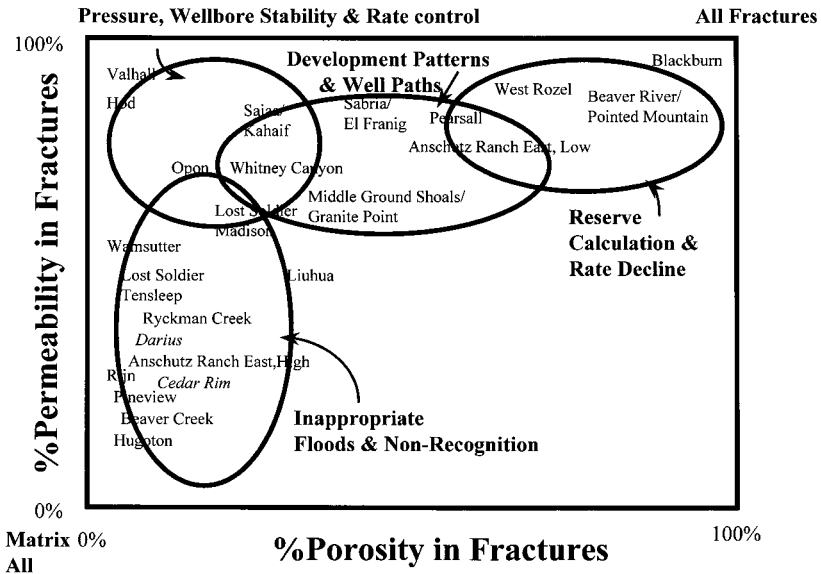


Figure 2-2 A visual depiction of the fractured reservoir classification of some of the fractured reservoirs studied by the author. Also depicted are production and evaluation problems encountered as a function of fractured reservoir type and relative position on this diagram.

optimum development and depletion. For anisotropic reservoirs in general, and fractured reservoirs in particular, several philosophical changes must be made in how we do our business. These include:

1. Quantification (both geological and petrophysical) in reservoir descriptions.
2. Interpretive evaluation of production history or history matching.
3. Reservoir modeling to understand the scaling of various geological and engineering data, and the ramifications of the numbers used.
4. A move toward total management and dynamic development as early as possible for optimum recovery in all phases of depletion.

Characteristically, in the past, reservoir management (development and depletion) in fractured reservoirs has relied heavily on production history data taken from early in the history of a field or from a look-alike field. A look-alike field is a produced field having similar characteristics to the one in question (Figure 2-3). Petrophysical and geological reservoir descriptions tended to be nonquantitative and were used to only a limited the extent in interpreting the history data and development plans.

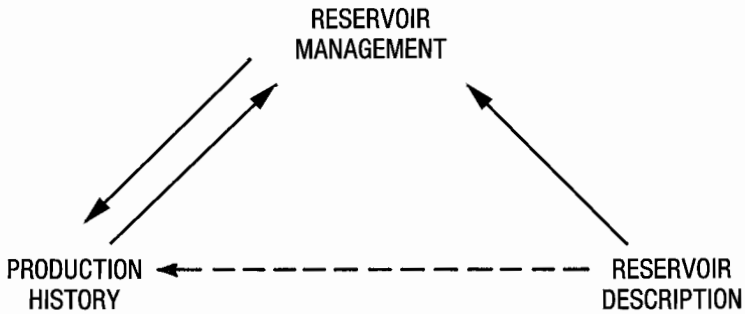


Figure 2-3 The “old” relationship between reservoir management decisions and input data.

Changes in technology and the current desire to improve recovery factors, especially in those fields with large reserves, allow us to change this procedure to a more integrated approach (Figure 2-4). Here optimum reservoir management is achieved through the use of reservoir modeling. These mathematical models integrate and iterate engineering and geological data of various scales and levels of quantification to achieve more accurate predictions of reservoir performance through time and under various assumed development and depletion schemes. Such interactive work requires changes in our method of data collection for the integrated approach to succeed.

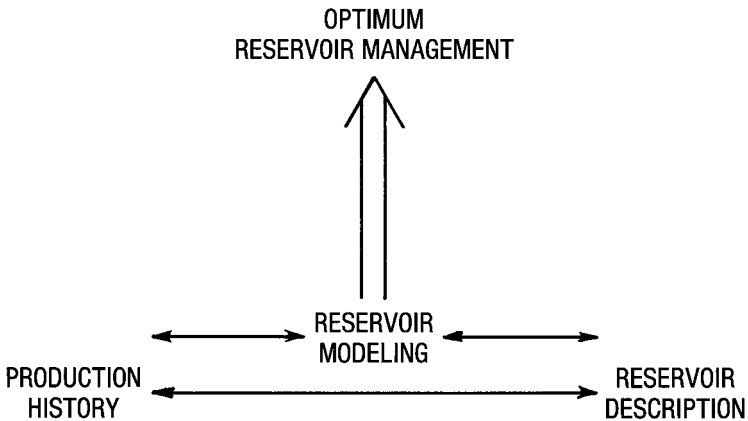


Figure 2-4 The “new” relationship between optimum reservoir management in fractured reservoirs and input data.

Reservoir Description

Geologists must learn to generate hard numerical data to not only define the size, shape, and distribution of relevant rock packages, but also to characterize the fluid-flow properties of these reservoir units. For too long, geologists have merely defined geologic units and left their in-depth quantification to the reservoir engineers who are generally less aware of the subtleties of reservoir variation and anisotropy. Quantification of these small-scale features and effects are most effectively handled by the geologist. Unfortunately, such quantification is often foreign to most geologists, but this must change for the unified approach (Figure 2–4) to become effective.

Geologists must learn to work up from the classical small-scaled core observations to understand how anisotropic features and flow characteristics combine to larger-scale reservoir performance. Observations must be made in light of defining potential reservoir compartmentalization and strong directional properties. Such work requires a synergistic melding of petrography, mechanics, and fluid-flow attributes in the total reservoir description.

Production History

In conducting evaluations, reservoir engineers deal with large-scale remote-sensed fluid-flow data, which is an amalgamation of all of the individual anisotropic parts or units within the reservoir. These data are often not interpreted in light of the details of reservoir composition because, like most large-scale remote-sensed data, it tends to be rather nonunique. Reservoir description is characteristically used only in the selection of an appropriate look-alike in the early stages of work. However, as more detailed quantitative reservoir descriptions and numerical reservoir models become available, this must change. Production history data will have to be interpreted in light of the details of reservoir makeup. This is possible with iterative modeling, much like inverse modeling of geophysical data. Models are first run that treat the reservoir more like a homogeneous, isotropic tank. With each progressive modeling run, more detail is added to the model, breaking it up into more response units and layers displaying more in homogeneity and permeability anisotropy as defined by the small-scale geological descriptions. At some point, results will not differ significantly with increasing model complexity. At this point, more detail is not necessary. As such, reservoir engineers will be moving relatively down in scale from the large-scale production data to smaller-scale interpretations of the data.

Reservoir Modeling

Reservoir models range from “look-alikes” to complex mathematical approximations. All are valid forms of modeling and should be viewed as effective and necessary vehicles for integrating and iterating various geological, petrophysical, and engineering data.

Look-alike models (produced fields that appear to have similar characteristics to the one in question) have always been popular prediction tools in the petroleum industry, both in exploration and production. They may be useful in general, but they have never proven very accurate in fractured reservoirs. This is due to the complex (almost unique) nature of most fractured reservoirs, and the general lack of quantitative descriptive data on the fracture and matrix properties necessary to determine which developed fields are truly analogous to the field in question. Because of this, we have often used very inappropriate look-alike models. However, with continued quantification in reservoir description, such modeling will become more and more meaningful.

Detailed mathematical modeling of fractured reservoir behavior and performance is relatively new within the industry. These finite differences and finite element techniques can depict pressure, temperature, fluid flow, saturation, and compositional behavior throughout the reservoir under various simulated depletion and treatment schemes. The modeling techniques have reached such a level of sophistication that these models can now begin to accept the reservoir complication evidenced in our reservoir descriptions at several scales.

Reservoir management decisions have often been made on the basis of different and often conflicting input data (Figure 2–4). In contrast, use of reservoir modeling as the primary integration of the various data permits reservoir management decisions based on the coherent, integrated modeling output-decisions that are more rational and straightforward.

Iteration

A very important aspect of the philosophical changes presented in this section is the facility for, and the necessity of, iterative steps in description or characterization, history matching, and modeling. Larger-scale quantification of reservoir descriptions and smaller-scale interpretation of history matching allows for a freer interaction between these disciplines. Iterative modeling facilitates this interaction by projecting the ramifications of the numbers chosen and in helping to define the scaling of detailed reservoir data up to large-scale (reservoir-scale) flow. Such scaling work helps us de-

fine the level of description complexity relevant to the reservoir performance above which accuracy is not improved.

Historic Production Distributions

Compared to normal reservoirs, fractured reservoirs are anisotropic and very inhomogeneous. This inhomogeneity can be shown by examination of frequency plots of field-wide rates and reserves, Figures 2–5 and 2–6. In a normal matrix-dominated reservoir, these distributions tend to be bell-shaped. However, in the fractured reservoir depicted in Figures 2–5 and 2–6, the distributions are highly skewed to the high end. The data shows that a few wells in the field dominate the reserves and are much higher in rates. To quantify this skewness in fractured reservoir properties, a data compilation was done for 20 produced fractured reservoir fields mostly from North America. The fields studied are shown in Table 2–14. The production data came mostly from Dwight’s Database.

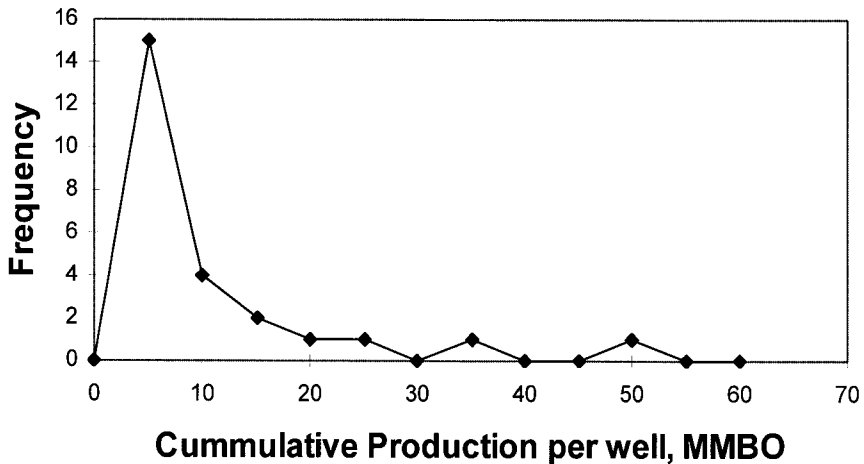


Figure 2–5 A frequency plot of cumulative production per well for the basement granite fractured reservoir in La Paz Field, Maracaibo Basin, Venezuela. This highly skewed distribution (log-normal versus bell-shaped) is typical of fracture-dominated reservoirs. Note that most wells produced about 5 million barrels of oil per day (MBOPD), while a few produced 7 to 10 times that amount.

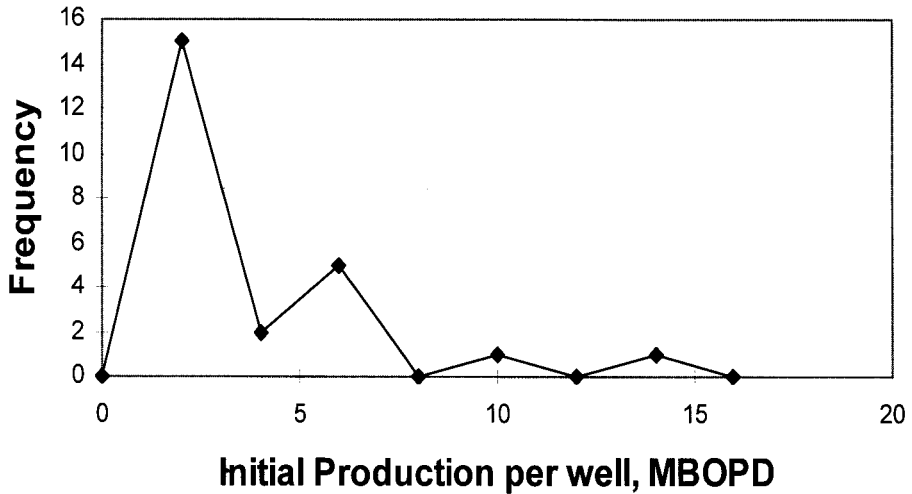


Figure 2-6 A frequency plot of Initial Potential (IP) or rate per well for the basement granite fractured reservoir in La Paz Field, Maracaibo Basin, Venezuela. This highly skewed distribution (log-normal versus bell-shaped) is typical of fracture-dominated reservoirs. Note that most wells produced are about 2 million barrels of oil per day (MBOPD), while a few produced at five to eight times that amount.

After studying the rate and reserve distributions of these fractured reservoirs along with those from two homogeneous matrix-only fields (Upper Valley and Waker Creek), the degree of skewness seems to be related to the degree of fracture control or fractured reservoir type (Figures 2-7 and 2-8). In general, the degree of skewness decreases as we go from a fracture-only reservoir (Type 1) to a matrix-only reservoir. Because it is difficult to visualize the differences in these distributions, a new format of display was designed to highlight these changes. Figure 2-9 depicts reserve distributions for the fields studied by plotting the percentage of wells drilled (ordered from lowest to highest) against the percentage of the total cumulative production of the field.

Table 2–14

Field	Formation	Rock Type	EOD	Cum., MMBOE	Max. Rate, BOPD
East Anschutz	Nugget	Sandstone	Eolian	564	7217
Ryckman Creek	Nugget	Sandstone	Eolian	64	3445
Pineview	Nugget	Sandstone	Eolian	15	540
Painter	Nugget	Sandstone	Eolian	167	3282
East Painter	Nugget	Sandstone	Eolian	138	4744
Lost Soldier	Tensleep	Sandstone	Eolian	138	
Wertz Dome	Tensleep	Sandstone	Eolian	42	
Rangeley (Sihco, 1976)	Weber	Sandstone	Eolian	4	1163
Middle Ground Shoals	Tyonek	Sandstone	Conglomerate	167	
Granite Point	Tyonek	Sandstone	Conglomerate	132	
Yellow Creek	Twin Creek	Carbonate	Shelf	6	679
Whitney Canyon	Madison	Carbonate	Shelf	33	2643
Lost Soldier	Madison	Carbonate	Shelf	40	1941
Wertz Dome	Madison	Carbonate	Shelf	3	642
La Paz	Cogollo	Carbonate	Shelf	575	14600
Trap Spring		Ignimbrite	Volcanic	13	1546
Dine-Bi-Keyah	Hermosa	Syenite Sill	Volcanic	18	1809
Florence	Pierre	Shale	Marine Sh		106
Point Arguello	Monterrey	Siliceous Sh	Deep Water Sh	131	10921
La Paz	Jr. Basement	Granite	Intrusive	209	12252
Upper Valley	Kaibab	Carbonate		24	273
Walker Creek	Smackover	Carbonate	Grainstone	16	336

(Capped)

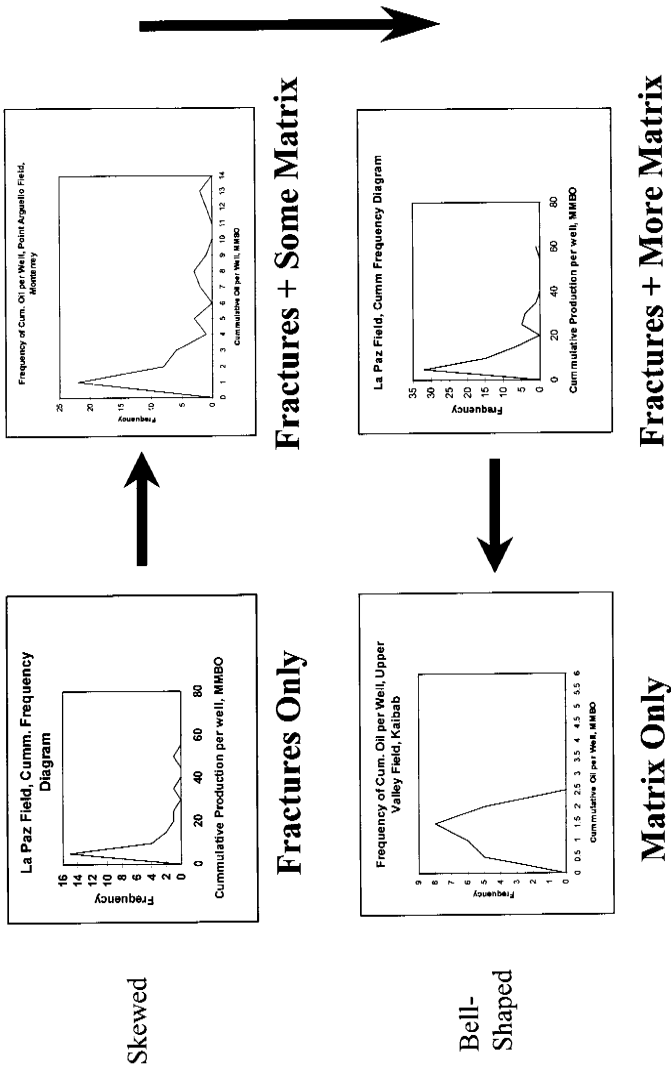


Figure 2-7 Selected frequency plots of cumulative production per well for reservoirs that range from matrix-dominated to fracture-dominated. The matrix-dominated distributions tend to be more bell-shaped while the fracture-dominated distributions tend to be highly skewed.

It is evident in this figure that there is great inhomogeneity in the cumulative production per well in these fields. As a reference point, in a truly homogeneous field every well would be average with each contributing an equal amount to the total field-wide cumulative production. Such a distribution would plot as a straight 45-degree line on this diagram, with every well giving an equal amount of reserves. The fractured reservoirs studied depart dramatically from that straight line. In fact, the shape and position of these curves appears to be a function of fractured reservoir type, with the Type 1 reservoirs having the greatest deviation and Types 2, 3, and 4 progressively moving toward the “homogeneous tank” straight line (Figure

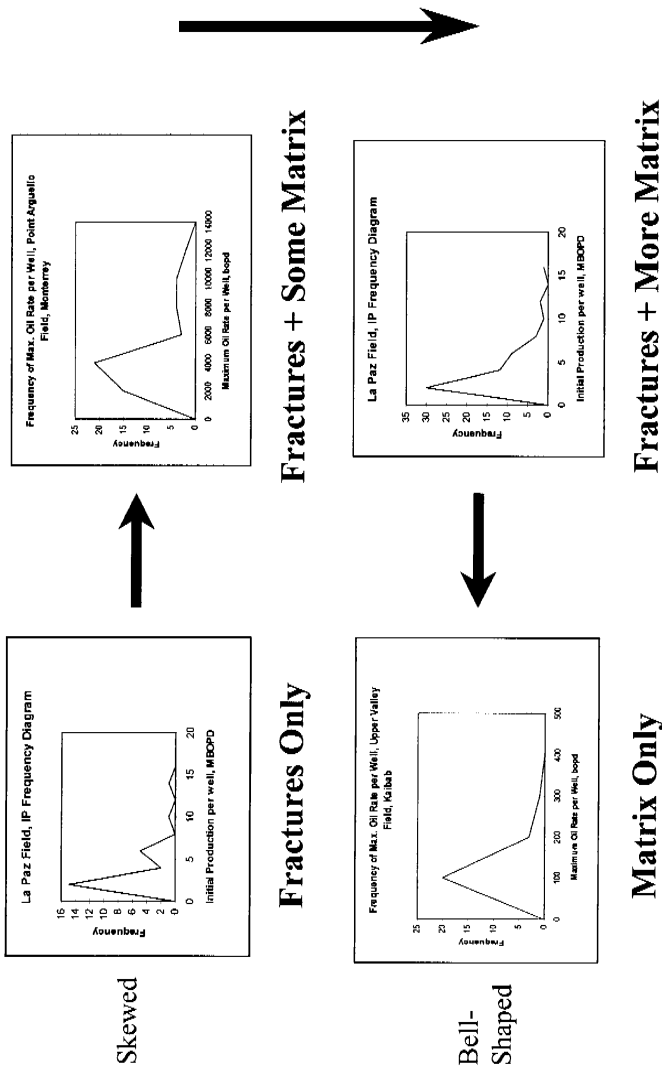


Figure 2-8 Selected frequency plots of maximum oil rate per well for reservoirs that range from matrix-dominated to fracture-dominated. The matrix-dominated distributions tend to be more bell-shaped or lightly skewed, while the fracture-dominated distributions tend to be highly skewed.

2–10). In this data set, in the Type 1 reservoirs the top 5-15 percent of the wells give 50 percent of the field’s reserves. This changes to 15-25 percent of the wells in Type 2 and 25-40 percent of the wells giving 50 percent of the reserves in Types 3 and 4. This change in distribution is logical in that reserves in Types 3 and 4 reservoirs are dominated by matrix storage. In these reservoirs, variations in fracture distribution have little effect on the amount of oil and gas produced. In the Type 1 and Type 2 reservoirs, reserves lie either directly within the fractures or require fractures to be produced from a portion of the matrix. In these reservoirs, variability in the fracture distribution creates large inhomogeneity in the reserve distribution.

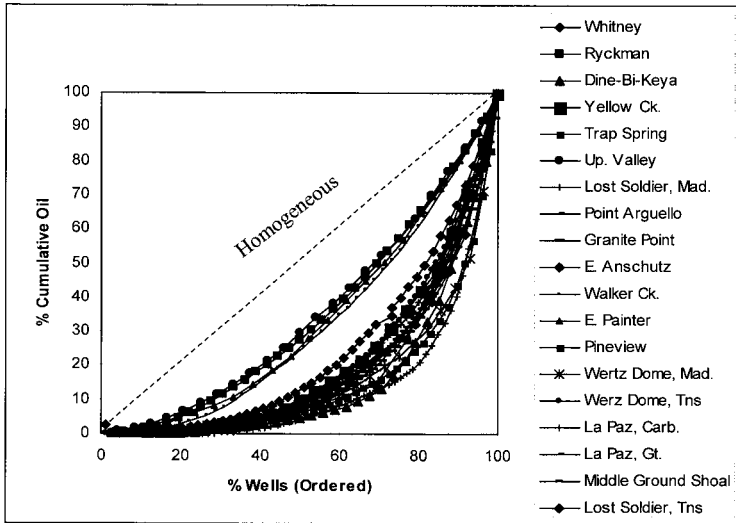


Figure 2-9 A percent cumulative oil versus percent wells cross plot for various fractured reservoirs. The wells are ordered from lowest to highest in cumulative production. Then the well's percentage contribution to the total production from the field is plotted for that well's percentage contribution to the total number of wells in the field. Fields in which every well had identical cumulative production would plot on a 45-degree line on this plot. Relatively homogeneous reservoirs would show a curve deviated slightly below that 45-degree line. Very inhomogeneous reservoirs, like fracture-dominated reservoirs, deviate substantially from that 45-degree line.

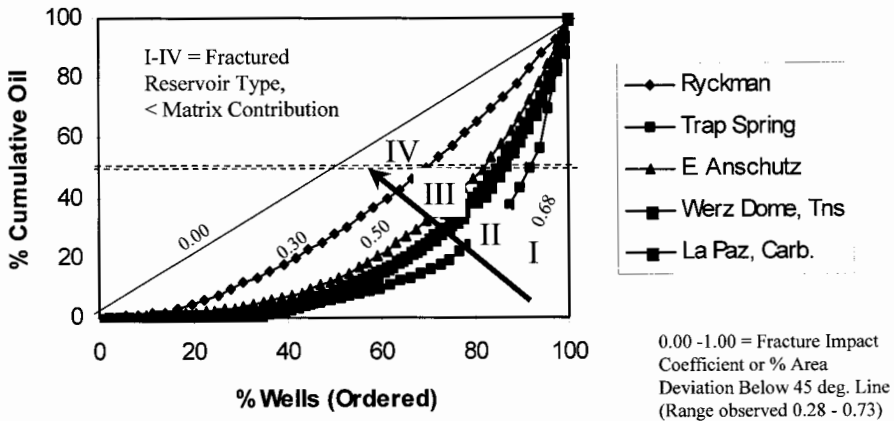


Figure 2-10 A percent cumulative oil versus percent wells cross plot for various fractured reservoirs similar to that in Figure 2-9. Depicted are reservoirs of varying fractured reservoir type (1-4) and their Fracture Impact Coefficient (percentage deviation from the homogeneous reservoir line).

A similar approach is used to investigate rate distributions in these same fractured reservoirs (Figure 2–11). In this plot, the percentage of wells is plotted against the percentage of liquid flow rate compared to the highest flow rate well in the field. The rate values used were the maximum monthly liquid flow rate the wells experienced during their life. On this plot, a homogeneous, all-average well field would plot as a horizontal line. As in the reserves plot, these fractured reservoirs display significant inhomogeneity with respect to rates, with only 10 percent of the wells having maximum flow rates of up to half that of the best well in the field. Compared to the reserves plot, this figure shows little discrimination by fractured reservoir type. In fractured reservoirs, rates are totally controlled by variations in fracture distribution, with more fractures giving more rate. Perhaps discrimination on the rate diagram will eventually be proven to be by fracture system origin (fold-related versus regional, etc.).

Another interesting observation in the production distributions in these fractured reservoirs comes from investigation of rates versus reserves in the wells from a field. Figure 2–12 shows an excellent linear correlation between rate and reserves in the wells from Type 1 fields, with progressively

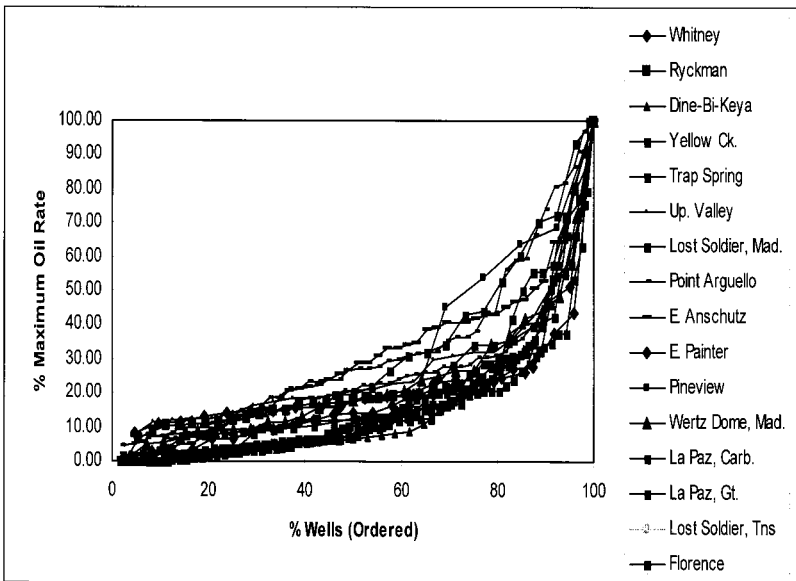


Figure 2–11 A percent maximum rate versus percent wells cross plot for various fractured reservoirs. The wells are ordered from lowest to highest in maximum rate. Then the well's percentage maximum rate compared to the maximum rate well in the field is plotted for that well's percentage contribution to the total number of wells in the field. Fields, in which every well had identical maximum rate, would plot as a horizontal line on this plot. Relatively homogeneous reservoirs would show a slightly deviated curve line. Very inhomogeneous reservoirs, like fracture-dominated reservoirs, deviate substantially from that 45° line.

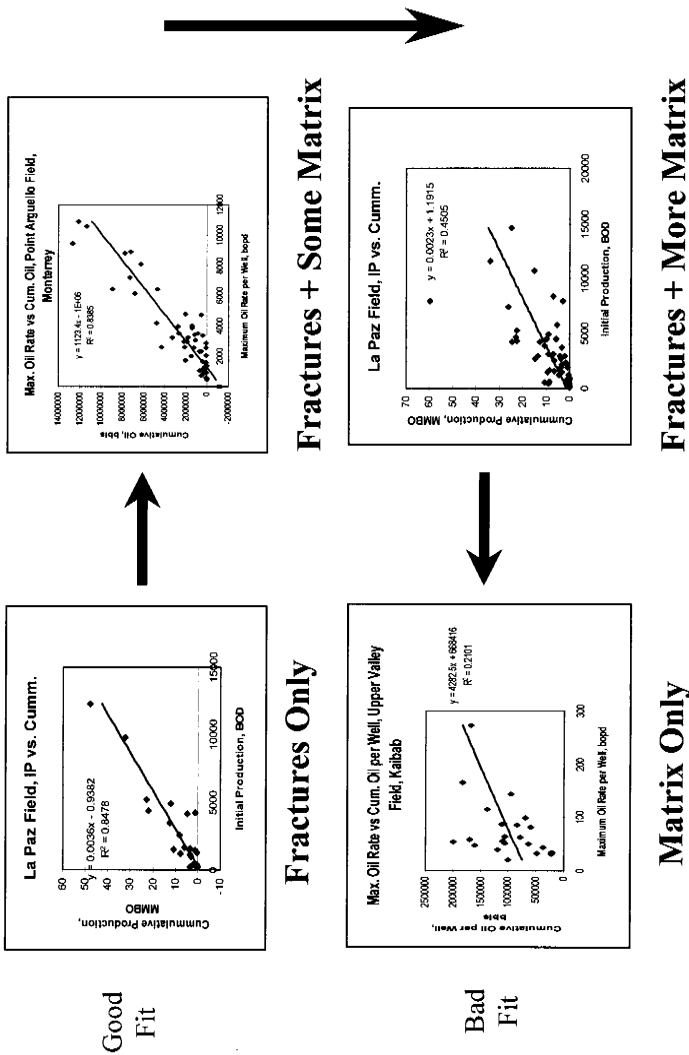


Figure 2-12 Selected cross plots of cumulative production per well versus maximum rate for reservoirs that range from matrix-dominated to fracture-dominated. In the matrix-dominated reservoirs correlation coefficients for cumulative and rate are low (~ 0.2), while the fracture-dominated correlations tend to be high (~0.9).

lower to very poor correlations moving to Type 2 to Types 3 and 4 reservoirs. Once again this is logical as reserves and rates are totally dependent on fracture abundance in Type 1 fractured reservoirs; the more fractures, the higher the rates and reserves. In Types 3 and 4 fractured reservoirs, more fractures give higher rate, but not higher reservoirs (those are stored dominantly in matrix pores).

There are several important aspects derived from these production distributions in fractured reservoirs. First, when creating early reservoir models for fractured reservoirs, we frequently do so by imputing a number of average or “standard” wells having the properties of the first wells in the field. In doing so, we never capture the variability because we don’t include

the really good wells that we are likely to encounter or the conversely the great number of poor wells. While with only one or two wells in the field, we will not know where our wells fit in the spectrum of possibilities, we can use these distributions to at least anticipate the likely variability (upside and downside).

Secondly, we can use distribution approaches such as this to circumvent fracture denial prior to developing secondary floods. For example, in a Type 3 fractured reservoir, we may have ignored the fractures during years of primary production. However, if we later embark on a secondary recovery-flooding project we cannot ignore the fractures as they will create strong directional flow. Creation of production distributions such as those described here can be used to prove that fractures play a role in the reservoir and that fractures must be incorporated into the secondary flood planning.

THOUGHTS ON RISK ANALYSIS IN FRACTURED RESERVOIRS

There is a variety of risk approaches used by the companies in the industry to judge the relative quality of drilling opportunities in their portfolio. They range from probability approaches to deterministic or various mixtures of the two. All, however, attempt to constrain the uncertainty of the various elements of aspects of the hydrocarbon system that is active and the trap itself. Regardless of the style used, in analysis of fractured reservoirs, attention must be paid to the presence of the fracture system and its reservoir properties, and to several standard engineering parameters.

Reservoir Presence Risk—Risk fracture system presence as well as matrix
Detection of Fractures—Detection of fractures on multiple data types reduces chance of failure

- Logs
- Core
- Welltests
- Mudlogs
- Drilling records
- Outcrop analogies

Distribution of Fractures (dependent on origin)—Are there “sweet spots?” Do fractures occur in restricted areas (single layers and hinge-related tectonic fractures) or in unrestricted areas (multiple layers with regional and diagenetic fractures). Restricted layers and areas may give higher rates while unrestricted ones may give higher reserves. Focus on restricted areas and layers causes uncertainty in well optimum locations and increases chance of failure.

Most Continuous Direction—Is there one dominant fracture orientation that can it be determined by structural, seismic, or production techniques? Is this reservoir a candidate for directional or horizontal wellbores? Higher continuity of trend reduces chance of failure.

Reservoir Porosity and Permeability Risk—Risk flow properties of fractures and matrix. Emphasis is on fracture porosity and fracture permeability and its relation to the matrix. Issues that become important are as follows:

Pore Pressure—Overpressured is a plus, normal pressure is neutral, underpressured is a negative in terms of fracture closure.

Fracture Morphology—From best to worst (vuggy, open, partially mineralized, slickensided, totally mineralized, gouge-filled or deformation bands).

Fracture/Matrix Communication (skin)—Restricted communication or crossflow in samples is a negative, while unrestricted communication is a plus.

Engineering Parameters—Several standard reservoir engineering parameters should be questioned in fractured reservoirs. These include the following.

We need to pay attention to *recovery factors* in a two-porosity system. The lower the permeability contrast between fractures and matrix the greater the recovery factor. Higher reservoir or pore pressure increases recovery factor in fractured reservoirs, while lower pressure reduces it.

Oil saturations in fractures are likely to be higher in fractures than in the matrix, but due to their small pore volume, will not significantly effect the reservoir performance.

Relative permeabilities in the fractures will be different for the fractures and the matrix. This difference may be significant and may need to be addressed in flow calculations.

The *economic limit* in fractured reservoirs may be smaller if the drainage area per well is larger than a matrix-only reservoir due to the presence of fractures. This reduces the number of wells necessary to deplete the reservoir and lowers development costs.

3

Detecting and Predicting Fracture Occurrence and Intensity

In exploring, developing, or evaluating a fractured formation, the zones of highest fracture intensity (closest fracture spacing) must be found and penetrated. These zones must either be detected in the wellbore, or they must be predicted. The following sections will discuss several techniques that have been used with various success in both detection and prediction of fractures and ultimately wellbore planning. These address the fifth and final phase of the fractured reservoir procedure.

DETECTION

All rock formations contain some fractures, and their presence in sufficient quantity to influence the reservoir is a matter of degree. The degree of fracturing present in a wellbore can be determined by either direct or indirect methods.

Direct Detection

There are three basic techniques:

1. Direct observation and analysis of core
2. Downhole cameras
3. Inflatable packers

Direct Observation and Analysis of Core

Unquestionably, the best method for detecting reservoir fractures is by observation of core material from the zone of interest, provided fracturing is not so intense as to impede core recovery. Carefully taken, whole-core material (including rotary side-wall cores) can provide fracture dip and intensity data as well as data on rock strength, rock fabric, and the interactive flow capabilities of the fractures and matrix. Oriented core material can, in addition, provide data on fracture azimuth. Such data facilitates in-depth quantitative analysis of fracture distribution and generation. Percussion sidewall cores are not recommended because the percussive event often generates numerous induced fractures into the sample.

Downhole Cameras

Small downhole photographic and television cameras can be used to take pictures of the wellbore. These give direct information on such physical features as hole size, bedding planes, fractures, and faults. With the addition of an orientation device, downhole pictures can provide the same gross directional data on fractures as oriented cores. Oriented cores will, however, provide rock composition, fabric, and strength data. Such data are often essential to a complete understanding of fractured reservoirs.

According to Fons (1960) and Aguilera and Van Poolen (1977), the photographic cameras are capable of taking up to 1,000 pictures per trip at downhole conditions of up to 200°F and pressures to 4,000 psi. In addition to normal photographic problems, the greatest drawback of this method is that this tool can only be used in dry, gas-filled, or clear water-filled wells. In addition, any drilling mud cake on the well wall may impede, or even eliminate, direct photography of the wellbore.

Impression Packers

Impression packers are bladders coated with a soft pliable material. The unpressurized packer is lowered to the zone of interest in the well and then pressurized. As the soft coating is pressed against the wellbore, it conforms to the topography of the hole, including fractures. The pressure in the packer is then released, and the tool is removed from the hole. Subsequent observation of the packer coating gives an idea of the physical character of the wellbore, hopefully including the fracture system. Impression packers have been used almost exclusively in the detection of hydraulic fractures (Haimson, 1975). This method works well for hydraulic fracture detection

in uncased holes, because the hydraulic fractures are wide and cut the drilling mud cake. Natural fracture systems, however, may not cut the mud cake or may not be of sufficient width to be seen in the rubber skin. Therefore, this tool is often limited for detecting natural reservoir fractures. In addition, very large or irregular wellbores characteristic of many fractured formations often cause overextension and blowouts in the packers, making the technique somewhat unreliable.

Indirect Detection

Indirect techniques include:

1. Primary well log evaluation
2. Flow or well test evaluation
3. Manipulation of reservoir rock property data

It is not the intention here to write an in-depth analysis of these techniques, but only to discuss what tools are available to students of fractured reservoirs. This discussion should serve as a basis for more detailed investigations by qualified log analysts.

Primary Well Log Evaluation

The following discusses nine logging tools used to detect reservoir fractures. In general, these tools have been used to detect (with varying degrees of success) high-intensity fractured zones and not to determine fracture spacing. Because responses used to detect fractures on well logs are nonunique, a detailed knowledge of the tool and the various rock property effects, which could cause fracture-like responses, is necessary for fracture detection by well logs.

Sonic Amplitude Log

This tool has probably been used more than any other to detect fractures. According to Morris and others (1964), compressional waves are attenuated more by vertical or high-angle fractures, while shear waves are more attenuated by horizontal and low-angle fractures. When a compressional wave encounters a fluid-filled fracture, its amplitude is reduced due to reflection at the interface. When a shear wave strikes a fluid-filled fracture, its amplitude essentially disappears (Aguilera and Van Poollen, 1977). In addition, one service company describes constructive/destructive interference as an indication of fractures that parallel the wellbore but do not intersect it.

Variable Intensity of 3-D Log

Variable intensity logs record depth and amplitude versus time after an acoustic transmitter pulse. A large portion of the sonic wave train is recorded and plotted out in a seismic like trace on the log. Amplitude changes are evidenced by changes in shading on the log; dark shades show the largest positive amplitudes, and light shades show the largest negative amplitudes. According to Aguilera and Van Poolen (1977), this tool is used for fracture detection by looking for jumbled or chaotic zones (fractured rock) on the log between zones of distinct banding of parallel wave lines (unfractured rock). Other analysts look not for jumbled zones on the record, but for specific W-shaped patterns. In both cases, however, unless the stratigraphic section is well known to the analyst, variations in lithology could be misinterpreted as fractured zones.

Caliper Log

With a good knowledge of the stratigraphic section, the caliper log can be a good tool for finding fractured zones in a well. In brief, it is assumed that highly fractured zones cave into the hole, thus enlarging the wellbore. Because normal hole enlargement can occur due to compositional differences, this tool works best in detecting relative fracture intensity differences in continuous, competent rock units such as carbonates. Any one of the different caliper tools (2-, 3-, 4-, or 6-arm) can be used to detect fractures. Each will, however, gives slightly different data about borehole configuration.

Electrical and Acoustic Borehole Imaging Logs

The dominant fracture detection tools in today's industry are the fracture imaging logs. These include acoustic and electrical resistivity tools. The acoustic tools image the topography of the wellbore, while the resistivity tools image fluids within open fractures. A comparison of the two tools is shown in Figure 3-1. This is a Schlumberger example of an ultrasonic borehole imager (UBI) and formation microimager (FMI) log of the same wellbore zone in a fractured granite section. The acoustic tool is often used when the well was drilled with oil-based muds because the resistivity imaging logs do not work well in these systems (improvements have been made allowing the resistivity imaging logs to be used in wells with these muds, but at the time of writing are not fully available). Also, the acoustic log is the best imaging log to define borehole breakouts for *in situ* stress direction determinations. The resistivity imaging logs, on the other hand, have finer resolution and can calculate a relative width or aperture of the fractures (in my experience, absolute apertures are not accurate, while relative aperture differences between fractures is).

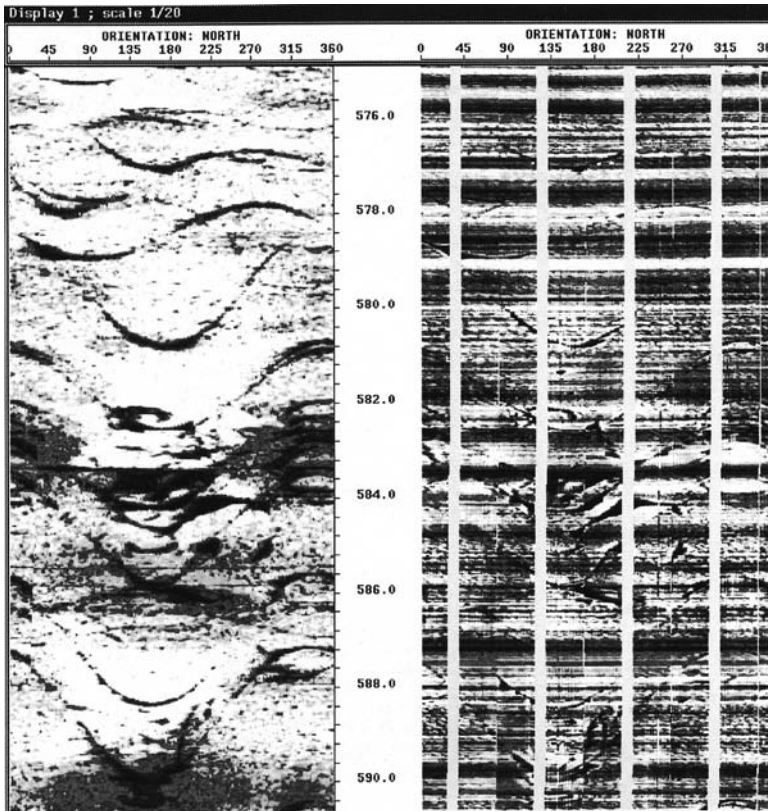


Figure 3–1 Example of natural fracture imaging of the same well interval on two varieties of borehole image logs. Left is an acoustic image (UBI Log) and right is an electrical resistivity image (FMI Log). Images courtesy of S. Hansen and Schlumberger.

The imaging logs give an unrolled “picture” (north to north) of the inside of the wellbore. Fractures that dip with respect to the wellbore axis show up as sinusoidal traces on the unrolled image (Figure 3–2). A critical tool to the interpretation of these images is the workstation interpretation platform. This program allows the interpreter to select points along the fracture trace and automatically calculate the strike and dip of the interpreted feature, whether it be sedimentary, natural fracture, or induced fracture. One company markets the use of a combined acoustic/resistivity tool. It is expensive due to the utilization of two imaging logs but when combined in the workstation allows for the computer enhancement of some mineralized fractures. An analysis of the resistivity imaging logs and how they are interpreted can be found in Trice (1999a and b).

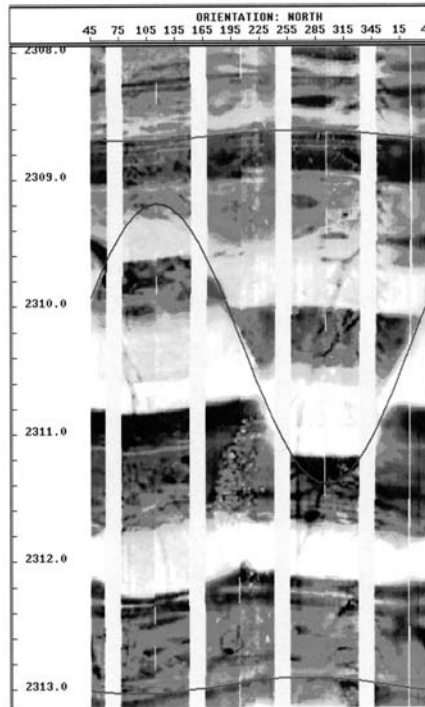


Figure 3-2 Example of how a fracture or fault is described and interpreted on an image log. The fracture trace in the wellbore shows up as a sinusoidal curve on the “unrolled” borehole image. This is an FMI resistivity image courtesy of S. Hansen and Schlumberger.

Dipole Sonic Log

The dipole sonic log utilizes both normal and shear wave acoustic data in the wellbore. The concept in the analysis of the data is that fractures in the rock mass do not effect the p-wave travel, while they do retard the s-wave travel. Analysis of the sonic anisotropy derived from this oriented tool allows the interpreter to determine the dominant fracture direction within the wellbore and perhaps an estimation of fracture porosity as well. This tool seems to work best in carbonate sections.

Induction Log

The induction log has been used to determine the presence of fractures using the assumption that the presence of fractures provides resistivity anomalies. This process depends on the invasion of vertical fractures with a nonconductive fluid (Aguilera and Van Poolen, 1977).

Microlaterolog

This tool, like the induction log, uses resistivity anomalies to locate fracture zones. The laterolog is affected by vertical resistivity changes while the induction log is affected by horizontal resistivity changes. The difference between amplitudes on the microlaterolog and induction log has been used as an indication of the presence of vertical versus horizontal fractures depending on which tool reads higher resistivity.

Dipmeter Log

The continuous four-pad dipmeter has been used to detect fractures in two different ways. In one, the dipmeter is used as a two-directional caliper measuring hole enlargement in one direction relative to another (maximum and 90 degrees from maximum enlargement). As in the caliper log, it is assumed that fractured zones cave into the hole parallel to the *in situ* fracture system. The second method assumes resistivity changes due to fluid-filled fracture planes to be evidenced by each of the four pads of the four-pad dipmeter. Vertical displacement in response to the four pads can be used to calculate fracture dip and strike.

Density Log Compensation Curve

This approach assumes that in a constant lithology (dense formation, such as clean carbonates), borehole roughness corresponds to the presence of fractures. The compensation curve acts as a very sensitive caliper to detect the roughness and, therefore, fractures. Of course, the detector is only about 2 in. in diameter. Therefore, it sees only a very small portion of the borehole circumference ($\cong 8\%$). But, since the detector is usually pushed into the major diameter of the wellbore, it may be looking at the most likely-to-be-fractured area, assuming the washout direction corresponds to fracture orientation.

Borehole Gravity Meter

While difficult to obtain and very difficult to interpret correctly, borehole gravity meter data can be used to detect large fractured zones in a well. The gravity meter determines the bulk density of a very large rock volume surrounding the wellbore. If there is very good data on the porosity and grain, and fluid density distribution in the rock, fracture porosity can be found. Provided the matrix data is very good and relatively consistent, and structure or terrain corrections can be handled, this tool has potential in not only finding fractures but in quantifying fracture porosity.

Flow or Well Test Evaluation

Included in this category are flow test methods prior to production as well as reservoir performance during production (production history). Well testing procedures in fractured reservoirs have been worked on extensively in the last 30 years. However, the procedures are often quite complicated and a complete discussion of them is beyond the background of this author. In general, such testing includes pressure buildup tests, pressure drawdown tests, and pressure interference tests. Several interesting papers on well test evaluation are Dyes and Johnston (1953), Russel and Truitt (1964), Odeh (1965), Adams and others (1968), Aguilera and Van Poolen (1977), and Aguilera (1995).

Manipulation of Reservoir Rock Property Data

There are several indirect techniques used to detect fractures, or the effect of fractures, in the reservoir from reservoir rock property data. Each of these deals with cross-plotting various core- or log-derived data. All of these techniques can only give an indication of fracturing, and should, therefore, be followed up with additional direct or indirect detection techniques to prove the existence of fractures in the reservoir.

Core Porosity Versus Core Permeability

Most rocks exhibit a loosely defined linear relationship between porosity and permeability. Cross-plotting core analyses porosity and permeability (plug or whole core) can establish this relationship. On such a plot, samples or groups of samples that plot anomalously high in permeability (with respect to the general porosity/permeability relationship defined for the rock type) are considered to be fractured (see Figure 3–3). This conclusion can be made because fractures may drastically affect permeability but may have little or no effect on porosity. Whole-core measurements generally work better than plug measurements in this technique.

Vertical Versus Horizontal Whole-Core Permeability

Due to the effect of bedding, most sedimentary rocks exhibit greater permeability parallel to bedding than perpendicular to it. Thus, on a vertical versus horizontal whole-core permeability plot, most rock samples will plot to the horizontal permeability side of the equal permeability line. If samples plot in or toward the vertical permeability side of the equal permeability line, fracturing should be suspected (see Chapter 1 “Fracture Width Versus Confining Pressure”).

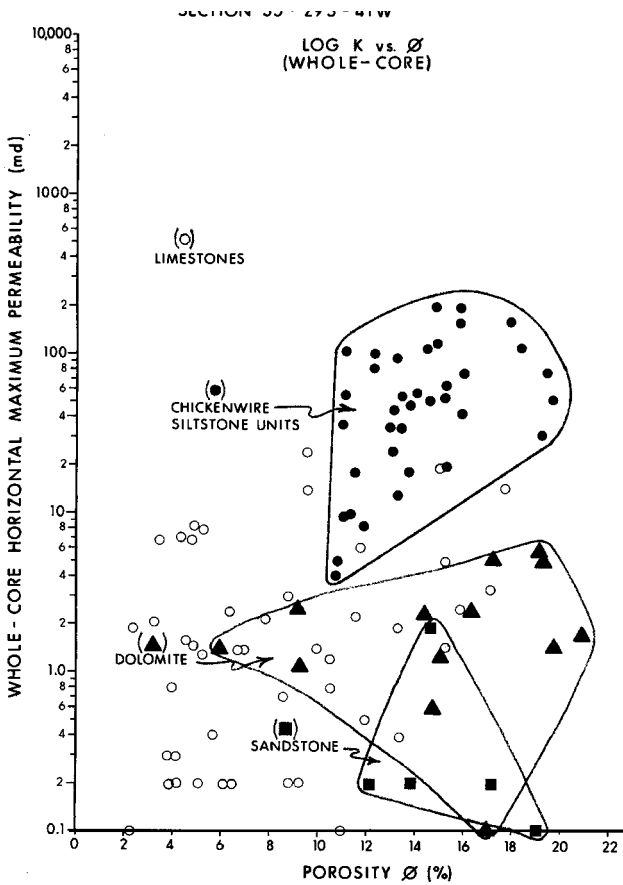


Figure 3-3 Whole core permeability versus porosity for a well containing chickenwire fractures siltstone. Note that the siltstone samples plot 10 to 100 times greater in permeability than sandstone samples of equivalent porosity.

Maximum Versus 90 Degrees-from-Maximum Horizontal Whole-Core Permeability

Vertical whole-core permeability is usually not run unless specifically requested. Generally only maximum and 90 degrees-from-maximum horizontal whole-core permeability is determined. In the standard analysis, a drastic discrepancy between the two horizontal permeabilities beyond what could be due to matrix anisotropy can be indicative of fractures.

Core Permeability Versus Flow Test Permeability

As most workers are aware, formation permeability measured in the laboratory on core samples and in production testing are somewhat different. Because the numbers are never identical, a comparison of core and flow-

test permeability is often done to give an idea of the normal range of measurement variability. However, flow test permeabilities that are extremely high with respect to their analogous core permeabilities, well above that of normal variability, are often considered to be fracture controlled.

Core Porosity Versus Porosity Determination from Neutron Log

This method assumes that core porosity represents a matrix porosity and neutron log porosity represents total porosity. Core samples that plot too low in porosity (with respect to normal variation) for a corresponding neutron porosity are considered to come from a fractured zone. The problem with this technique is that fracture porosity is generally too low to observe numerically on a neutron log,

Resistivity Versus Log Porosity

When resistivity is plotted against log-derived porosity, the slope of the resulting curve is the porosity exponent m . In some naturally fractured reservoirs this slope (m) is smaller than the analogous matrix porosity exponent determined on unfractured samples in the laboratory. When this happens, fracturing is suspected.

Sonic and Neutron or Density Log Curve Separation

Curve separation between two porosity logs, the sonic and either the neutron or density porosity tools, can be used to indicate fractures. The sonic-derived porosity is assumed to indicate matrix porosity, while the neutron or density-derived porosity is assumed to represent total porosity. The difference or separation between the two curves is, therefore, assumed to be a measure of fracture porosity. Fracture porosities derived using this technique are in some cases unreasonably large.

Remote Sensing

One method of very indirect detection of natural fractures in the subsurface is remote sensing (Blanchet, 1957). These approaches are basically extrapolations of surface data derived from remotely sensed images to subsurface formations. The basic data types used are radar imagery, and various types and scales of black and white or color photographs from low-altitude to satellite-based scales.

Structural, fracture, and/or lineation data are extracted from the images with emphasis on fabric data and specific locations of the larger features (Nelson, 1983). Assumptions are then made that high-intensity fracture/linear zones continue with depth (Wheeler, 1980), and that features, which are

long in map view, continue deep through the section (Nur, 1978). To what degree these assumptions are valid is not completely known at this time. Structural features can be delineated effectively from remote sensing imagery, especially from low-altitude stereo pairs (Norman and Partridge, 1978). This can in turn be used to find areas containing tectonic fractures. Using the models presented in Chapter 1 under "Tectonic Fractures," subsurface orientations can then be predicted. Fracture intensity must then be predicted using the principles discussed later in this chapter. The correspondence of surface and subsurface fracture data in an eastern U.S. oil field is given in Overby and Rough (1971). For further reading, see Prost (1994).

Application of Direct and Indirect Techniques

The best procedure appears to be empirically determining the best logging or technique suite, which works for the formation of interest in a particular area. If interest moves to other units or other areas, new suites may need investigation.

Most tools and techniques described here will work in some manner for fracture detection, but they will not give a quantitative or even a relative measure of how many fractures exist in the reservoir. In general, detection tools give none of the quantitative fracture data necessary to evaluate a fractured reservoir and, in fact, are probably no more accurate at finding fractures than are geologic and rock mechanics predictions (Hirsch and others, 1981). However, these tools are often important in isolating fractured zones or units where concentrated quantification is needed to properly evaluate the recovery potential and plan a production strategy. If fracture presence and intensity in a fractured reservoir cannot be detected in the wellbore, it is necessary to predict them. The following discusses the techniques and parameters currently available for those predictions.

PREDICTION OF SUBSURFACE FRACTURE SPACING

Fractures are virtually always present in rock. However, they are most often distributed in an ineffective manner with respect to reservoir fluid flow. The geologist's task is to determine when and where fracture distribution becomes effective, and to plan development-drilling programs to take best advantage of the fractures that are there.

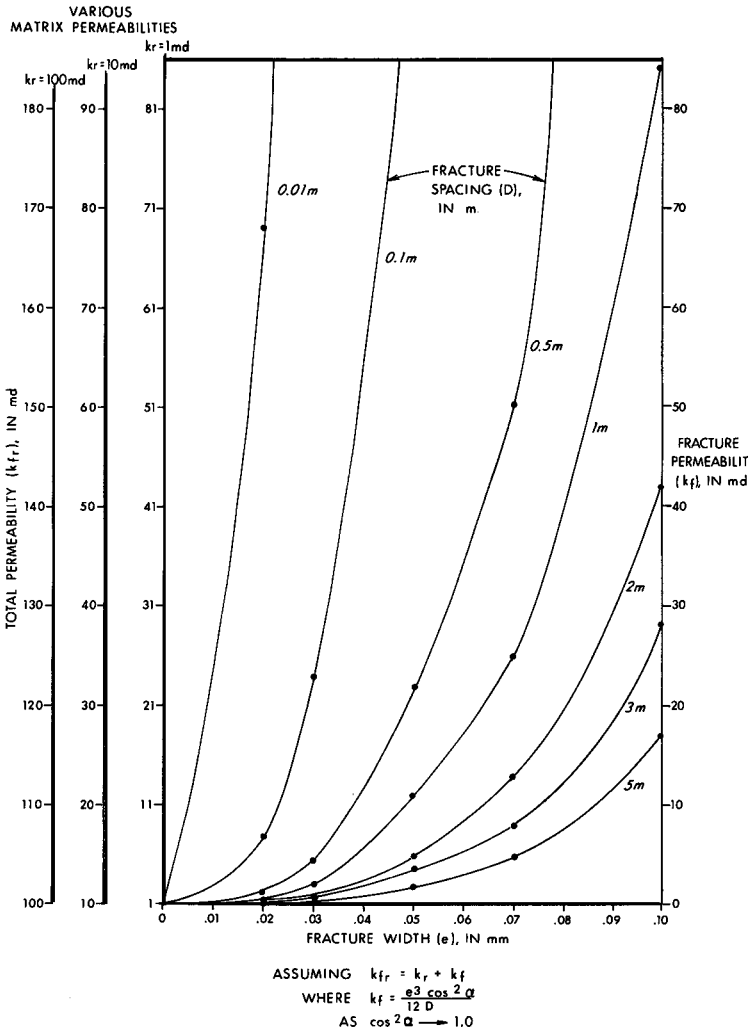


Figure 3-4 Graph of Equation 1-5, which depicts total formation permeability as a function of fracture width, fracture spacing, and matrix permeability.

Effective fracture distribution can be approximated with Parsons' equation (Equation 1-5 in Chapter 1). This equation incorporates matrix and individual fracture permeability as well as orientation and spacing of the fracture sets present. A graphical representation of the relationship between fracture permeability, fracture spacing, and fracture width can show the relative importance of each parameter (Figure 3-4).

Subsurface fracture and matrix permeability can be approximated in the laboratory as related in Chapter 1. Subsurface fracture orientation can be determined in some cases by core observation and by predictions based on the relationships discussed in Chapter 1.

Several geological parameters are important in controlling fracture spacing in subsurface rock units:

1. Composition
2. Grain size
3. Porosity
4. Bed thickness
5. Structural position

Relative fracture spacing can be predicted through the analysis of these parameters. In general, relatively stronger, more brittle rocks will contain closer-spaced fractures. Therefore, any parameter that strengthens or embrittles a rock will increase its fracture intensity during deformation. The remainder of this section will discuss these five parameters. This discussion should be considered an outline of present knowledge on the subject.

Composition

Several authors have pointed out the relationship between fracture spacing-or density-and lithology (Stearns, 1968b; Stearns and Friedman, 1972; and Currie, 1974). This observation is characteristically related by authors to the strength or ductility of the rocks involved (Figures 3-5 and 3-6). In general, rocks with a high percentage of brittle constituents will have closer-spaced fractures than those with a lower percentage. (This, of course, assumes similar stress and environmental conditions for the two rocks.) In most sedimentary reservoir rocks, the primary brittle constituents would generally be the various forms of quartz, feldspar, dolomite, and sometimes calcite (Figure 3-7).

Porosity

Rock strength decreases with increasing porosity. This relationship has been worked out by Price (1966), Dunn and others (1973), and Hoshino (1974). The relationship is, however, not linear (Figure 3-8).

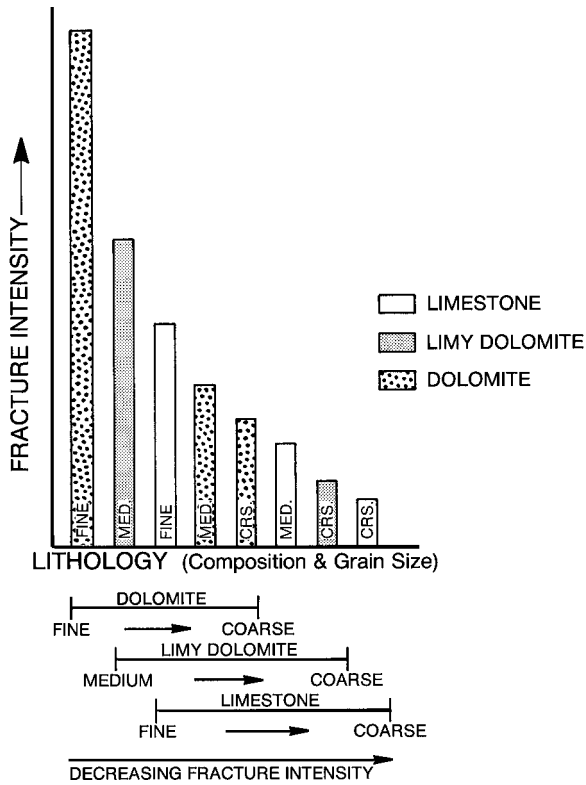


Figure 3-5 Histogram showing relative tectonic fracture intensity as a function of lithology (mineral composition and grain size). Modified from Sinclair (1980).

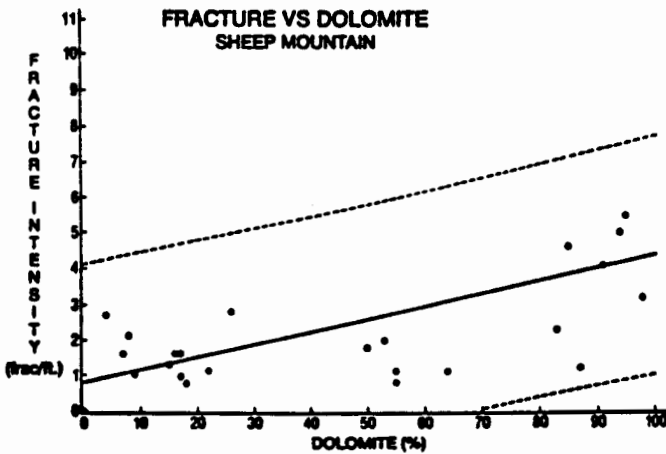


Figure 3-6 Outcrop measurements of fracture intensity and corresponding percent of dolomite in the Mississippian Madison Limestone on Sheep Mountain Anticline, Bighorn Basin, Wyoming.

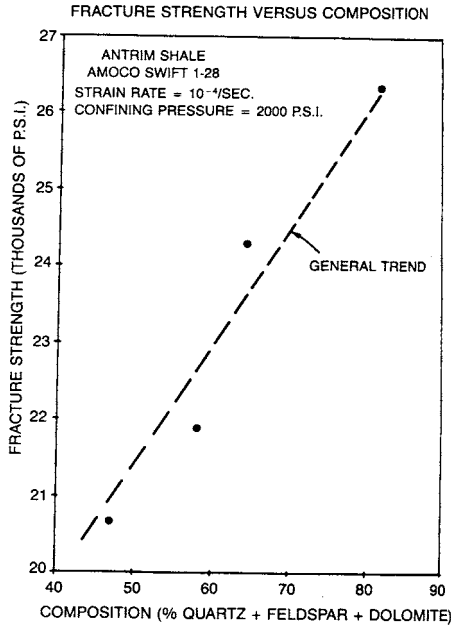
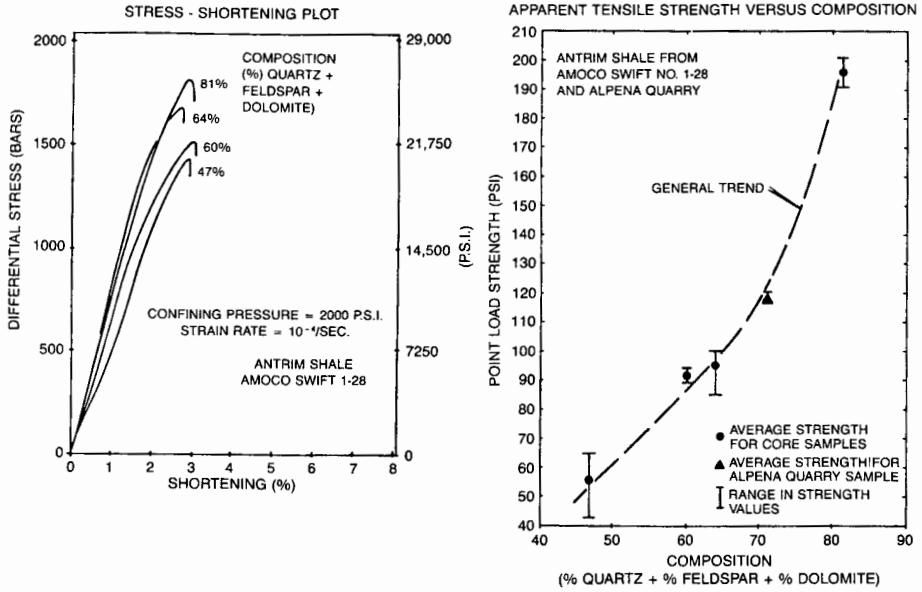


Figure 3-7a, b, and c Effect of mineral composition on the strength of core and outcrop samples of Devonian Antrim shale, Otsego County, Michigan. Composition is defined by the abundance of brittle minerals present (quartz, feldspar, and dolomite).

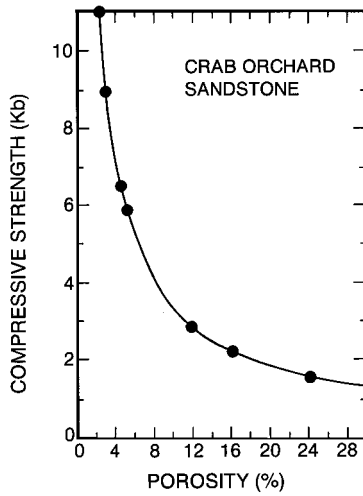


Figure 3-8 Compressive strength as a function of porosity. After Dunn and others (1973), courtesy of American Geophysical Union.

In general, lower-porosity rocks of similar composition and fabric will have closer spaced or more numerous fractures than relatively higher-porosity rocks (Figure 3-9). In addition, within sandstones, lower-porosity rocks may have less intensely deformed shear fractures than higher porosity equivalent sandstones.

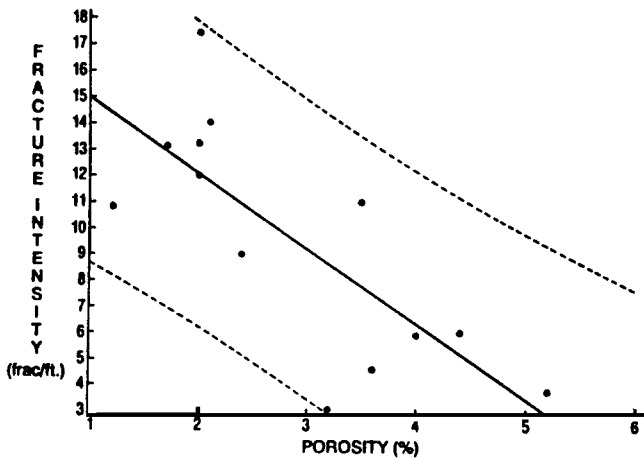


Figure 3-9 Outcrop measurements of fracture intensity and corresponding percent of porosity in the Lower Paleozoic Dolomite on an anticline near Gibson Reservoir, Sawtooth Mountains, Montana. Note the decreasing fracture intensity with increasing porosity in the rock. Measurements were made by B. Ward.

Grain Size

In well-sorted clastic rocks, decreasing constitutive grain size increases compressive and tensile strength (Gallagher, 1976; Ramez and Mosalamy, 1969). This increase in strength is apparently due to an increase in specific surface energy (a surface-to-volume function) as the grain diameter becomes smaller (Brace, 1961).

The observation is also made that in a clean clastic section, such as the Mesozoic rocks of the Colorado Plateau, decreasing grain size gives increasing fracture intensity. This effect is often hard to single out, however, because beds of finer grain size are often thinner than corresponding coarser grained beds.

No quantitative relationship between constitutive grain size and fracture spacing currently exists. The qualitative relationships that can be shown deal with the effect of grain size on fracture strength and the subsequent effect of strength on fracture intensity (Figures 3–10 through 3–12).

Bed Thickness

Considering all other rock parameters and loading conditions to be equal, thinner beds will fracture at a closer spacing than thicker beds. This general relationship has been documented in the literature by Bogdanov (1947), Harris and others (1960), Price (1966), Sowers (1970, 1972), McQuillan (1973), and Ladiera and Price (1981). Examples of some of their data as well as new data by this author are included in Figures 3–13, 3–14, and

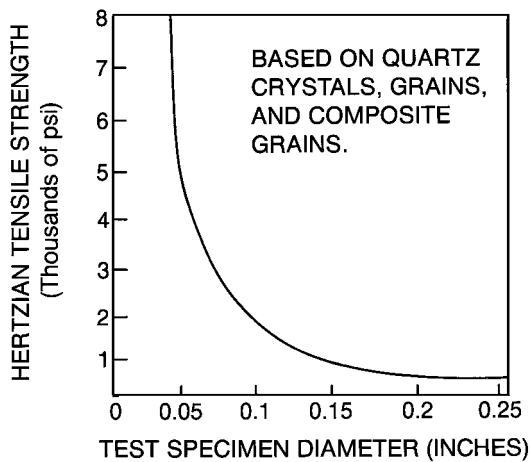


Figure 3–10 Tensile strength as function of grain diameter (specimen diameter for composite grains). After Gallagher (1976), courtesy of Utah Engineering Experiment Station.

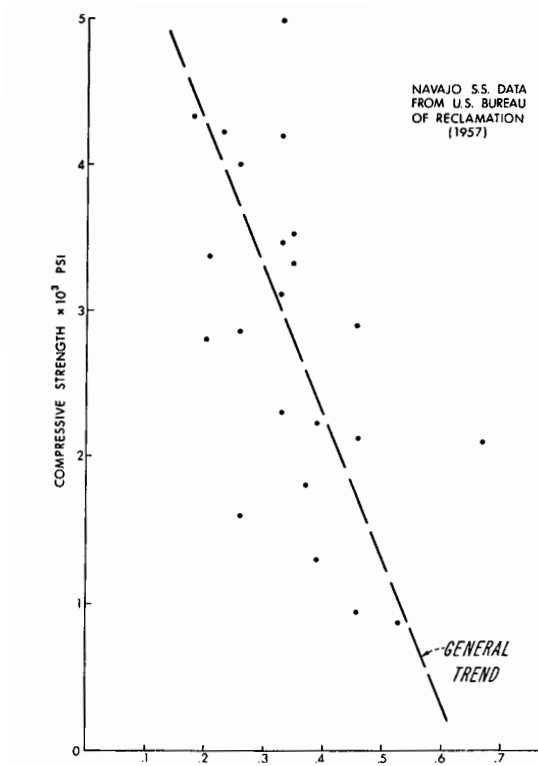


Figure 3-11 Uniaxial compressive strength versus average grain diameter plot for Jurassic Navajo Sandstone samples from near Page, Arizona.

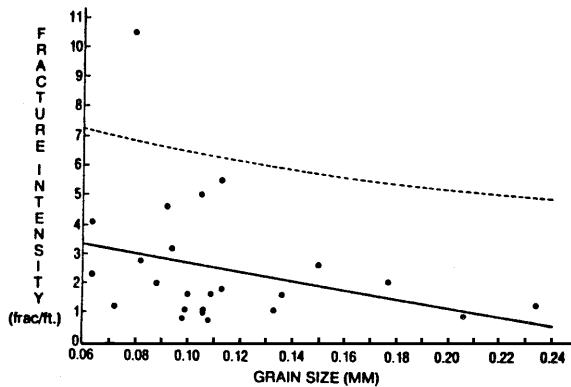


Figure 3-12 Outcrop measurements of fracture intensity and corresponding grain size in the Mississippian Madison Limestone on Sheep Mountain Anticline, Bighorn Basin, Wyoming. Note the slight decrease in fracture intensity with increasing grain size in the rock. Measurements were made by B. Ward.

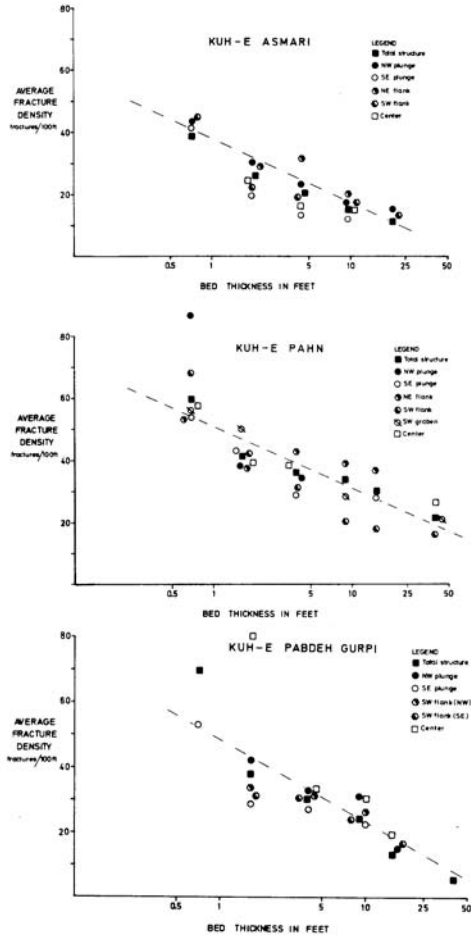


Figure 3-13 Tectonic fracture spacing versus bed thickness plot for carbonate rocks on three outcropping folds in the Middle East. From McQuillan (1973), courtesy of AAPG.

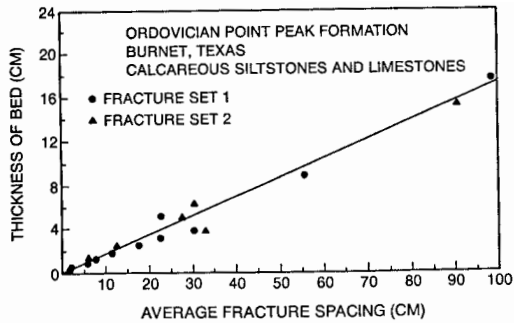


Figure 3-14 Bed thickness versus fracture spacing plot from Sowers (1970).

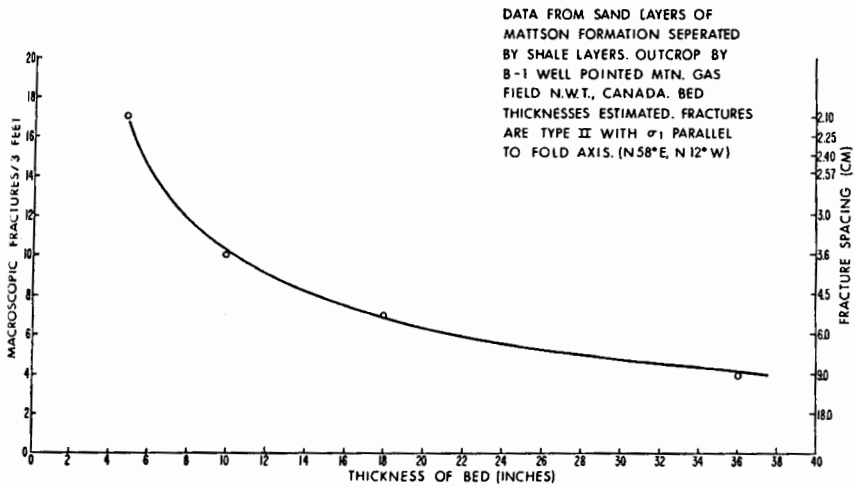


Figure 3-15 Tectonic fracture spacing versus bed thickness plot from outcrop data, Pointed Mountain Field, N.W.T., Canada.

3-15, and summarized in Figure 3-16. This relationship, which has been statistically verified by Quillin (1983), can be used to predict subsurface fracture spacing from both core and outcrop data. For instance, if fracture data are available in outcrop from a lithology similar to a subsurface rock of interest and in the same structural position, the change in fracture intensity due to a bed thickness change can be obtained. This can be done by plotting bed thickness against fracture spacing (Figure 3-16), and constructing a straight line through the data points and, in some cases, the origin. Interpolation and extrapolation of these thickness/spacing data can then be made from the outcrop to the subsurface unit. Ladiera and Price (1981), however, take a slightly different approach to constructing these lines, making them two straight-line segments instead of one, although the physical significance of the two slopes is not clear.

A similar approach can be used when working with core data. Often the diameter of the core is too small to intersect enough fractures parallel to the core axis to allow for spacing measurements in the thicker, possibly more productive units to be made. Data on several thin beds with measurable fracture spacings can be extrapolated to the thicker units with unknown spacings.

These relationships should be used only when all other parameters discussed in this section are held constant. Though thinner beds have higher fracture spacing than thicker beds, care must be exercised in extrapolation

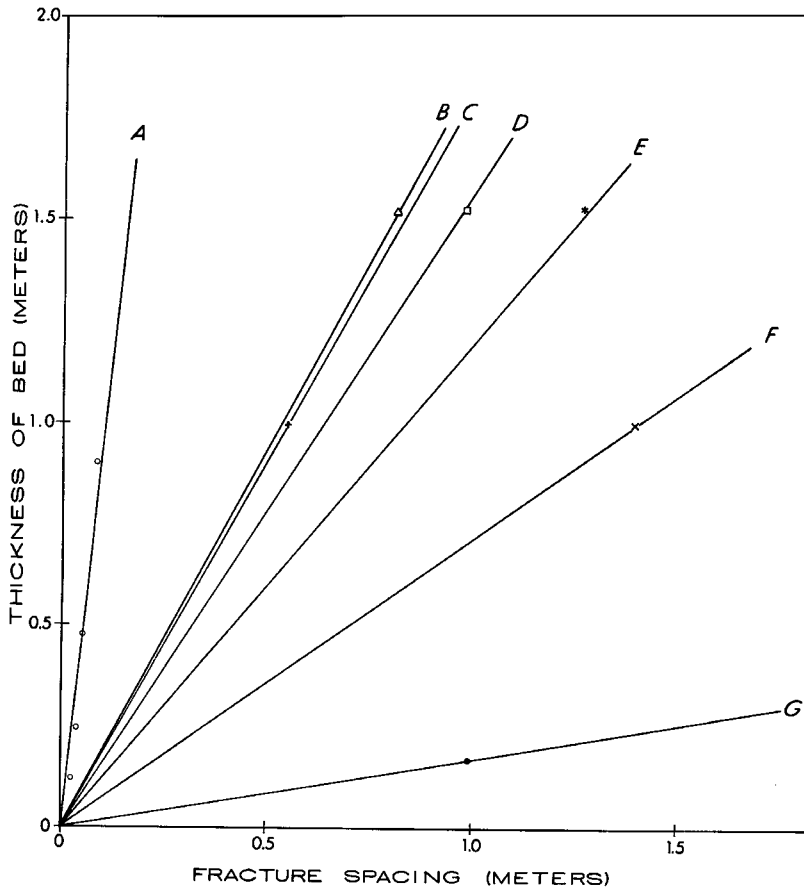


Figure 3-16 Bed thickness versus fracture spacing, composite diagram. Data is from (A) Figure 3-15; (B, D, E) McQuillan (1973); (C, F) Bogdanov (1947); (G) Sowers (1970). In all but curve (A), symbols are not data points but slope construction points from the original published data.

because often two parameters change spacing in the same way at the same time. For example, finer-grained sandstones often occur in thinner beds than their coarser-grained equivalents. If just the difference in bed thickness were used in extrapolation from a bed thickness versus fracture spacing curve in a sandstone that also saw a reduction in grain size, predicted spacing would be too low. Two works that deal with the theoretical basis for bed thickness effects on fracture intensity are Hobbs (1967) and Sowers (1972). Sowers concluded that extension fractures could be treated by an instability function with their spacing controlled by elastic differences between the beds and the bed thickness.

Structural Position

Rocks undergoing fracture exhibit increased fracture intensity with increased strain. For example, in outcrop, brittle quartzite will contain closer-spaced fractures after experiencing 10 percent strain than after 2 percent strain. Considering fracture alone, this relationship is only qualitative. If some ductile behavior occurs, the relation becomes more complex. Price (1966, page 143) relates the number of fractures developed in a rock to the strain energy originally stored in the rock. He writes:

$$W = \frac{1}{2}\sigma \times \epsilon \quad (3-1)$$

where w = strain energy
 σ = stress component
 ϵ = resulting strain component

Assuming from linear elasticity

$$\epsilon = \sigma \times E \quad (3-2)$$

where E = Young's modulus, and

$$w = \sigma^2/2E \quad (3-3)$$

Price concludes that a rock with relatively high calculated strain energy will have more frequent fractures than a rock of equal thickness with relatively low calculated strain energy. Price does point out that this is only one relative or qualitative approach to fracture intensity predictions. The major use of the total strain approach is in predicting fracture intensity with structural position. This can be done in two ways. First, by analytically solving boundary value problems or by applying finite element approximations, we can determine stress and strain distribution in simple geologic models. These general strain maps or cross sections can be combined with structural geometry from seismic data and fracture intensity data from a core to predict changes in fracture intensity away from the wellbore (Figure 3-17).

A second way that fracture intensity with structural position can be predicted is by using the radius-of-curvature or rate-of-change-of-dip approach. This method (with several variations) has been used with success by Murray (1968) and McCaleb and Wayhan (1969). This approach as-

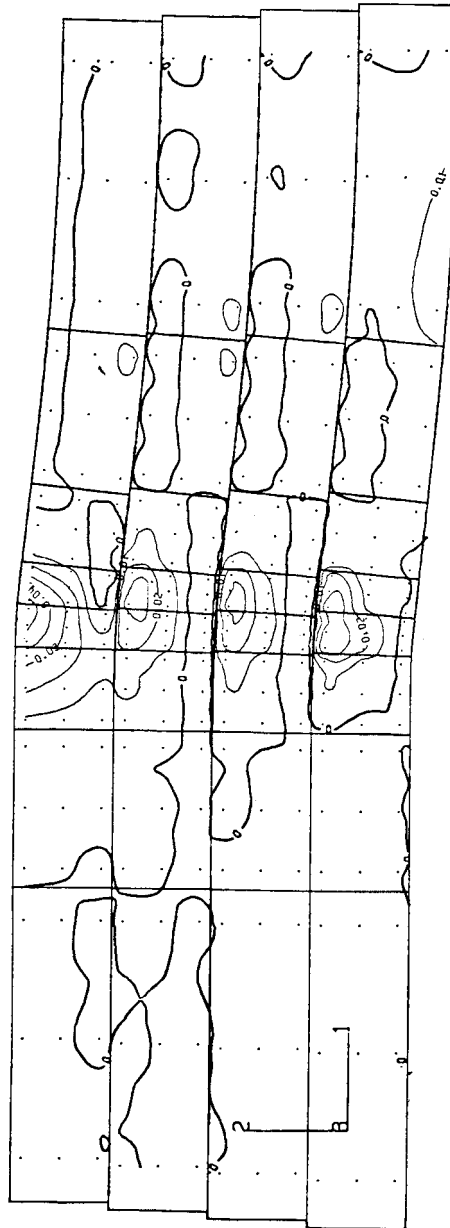


Figure 3-17 Finite element mathematical modeling of a four-layer fold developed by fault displacement from below. Contours are for equivalent plastic distribution in the model. Courtesy of N.G. Higgs.

sumes that flexure-related fracturing will occur in its highest intensity (lowest fracture spacing) where rate of change of dip or curvature is a maximum (see Figure 3-18). The assumptions of this technique are that:

1. The rock involved is brittle and fails predominantly by fracturing.
2. An increase of curvature gives an increase in strain.
3. This increase in strain gives an increase in fracture intensity.

This fracture intensity prediction method lends itself quite well to log- and seismic-derived subsurface data. An example of the relationship between curvature and fracture intensity for two very different rocks at Lost Soldier Field in Wyoming is given in Figure 3-19.

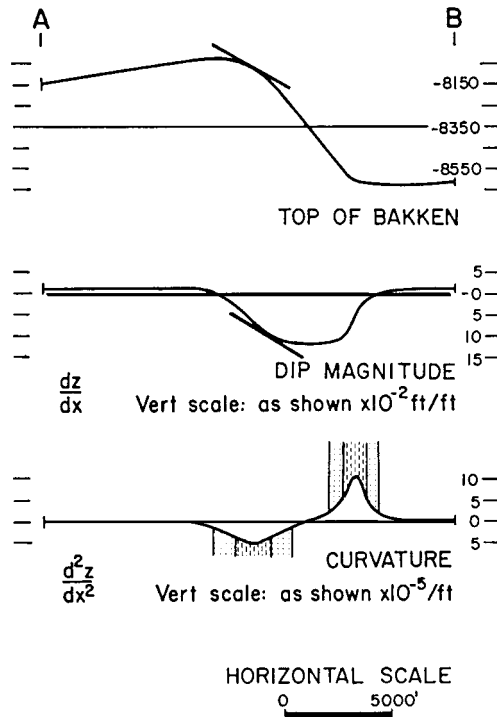


Figure 3-18 Curvature approach to predicting zone of high tectonic fracture intensity. From Murray (1968), courtesy of AAPG.

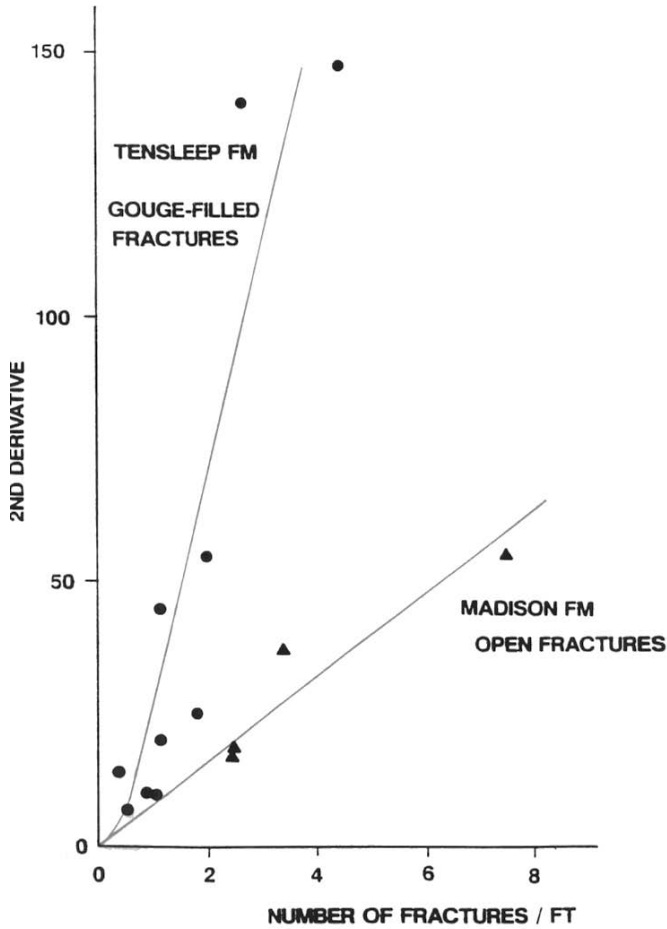


Figure 3-19 A cross plot of second derivative curvature versus fracture intensity derived from core observation for two fractured reservoirs in Lost Soldier Field, Wyoming. Two distinct relationships are shown for gouge-filled fractures in Pennsylvania Tensleep Sandstone and open fractures in Mississippian Madison Limestone. Measurements were made by J. Tilden and H. Harrison.

SUMMARY

The strength and ductility of a reservoir rock are important parameters in determining fracture intensity. In outcrop, strong rocks fracture more intensely than weak rocks. In shallow crustal fracturing, strong rocks are usually brittle. As such, they cannot sustain much strain before failing, and they fail predominantly by fracture. This is why in most rock sections the stronger, more brittle rocks contain relatively more fractures than the more ductile rocks, which can dissipate strain more efficiently by various methods.

In reality, fracture intensity is probably related to strain or a combination of stress and strain. Fracture toughness or the area under a laboratory stress-strain curve(s) from origin to fracture has been used by some to predict relative fracture intensity. If the rocks behave in a brittle manner, the greater the fracture toughness (greater area gives greater fracture toughness), the greater the fracture intensity or smaller the fracture spacing. However, most sedimentary rock sections, in which we try to predict fracture intensity, display minimal differences in strain at failure under a given set of conditions. Because of this, the area under the curves (fracture toughness) is predominantly a function of stress or strength. This is probably why strength correlates relatively well with fracture intensity in outcrop for brittle rocks.

For two equally brittle rocks, the stronger of the two will contain closer-spaced fractures. The problem of prediction by strength becomes more complicated, however, when the style of loading is considered. If a layered rock package is end-loaded so that each unit is in contact with the forcing member (say a piston), the strong brittle units would sustain the greater stress difference. If, on the other hand, the load is applied perpendicular to the bedding, it is the ductile, usually weaker rock that sustains the majority of the strain.

Both strength and ductility are important in controlling the fracture process in rock. Both do not vary together in all rocks. For example, in many rocks, strength increases with increasing ductility. This change, however, is generally brought about in the laboratory by significant changes in environmental parameters, such as large increases in confining pressure or temperature. Changes in rock ductility are difficult to quantify and are most useful in defining large variations in environmental parameters in natural deformations. Rock strength in the brittle field, on the other hand, is very useful in defining rock property variations. In fractured reservoirs, we are generally dealing with rock packages that have not experienced large variations in environmental parameters; within one unit or between units. The rocks of interest in these reservoirs, for the most part, are brittle. The sig-

nificant variations present are petrologic. Because we deal with predominantly brittle deformations that vary in petrology and not in environmental conditions, strength is considered a more sensitive indicator of fracture intensity than contrasts in ductility.

In summary, for most outcrops exhibiting regular fracture patterns, it is the stronger more brittle rock units that contain the most numerous fractures. The strength/fracture spacing relationship has been addressed by two related papers: Hugman and Friedman (1979), and Sinclair (1980). Hugman and Friedman (1979) showed experimentally that grain size, composition, and porosity directly influenced the strength of carbonates, in that order. Sinclair (1980) reported the same relative effect of grain size, composition, and porosity on outcrop measured fracture spacing in fold-related tectonic fractures in carbonate rocks in Montana (Figure 3–20).

Five rock variables and their effect on fracture spacing have been discussed briefly in this section, and all are intimately interrelated. Strain at failure is a function of the strength and ductility of the rock, which in turn is a function of the composition, size, and fabric of the constitutive particles that make up the rock as well as the physical environment to which it is subjected. It has long been known that the exact rock strength and ductility or elastic modulus determined in the laboratory is a function of sample size. In this way, *in situ* bed thickness changes may also be affecting fracture spac-

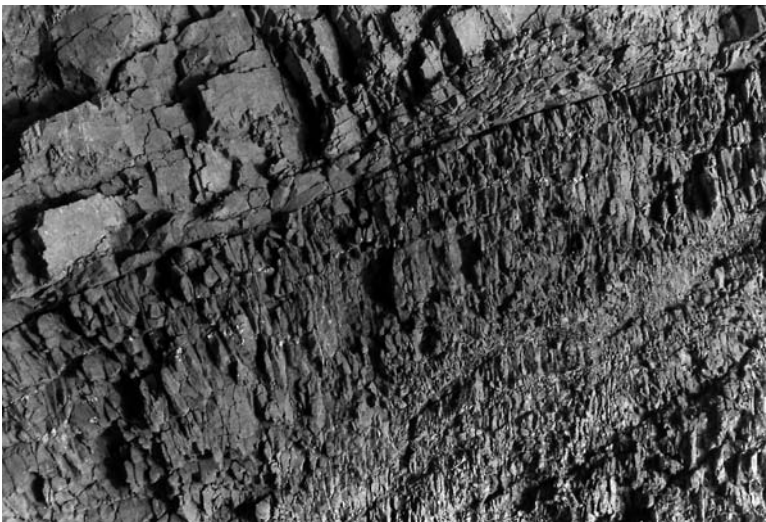


Figure 3–20 Outcrop fracture intensity variations as a function of rock composition. Higher fracture intensity layers are carbonates with larger amounts of dolomite, while lower fracture intensity layers are carbonates with higher amounts of calcite. These are tectonic fold-related fractures on a thrust belt anticline along the Sun River in the Sawtooth Mountains of Montana. Outcrop field of view is about 5 ft.

ing by altering rock strength and ductility. In some instances, data on one parameter are available while data on another, perhaps more pertinent parameter, are not. The important point to note is that a knowledge of several of these variables can allow us to predict fracture intensity in one unit relative to others. In this way, suites of mechanical tests on the rock types of interest, tests, which investigate the relative importance of several rock variables along the lines of Hugman and Friedman, can be an excellent tool for extrapolating limited rock data to the subsurface. The good correlation between the laboratory predictions of Hugman and Friedman (1979) and the later field measurements reported by Sinclair (1980) are cause for optimism.

Picking Well Locations and Well Paths in Folded Fractured Reservoirs

The porosity and permeability of natural subsurface fracture systems are a function of fracture spacing or intensity (how many fractures) and fracture aperture available for fluid flow (how wide they are). Horizontal wells can be used to optimize the contribution of both parameters in fractured reservoirs. Since we can do little in early exploration to actively high-grade fracture aperture, much of our exploration activity in these reservoirs involves high-grading fracture intensity.

Fracture intensity can be defined and predicted by a combination of material property variations (a function of mineral composition, porosity, grain size, and mechanical bed thickness), *in situ* conditions (depth, pore pressure, temperature, and rate of deformation), and strain distribution within the section (structural position). Because we are mostly interested in determining fracture intensity distributions in individual structures, the environmental parameters at fracturing are usually assumed to have been constant over the vertical and horizontal limits of the field, thus having little effect on relative fracture intensity variations. This leaves us with lithology and structural position as the prime factors to work with in picking optimum well locations, borehole trajectories, and completion zones.

Past experiences with fractured carbonate reservoirs have led us to conclude that, in many cases, lithologic variations have a somewhat larger effect on fracture intensity than does structural position. This conclusion will be detailed with the use of four carbonate rock sections of similar age and composition in the remainder of this manuscript.

Fracture Intensity

Outcrop observations from one section in the Western Wyoming Thrust Belt were used to detail fracture intensity variations in the Lower Paleozoic carbonates. This interval is typical of productive fractured reservoirs throughout the western U.S. and Canada. To accomplish this, measurements were made at five localities, four of which involved the Mississippian Madison limestone. The remaining locality contained both the Devonian Bighorn Dolomite and the overlying Devonian Darby calcareous siltstone. At each field locality, several fracture-measurement stations were selected where fracture spacing was recorded. These stations were selected to gain an understanding of both the vertical and lateral variation in fracture intensity within the folded section.

At each station, the following information was recorded: strike and dip of fractured bed, bed thickness, and the number of fractures encountered along two measurement lines. For exposed bedding surfaces, measurement lines 3 ft. long (0.984m) were laid out parallel to bed strike and parallel to bed dip. For measurements in cross section or cliff faces, measurements were taken parallel and perpendicular to bedding along the outcrop face.

At each station, the two fracture intensity numbers (fractures/foot) were averaged and plotted on perspective outcrop sketches (Figures 3–21 through 3–25). These figures depict both vertical and lateral variations in fracture intensity in deformed geometries similar to those producing in the subsurface in this area, for example, Whitney Canyon Field.

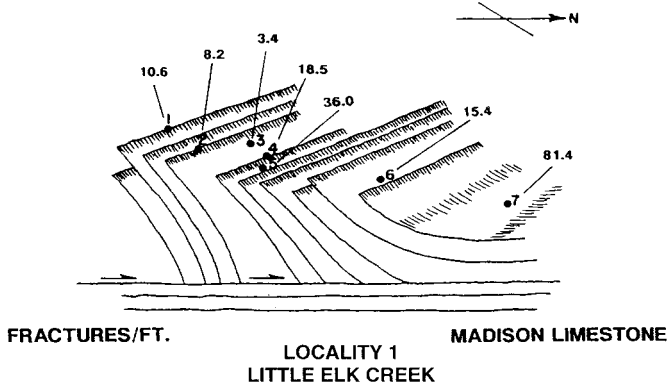


Figure 3–21 Fracture intensity measurements as a function of structural position in outcrops of Madison Limestone at Little Elk Creek in the Western Wyoming Thrust Belt. Measurements were made by S. Serra. From Nelson and Serra (1995). Figure reproduced with the permission of the Canadian Institute of Mining, Metallurgy and Petroleum.

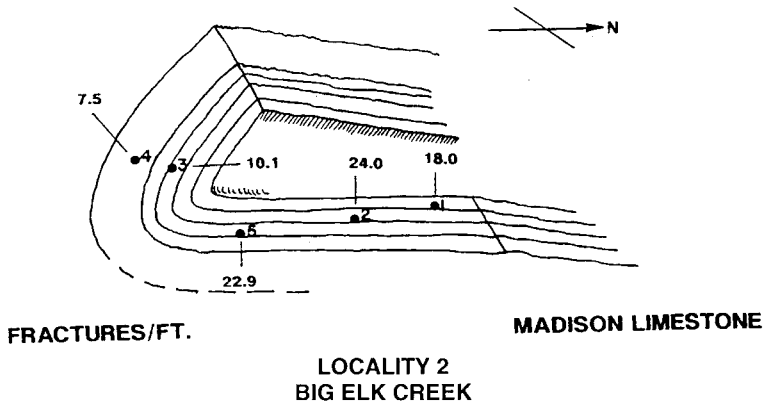


Figure 3-22 Fracture intensity measurements as a function of structural position in outcrops of Madison Limestone at Big Elk Creek in the Western Wyoming Thrust Belt. Measurements were made by S. Serra. From Nelson and Serra (1995). Figure reproduced with the permission of the Canadian Institute of Mining, Metallurgy and Petroleum.

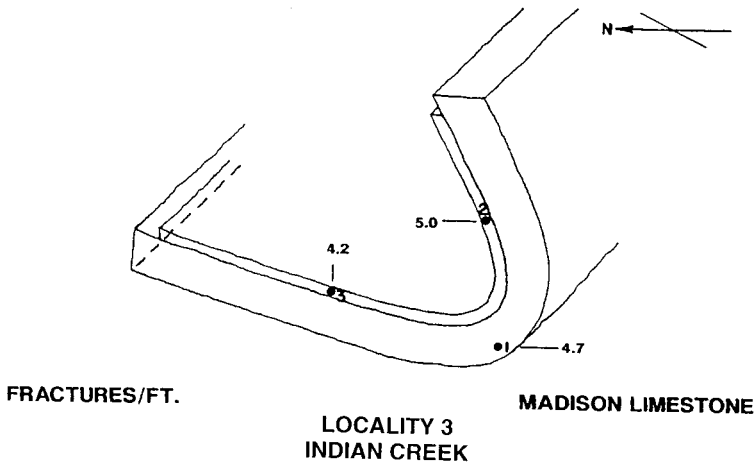


Figure 3-23 Fracture intensity measurements as a function of structural position in outcrops of Madison Limestone at Indian Creek in the Western Wyoming Thrust Belt. Measurements were made by S. Serra. From Nelson and Serra (1995). Figure reproduced with the permission of the Canadian Institute of Mining, Metallurgy and Petroleum.

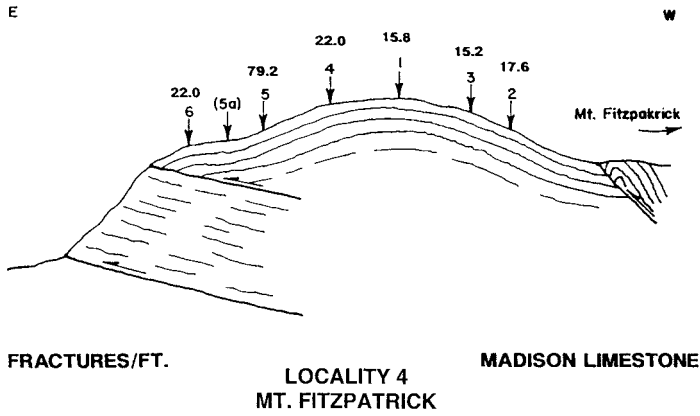


Figure 3-24 Fracture intensity measurements as a function of structural position in outcrops of Madison Limestone at Mt. Fitzpatrick in the Western Wyoming Thrust Belt. Measurements were made by S. Serra. From Nelson and Serra (1995). Figure reproduced with the permission of the Canadian Institute of Mining, Metallurgy and Petroleum.

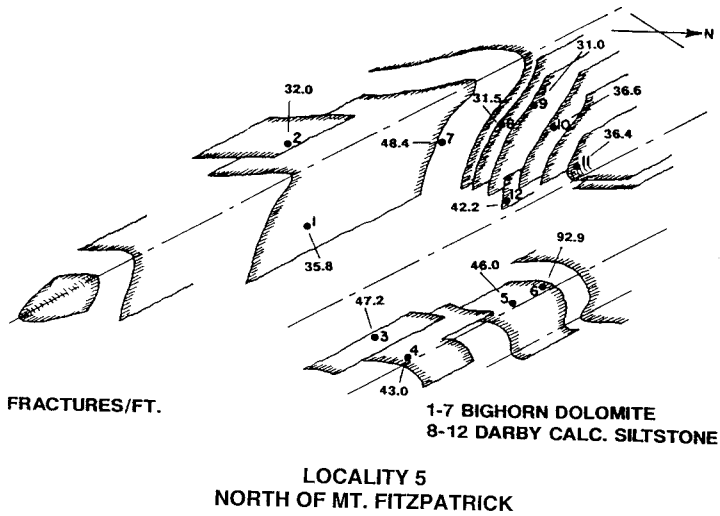


Figure 3-25 Fracture intensity measurements as a function of structural position in outcrops of Bighorn Dolomite and Dary Siltstone north of Mt. Fitzpatrick in the Western Wyoming Thrust Belt. Measurements were made by S. Serra. From Nelson and Serra (1995). Figure reproduced with the permission of the Canadian Institute of Mining, Metallurgy and Petroleum.

They show variations of both a primarily stratigraphic nature (such as in Figures 3–21 and 3–22) and of a primarily structural nature. While it is true that fracture intensities in surface outcrops are often somewhat higher than equivalent situations in the subsurface due to the combined processes of weathering and unloading, it is assumed that these processes affect individual outcrops equally. Thus, while intensities in outcrop may not be identical to those of equivalent situations in the subsurface (usually higher at the surface). The relative intensities among layers and within one layer as it crosses the structure are probably similar if not constant. As such, while absolute values may not be accurate, these fracture intensity variation maps can be compared with either laboratory measurements or predictions of hydraulic fracture aperture to estimate subsurface fracture porosity and fracture permeability variations likely to be encountered in the subsurface.

An alternate way of viewing these data is by use of frequency diagrams of the combined data. A histogram of all Wyoming Thrust Belt field measurements taken is displayed by rock type in Figure 3–26. Such distribution diagrams are standard for most reservoir engineering approaches when assigning average properties to reservoir models.

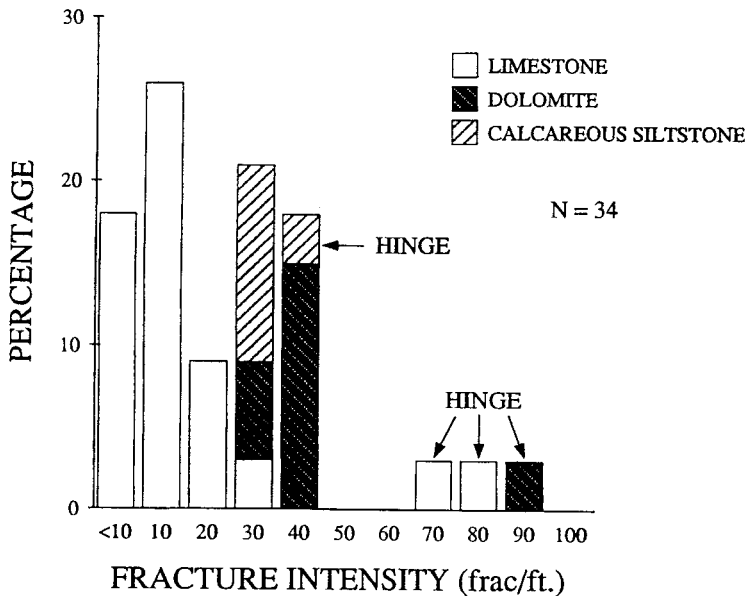


Figure 3–26 Diagram showing the frequency of fracture intensity measurements for fold-related fractures measured in the outcrops shown in Figures 3–21 through 3–25. Highlighted are various rock types measured and hinge versus flank positions. From Nelson and Serra (1995). Figure reproduced with the permission of the Canadian Institute of Mining, Metallurgy and Petroleum.

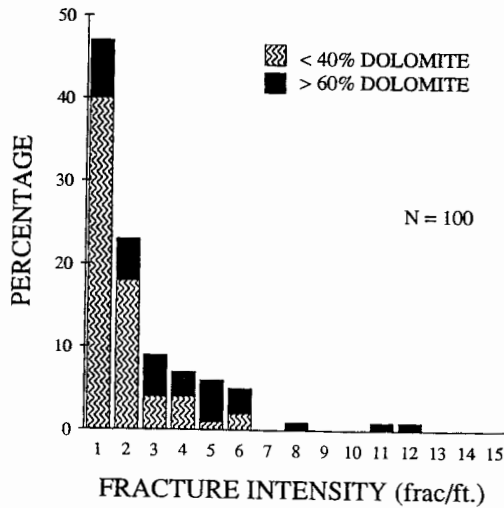


Figure 3-27 Diagram showing the frequency of fracture intensity measurements for fold-related fractures measured in the outcrops of Madison Limestone at Sheep Mountain in the Bighorn Basin of Wyoming. These measurements were all taken from the backlimb of the asymmetric anticline. Highlighted are measurements in rocks of less than 40 percent dolomite and greater than 60 percent dolomite. From Nelson and Serra (1995). Figure reproduced with the permission of the Canadian Institute of Mining, Metallurgy and Petroleum.

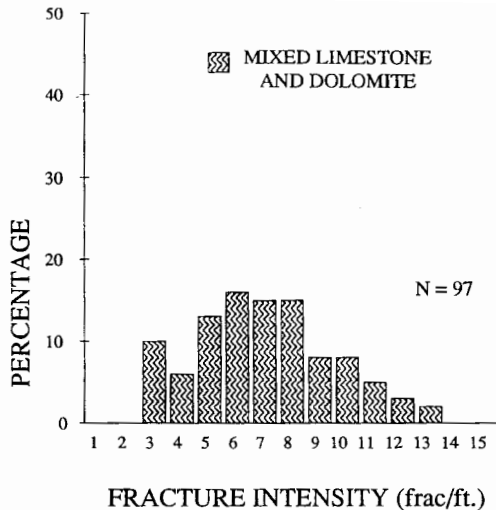


Figure 3-28 Diagram showing the frequency of fracture intensity measurements for fold-related fractures measured in the outcrops of Madison Limestone at Sheep Mountain in the Bighorn Basin of Wyoming. These measurements were all taken from the forelimb of the asymmetric anticline. The rocks are a mixture of limestone and dolomite. From Nelson and Serra (1995). Figure reproduced with the permission of the Canadian Institute of Mining, Metallurgy and Petroleum.

This distribution compares favorably with data collected in a similar manner from three equivalent Madison and Darby sections at (1) Sheep Mountain, (2) a Rocky Mountain foreland structure in the Bighorn Basin (Figures 3-27 and 3-28), and, (3) from a Mississippian carbonate section from leading edge anticlines in the Rundle Group in the Canadian Thrust Belt near Grade Cache, Alberta (Figure 3-29). These three fracture intensity distributions display data from similar rock packages, but are from different locations involving various structural styles, field observers, and sizes of dataset. For example, the Sheep Mountain dataset is from a basement cored foreland “drapefold,” has the lowest overall fracture intensity and contains the greatest number of observations: N=197. The remaining two are from higher overall intensity “leading edge” anticlines in Laramide thrust belts, but contain fewer overall observations: N=51 for the two combined.

The Wyoming Thrust Belt observations (Figure 3-26) show that for measurement stations outside of fold hinges, lithology controls fracture intensity, with the dolomites most fractured and the limestones the least fractured. The calcareous siltstones are intermediate in fracture intensity, but have only slightly less fracture intensities than the dolomites. This distribu-

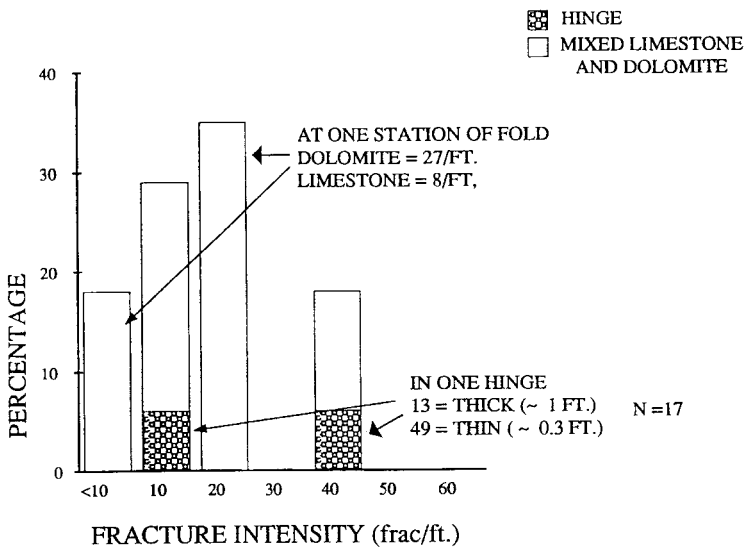


Figure 3-29 Outcrop-based fracture intensity frequency diagram for carbonates of the lower Paleozoic Rundle Group from leading edge anticlines in the Western Canadian Thrust Belt, Alberta. Frequency is expressed as percent of total population.

tion is logical and predictable. The general composition relationship for nonhinge sections is also shown in the Sheep Mountain backlimb dataset in Figure 3–27, where the higher fracture intensity observations are dominantly from dolomites. Unfortunately, the Rundle Group and Sheep Mountain forelimb datasets were not generally collected by lithology, making a parallel lithologic comparison impossible. However, at one station outside of a hinge on a fold in the Rundle Group, adjacent limestone and dolomite measurements were taken. There, the dolomite had 3.4 times the fracture intensity of the limestone (limestone = 8, dolomite = 27/foot or 27/0.3048m), thus generally substantiating the lithologic control in this dataset as well.

Hinge or forelimb deformation increased fracture intensity in all three datasets. However, the increase is variable and heavily influenced by rock type and bed thickness. For example, the Wyoming Thrust Belt dataset shows an increase in fracture intensity in all three lithologies in hinge zones, with the multiplier varying by rock type. The less brittle limestones, while lower in nonhinge fracture intensity, increased six to eight times within hinges; while the more brittle dolomites increased only a factor of 2.2. Such changes have also been seen and reported for the equivalent section in the Sawtooth Range of western Montana. Calcareous siltstones increased only 1.3 times, giving an intermediate fracture intensity response, but was relatively undersampled at 15 percent of the data. This is supported by the Madison Limestone map in Figure 3–24, where a four to five times increase in intensity is related to a gentle synclinal hinge, and in Figure 3–25, Stations 3 through 6, where dolomite fracture intensity increased only two times due to hinge strain.

Comparison of the Sheep Mountain backlimb and forelimb data shows an increase in average intensity in the high strain forelimb (roughly from 2 to 7 fractures/foot, /0.3048m, geometric average). However, the range in the forelimb population is slightly smaller (10 versus 11 for the backlimb), while the highest intensity only increased one fracture/foot over the backlimb. The major change is in the shape of the two distributions, from a very skewed distribution for the backlimb to a more symmetric one for the forelimb. As in the Wyoming Thrust Belt data, the higher intensity backlimb or nonhinge lithologies increased in the equivalent section in the forelimb less than the lower baseline lithologies.

Because of different sampling procedures, the Rundle data does not depict rock type or relatively significant numbers of hinge measurements, but does depict another important controlling parameter, bed thickness. The two hinge measurements shown in this figure are from two lithologically similar beds in the same hinge, but with different bed thicknesses. Here, a

decrease in bed thickness from 1.0 to 0.3 ft. (0.3048 to 0.1016m) increases the fracture intensity 3.8 times (from 13 to 49 fractures/foot, or fractures /0.3048m).

Analysis of these three above-mentioned datasets shows several interesting common characteristics including: (1) backlimb or nonhinge intensity distributions are wider or more variable than forelimb or hinge distributions; (2) brittle rocks such as dolomites have the highest fracture intensities in backlimb or nonhinge areas and in forelimb areas, but their increase within the hinge is less than that of the less brittle limestones possessing lower base level backlimb intensities; (3) restricted areas of nonhinge rock can exhibit as high or nearly as high fracture intensities as equivalent rock in hinge areas; and (4) the leading-edge folds are nearly an order of magnitude higher in fracture intensity than the foreland folds.

Well Trajectory

Assuming that the above observations hold in general for folded carbonate sections, several strategies can be invoked to optimize well trajectories or well paths in the exploration and exploitation phases for such reservoirs. These strategies consider relative fracture spacing variations among rock layers and how they range from backlimb, to hinge, to forelimb, as well as the dominant azimuth of fractures in these same fold domains. Optimum wellbore azimuth can be calculated when various sets of fractures exist with different spacings and stress-dependent widths. Such an approach is used in this discussion, except that the azimuthal variation of the *in situ* stress is considered small to negligible.

A hierarchy of optimized well paths for a typical asymmetric carbonate fold is given in Figure 3–30. The highest predicted production rates occur along wellpath A on Figure 3–30. At A, the well should encounter high intensity (low spacing) Type 2 fractures subparallel to the fold axis (Type 2 fractures are perpendicular to bedding and are subparallel to the bedding strike). The fracture intensity of all layers will increase when entering the hinge (assuming all are brittle and deform by fracture) with the difference in intensity among layers subdued in the hinge(s) compared to the flanks. As a result, the wellpath should intersect as many layers as possible in an azimuth perpendicular to the Type 2 fractures, or in the dip direction (well trajectory A on Figure 3–30).

Depending on the level of strain in the forelimb of the fold, wellbore A could be deepened to develop the steep limb of the structure, shown as wellbores B and B' on Figure 3–30. Wellbore B continues in the dip direction and would be optimum for intersecting Type 2 fractures from the limb that

has experienced a “migrating hinge” during fold development. Path B’ (bisecting dip and strike directions) attempts to intersect both Type 1 (perpendicular to bedding and subparallel to dip direction) and Type 2 fractures as might be expected in a “fixed hinge” development of the fold. The optimum azimuth of B’ would be dependent on the relative abundances of types 1 and 2 fractures. Once determined or predicted, published nomographs could be used to obtain this azimuth. Caution should be observed in booking reserves in the forelimb of such structures, however, until a well has tested the flank. Some folds have experienced high strain, high mean stress conditions in the forelimb, causing the limb to deform ductilily or in a compactive manner rather than by dilation involving fractures.

Well path C in Figure 3–30 is the next best predicted producer. It attempts to cross-cut Type 1 fracture sets in the backlimb of the fold. These fracture sets are less abundant than the Type 2 fractures in the hinge, but tend to be larger and interconnect greater vertical and lateral dimensions in the fold. The result on production is that C may have lower flow rates than A, B, and B’ but may eventually communicate greater reserves per well. Rates are lower because all layers will have lower fracture intensity than the hinge. However, certain optimum layers will have fracture spacings almost as good

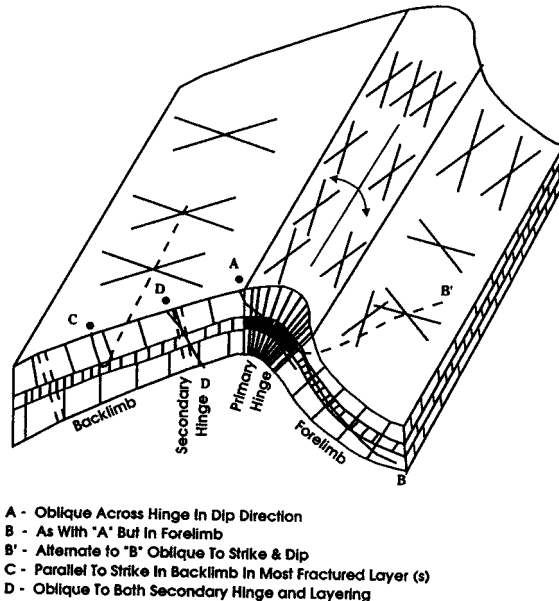


Figure 3–30 Diagram showing the frequency of fracture intensity measurements for fold-related fractures measured in Mississippian carbonate outcrops in the thrust belt in western Alberta. From Nelson and Serra (1995). Figure reproduced with the permission of the Canadian Institute of Mining, Metallurgy and Petroleum.

as that of the average of the hinge. The key to wellbore C is to select the optimum layer(s) and to have the horizontal portion of the wellbore run parallel to its boundaries and completely within it (wellbore C, Figure 3–30).

Another possible target in such a fold is shown as wellbore D on Figure 3–30. This trajectory attempts to develop more minor secondary hinges with relatively small dip inflections that sometimes occur on the backlimb of folds. These contain small swarms of Type 2 fractures that cut multiple layers within the fold. The optimum well path would cross the hinge and cross the layering in an oblique manner. Rates and reserves for these completions should be quite variable.

Several unique datasets of outcrop-derived fracture intensity in carbonate rocks depict the relative importance of lithologic and structural control on fracture distribution. It has been shown through various views of the data that lithology is a dominant control on fracture intensity especially in non-hinge areas of folds and that it also controls the relative increase in intensity within hinge zones to a lesser extent. Further, it appears that these characteristics predict fractured reservoir potential in restricted, optimum zones in backlimb or nonhinge fold areas that are as good as average hinge zone properties.

Several rules of thumb could be used to predict hinge zone fracture intensity. Limestone backlimb fracture intensities could increase four to eight times within hinge zones, whereas dolomites might increase only two to three times.

Overall, these four datasets in equivalent carbonate sections indicate that the fracture intensities of leading-edge thrust-related anticlines (Wyoming Thrust Belt and Rundle Group datasets) are nearly an order of magnitude higher than those of foreland anticlines (Sheep Mountain and Lost Soldier/Wertz Field datasets). This is logical as the leading edge folds were probably folded and unfolded more than once as the section passed through thrust ramps during emplacement, whereas the foreland folds experienced folding only once.

In terms of drilling directions, results indicate that backlimb wells should follow optimum stratigraphic layers, possibly in the strike direction; while hinge wells should cross-cut multiple horizons, possibly in a general dip direction. Optimum forelimb well tracks are dependent on rock type and the history of migrated or fixed hinges. Tracks cross-cutting layers and varying in azimuth from dip-parallel to 45 degrees to dip azimuth are possible.

4

Analysis of Anisotropic Reservoirs

Three main features can create strong reservoir anisotropy with respect to fluid flow:

1. Bedding and crossbedding (a primary rock fabric)
2. Stylolites
3. Fractures

Stylolites and fractures are both secondary features due to deformation or physical diagenesis of rocks. This chapter discusses these three features and how their effects on reservoir anisotropy can be quantified.

STYLOLITES

A stylolite is a common diagenetic rock feature that occurs most frequently in limestones, dolomites, and sandstones (Figure 4–1). As Park and Schot stated (1968, page 175):

Generally, stylolites are recognized as irregular planes of discontinuity between two rock units; the irregularities display the shape of “stylas,” the Greek word for columns and pyramids. Consequently, the two rock units appear to be interlocked or mutually interpenetrating along a very uneven surface. This surface is referred to as a stylolite, which is most commonly characterized by the concentration of relatively insoluble constituents of the enclosing rock.

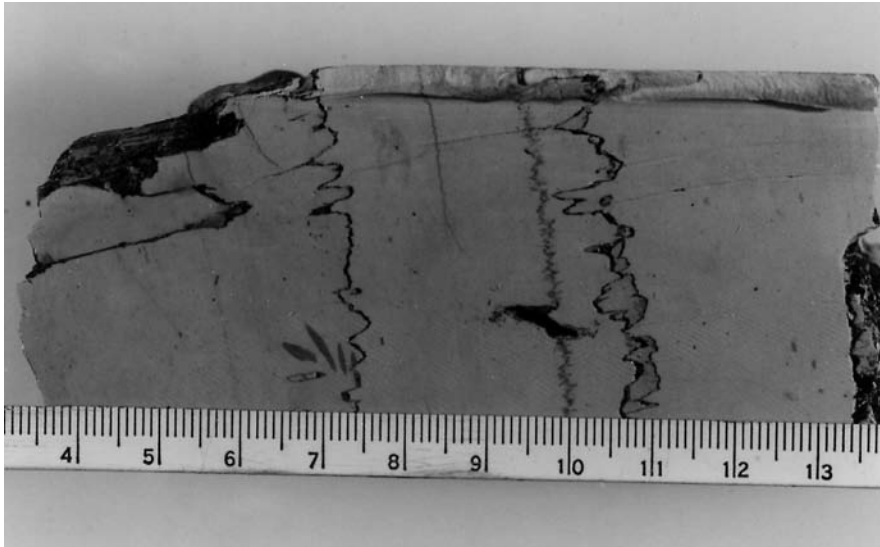


Figure 4-1 Example of typical stylolite morphology: core sample of Cretaceous chalk from the Amoco Norway 2/5-1 Well North Sea, 10,721 ft. Note the large variation in stylolite amplitudes. From Nelson (1981a). Courtesy of AAPG.

The seam material is generally fine-grained, dark-colored, and displays a degree of foliation parallel to the seam. As a result, the stylolite acts as a permeability discontinuity within the reservoir rock. Several classification schemes have been proposed for stylolites. Wanless (1979), for example, categorizes them on the basis of the presence and degree of suturing of seam material. Park and Schot (1968), on the other hand, classify them on the basis of the two-dimensional geometry expressed by the seam and its relation to sedimentary bedding. In addition, they define two scales of stylolites: those which have suture amplitudes larger than the grain diameter of the rock above and below the stylolite (aggregate stylolites), and those which have amplitudes smaller than the grain size of the host rock (intergranular stylolites). Aggregate stylolites will be discussed in the remainder of this chapter.

Stylolites are generally thought to be the result of pressure solution, a process that involves the creation of nonuniform solubility of mineral grains in an aggregate in response to a state of differential stress. Material goes into solution at highly stressed surfaces of the grains and is then either reprecipitated at surfaces of lower stress or removed from the system.

Stylolites and Their Contribution to Reservoir Anisotropy

Stylolite zones often have a variety of natural and induced fractures associated with them. The natural fractures intimately associated with the stylolite zone owe their origin to the same stress state that caused the stylolite. They have a distinct morphology and can, as the stylolites themselves, be used as a paleo-stress indicator (Choukroune, 1969; and Nelson, 1981a), (Figure 4–2).

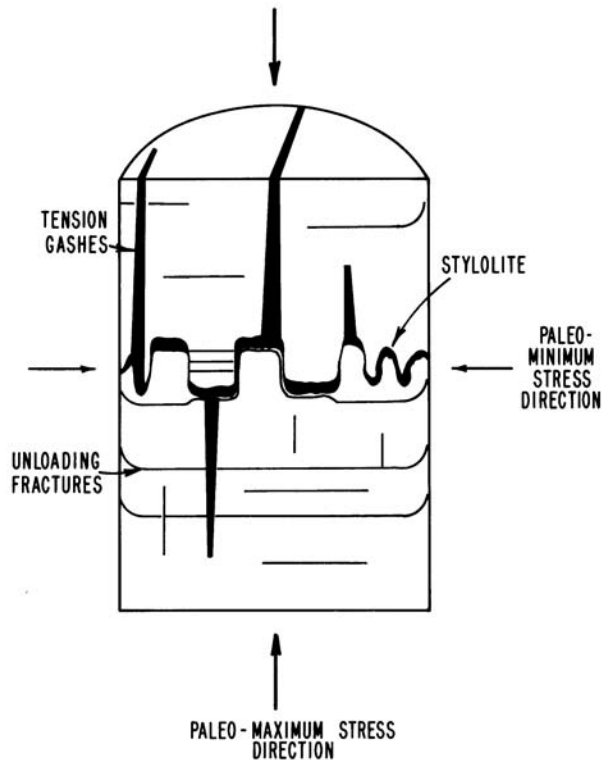


Figure 4–2 Schematic diagram showing geometric relation of stylolites, tension gashes, unloading fractures, and the paleo-state of stress that caused them. From Nelson (1981a), courtesy of AAPG.

Fractures Associated with Stylolites

Tension Gashes

As shown in Figure 4-2, the columns or “peaks and valleys” of a stylolite parallel the maximum stress or strain direction during formation (Choukroune, 1969; Groshong, 1975; and Nelson, 1981a). In some cases, there is a set of parallel fractures associated with stylolites that also follows this same maximum stress direction (Figure 4-2). These were called “tension gashes” by Choukroune (1969). They are probably not true tension fractures but extension fractures derived from the same compressive state of stress as the stylolite (Nelson, 1979). Many authors erroneously ascribe these fractures to an origin separate from that of the stylolites. Choukroune (1969) is the first to correctly point out the intimate association between stylolites and tension gashes.

These tension gashes are generally only a few inches in length, and parallel the peaks and valleys or columns of the stylolite. The fractures are often wedge-shaped and terminate at the stylolite seam at their wider end. Often they are filled with coarse, highly twinned calcite. Tension gashes rarely occur in the rock more than a few inches removed from stylolite. This fracture/stylolite association has been observed many times in stylolite zones from all over the world. It is a common and logical association (Figure 4-3).

Unloading Fractures

A second fracture set associated with some stylolites is made up of unloading fractures (Nelson, 1979, 1981a). While these fractures trend roughly parallel to the stylolite seam, they occur more precisely perpendicular to the maximum paleo-stress direction (Figure 4-2). They occur either at the seam itself or within the rock in the general vicinity of the stylolite. Because of surface texture and orientation they must be either extension fractures or true tension fractures formed by unloading or relaxation of the rock parallel to the maximum stress direction. This unloading is compatible with the original loading direction inferred from the stylolite (Figure 4-4).

Unloading fractures may develop in cores when they are taken out of their subsurface stress environment. These particular fractures are, therefore, generally induced and not true reservoir fractures. Some unloading fractures may, however, develop in reservoirs. For example, vertical, tectonic stylolites in the Twin Creek Limestone of the Western Wyoming Thrust Belt formed during thrusting. When thrusting ceased, relaxation parallel to the movement direction formed unloading fractures associated with the stylolites. All tension gashes and unloading fractures were subsequently filled with a later-stage calcite cement indicating their subsurface occurrence (Figure 4-5).



Figure 4-3 Examples of association of stylolites and tension gashes in 4-in. diameter core of Yamama Limestone, Darius Field (Wells D-3 and D-4), Persian Gulf. From Nelson (1981a), courtesy of AAPG.

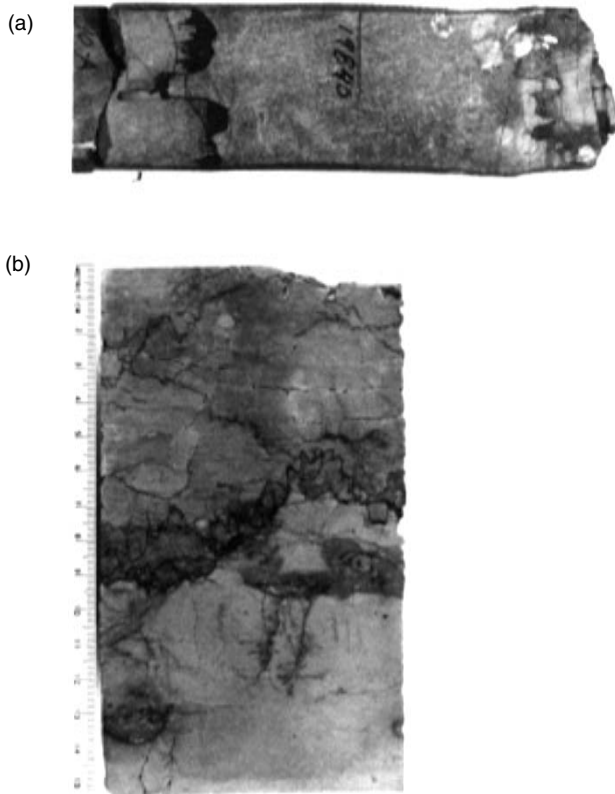


Figure 4-4 Core examples of association of stylolites and unloading fractures. Unloading fractures shown are induced and do not occur naturally in the subsurface. (a) Smackover Limestone, Amoco Amos 32-12, Baldwin County, Alabama; (b) Yamama Limestone, Darius Field, D-3 Well, Iran. Such induced fractures can give overly optimistic core test permeabilities. From Nelson (1981a), courtesy of AAPG.

While unloading in the direction of the *in situ*, maximum stress direction can and does occur in outcrop and in many cores, fractures interpreted as unloading fractures most often occur closely associated with stylolites. This association may indicate that pressure solution has not dissipated all of the stress concentration in that zone, therefore relieving it by unloading when removed from its subsurface restraints. This may indicate either a threshold value of stress difference for stylolitization to proceed, or possibly a rate problem—i.e., stylolitization too slow to dissipate all of the *in situ* stress concentration.

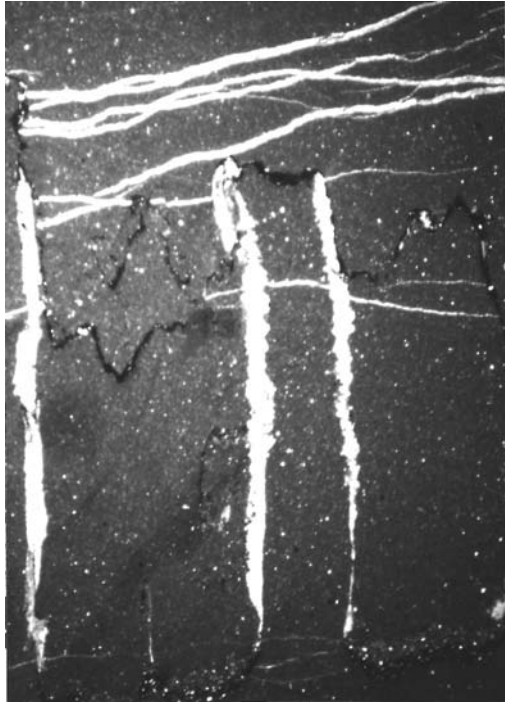


Figure 4-5 Thin section photomicrograph of natural unloading fractures associated with stylolite in Twin Creek Limestone core, American Quasar 3-1, Pineview Field, Summit County, Wyoming. From Nelson (1981a), courtesy of AAPG. (Magnification 16x.)

Stylolite Columns

Stylolite columns are bounded by slip surfaces that separate portions of the seam, which are advancing in either opposite directions or in the same direction at different rates (Figure 4-6). The columns often are slickensided and are sometimes filled with secondary mineralization. If secondary minerals are emplaced before stylolitization has ceased, the filling material becomes highly twinned and translated, i.e., crystallographic distortions (Figure 4-7).

Stylolite-Related Fractures and Strain During Deformation

Not all stylolites have tension gashes associated with them. The presence of tension gashes must, therefore, indicate something unique about the origin of the stylolite zones that possess them.

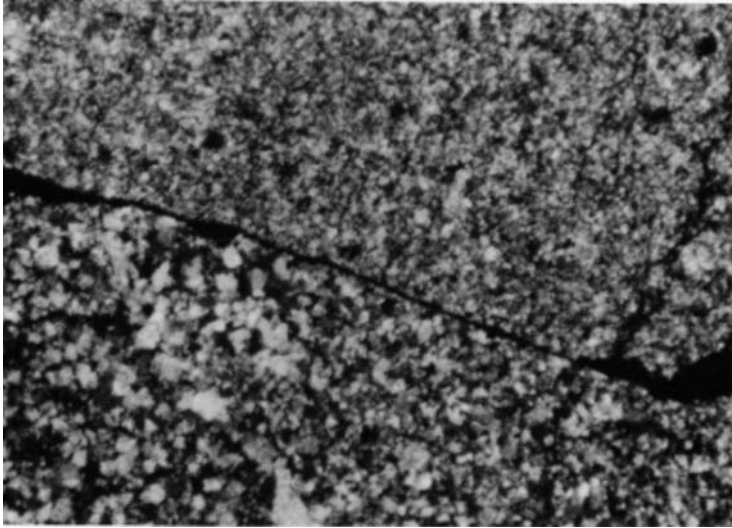


Figure 4–6 Stylolite column in thin section of Smackover, Amoco Amos 32-12, Baldwin County, Alabama. From Nelson (1981a), courtesy of AAPG. (Magnification 52x.)

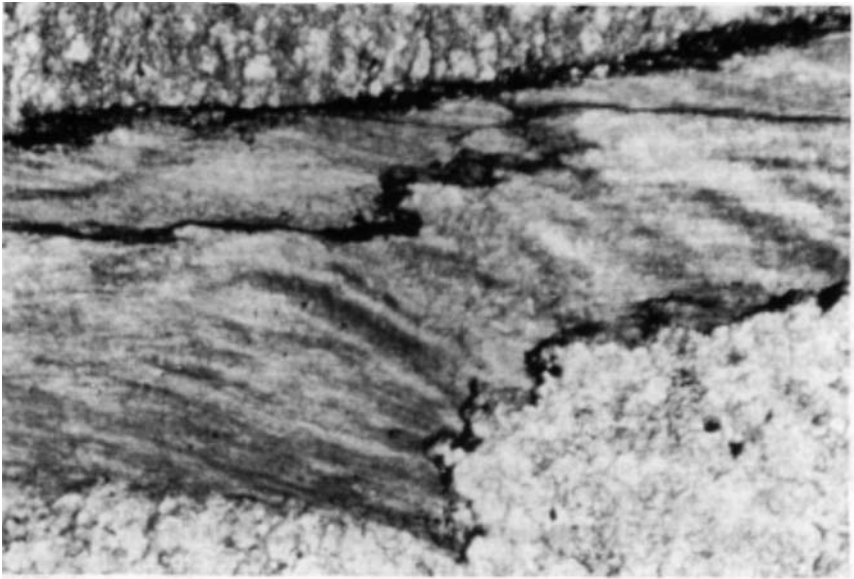


Figure 4–7 Crystallographically translated (deformed) carbonate crystals in stylolite column, Smackover, 19,847 ft., Amoco No. 2 Amos, Baldwin County, Alabama. From Nelson (1981a), courtesy of AAPG. (Magnification 57x.)

Stylolite zones display several associated displacement or strain patterns (Figure 4–8). A stylolite without fractures deforms the rock by uniaxial compaction, parallel to the maximum stress direction (Figure 4–8a). The laboratory test that most accurately reflects this state of strain is the uniaxial strain test (Brace and Riley, 1972; and Nelson, 1981b). The deformation of stylolite zones with associated tension gashes is, on the other hand, quite different and shows movement patterns that are more complicated (Figure 4–8b). Not only is there compaction parallel to the maximum principal stress direction, but there is also extension parallel to the minimum principal stress. These strain patterns are identical to those developed in standard laboratory triaxial compression tests (Figure 4–8c). In addition, this movement and strain pattern is identical to that accomplished by typical tectonic fracture sets (shear and extension fractures).

If stylolites with tension gashes are considered tectonic in origin, this association is not surprising. Deformationally, tectonic stylolites and tectonic fractures often appear to be two sides of the same coin. They can accomplish the same strain patterns during deformation although possibly at different rates.

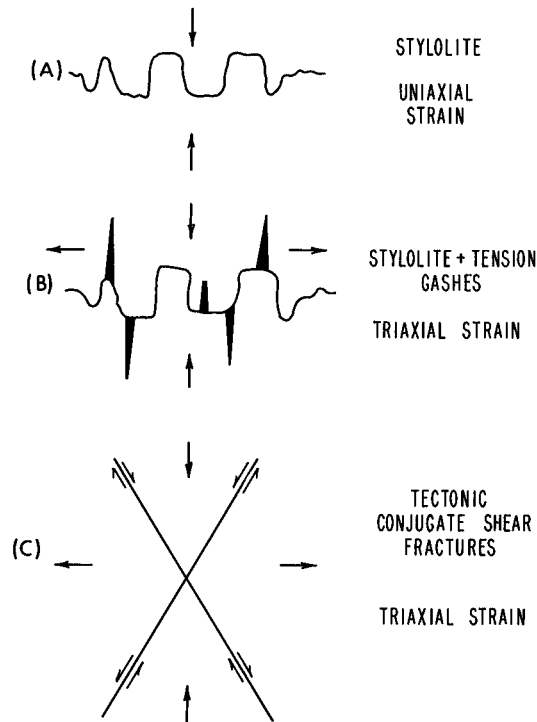


Figure 4–8 Idealization of movements associated with stylolites and fractures, assuming vertical maximum principle stress. From Nelson (1981a), courtesy of AAPG.

To accommodate movement patterns similar to tectonic fracture sets most efficiently, any fracture associated with a tectonic stylolite would tend to be an extension and not a shear fracture, i.e., no additional shortening parallel to the maximum stress direction and maximum extension parallel to the minimum stress direction. This agrees with observations of stylolite zones.

In general, any slow-rate tectonic process that involves soluble rocks that are pressure-soluble with a compaction in one direction and an extension at 90° to it should have stylolites with associated tension gashes. If the process involves only uniaxial compaction, stylolites without tension gashes should occur. A rapid-rate tectonic process may favor tectonic fracture sets instead of stylolitization. Thus, overburden-related stylolites may not possess tension gashes, while some tectonic stylolites may.

Fletcher and Pollard (1981) have an alternate point of view on the generation of tension gashes. In their model, tension gashes are generated by shear stresses along the seam, which are related to stylolite propagation at the ends of the seam. The model is quite innovative and envisions stylolitization mathematically as the inverse of an opening stable crack. While this seems an excellent approach, it does not explain why some aggregate stylolite occurrences have well-developed tension gashes and others do not.

Effect of Stylolite Zones on Porosity and Permeability

In general, the major effect of a stylolite in a reservoir is the creation of a highly directional, narrow zone of reduced porosity and permeability. These features can be treated in the same way as are tectonic gouge-filled fractures in reservoir analysis.

Stylolites are generally found in the lower-porosity portions of a core (Dunnington, 1967; Wood and Wolfe, 1969; Patrick and others, 1972; and Nelson, 1983). A number of these relatively low-porosity zones may be original or due to pre-stylolitization diagenesis and, therefore, localize stylolitization by causing stress concentrations. The remainder of these lower-porosity zones may be post-stylolitization or syn-stylolitization and due to local precipitation of pressure-dissolved material. Either case gives relatively low porosity associated with stylolites.

Because of the lower-porosity surrounding many stylolites and the presence of the fine-grained seam material, stylolite zones have a more reduced permeability compared to the adjacent underformed rock above and below (see Figure 4-9, top). This permeability reduction is greater perpendicular to the stylolite than parallel to it.

The presence of tension gashes and unloading fractures can drastically increase laboratory-measured permeability near stylolites. Therefore, great care should be taken in analyzing such data. Many of the associated unloading fractures are induced during or after coring and are not, therefore, reservoir features. Likewise, tension gashes related to one period of stylolization are always parallel (therefore, not interconnected) and their permeability is relevant only to the size of the measurement sample (plug or whole-core) and not to reservoir permeability (Figure 4-9). For example, three 4-inch-long, open parallel fractures will have a great effect on permeability in any laboratory-size measurement sample but will have no significant effect on reservoir flow.

Stylolites as an Indicator of Mechanical Properties

While much has been published on pressure solution and stylolization in the past (Stockdale, 1922, 1926, 1936, 1943, 1945; Bastin, 1940;

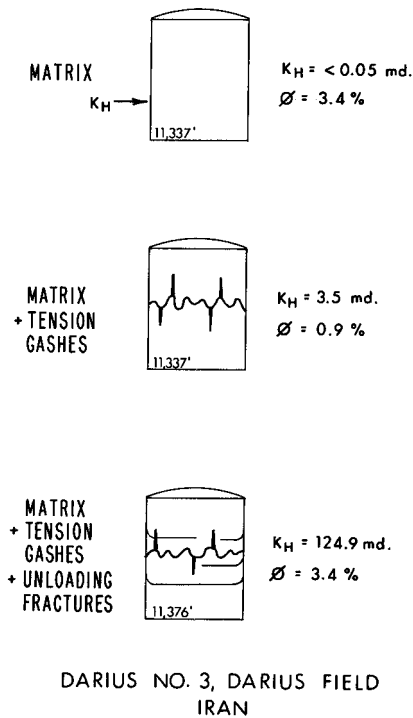


Figure 4-9 Effect of stylolites and associated fractures on laboratory permeability analyses. From Nelson (1981a), courtesy of AAPG.

Mossop, 1972; Bathurst, 1976; deBoer, 1977a, 1977b; and deBoer and others, 1977), the processes that determine the location of stylolites have been largely unaddressed. The following pages will briefly examine the localization of aggregate stylolites in light of the rocks' mechanical properties.*

Location of Stylolite Initiation

As defined in Durney (1972), pressure solution is "the phenomenon of dissolution of minerals under a nonhydrostatic stress." The grains of an aggregate tend to dissolve more at highly stressed surfaces than at surfaces of relatively low stress. Subsequently, the dissolved material is either reprecipitated at less stressed surfaces or transported out of the system.

Obvious areas of high stress concentration necessary to initiate pressure solution occur at grain-to-grain contacts (low contact areas) where suturing and microfracturing often occur (Heald, 1955; Trurnit, 1968; and Gallagher, 1976). A simple description of stress concentrations or gradients in the formation of larger aggregate stylolites where contact areas are large is, however, more difficult to accomplish.

Park and Schot state (1968, p. 188) ". . . in order for stylolites to develop (during diagenesis), inhomogeneities in fabric or composition, or both, in the sediment to promote pressure solution and explain the presence of seam material appear to be a prerequisite." Several mechanisms for localizing stylolitization have been proposed. These mechanisms may be manifested in rock property variations and identified on point-load hardness maps.

Once stylolitization is initiated along a plane, its growth and propagation can be modeled using the work of Fletcher and Pollard (1981). Their model envisions the compaction and propagation of a stylolite to be analogous to the opening and propagation of a crack. Thus, the mechanics of Griffith crack propagation (dilatency) can be used for the stylolite (compaction). The stylolite is, therefore, viewed as an anticrack with a sign change in the crack propagation mathematics.

Lithologic Boundaries

Stylolite seams often separate rocks of different lithology or rock composition (Park and Schot, 1968; Wood and Wolfe, 1969; Whitcombe, 1970; Collins and Smith, 1975; and Wariless, 1979). The most common occurrence of this lithology-related localization is that of dolomite and limestone in contact across a stylolite surface (Figure 4-10).

*Aggregate stylolites as used in this book are those whose amplitude is larger than the grain size of the rock in which they form (Park and Schot, 1968).

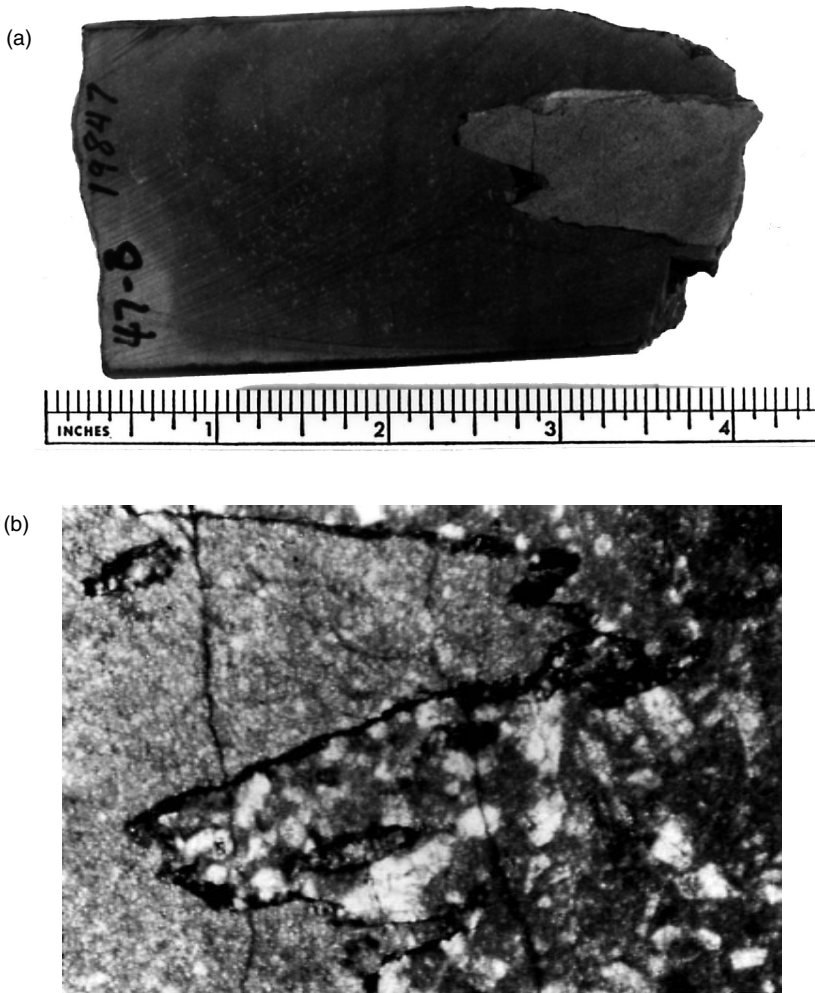


Figure 4-10 Examples of lithologic differences across stylolites. (a) Stylolite in Yamama Limestone from the Darius #3, Persian Gulf. Fine-grained dolomite to the left is in contact with coarse-grained limestone to the right of the stylolite. (b) Smackover Limestone sample from 19,847 ft. in the Amoco #2 Amos, Baldwin County, Alabama. The darker material to the right of the stylolite is stained limestone, while the lighter material below is unstained dolomite.

Such contacts are often explained (especially in low-amplitude stylolites) by assuming that the stylolite began within the limestone and subsequently dissolved calcite in both directions until the less soluble dolomite was encountered. Solution is then plausibly envisioned to either slow or cease on the dolomite side of the stylolite and continue on the limestone side. An alternate explanation considers initiation at the lithologic boundary due to a stress concentration (stress gradient) arising from a mismatch in

mechanical properties. The development of lithologic boundary-related stress gradients is discussed in Sowers (1972).

Low-Porosity Zones

Stylolites are generally found in zones of relatively low porosity in core material (Dunnington, 1967; Wood and Wolfe, 1969; Patrick and others, 1972; Mapstone, 1975; and Klopp, 1975). This association could be initiated either early or late in diagenesis. As pointed out previously, the low relative porosity could be early and localize subsequent stylolite formation; or the low relative porosity could be late and due to reprecipitation of stylolite-related pressure-dissolved material. The distinction is important in a mechanical sense because many rocks such as chalk and clean, well-sorted sandstones vary in mechanical properties directly as a function of porosity (Dunn et al., 1973; Hoshino, 1974; and Yaalon and Singer, 1974; Figure 4–11). As such, porosity variations in an otherwise homogeneous section may mechanically localize stylolitization within or at the boundaries of porosity layers in a manner similar to those already described. In any event, whenever formed, this association may be useful in defining small-scale reservoir properties (porosity) and other small-scale petrophysical property variations in core by stylolite distribution.

Discontinuities

Aggregate stylolites often occur on planes of discontinuity within the rock mass, such as bedding planes, pre-existing fractures, and thin “shale stringers” or clay layers. Such associations have been previously documented in Stockdale (1943), Blake and Roy (1949), Heald (1955, 1959), Manten (1966), and Wood and Wolfe (1969).

Physical breaks such as bedding planes and fractures could affect stylolitization by perturbing the stress state in the immediate vicinity of the opening (Sowers, 1972). Clay layers, on the other hand, could affect stylolitization by either acting as a small-scale lithologic contact or as a catalyst to the pressure-solution process (Heald, 1959).

The Concept of Stress Concentration Localization

Stylolites have been treated phenomenologically, with little regard to their distribution and position. Stylolitization is a major rock deformation mechanism initiated in response to both overburden and tectonic stresses and is not distributed randomly within rock masses. Indeed, their occurrence tells us something about the long-term load-bearing capabilities of the

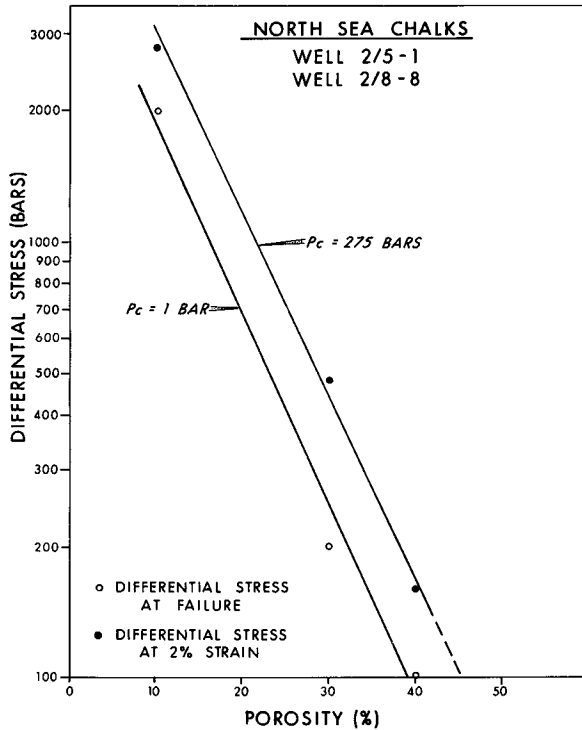


Figure 4-11 The relationship between differential compressive stress at failure and porosity for the chalk section in the Norwegian North Sea (Valhall Field). Data were derived from triaxial compression tests at the confining pressures (P_c) shown. Tests were run at room temperature and humidity at a strain rate of 10^{-4}sec^{-1} . From Nelson (1983), courtesy of AAPG.

rocks involved as well as the inhomogeneities in the paleo-stress field within the rock mass.

On a large scale, stylolites occur in rock types that contain an abundance of minerals that are susceptible to pressure solution (Heald, 1955). On a smaller scale, they occur at places within the rock where stresses are concentrated due to the physical make-up or internal geometry of the body. This association may permit definition of the mechanical property distribution within the section by observation of the stylolite distribution. This mechanical property distribution may in turn define the lithologic and reservoir quality distribution within the section.

In order to define more accurately the mechanical discontinuities in rock, which could give rise to stress gradients and subsequent stylolitization, hardness testing was done on several core samples containing stylolites. Point-load hardness maps were constructed for several stylolite zones (Figures 4-12 through 4-19).

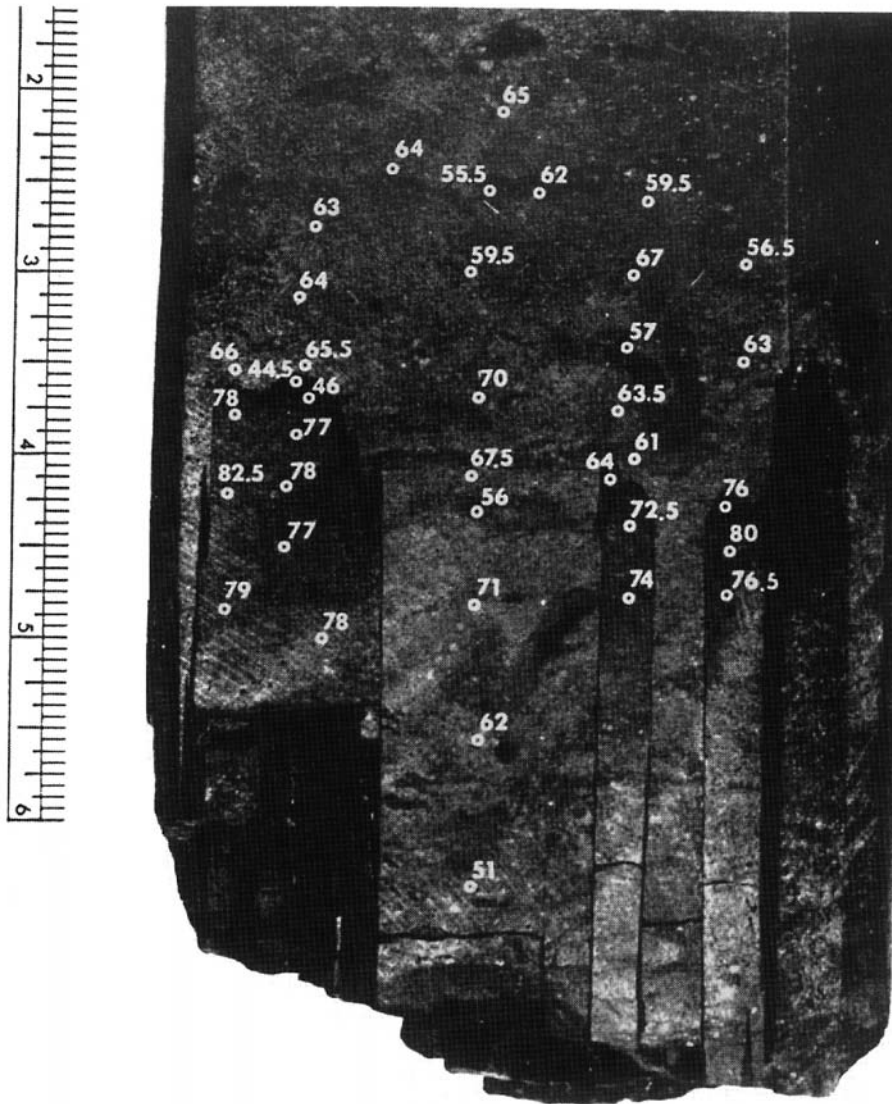


Figure 4-12 A map of point-loaded hardness in the rock surrounding a stylolite in Mission Canyon Limestone. The rock is from the Gulf 1-10-2a Well, Littleknife Field, North Dakota, 9,954-ft. depth. Note the variation in hardness across the stylolite. The arrow refers to the approximate location of Figure 4-3. From Nelson (1983), courtesy of AAPG.

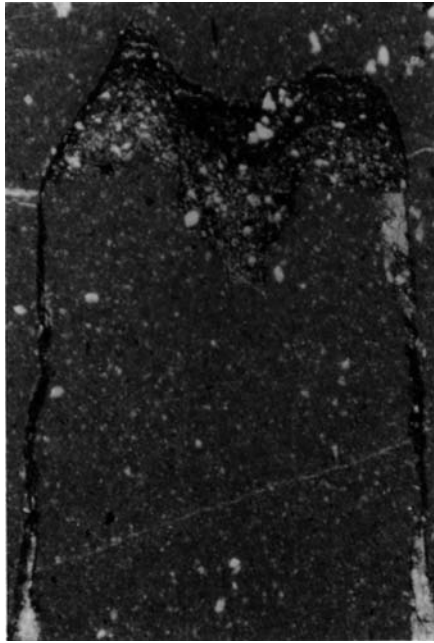


Figure 4-13 Photomicrograph taken from the sample in Figure 4-12 showing the general morphology of the stylolite seams in this sample. From Nelson (1983), courtesy of AAPG. (Magnification 14x.)

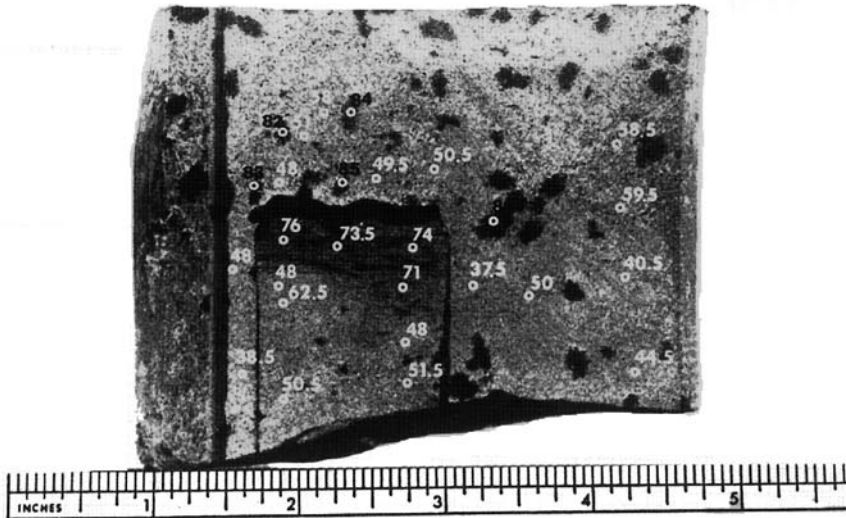


Figure 4-14 A map of point-loaded hardness in the limestone surrounding a stylolite. The core sample is from Stoltz, Wagner and Brown, No. 1 Rose Well, Kearny County, Kansas. Black numerals indicate hardness values for anhydrite blebs within the limestone. The arrow shows the approximate location of Figure 4-15. From Nelson (1983), courtesy of AAPG.

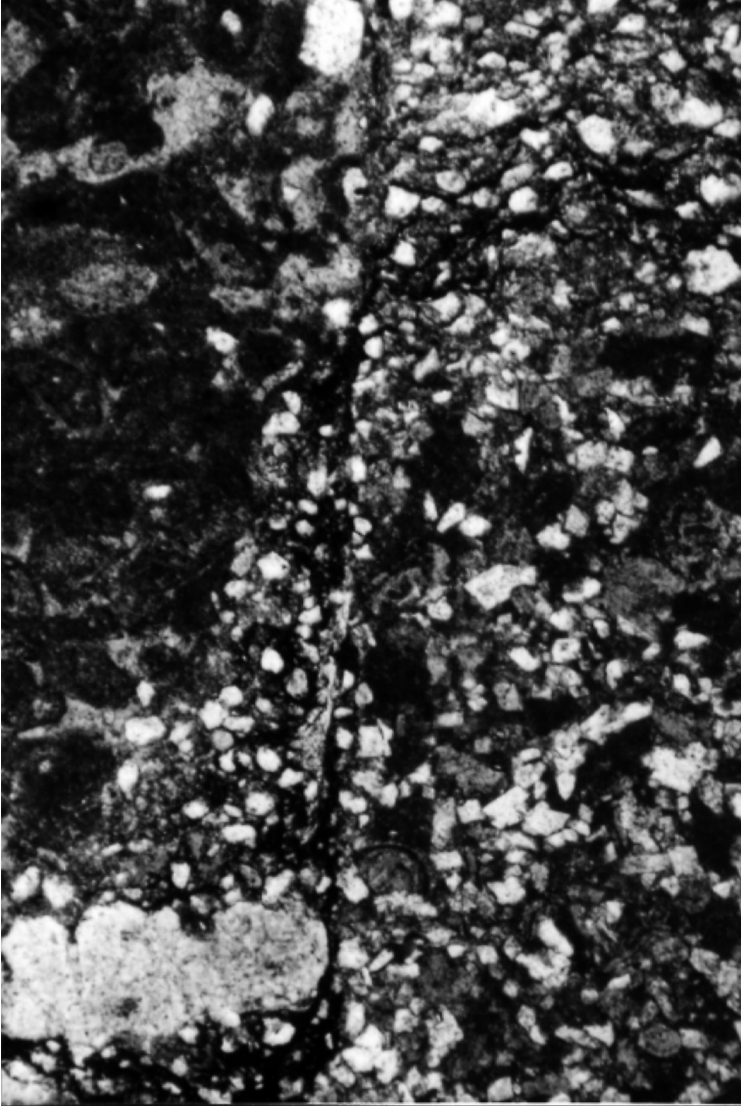


Figure 4–15 A photomicrograph taken from the sample shown in Figure 4–14. Note the difference in rock texture across the column and its relation to point-loaded hardness. From Nelson (1983), courtesy of AAPG. (Magnification 57x.)

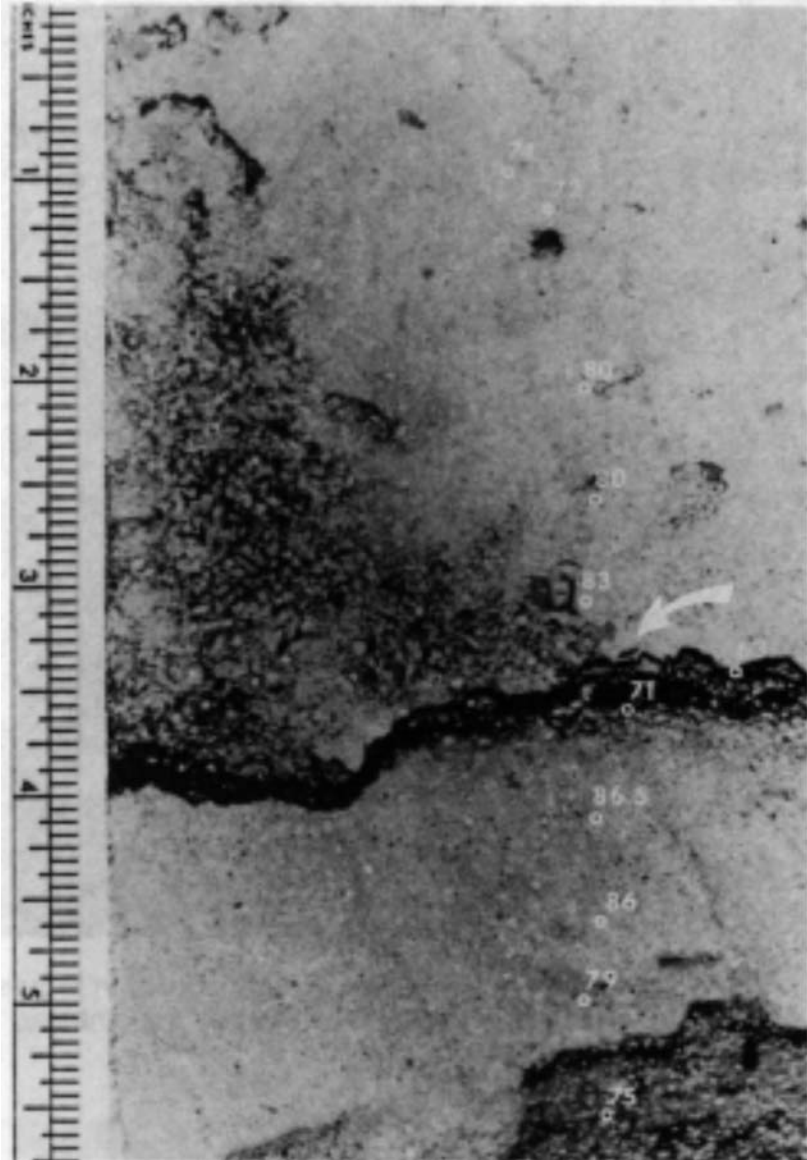


Figure 4-16 A map of point-loaded hardness surrounding a stylolite in a Chase Limestone layer. The core sample (Sample 20) is from the Amoco Miles #2 Well, Panoma Field, Kearny County, Kansas, 2,631-ft. depth. Note the radial increase in hardness toward the stylolite. The arrow points to the approximate location of Figure 4-17. From Nelson (1983), courtesy of AAPG.

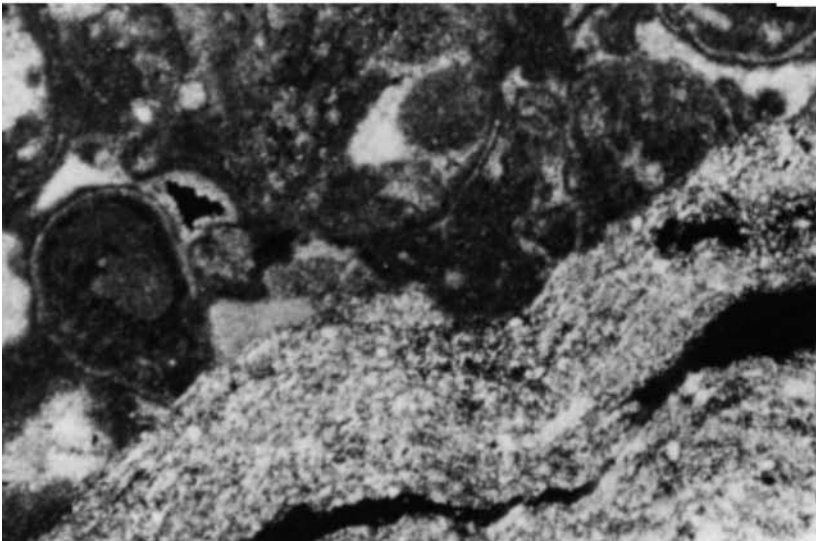
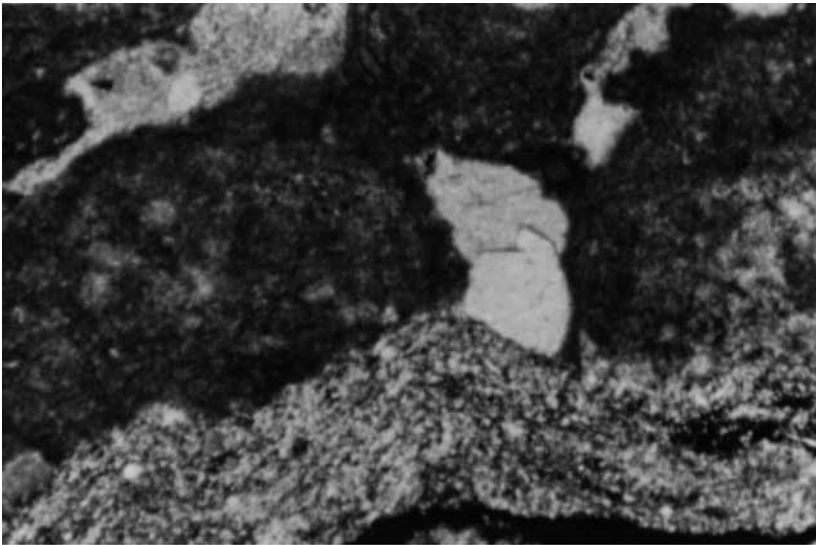


Figure 4–17 Photomicrographs of the sample in Figure 4–16. Both photographs show the stylolite seam. From Nelson (1983), courtesy of AAPG. (Magnification 65x.)

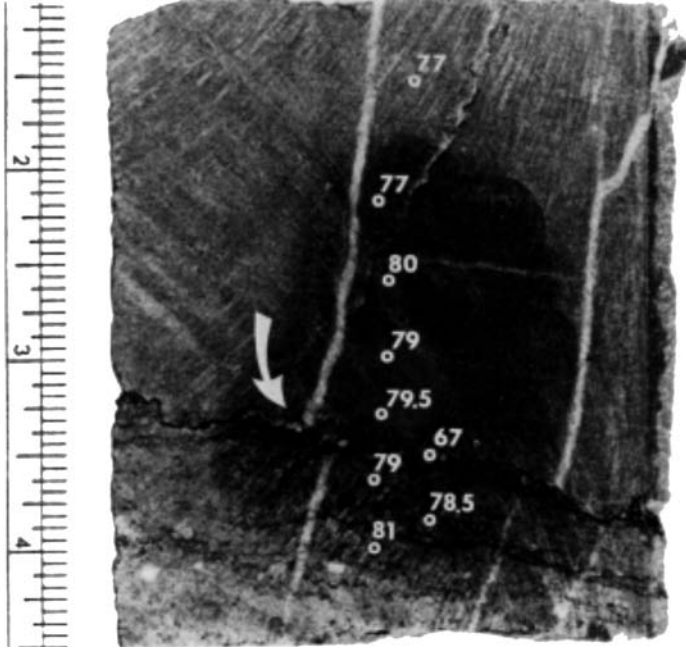


Figure 4-18 A map of point-loaded hardness in the rock surrounding a stylolite in Yamama Limestone. The core sample is from the Darius 17, D-4 Well, Iran, 11,144-ft. depth. Note that this very low-porosity rock shows no significant variation in point-load hardness. The arrow refers to the approximate location of Figure 4-19. From Nelson (1983), courtesy of AAPG.

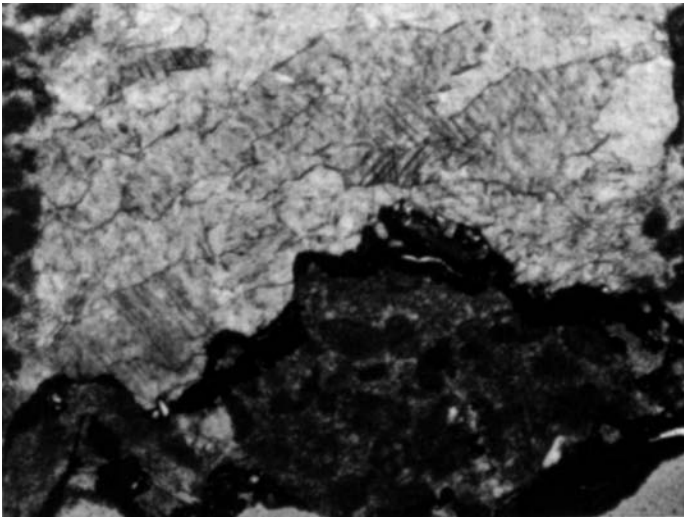


Figure 4-19 Photomicrograph taken from the sample in Figure 4-18. The lighter calcite in the center is the base of one of the calcite-filled tension gases in Figure 4-18. From Nelson (1983), courtesy of AAPG. (Magnification 57x.)

The values plotted on these maps are relative penetration of a ball of constant diameter driven by a constant load and are related to penetration hardness.* These numbers are in a loose way related to rock strength and ductility. Relative values of strength can be obtained by calibrating the tests with samples of known compressive and tensile strength. In general, on these maps, the larger numbers represent the stronger and usually more brittle rock.

Hardness maps of stylolite zones indicate that they may have been initiated at a lithologic or mechanical interface within the rock (Figures 4–12 and 4–14). This is suggested by the great hardness variations across the stylolite seams and, to some degree, across the columns. It is further substantiated by thin-section observations that show a great variation in both porosity and dolomite-to-calcite ratio across the stylolite (Figure 4–13) and a large variation in grain size across the column (Figure 4–15). All of these indicate the possibility of mechanically dissimilar rocks in contact across the initial pressure solution surface.

Other maps show stylolites with a small but gradual decrease in rock hardness with increasing distance from the seam (Figure 4–16). From thin-section observations (Figure 4–17), this increase in hardness near the seam often appears to be related to redeposition of material dissolved to form the stylolite. The width of porosity reduction by re-precipitation around a seam could be measured by empirically calibrating thin-section-derived porosity values with the point-load values. This porosity zone width could then be used to estimate the spacing of stylolites at which all effective porosity would be destroyed by reprecipitation. Stylolites showing no significant hardness variation associated with them are also seen (Figure 4–18). This is probably due to the very low bulk porosity of the sample (< 1.0 percent in Figure 4–18). Such a stylolite may, however, have initiated at a bedding plane or a pre-existing fracture that localized subsequent pressure solution (Figure 4–19). Because of its insignificant hardness variation, a sample yielding such as a point-load map would probably not be chosen for any subsequent small-scale data collection.

In general, hardness mapping may be an easy, informative procedure to determine the origin and time of stylolitization. These in turn can provide insight into lithologic and reservoir property distribution variations on a small scale, provided additional observational work (most specifically, thin-section observation) is performed on the samples. Point-load testing, like many other forms of data collection, gives a nonunique result. Such point-

*Hardness testing was performed on Rockwell Hardness Tester Model 4JR with a 1/8-in. ball and chuck and a 100-kg load.

load mapping should be used as a reconnaissance technique for locating pertinent locations for detailed observations such as cathodoluminescence and UV fluorescence. If, within a particular unit, a significant correlation exists between generalized stylolite location and the petrologic and/or mechanical property variation, such as modulus or porosity maps, the distribution of stylolites may be used effectively in reservoir property descriptions.

DEVELOPMENT OF PERMEABILITY TENSORS FOR ANISOTROPIC RESERVOIRS

“Reservoir quality” is a broad term that includes many parameters that either influence or determine the volume and mobility of the various fluid phases held within the rock. For simplicity, this section will focus primarily on differences in porosity and permeability brought about by geologically significant variations in rock character. These two parameters are the most used and most easily measured of those used to evaluate reservoir performance.

In this type of study, an attempt is made to determine the effect of individual petrologic features in small-scale, oriented, standard-permeability plugs and to subsequently show the combined effect of these features in larger-scale, whole-core analysis. The study will address both reservoir inhomogeneity (the similarity or dissimilarity of properties of one piece of the reservoir with another) and reservoir anisotropy (the variation of certain properties, such as permeability, with direction at any single point within the reservoir).

The reservoir chosen as an example was the Jurassic Nugget Sandstone from the Ryckman Creek Field of the Western Wyoming Thrust Belt. Excellent unslabbed core material was available from the Ryckman Creek Working Interest No. 6 Well, Unita County, Wyoming. The petrology of this rock allows us to investigate the effects of grain size, cementation, and the quality and orientation of crossbedding and fracturing.

The selected core samples come from the top 336 ft. of the approximately 800-ft. thick Nugget Sandstone. Whole core porosity and three-direction permeability analyses were performed on it. The entire core was peel-scaled at the rig to preserve reservoir saturations.

This work was performed with the assistance and collaboration of Howard Cotton of Amoco Research. A description was first made of the un-

wrapped portions of the core. This visual description emphasized grain size and the character and orientation of the crossbeds and fractures.

From the 177 unwrapped whole-core samples, 36 were selected as excellent examples of certain individual or combined features. Each of the 36 samples was measured for standard permeability plug analysis. These plugs were chosen to sample either fractures (F) or crossbedding (B). Plugs were taken such that the axis of one plug was perpendicular to the feature B-1 and F-1, one was at 45° to the feature B-2 and F-2, and one was parallel to the feature B-3 and F-3.

One of the purposes of the sets of three plugs is the eventual creation of the two-dimensional permeability tensor associated with the individual feature. Because permeability is a tensor quantity, only these three permeability components (directions and magnitudes) are needed to describe permeability in any direction. Permeability tensors for various features can be added together to determine their combined effect on flow in the reservoir (Figure 4–20).

In addition to the plug “sets,” one “random plug” (R-4) was taken perpendicular to the whole-core axis. This plug was taken “blindly” wherever space permitted to simulate the standard plug analysis procedure used by various core-testing facilities.

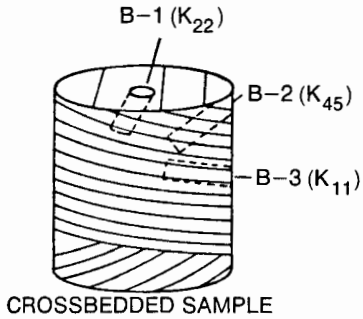
Crossbedding

Crossbedding is an arrangement of laminations transverse or oblique to the main planes of stratification in clastic rocks (Trowbridge, 1962). At its smallest scale, a crossbed is recognized by an alternation in grain size and/or composition. In the Nugget Sandstone, crossbedding is predominantly a grain size alternation.

Crossbedding, has a profound influence on the permeability-porosity relationship in the Nugget Sandstone reservoir (Rose, 1983). This influence manifests itself not only in terms of the orientation of bedding, but also in the visual quality or distinctness of the crossbedding.

The effect of the presence and orientation of crossbedding is best shown on standard porosity-permeability cross plots; for example, (ϕ -k) relationship for the Nugget Sandstone plugs that have no bedding or fracturing (Figure 4–21), and ϕ -k relationship for crossbedded Nugget Sandstone plugs as the angle between the measurement direction and the crossbed planes varies from 90° to 45° to 0° (Figures 4–21a–c). These ϕ -k relationships are summarized in Figure 4–22.

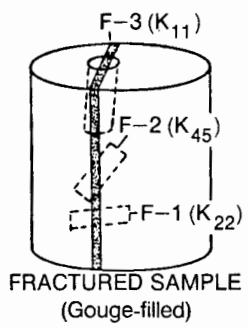
It is evident in Figure 4–22 that there is more than an order of magnitude (10 times) higher permeability at a given porosity for samples measured



$$\begin{vmatrix} K_{11} & K_{12} \\ K_{21} & K_{22} \end{vmatrix} = B_{ij}$$

BEDDING

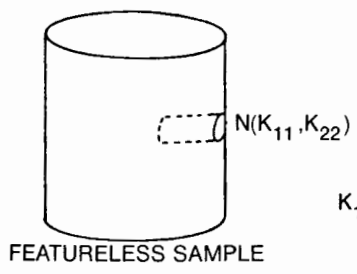
$$K_{12} = K_{21} = 0$$



$$\begin{vmatrix} K_{11} & K_{12} \\ K_{21} & K_{22} \end{vmatrix} = F_{ij}$$

FRACTURES

$$K_{12} = K_{21} = 0$$



$$\begin{vmatrix} K_{11} & K_{12} \\ K_{21} & K_{22} \end{vmatrix} = M_{ij}$$

MATRIX

$$K_{11} = K_{22}, K_{12} = K_{21} = 0$$

K_{11} , K_{22} , and K_{45} Can Be Used To Construct The Permeability Ellipse, See Long (1983).

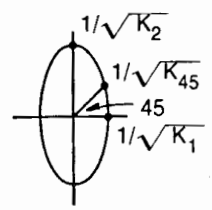


Figure 4-20 Orientation of permeability plug sets with respect to the features they represent are shown along with the permeability tensor components.

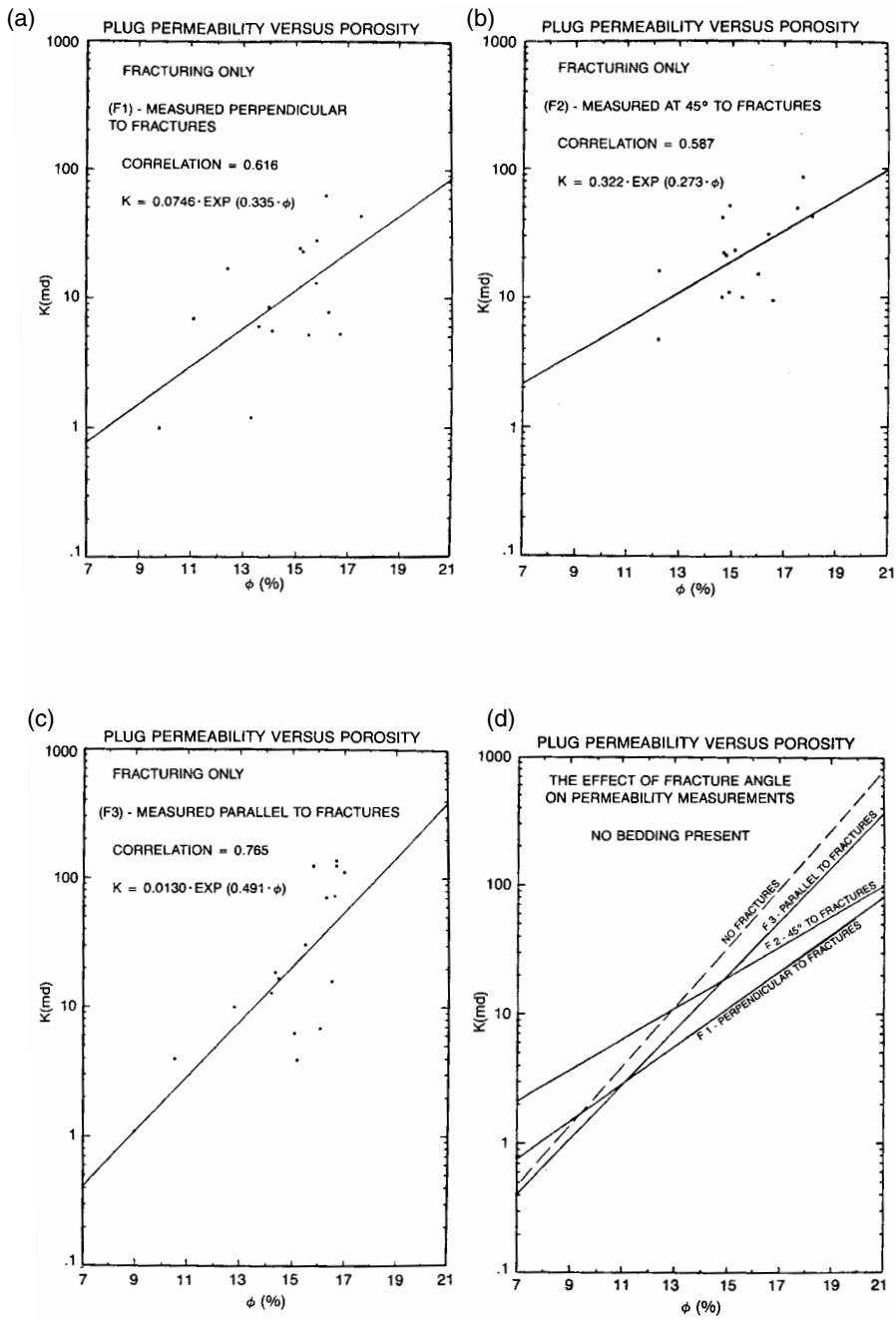


Figure 4-21 Porosity-permeability relationships as the angle between measurements direction and the crossbed plane varies from 90° (a), to 45° (b), to 0° (c), and to plugs that show neither bedding nor fractures (d).

parallel to bedding than samples measured perpendicular to bedding. The “no bedding” line on Figure 4–22 plots lower in permeability than the parallel-to-bedding crossbed curve over most of its range. This is due to the segregation of grain sizes in the crossbedded sandstones, causing alternating coarse and fine layers. When this happens, the well-sorted coarse layers with their higher permeability dominate the fluid flow.

Fractures

The effect of fractures on porosity and permeability in this core is less distinct than that of crossbedding. Because the majority of tectonic fractures in this core are gouge-filled shear fractures, the granulated rock in the fracture planes should, due to a reduction in grain size and sorting, reduce permeability perpendicular to the fracture plane and have little or no effect on flow parallel to the fracture plane. The effect of fractures on the porosity-permeability (Figure 4–23) is similar in form but smaller in magnitude than that of the crossbeds (Figure 4–21). To fully understand the combined effects of crossbeds and fractures, it is first necessary to understand the (ϕ -k

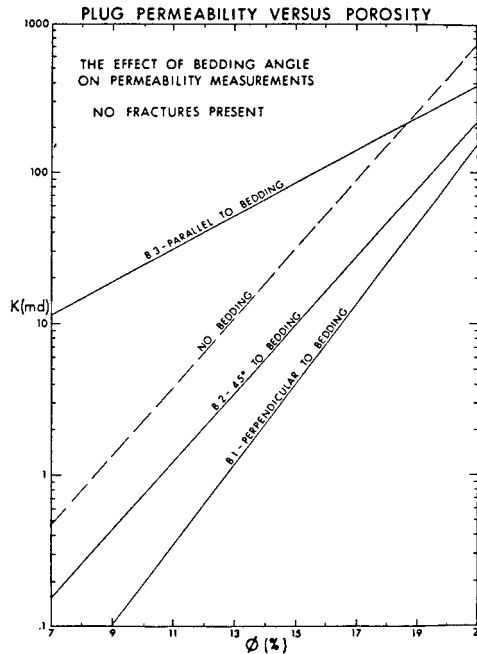


Figure 4–22 Porosity-permeability plot summary showing the effect of bedding and bedding angle.

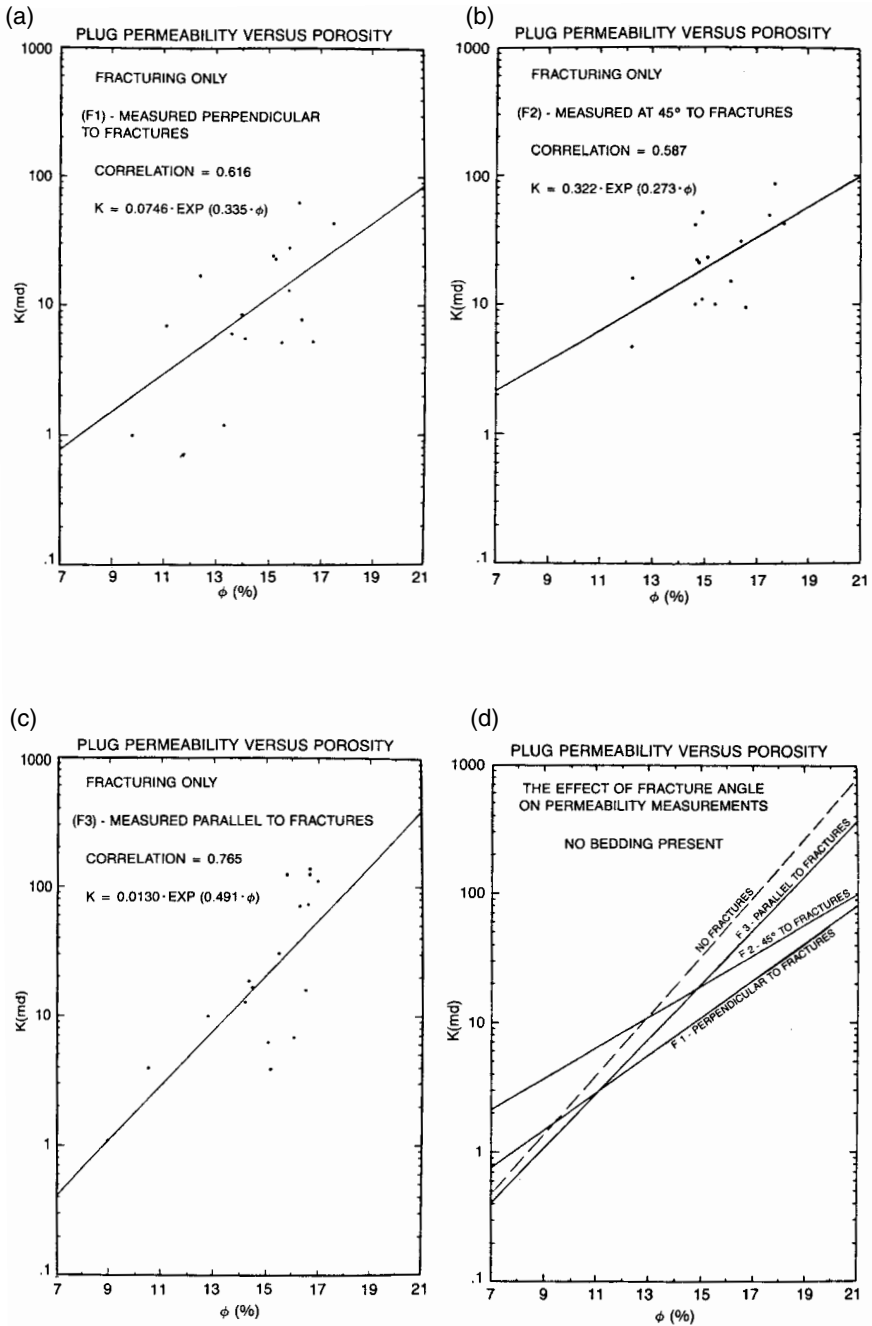


Figure 4-23 Porosity-permeability relationships are shown as the angle between the measurement direction and the fracture planes varies from 90° (a), to 45° (b), to 0° (c). A summary of the relationships is shown in (d).

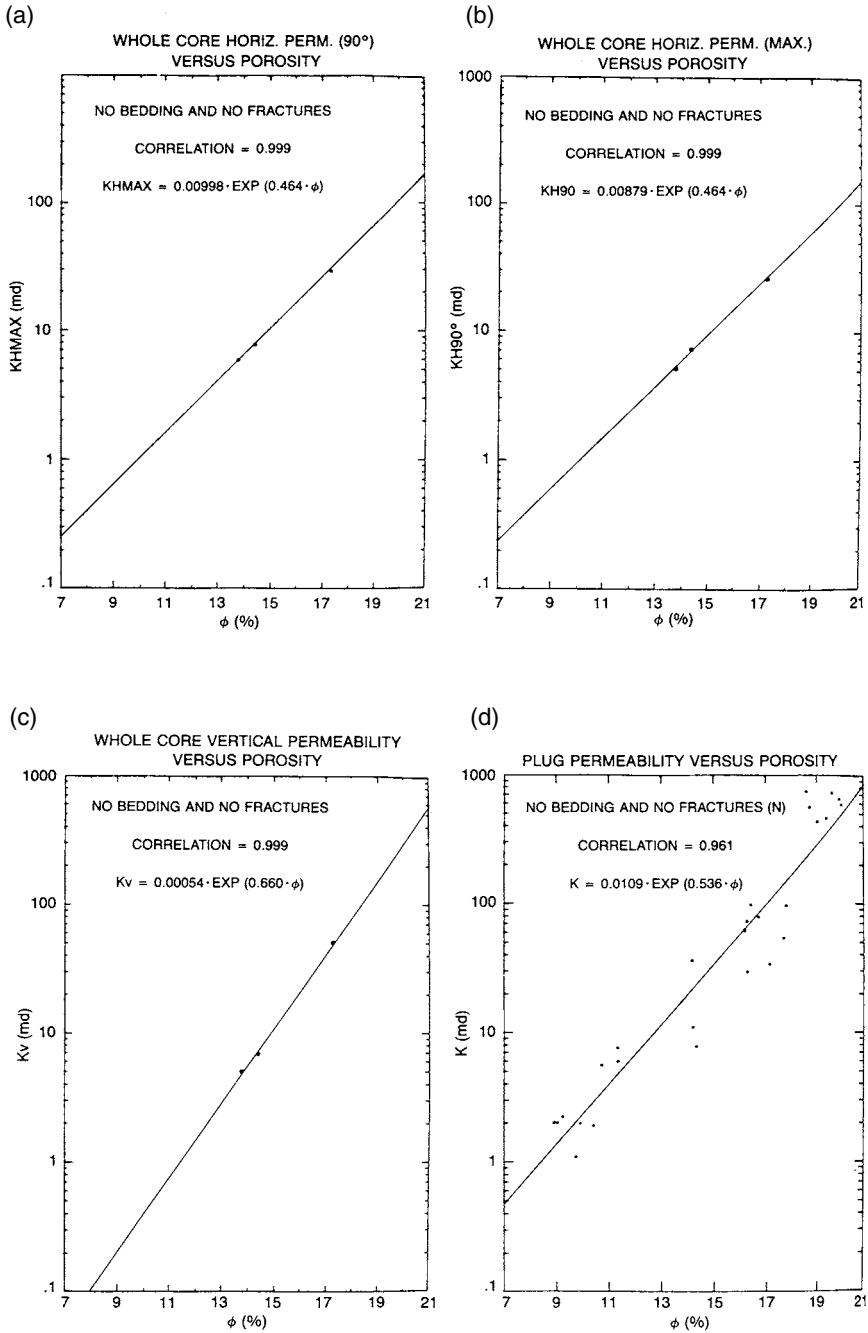


Figure 4-24 Whole-core (a, b, and c) and plug (d) porosity-permeability relationships for nonbedded, nonfractures Nugget Sandstone.

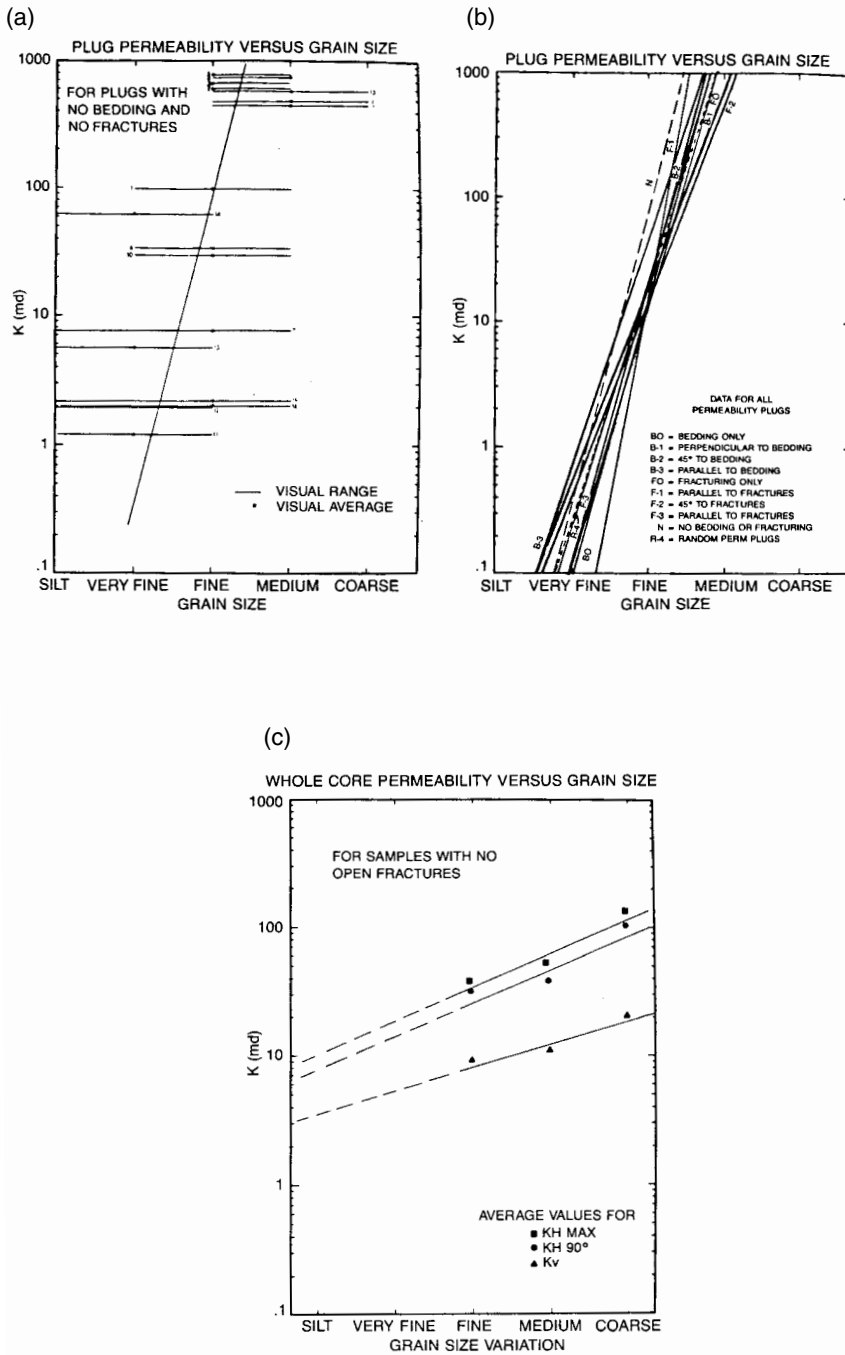


Figure 4-25 Variations in permeability with grain size.

relationship for the visually nonbedded, nonfractured Nugget Sandstone (Figure 4-24). These data provide the base level ϕ -k relationship in this rock. As would be expected in these visually featureless rocks, the permeability in three directions is nearly equal for each of the whole core samples.

Other Factors

Grain Size

The Nugget Sandstone in this core is fine-grained (0.125 to 0.25 mm), with a range from silt size (< 0.063 mm) to coarse-grained (0.5–1.0 mm) sand. Variation in permeability with grain size is obscure in the crossbedded and fractured plugs. A good relationship is, however, seen in the data for the nonbedded, nonfractured plugs (Figure 4-25a). As would be expected, the coarser the grain size, the higher the permeability. The poorly developed trends for the fractured and bedded plug data and the nonbedded, nonfractured trend are quite similar (Figure 4-25b). A similar, but less dramatic effect, is seen in the whole core data (Figure 4-25c).

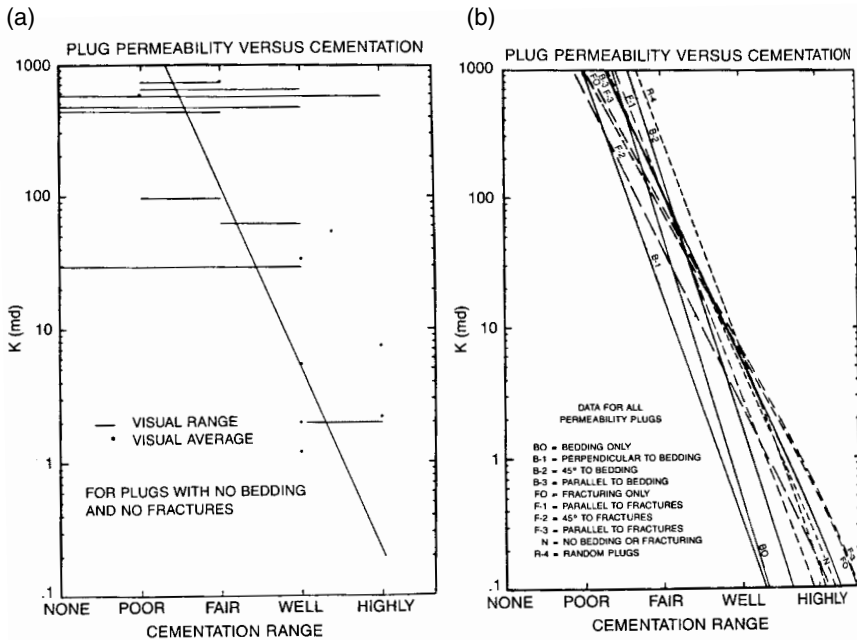


Figure 4-26 Variations in permeability with cementation.

Cementation

A visual estimation of the degree of cementation was made for each plug used in this study. This estimation is, of course, highly subjective. As with the grain size data, the relationship between cementation and permeability is weakly defined in both the fracture and bedding plug data, and somewhat more well defined in the nonfractured, nonbedded plug data (Figure 4–26).

Scaling

The major aim of this work was to show how individual petrologic features combine to dictate reservoir flow. The combining of these parameters requires the comparison of petrophysical data obtained at various scales.

As with the grain size data, the relationship between cementation and permeability is weakly defined in both the fracture and bedding plug data, and somewhat more well defined in the nonfractured, nonbedded plug data (Figure 4–26).

Random Plugs

In general, the random plugs seem to plot intermediate in position on the grain size and cementation versus permeability compilation plots and on the ϕ -k compilation plot (Figure 4–27).

Scaling

The major aim of this work was to show how individual petrologic features combine to dictate reservoir flow. The combining of these parameters requires the comparison of petrophysical data obtained at various scales.

A plot of the ϕ -k relationships for both the plug and whole-core data shows that for a given porosity the whole-core fit gives a lower permeability than the analogous plug permeability (Figure 4–28a). In all three curves, the whole-core permeability is lower than the average permeability of the plugs taken from them. If we assume that the larger the sample of the reservoir the closer it reflects the true petrophysical properties of the reservoir, we must conclude that plug data gives too optimistic a permeability for this rock.

One of the more instructive forms of display of whole-core data is the directional permeability plot (Figures 4–29 and 4–30). These plots characteristically give a strong indication of fracture and crossbed control of

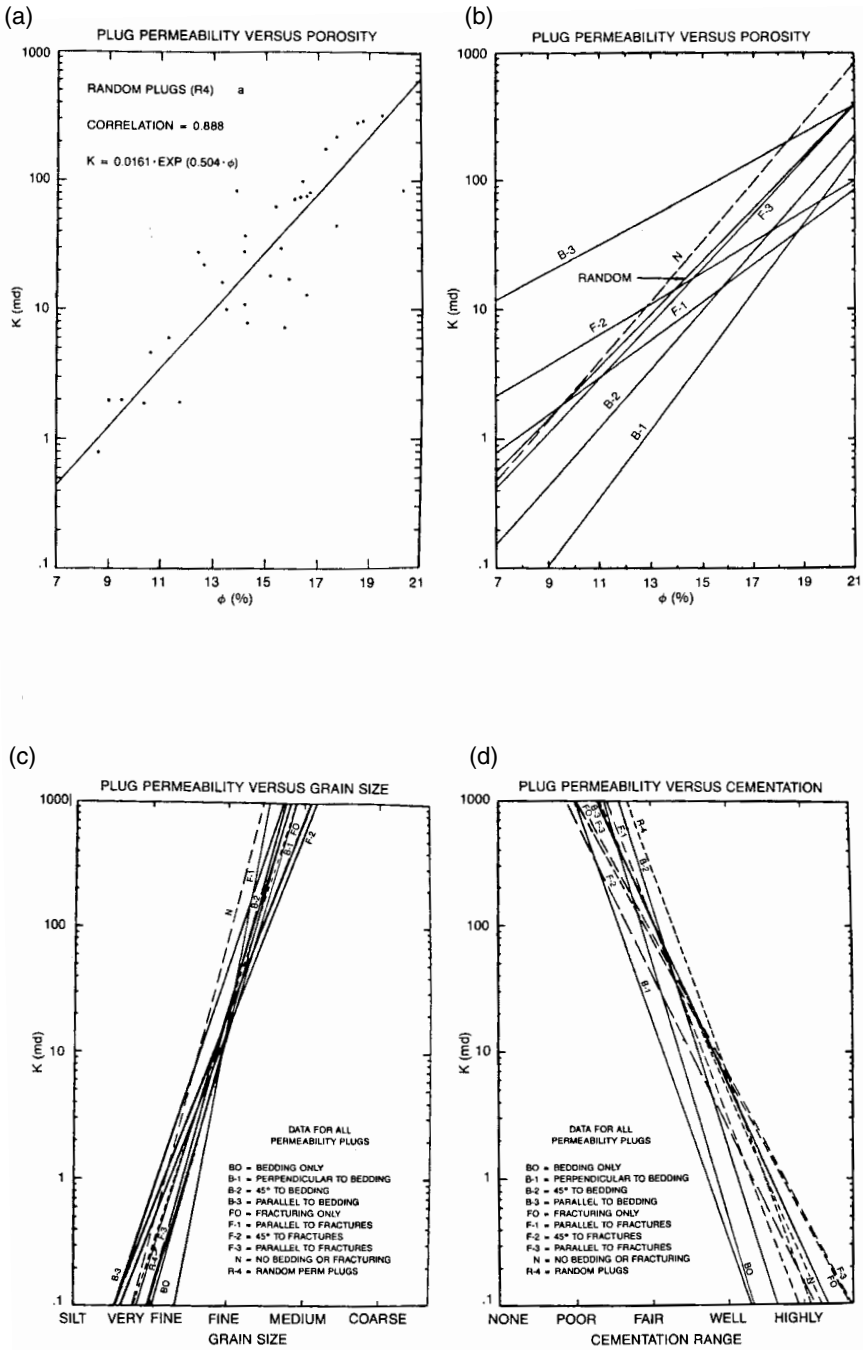


Figure 4-27 Comparison of random plug analyses.

permeability in a reservoir rock. Ideally, in a nonfractured, horizontally bedded sandstone, the data points should plot near, and slightly to the K_{Hmax} side of, the equal permeability line. Pronounced crossbedding should reduce both K_{H90° and K_v relative to K_{Hna} . This would move data points off of the equal permeability line toward K_{Hmax} into the lower right-hand portions of the plotted fields (Figures 4-29 and 4-30). The effect of vertical fractures, either open or gouge-filled, would be to either increase K_v (open), or reduce K_{H90° (gouge-filled) relative to K_{Hmax} . In addition, vertical open fractures would increase K_{Hmax} , relative to K_{H90° . The end result would be a movement of the data points away from the equal permeability line into the lower right-hand portion of the plotted field (Figure 4-30) and into both the upper left-hand and lower right-hand fields of Figure 4-29. A substantial number of data points do, in fact, indicate crossbedding- and fracture-related displacements (Figures 4-29 and 4-30).

Data fields on Figures 4-29 and 4-30 relative to the equal permeability line can be expressed in permeability ratios (K_v/K_{Hmax} , and K_{H90°/K_{Hmax}). These ratios can be plotted as a function of depth. By core observation, relevant cut-off values for the ratios indicative of specific control can be generated. These ratio cut-off values can be highlighted as having specific anisotropic effects. In this study, on the basis of sample descriptions,

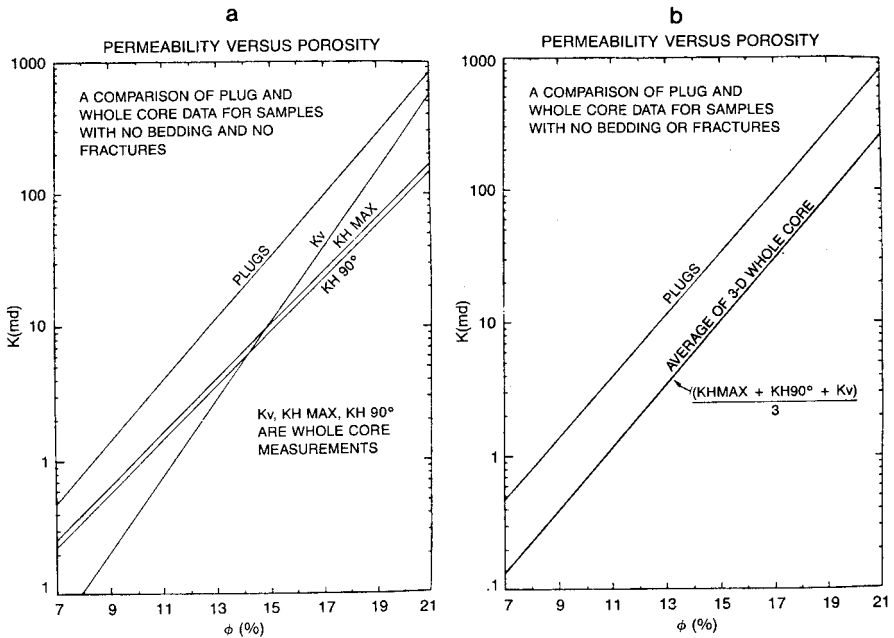


Figure 4-28 Permeability relationships for corresponding plug and whole-core data.

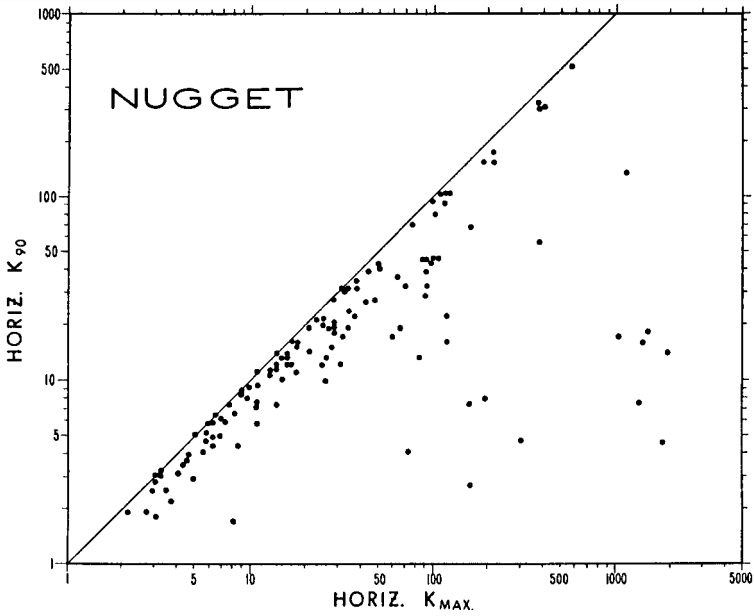
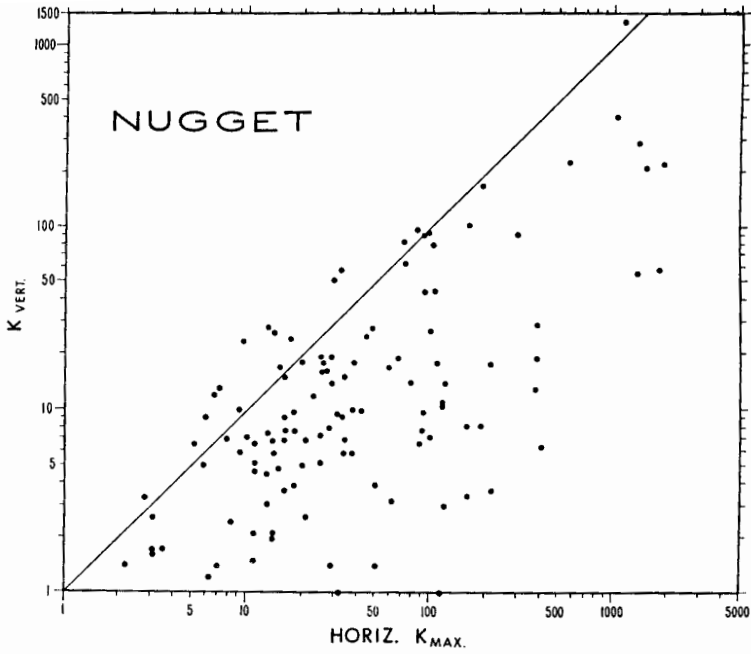


Figure 4-29 Whole-core, directional permeability plot, vertical versus maximum horizontal permeability, with equal permeability line show.

Figure 4-30 Whole-core directional permeability plot, maximum horizontal versus 90° to maximum horizontal permeability, with equal permeability shown.

$K_{H90}/K_{Hmax} < 0.5$ indicates fractures, while $K_v/K_{Hmax} > 1.0$ indicates fractures and $K_v/K_{Hmax} < 0.2$ indicates either strong crossbedding or fractures, or both (Figure 4-31).

Permeability Tensors for Crossbedding and Fractures

In an anisotropic porous media, the magnitude of permeability is dependent on the measurement direction. As such, because it has a direction and a magnitude, a permeability measurement is a vector quantity. The array of permeability vectors, or the permeability field, at a given point in a rock can be treated mathematically as a second-order tensor much like stress and strain (Evans, 1982; van Golf-Racht, 1982, p. 434; and Rose, 1983). The utility of this treatment is that such tensors can be translated and rotated through matrix algebra from one frame of reference to another. This means that once these specific permeability components are described, the permeability in any direction can be calculated. In addition, permeability tensors for the effect of specific features can be added and subtracted via matrix algebra to determine their combined effects in the material.

In this section we will show how permeability tensors can be created for crossbedding and gouge-filled fractures and how the tensors can be individually rotated and added together to approximate whole-core permeability and ultimately reservoir performance. This discussion assumes a limited knowledge of tensor mathematics and matrix algebra. An excellent discussion of tensor concepts and tensor mathematics can be found in Chapters 1 and 2 of Nye (1957).

The individual sets of three permeability plugs were taken such that they fully describe the permeability tensor in directions coincident with the principal permeability planes (Figure 4-20). The tensor reflecting the effect of crossbedding or gouge-filled fractures can be calculated by subtracting the isotropic matrix permeability tensor (M_{ij}) from the bedding and fracture tensors (B_{ij} and F_{ij}) to give the appropriate permeability deviator tensors.

Using the notation of Figure 4-20, B_{ij} , F_{ij} , and M_{ij} can be calculated for any porosity using the least-squares fit equations for the ϕ - k relationships generated in this study. These equations are summarized in Table 4-1. The matrices generated for the given porosity value can then be subtracted via matrix algebra to give two new tensors, which depict the effect of crossbedding ($B'\phi$) and fractures ($F'\phi$) relative to the featureless matrix:

$$B_{ij} - M_{ij} = B'_{ij} \quad (4-1)$$

$$F_{ij} - M_{ij} = F'\phi \quad (4-2)$$

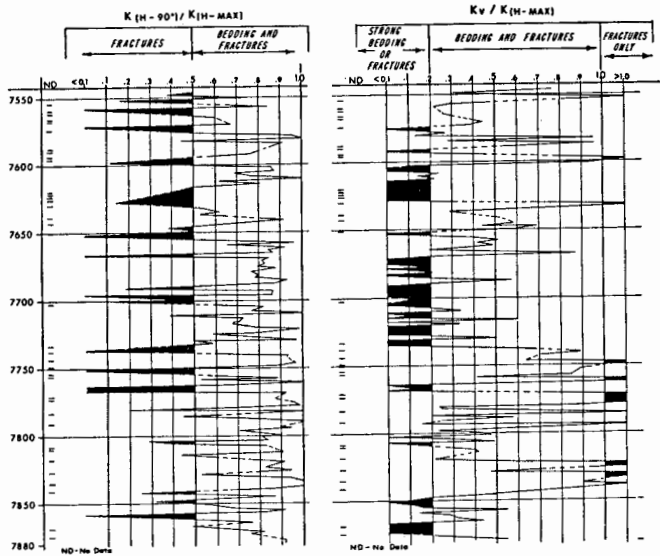


Figure 4-31a Replot of figures 4-29 and 4-30 with fields and cut-off ratios depicted for strong anisotropic effects of crossbedding and fractures.

These matrices are described in the principal permeability directions. To determine the effect in a whole-core sample, each matrix must be rotated via matrix algebra to conform with the orientation of these physical features in the core. The average dip of crossbedding in this core is 22° and the average dip of gouge-filled fractures is 78° , relative to the core axis. To simulate k_v and k_{Hmax} in a two-dimensional whole-core analysis, F'_{ij} must be rotated through 78° and B'_{ij} through 22° . The rotated matrices are then added and recombined with M_{ij} to simulate whole-core permeability (Figure 4-32a).

To more accurately simulate subsurface permeabilities and changes in permeability during reservoir draw-down or depletion, B_{ij} , F_{ij} , and M_{ij} can be altered to accommodate changes in the components due to an applied external load, such as confining pressure. Curves showing percentage reduction in permeability (k/k_0) as a function of stress (σ_3 or $\sigma_1 - \sigma_3$) for the individual permeability plugs taken in this study (B-1, B-2, B-3, F-1, F-2, F-3, and N) could be created by subjecting these plugs to stress tests in the laboratory. Equations of curves similar to those shown in Table 4-1 for each component could then be calculated to show how to reduce the components as a function of applied load or pore pressure depletion. Unfortunately, such tests would have to be run at many porosities because the form of the (k/k_0

versus σ_3) line will undoubtedly be different for high- and low-porosity sandstones.

In addition to the permeability tensors, the oriented permeability plug data can be used to generate ellipses representing the two-dimensional permeability array for flow parallel to pressure gradient. These are created using the k_{11} , k_{22} and k_{45} data (see Figure 4-20 and Table 4-1).

The cross permeability terms k_{12} and k_{21} are not especially relevant to geologists working in reservoir development. They represent the permeability for flow in a direction 90° to the pressure gradient. Of more relevance is the permeability representing flow parallel to the gradient in all directions around a point. Figure 4-32b displays these data from this study in a format described in Long (1983).

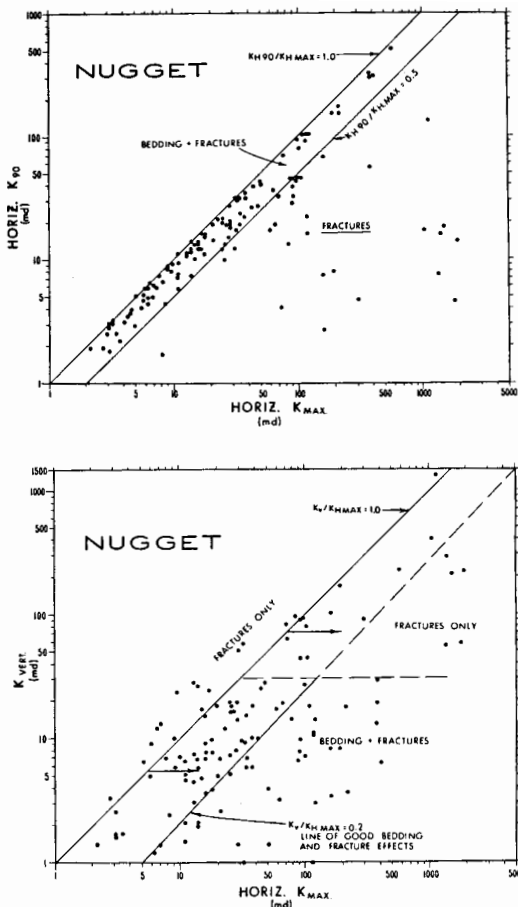


Figure 4-31b Permeability ratio values plotted in log form with cut-off ratios representing strong anisotropic effects of crossbedding and fractures from Figure 4-3a highlighted.

Table 4-1
A Summary of the Least-Squares Fit Equations for the Plug Data

Bedding

$$B_{ij} \quad k_{11} = 2.04 \times \exp(0.251 \times \phi)$$

$$k_{22} = 0.000387 \times \exp(0.615 \times \phi)$$

$$k_{45} = 0.00396 \times \exp(0.521 \times \phi)$$

Fractures (Gouge-Filled)

$$F_{ij} \quad k_{11} = 0.0130 \times \exp(0.491 \times \phi)$$

$$k_{22} = 0.0746 \times \exp(0.355 \times \phi)$$

$$k_{45} = 0.322 \times \exp(0.273 \times \phi)$$

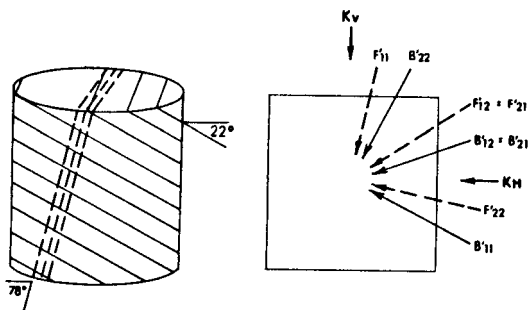
Matrix

$$M_{ij} \quad k_{11} = k_{22} = 0.0109 \times \exp(0.546 \times \phi)$$

$$(a) \quad \begin{matrix} B_{ij} \\ F_{ij} \end{matrix} \begin{vmatrix} B_{11} & B_{12} \\ B_{21} & B_{22} \end{vmatrix} - M_{ij} \begin{vmatrix} M_{11} & M_{12} \\ M_{21} & M_{22} \end{vmatrix} = \begin{matrix} B'_{ij} \\ F'_{ij} \end{matrix} \begin{vmatrix} B'_{11} & B'_{12} \\ B'_{21} & B'_{22} \end{vmatrix} \begin{vmatrix} F'_{11} & F'_{12} \\ F'_{21} & F'_{22} \end{vmatrix}$$

$$\begin{matrix} B'_{ij} \text{ (ROTATED } 22^\circ) \\ + F'_{ij} \text{ (ROTATED } 78^\circ) \\ + M_{ij} \text{ (ISOTROPIC)} \end{matrix}$$

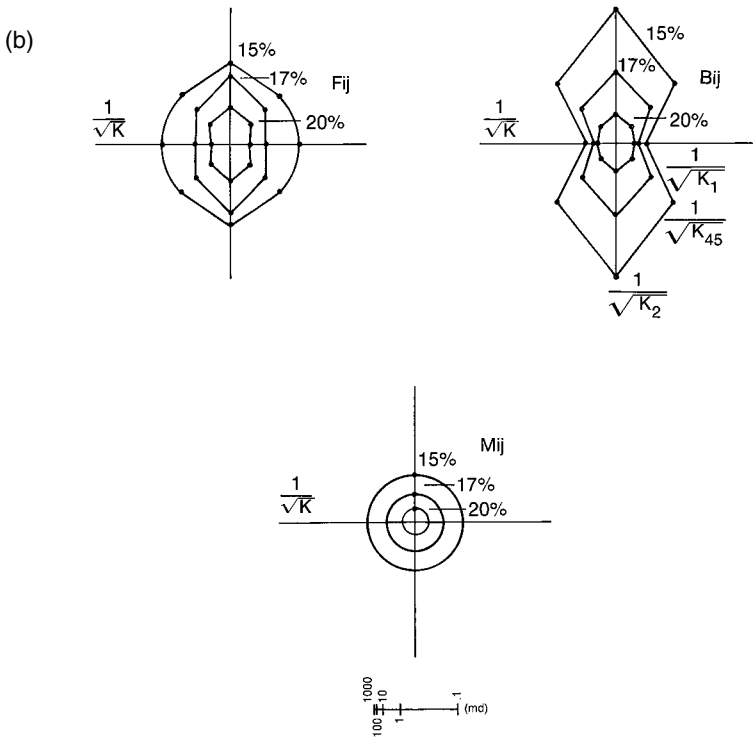
TOTAL (RESOLVED TO K_V & K_H)



ASSUMING THE AVERAGE WHOLE CORE POROSITY OF 15%

RESOLVE TO	CALC.	AVG. WHOLE CORE (No Open Fractures)
K_V & K_H	$K_V = 14.6 \text{ md}$	10.6 md
	$K_H 90^\circ = 52.5$	38.5
	$K_V/K_H 90^\circ = 0.28$	0.27

Figure 4-32a Schematic diagram showing how tensors for bedding (B'_{ij}), fracturing (F'_{ij}), and matrix (M_{ij}) are rotated and added together to depict total permeability. Shown in a comparison of the tensor manipulation and an average whole-core example for Nugget sandstone with the average porosity (15 percent), the average bedding dip (22°), and the average fracture dip (78°).



Assumes Symmetry of Plot.
Flow Measured Parallel To Pressure Gradient.

Figure 4–32b Directional permeability diagrams for bedding fractures and homogenous matrix at 15, 17 and 20 percent porosity (see Figure 4–20 and Table 4–1); for flow parallel to pressure gradient.

Relative Effect of Rock Parameters

Analysis of the data presented shows that variation of orientation in crossbedding and gouge-filled fractures affects the ϕ -k relationship in this rock more than grain size and degree of cementation variation. Of the two, crossbedding appears to dominate in its effect on permeability porosities below about 18 percent and appears roughly equal to fractures above about 18 percent.

Continuity of Features Within the Reservoir

Once the relative effects of the individual petrologic features have been shown, it is instructive to determine how continuous these features are both vertically and horizontally in the reservoir. Because the core used in this study samples a representative productive Nugget Sandstone section, a good idea of vertical reservoir continuity is known. In general, by visual and thin-section observations this core displays fairly constant grain size, moderate variations in cementation, and large variations in the amount and quality of crossbedding and fracturing. The result is great vertical variations in porosity and permeability. Because this is a crossbedded sandstone, one might expect similar variations in petrologic parameters and their resulting porosity and permeability in the horizontal direction.

Indeed, because these reservoirs are made up of dune packages, and these crossbed packages and the fractures within them possess a high degree of preferred orientation, horizontal porosity and permeability are inhomogeneous from point to point and distinctly anisotropic in three dimensions at any point.

The Nugget Sandstone in the Western Wyoming Thrust Belt is predominantly an Eolian deposit, although some marine influence is undoubtedly present. According to Potter and Pettijohn (1963), the strike of a sand dune is generally perpendicular to the wind direction at the time of formation. The inclination of crossbeds with respect to true bedding is a maximum in the direction parallel to the wind direction, about 26°, and approaches zero in the direction perpendicular to the wind direction. Paleo-wind directions are determined for an area by statistically analyzing crossbed dip directions. A general knowledge of the average paleo-wind direction in an area does, then, reflect the statistical distribution of crossbed inclination directions. This, in turn, reflects for us a regional anisotropy in permeability parallel to the major bedding surface (top and bottom of the formation). Ideally, regional horizontal permeability in an Eolian, crossbedded sandstone would be greatest perpendicular to the average paleo-wind direction and least parallel to it.

Poole (1962) reports paleo-wind directions for the Nugget Sandstone from northeast Utah and northwest Colorado near the Western Wyoming Thrust Belt. His data show a generalized paleo-wind direction of roughly N-S. If these data are similar to the Ryckman Creek Area, regional permeability may be greatest E-W and least N-S. Preliminary analysis of the dipmeter data from the subject well indicates a poorly defined W-NW

paleo-wind direction. More work on wind directions in this field would be necessary to further determine regional permeability trends due to cross-bedding.

The effect of fracturing on horizontal permeability in this rock is to greatly increase permeability anisotropy. As pointed out in Stearns (1968b) and Nelson (1979), fracture planes have definite and reproducible orientations with respect to structural strike in a fold such as at the Ryckman Creek Field. Major permeability trends should run near-parallel and near-perpendicular to the axis of the structure. Open fractures would increase reservoir permeability parallel to the fracture plane, while gouge-filled fractures would decrease reservoir permeability perpendicular to the fracture plane.

Data Types

This study of the Nugget Sandstone used three different data types: random plug data, oriented plug data, and 3-D whole-core data. Obviously, not all data types are necessary in every standard analysis of a reservoir such as this. The type of data to use depends to a great deal on the type of simulation to be made.

The random plug analysis, for example, gave a very good representation of the data as a whole. The random plugs plot intermediate on the ϕ -k diagram with respect to the oriented plugs, and somewhat closer to the whole-core data than the plugs as a whole. The random plugs with a correlation coefficient for σ -k of 0.888 represent the total of several petrologic effects quite well. If a homogeneous reservoir is assumed, the random plug analysis gives a good representation of the reservoir. However, while considered appropriate in many primary production models, this assumption is often invalid for modeling secondary and tertiary recovery in anisotropic reservoirs. Reservoir inhomogeneity and anisotropy are not well defined by the random plug analysis.

The 3-D whole-core data (k_{Hmax} , k_{H90} , k_v) is the best to use for reservoir analysis incorporating anisotropic features. Data plots, such as Figures 4-29, 4-30, and 4-31 can be used to define this anisotropy. Once anisotropy is defined on whole-core analyses, the numerical effect of mixed features can be determined with oriented plug analysis as performed in this study.

Permeability Anisotropy and Stylolites

As pointed out earlier in this chapter, stylolites can create a strong permeability anisotropy within a reservoir. Permeability tensors can be created

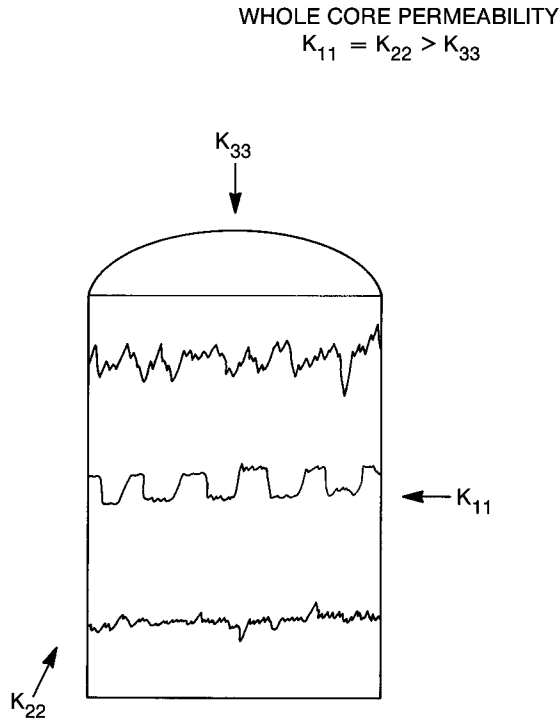


Figure 4–33 Effect of parallel stylolites on 3-D whole-core permeability.

for the effect of stylolites similar to that created for fractures. In calculating the principal permeability components of the second order tensor (k_{11} , k_{22} , k_{33}) two conceptual approaches can be taken. The first envisions the presence of parallel stylolites within the reservoir, as is often observed in core samples (Figure 4–33). In this case permeability measured perpendicular to the stylolite seam is usually the minimum permeability component (k_{33}). The maximum and intermediate reservoir permeability components are assumed to be equal and parallel to the seam ($k_{11} = k_{22}$). The second conceptual approach envisions that the stylolite seams anastomose or interconnect in three dimensions within the reservoir (see Figure 4–34). In this case, the overall permeability effect will be equal in all directions, creating an isotropic permeability tensor for stylolites ($k_{11} = k_{22} = k_{33}$).

In either model, measurements of permeability parallel and perpendicular to stylolite seams with respect to normal matrix permeability can allow for the creation of the stylolite permeability tensor (measurement with stylolite minus matrix permeability in that same direction gives the effect of the stylolite along that line).

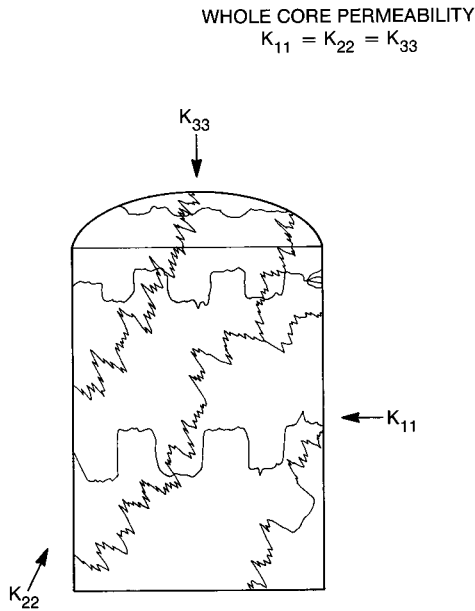


Figure 4–34 Effect of intersecting or anastomosing stylolites on 3-D whole-core permeability.

Combined Tensors

Once the permeability tensors are created for the various fabric elements within a rock, they can be numerically manipulated to depict the combined effect of all oriented anisotropic features: B_{ij} for bedding, F_{ij} for fractures, S_{ij} for stylolites, and M_{ij} for homogeneous matrix (Figure 4–35).

The tensor components and their directions can be derived from statistically analyzing numerous oriented permeability plugs and appropriate whole-core samples. Therefore, the values may vary in error and quality with the amount of data available and may not match exactly the values in the reservoir on a foot-by-foot basis. They do, however, allow prediction of combined effects within the nonsampled, interwell portions of the reservoir where the individual features change in abundance and orientation in a predictable manner with respect to formational boundaries and the long axis of the wellbore. Future predictions of interwell areas for reservoir modeling in anisotropic reservoirs will rely heavily on permeability tensor analyses similar to those discussed here.

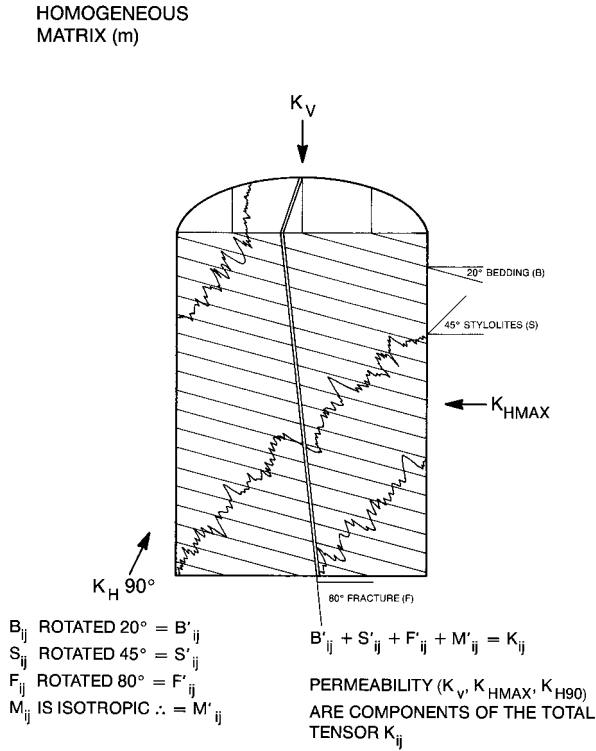


Figure 4–35 Schematic diagram showing various permeability tensors including that for stylolites would be rotated and added to simulate or correspond to 3-D whole-core analyses. Also see Figure 4–32.

STATISTICAL DATA IN RESERVOIR MODELING

Reservoir Domains or Compartments

Reservoirs are considered to be anisotropic when they possess significant variation in physical properties (porosity, permeability, wettability, etc.) in three dimensions. The Nugget Sandstone reservoirs of the Western Wyoming Thrust Belt all fall into this category. Reservoir anisotropy and heterogeneity are due to primary sedimentary fabric and variations in physical and chemical diagenesis. Such anisotropy can lead to several potential reservoir problems. These include:

1. Reservoir compartmentalization
2. Anisotropic fluid flow
3. Difficulties in recovery planning
4. Uncertain economic forecasts

In the Nugget Sandstone, reservoir anisotropy is the result primarily of the presence of crossbedding and natural fractures of various morphology (Figure 4–36).

In describing anisotropic reservoirs such as the Nugget sandstone, for the purposes of reservoir modeling, three general approaches can be used to represent the distribution of reservoir properties (Figure 4–37) (Lelek, 1983). In the first (Figure 4–37a), anisotropic properties are of such a small scale and so variable in distribution that a single-layer homogeneous model of the reservoir can be used. This model is characterized by reservoir properties that are extracted or averaged in some manner from the entire data population. Such models are frequently supported by the statement, “the rocks are so heterogeneous they are homogeneous.” These models or descriptions are most valid when the reservoir properties of interest vary in a nonsystematic or nonsegregated manner. This approach is least valid when domains of similar reservoir properties exist within the material.

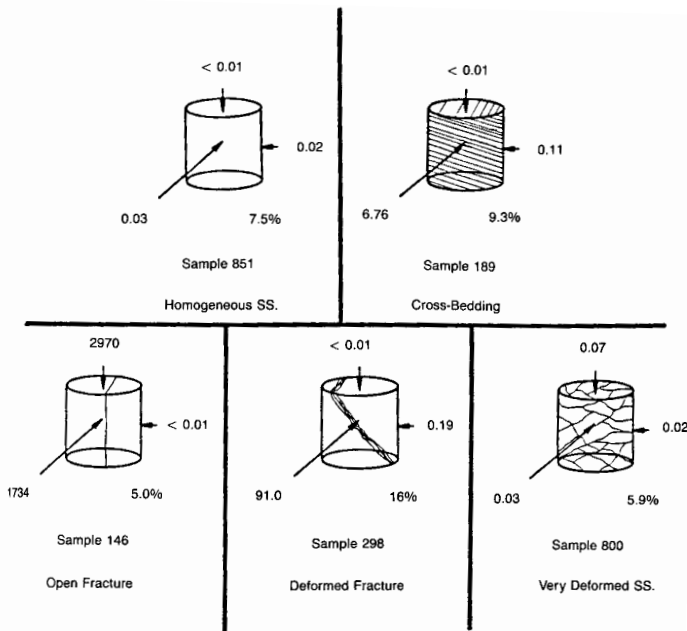


Figure 4–36 The effect of heterogeneities on 3-D whole-core permeability are shown. Sample porosities are given in percent, and permeabilities in millidarcies. All samples are from the Champlin 458, Amoco D-3 Well, Anshultz Ranch East Field.

In the second approach to modeling reservoir property distribution (Figure 4–37b), properties are assumed to be layered, varying primarily in the vertical dimension while being continuous or homogeneous in the lateral direction. This approach is the most frequently used in modeling sedimentary rocks with normal intergranular porosity. Layering is generally accomplished by the correlation of porosity, gross lithology, or flow rates from well to well. It is assumed that no significant or unexpected variation in properties exists along each layer between correlation points. In lieu of any reason to expect variation outside the known data population or any expectation of property segregation due to depositional processes, this is the most appropriate approach in modeling a normally bedded, nonfractured sedimentary reservoir.

The third approach to modeling reservoir property distribution (Figure 4–37c) assumes the presence of domains of like reservoir properties that vary both vertically and laterally on a large scale within the reservoir. This “brick-like” distribution of properties can occur because of sedimentary texture or fabric, such as in Eolian dune sequences, or because of the inhomogeneous distribution of natural fractures. The Nugget Sandstone at East Anschutz can be characterized as a brick-work reservoir. The greatest difficulty with this approach to reservoir description is its complexity. Because this approach does not a priori assume continuity in the lateral direction, as in the layered approach, construction of the domain distribution from a limited amount of one-dimensional well data becomes very difficult.

The reason this approach is considered more appropriate than the simpler layered approach (Figure 4–37b) lies not in the porosity distribution but the permeability distribution within the reservoir. Crossbedding and natural fractures show a high degree of preferred orientation that produces anisotropy. As such, directional reservoir properties, for example permeability, vary dramatically in three dimensions. Porosity as measured in either core or logs is a bulk property that has no inherent directionality. Any lateral continuity of porosity evidenced within the reservoir does not necessarily indicate permeability continuity or layering.

The most difficult part of creating a reservoir description for the purposes of detailed reservoir modeling is the melding of diverse data types into a coherent package. Definition and correlation must proceed from simple one-dimensional descriptions, to more difficult two-dimensional correlations, and finally to complex three-dimensional definitions of reservoir response units.

Consider a small slice of a hypothetical sandstone reservoir, which is made up of 16 individual crossbed units (Figure 4–38a). These units or “pods” of sandstone are defined by the presence, strike and dip of cross-

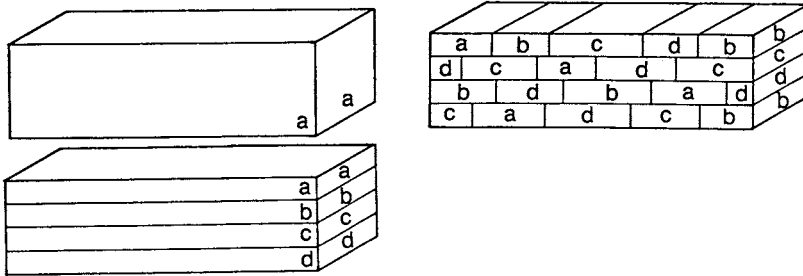


Figure 4-37 The various methods by which reservoir properties can be modeled in a petroleum reservoir. (Upper left) Homogeneous model in which properties vary in a small and statistically random fashion. (Lower left) Layered model in which properties vary primarily in the vertical dimension while being relatively continuous in the lateral direction. (Right) Domain model in which properties are distributed in domains of like reservoir properties and varying in both vertical and horizontal dimensions.

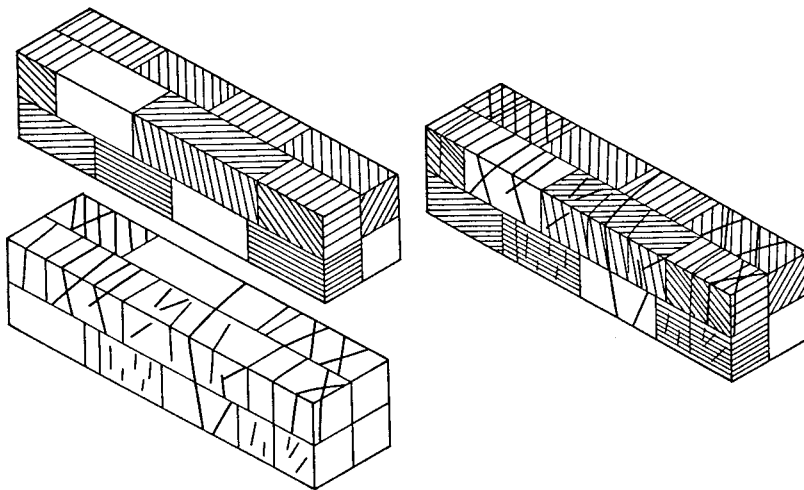


Figure 4-38 (Upper left) Idealized slice of an Eolian Sandstone reservoir broken up into units of nonbedded and crossbedded material of various crossbed orientation. (Lower left) Possible fracture distribution within this slice with open fractures and deformed fractures. (Right) Complexity of the reservoir as those various anisotropic fractures are added together. Anisotropic response units can be defined from the addition of these various factors.

beds, grain size, and porosity-permeability relationship of the material. Now imagine a nonhomogeneous fracture distribution (Figure 4-38b). The combined crossbed and fracture data for this hypothetical reservoir slice would produce a highly compartmentalized reservoir (Figure 4-38c). The combined fracture and crossbed data can be coded to represent blocks of like permeability anisotropy or response in fluid flow (Figure 4-39).

Basic to such a process is a complete one-dimensional description of each well. Environment of Deposition (EOD), sample type (sample categories defined by the presence and relative orientation of predetermined features), and petrophysical units can all be interpreted on sample or core logs. These one-dimensional units can then be correlated in the second dimension to the next well studied. The two-dimensional correlation of the two individual well data sets shows that while porosity is often roughly correlative, large portions of the sample type and EOD units are not. Communication or continuous layering between wells would, therefore, be suspect.

Three-dimensional correlation and definition of reservoir units proceed along the same lines as the two-dimensional correlations and utilize prospective fence diagrams. In this way, limits or size constraints can be placed on the individual reservoir response units. These response units may often be defined by the EOD units (modified or further subdivided by pods of material of relatively constant crossbed orientation) and sample type layering (chosen at a scale commensurate with the EOD or porosity unit size).

These 3-D response units *must* then be analyzed and modified to fit the large-scale reservoir data derived from the early production data and multiple well tests and finally iterated into the mathematical models in a manner similar to that described in Barbe (1983). Only through this small-scale to large-scale correspondence can the most valid, yet least complex reservoir description be determined. In order to better deal with complex reservoirs in the future, more work and data is required (see Table 4–2).

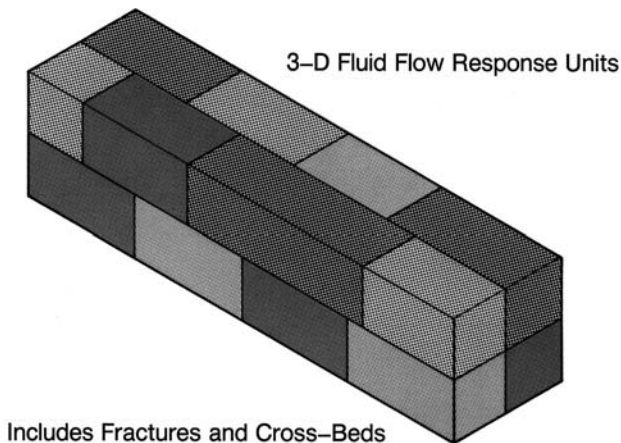


Figure 4–39 The various anisotropic fractures depicted in Figure 4–38 can be added together to form response units, which act as entities on units with respect to fluid flow. These are shaded here to show their 3-D fluid flow affinities to other crossbed/fracture units within the reservoir.

Table 4–2
Research Needed in Anisotropic Reservoir Analysis

1. Determine the relative importance of various petrophysical/petrological parameters on fluid flow.	<i>Which parameters?</i>
2. Learn to more accurately superimpose anisotropic effects of various rock fabrics.	<i>How they add?</i>
3. Tie petrophysical data to reservoir engineering data.	<i>Scaling?</i>
4. Determine the proper level of geological/petrophysical complexity necessary for effective reservoir modeling.	<i>How complex in modeling?</i>

By the general method described above, geological and petrophysical data can be used in effective reservoir management, either directly or through the use of reservoir modeling techniques. In this way, optimum reservoir management can be approached through time.

Averaging Techniques in Three Dimensions

Once an anisotropic reservoir is modeled into domains or flow compartments for modeling, it is necessary to assign flow properties to these units or blocks. The rock within these domains must be quantified by a single set of characteristic directional and nondirectional parameters (such as porosity, directional permeability, permeability ratios, directional permeability-porosity relationships, saturations, relative permeabilities, etc.). Methods of characterizing these blocks of material are, however, problematic.

In highly anisotropic reservoirs, there are usually several features, or orientations of single features, that cause a large scatter on standard reservoir property cross plots, such as porosity versus permeability and vertical versus horizontal permeability (see Figure 4–40). As pointed out earlier, these features include such things as bedding, crossbedding, fractures, and stylolites.

To reduce the scatter in such data and derive a statistically tighter relationship for domain characterization, smaller, statistically tighter data sets are used. The data sets are derived from detailed descriptions of each porosity/permeability sample taken in the reservoir. Three-dimensional whole-core analyses are essential in this regard. Sample types can be defined on the basis of the presence and orientation of various anisotropic features relevant to that reservoir (Table 4–3).

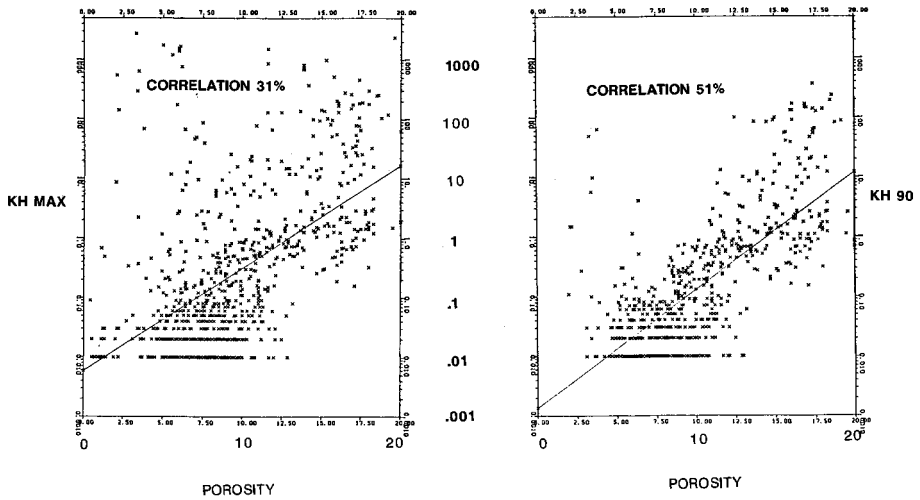


Figure 4–40 Whole-core porosity-permeability diagrams for all samples in the Champlin 458, Amoco 3-D Well, Anschutz Ranch East Field. Note that correlation quality is only 31 percent for the K_{Hmax} plot and 51 percent for the K_{H90} plot.

Table 4–3
A Sample Type Classification for Nugget Sandstone
at Anschutz Ranch East

1. NB, NF
2. NB, $F < 45^\circ$
3. NB, $F > 45^\circ$
4. $B < 20^\circ$, NF
5. $B < 20^\circ$, $F < 45^\circ$
6. $B < 20^\circ$, $F > 45^\circ$
7. $B > 20^\circ$, NF
8. $B > 20^\circ$, $F < 45^\circ$
9. $B > 20^\circ$, $F > 45^\circ$

where NB is no bedding
 NF is no fractures
 B is bedding
 F is fractures
 90° is parallel to core axis
 0° is perpendicular to core axis

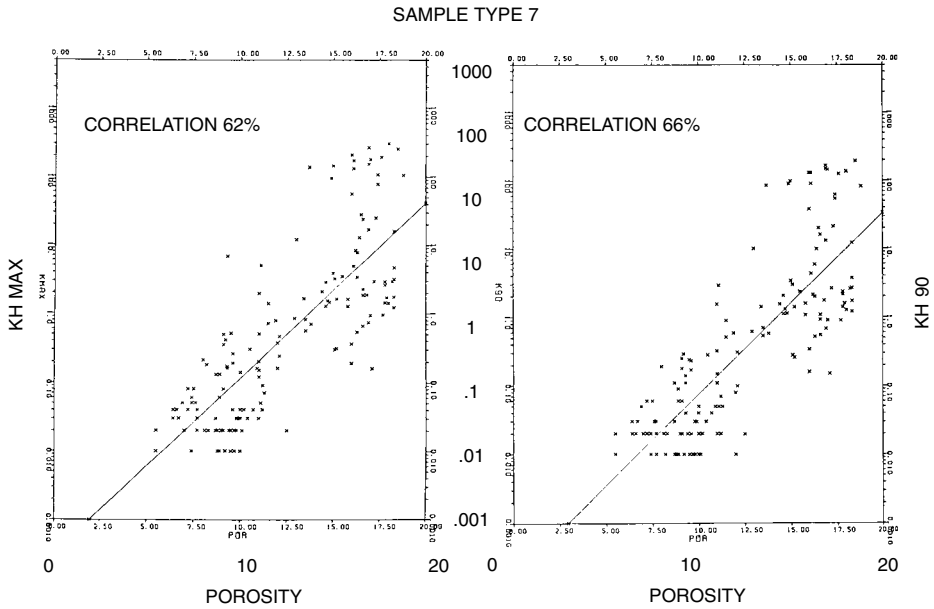


Figure 4-41 Whole-core porosity-permeability diagrams correlative to those in Figure 4-40, but for only sample Type7 data (bedding dip greater than 20° , unfractured.) Corresponding correlation quality has risen to 62 percent for the K_{Hmax} plot and 66 percent for the K_{H90} plot.

The sample sets, then, are groups of samples with common anisotropy attributes. The sample set data can be cross-plotted in a form similar to that of Figure 4-41 for one sample type in which the original scatter in the data is much reduced (Figure 4-41). We can then characterize a reservoir domain or block by the presence and orientation of the features present (dominant sample type) and use the relatively cleaner sample type data to characterize the block.

The tighter sample type data population is the first step toward characterization. However, this data population must still be reduced to a set of individual values representative of the domain. This is most frequently done by averaging the data in some manner. Three of the averaging techniques available to us for this purpose give harmonic, arithmetic, and geometric means. (Equations for the calculation of these means are given in Appendix C.)

Permeability values for any sample population have a frequency distribution (Figure 4-42). Both are log-normal distributions with one (4-42a) being a nonskewed distribution and one (4-42b) a skewed distribution. These are similar in form to the fracture width distributions discussed previously. Notice that there is small variation in the three different averages

in the nonskewed distribution (Figure 4-42a). In this case all techniques would give somewhat similar values. In the skewed distribution, however, a great variation in the averages exists (Figure 4-42b). In such a population, the averaging technique used becomes very important. For fractured reservoirs and, indeed, all highly anisotropic reservoirs, the geometric mean is currently considered the most appropriate of the three in domain characterization.

Calculation of relevant permeability ratios is another important factor in domain characterization. Two basic approaches can be used: one involves calculating the average of all the individual ratios in the data population, while the other involves the creation of a single ratio using average permeability values. In my experience it is best to create directional permeability ratios (k_v/k_{Hmax} , k_{H90}/k_{Hmax}) by taking the ratio of the geometric mean of each permeability population (geometric mean K_v /geometric mean K_{Hmax} , etc.). These ratios are input into reservoir models for reservoir characterization.

Three-Dimensional Correlation of Reservoir Properties in Fractured Reservoirs

In correlating domain characteristics in three dimensions, several procedures must be considered. First the analyst must look for vertical and horizontal continuity in the data: 1-D correlations of reservoir properties within wells, 2-D correlations between individual wells along sections, and 3-D correlations among a network of numerous wells. Next, the interwell areas must be categorized by knowledge of rock type geometries, fracture continuity by fracture origin, and rock controls on fracture morphology. This interwell area characterization, which is based substantially on prediction, must then be backed up with multiple-well test data to support or refute the predictions.

These three-dimensional correlations and the quantitative data ascribed to them must then be displayed graphically in three-dimensional perspective. This is important because geologists generally think and work in three-dimensional representations and because it is easier to spot major discontinuity surfaces and their orientation in such presentations. Lastly, the three-dimensional correlations and characterizations based on data points and interwell predictions must be modified iteratively through the use of physical or numerical reservoir models and production values when available. This is often the only way to truly characterize fluid flow effects within the reservoir.

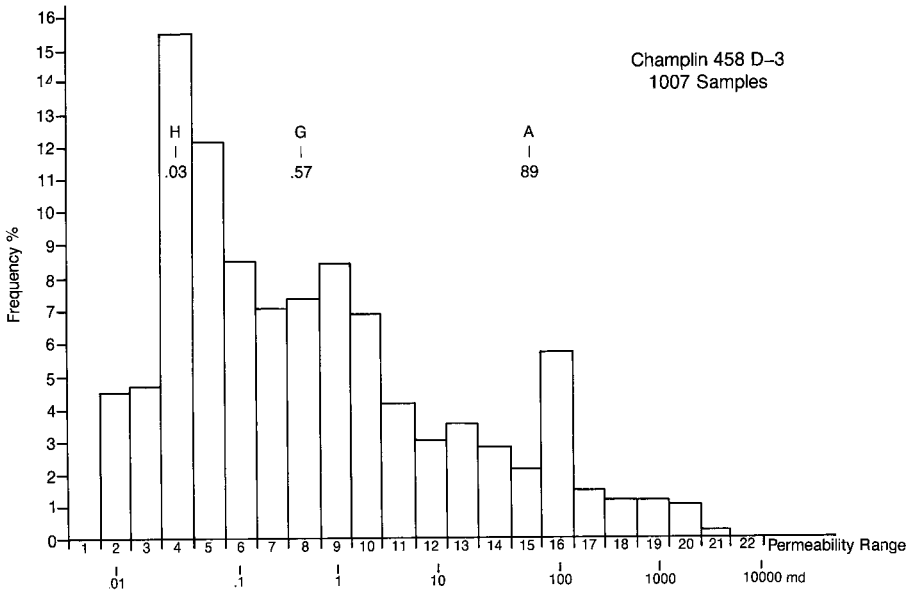
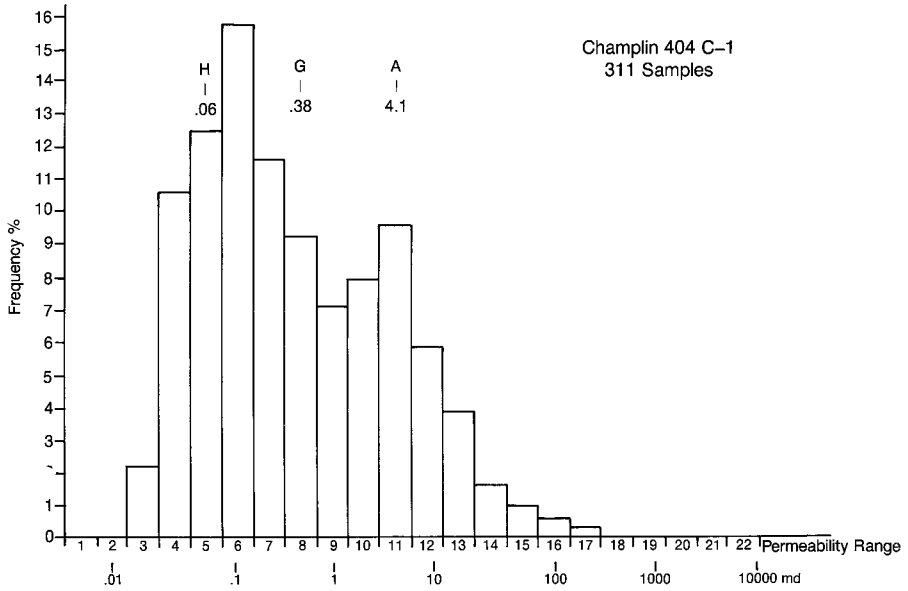


Figure 4-42 Permeability frequency diagrams for k_{Hmax} whole-core data, Nugget Sandstone, Anschutz Ranch Field, Wyoming Thrust Belt. Depicted are the harmonic (H), geometric (G), and arithmetic (A) means for lightly skewed (a) and heavily skewed (b) populations.

Statistical Characterization of Block Sizes

Most equations for fracture permeability and fracture porosity require the use of a fracture spacing term. For reservoir modeling and predicting the dynamics of reservoir flow, however, fracture spacing data is usually recalculated into matrix block size and shape (Aguilera, 1995, p. 518; and Van Golf-Racht, 1982, p. 99). Engineers find data in this form is very useful for defining fracture/matrix cross flow, matrix recovery factors, and pressure distributions within the dual-porosity system. Numerous publications deal with the statistical characterization of matrix block size and shape in fractured reservoirs. Of interest is Ghez and Janot (1972).

STIMULATION IN FRACTURED RESERVOIRS

Very efficient fracture stimulations can be performed in rocks that contain an extensive natural fracture system. In a fracture job (either explosive or hydraulic), productivity increase is directly related to the extent and surface area of the generated fractures. One fracture plane with the wellbore as a general midpoint is generated during a hydraulic fracture treatment. This single fracture can be propagated hundreds to thousands of feet into the formation and has a minimal amount of “fines” associated with its generation. In a “shot” well, many explosive fractures are generated radially around the wellbore. These fractures are, however, much shorter than hydraulic fractures (substantially less than 100 ft. in length) and are associated with an abundance of fine particles during their generation. These differences are important in considering a fracture stimulation program in a naturally fractured reservoir.

In induced fracture stimulation of an unfractured formation, the fracture surface area generated is calculated from the energy input and the amount and physical properties of the fluid injected. In a naturally fractured reservoir, the effective fracture surface area can be higher than that calculated for the fracture job due to the interaction of natural and induced fractures. Figures 4-43 through 4-46 depict various hypothetical natural and induced fracture combinations and the isopotential lines associated with these fractures. These drawings assume a matrix with low permeability and equal and near-infinite conductivity of the fractures. Though this is not the case in nature, it is used to simplify the situation for illustrative purposes.

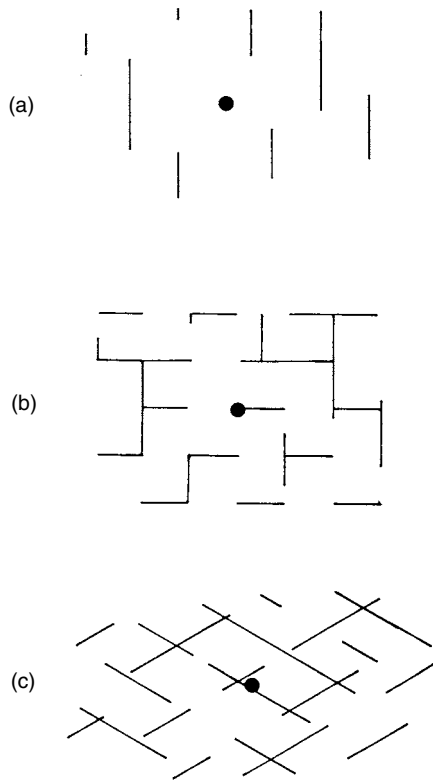


Figure 4-43 Three natural fracture systems (a) monodirectional, (b) orthogonal, and (c) oblique. Black dot represents the wellbore.

Hydraulic fractures are very efficient in draining large areas, especially in an interconnected fracture system or in a mono-directional fracture system if the strike of the hydraulic fracture is at high angles to the natural fracture trend. As unidirectional natural and induced fractures approach parallel, drainage is less efficient. Explosive or radial fracture patterns may communicate and drain better in interconnected fracture systems than in unidirectional ones. However, due to the multiple directions of fracturing in explosive stimulation, the strike of the natural fracture system becomes less important in drainage efficiency. Radial fractures are bound to intersect a natural fracture system of any strike provided the fracture spacing is small and is developed close to the wellbore.

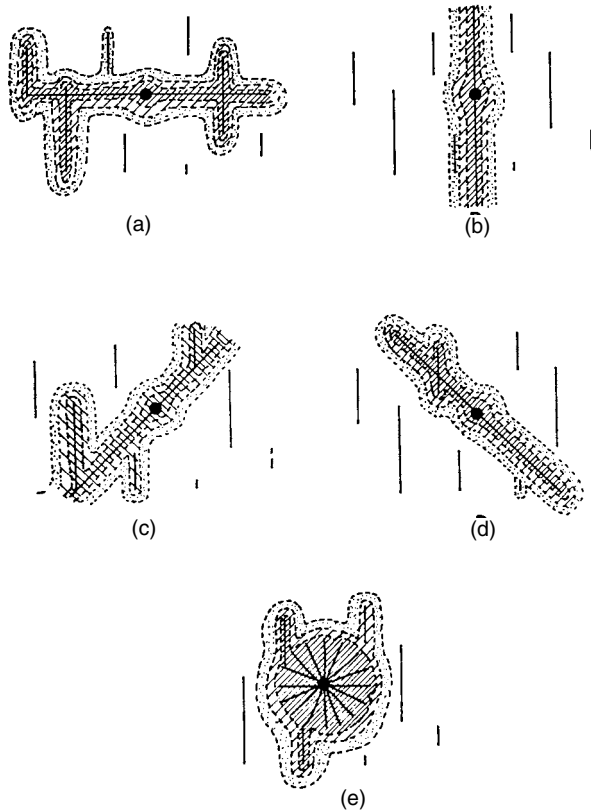


Figure 4-44 Three isopotential lines surrounding various induced fracture directions in a monidirectional natural fracture system; (a-d) are hydraulic fracture treatments, (e) is an explosive fracture treatment.

While in one instance, a correlation between wellbore hydraulic fracture orientations and the surface fracture orientations has been documented in Overby and Rough (1968), many downhole techniques for predicting hydraulic fracture directions have become popular. From cores within a field and predictions based on empirical relationships between fractures and geological structures, the strike distribution of a natural fracture system can be estimated. With the aid of mechanical tests on selected core samples and high-quality *in situ* stress measurements, the preferred hydraulic fracture

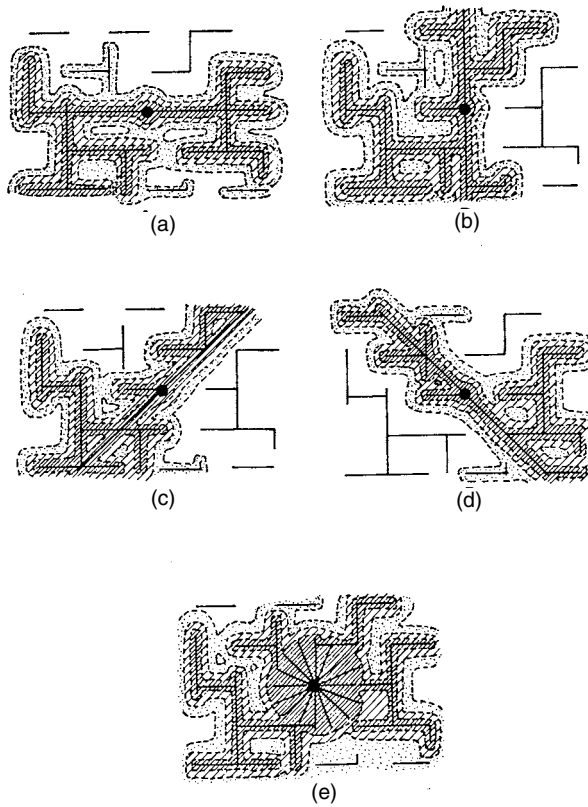


Figure 4-45 Three isopotential lines surrounding various induced fracture directions in an orthogonal natural fracture network; (a–d) are hydraulic fracture treatments, (e) is an explosive fracture treatment.

direction may be predicted in some cases (Smith et al., 1978; and Logan, 1983). If in a closely spaced natural fracture system, it is found that designed hydraulic fractures cross the natural system at high angles, a hydraulic fracture stimulation would be most efficient. If on the other hand the potentially developed fracture plane intersects the natural system at low angles, the explosive system may be more efficient at intersecting the greatest number of natural fracture planes. In a highly interconnected system of closely spaced natural fractures, both stimulation techniques would probably be efficient. The major deciding factors would be cost and safety.

Explosive fracturing has been of use in earlier-produced naturally fractured reservoirs where wells were characteristically completed open hole.

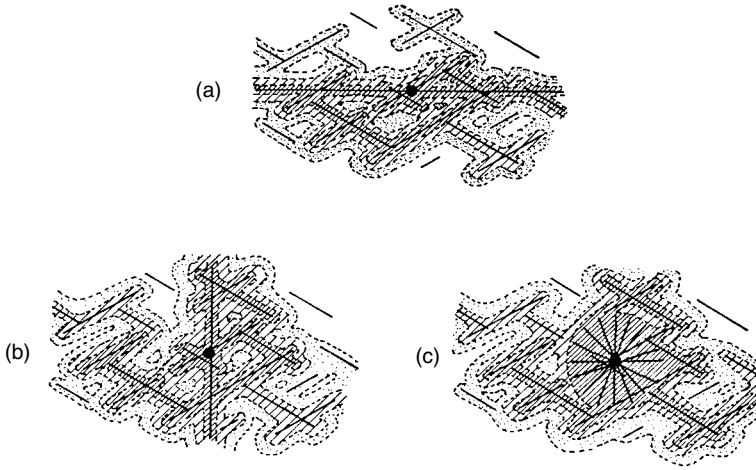


Figure 4-46 Schematic diagrams depicting three isopotential lines surrounding various induced fracture directions in an oblique natural fracture network; (a–d) are hydraulic fracture treatments; (e) is an explosive fracture treatment.

Production engineers today discourage explosive fracturing due to wellbore damage, safety, and casing problems. However, if carefully designed by the geologist, engineer, and driller, explosive fracturing may still be valuable in specific highly fractured reservoirs, especially in light of the new low-velocity explosives currently available.

In the Big Sandy Field of Kentucky and West Virginia, such a natural fracture system exists in the Devonian Black Shales. A study of hydraulic versus explosive fracturing was performed for the Department of Energy to determine which stimulation process is most efficient (Ray, 1976). In most cases, the hydraulic fracture stimulation yielded higher flow rates and better production than the explosive fracturing. The hydraulic fracture treatment was always significantly greater (as much as 115 percent better) in wells of low initial, pre-stimulation flow. In the highest initial flow rate wells, which probably possess more intense natural fracture systems, this difference was as low as only about 9 percent in the second year of production. In very fractured reservoirs, a 9 percent increase must be balanced against the higher cost of the hydraulic fracture jobs.

The discussion of the interaction of natural and induced fracture systems has assumed no inhibition of the generation of induced fractures by the presence of a pre-existing natural fracture system. Indeed, natural fractures can: (1) control the orientation of a hydraulically induced fracture; and (2) inhibit the generation of a hydraulic fracture.

Natural fractures in a reservoir impart a mechanical anisotropy to the rock mass. This anisotropy can be a plane of weakness, as in the case of an open fracture, or a plane of strength, as in the case of a fracture filled with gouge material or secondary mineralization. The orientation of a hydraulic fracture plane is controlled by the *in situ* state of stress in the rock mass. When this state of stress approaches hydrostatic (all three principal stresses near equal, or a very low differential stress), anisotropies within the rock can dominate fracture orientation (Smith et al., 1978; and Logan, 1983).

Work by Komar and Frohme (1973) on one type of rock has shown that if the *in situ* differential stress is less than 200 psi, mechanical anisotropies within the rock control hydraulic fracture orientation. These anisotropies could be sedimentary structures, rock fabric, or fracture planes. When *in situ* differential stresses are above 200 psi in this rock, the state of stress may control generated fracture orientations.

The presence of natural fractures can inhibit the generation of hydraulic fractures. If a well-developed, open fracture system is present in a reservoir prior to hydraulic fracturing, the fracturing fluids may open and prop the natural system, and never break the rock regardless of the state of stress (Blanton, 1982). This may be evidenced in fracture jobs in which a distinct breakdown pressure is never attained on a pressure-time record.

The control of generation and propagation of hydraulic fractures by natural fracture systems just described does not apply to explosive fracturing because of the very rapid strain rate involved in explosive stimulation.

5

Analysis Procedures in Fractured Reservoirs

Previous chapters have developed the general concepts and approaches necessary for effective evaluation of fractured reservoirs. This chapter will now step back and discuss how we determine we have a fractured reservoir and how we obtain the detailed data we need from core and outcrop observations and production techniques.

SCREENING TOOLS IN DEFINING A FRACTURED RESERVOIR

Natural fractures occur in all subsurface formations. However, as pointed out in Chapter 1, “A *fractured reservoir* is defined as a reservoir in which naturally occurring fractures either have, or are *predicted* to have, a significant effect on reservoir fluid flow either in the form of increased reservoir permeability and/or reserves or increased permeability anisotropy.” In practice, how do we determine if the natural fractures present have or will have this significant effect? To do this, screening tools can be created by which the analyst can begin to define this effect. These questionnaires can range from the simple to the complex and are used to direct the analyst to the key observations necessary. One such simple tool or checklist is shown in Table 5–1.

Table 5-1
Simple Fractured Reservoir Screening Tool

If you answer “Yes” to any of these questions, you may have a Fractured Reservoir:

- Do well test or whole core permeabilities exceed typical porosity-permeability relationship by an order of magnitude?
 - Do some wells in the field experience water influx much earlier than others?
 - Are well rates extremely variable across the field?
 - Do injected fluids show up earlier or in different wells than expected?
 - Are flow rates after casing and perforating substantially lower than open hole tests?
 - Do your drilling wells experience unexpected high mud losses or unintended variable drilling rates?
 - Do your wells experience rapid decline in rates?
-

In this simple tool emphasis is on flow behavior in the field. Other, more discipline-based tools can be addressed to screen the reservoir at earlier stages of its maturity. Examples of such discipline-based questionnaires are given in Tables 5-2 through 5-6.

Table 5-2
Fractured Reservoir Screening Tool Based on Geological Data

“Yes” Answers Point Toward the Presence of a Fractured Reservoir

1. Do you observe significant number of natural fractures (>1/ft.) in core or on well-processed imaging logs?
 2. Do outcrops of the relevant formation(s) on structures of similar origin contain abundant natural fractures?
 3. Are well test Kh’s a factor of two or more greater than those observed from core analysis?
 4. Do numerical structural deformation models using mechanical properties of the formation of interest and relevant structural geometry and deformation paths predict significant brittle strain in the trap?
 5. Do calibrated restoration strains from kinematic forward modeling predict significant brittle strain in the trap?
-

Table 5–3
Fractured Reservoir Screening Tool Based on Geophysical Data

“Yes” Answers Point Toward the Presence of a Fractured Reservoir

1. Do various forms of seismic attributes based on amplitude anomalies display azimuthal response within the trap?
 2. Does shear wave birefringence techniques show a strong azimuthal anisotropy within the trap?
 3. Do seismic dim zones correlate with structural curvature in the structure or map parallel to regional fracture trends in the area?
 4. Do interval velocities for the potential fractured reservoir vary significantly throughout the trap or structure?
-

Table 5–4
Fractured Reservoir Screening Tool Based on Drilling Data

“Yes” Answers Point Toward the Presence of a Fractured Reservoir

1. Do restricted zones in the formation exhibit penetration rates higher than expected and does this occur in more than one well?
 2. When drilling certain “hard” formations, does the drill string exhibit an unusual amount or “chatter” of vibration?
 3. Do we experience sporadic and rapid mud losses within the formation, and do they correlate across the field/trap?
 4. Do zones of mud loss become periodic within the formation?
 5. Does the well experience unusual pressure kicks, especially in tight portions of the formation?
 6. Do production logs (spinner, temperature, acoustic) display restricted zones of high fluid entry in a step function manner?
-

Table 5–5
Fractured Reservoir Screening Tool Based on
Reservoir Engineering Data

“Yes” Answers Point Toward the Presence of a Fractured Reservoir

1. Is there a very good correlation between maximum rate and cumulative production within the field?
 2. Do pressure transient tests display a dual porosity behavior?
 3. Does history matching require greater than anticipated flow rates or drainage areas?
 4. Do well tests indicate the presence of fluid flow barriers or point sources away from the wellbore, and can these be mapped using multiple wells?
 5. Do multiple well tests or flood pilots indicate strong preferential flow directions or high permeability azimuths?
-

DATA TYPES AND CONSTRAINTS AS
A FUNCTION OF WHEN THE FRACTURED
RESERVOIR IS DISCOVERED

As pointed out in previous sections, fields are often discovered to contain fractured reservoirs long after production is initiated. This occurs either because of the paucity of appropriate data at the early stages of evaluation or a general lack of focus on fracture related issues within the reservoir. A major problem related to the delay of “discovery” of the effect of the fracture system is the limitations it places on collection of needed data from the field and the formation. For the purposes to this discussion, Table 5–6 defines three exploration and development phases.

Table 5–6
Work Procedures once a Fractured Reservoir is “Discovered”

-
- The Industry often resists defining fields as fractured reservoirs for as long as possible (Fracture Denial).
 - We can often “make it fit” during primary recovery, but it becomes evident during secondary recovery.
 - When we “discover” we have a fractured reservoir impacts the work plans we can accomplish.
 - 1)exploration/access,
 - 2)primary/production,
 - 3)secondary/harvest
-

Table 5–7 lists some of the major data types used in evaluating fractured reservoirs. However, not all of these can be brought to bear if fracture effects are understood later in the reservoir maturity cycle. Tables 5–8 through 5–10 display a version of data constraints and subsequent recommended procedures as a function of when the fracture system was discovered.

Table 5–7
Data Types Useful in Fractured Reservoir Analyses

<ul style="list-style-type: none"> • Cores • Borehole Image Logs • 2-D Seismic • Core Analysis (Plug, Whole Core/3-D Whole Core) • Structural/Fracture Modeling • Single and Multiple Well Tests • Tracer Tests • 3-D Seismic 	<ul style="list-style-type: none"> • History Matching • Reservoir Simulations • Directional Permeability Data • Water Breakthrough • 4-D Seismic • Drainage Area Calculations
---	---

Table 5–8
Data Constraints and Procedures When a Fractured Reservoir is “Discovered” During 1) Exploration/Access

Data Constraints

- Little dynamic data available
- Limited number of wells
- Predictions dominate the fracture descriptions

Procedures

- Obtain cores and/or image logs in all early wells
 - Predict natural fracture distributions
 - Select optimum well locations and well paths
 - Determine and map *in situ* stress from breakouts, etc.
 - Determine fractured reservoir type
 - Evaluate reserves, variability, and risk
-

Table 5–9
Data Constraints and Procedures When a Fractured Reservoir is
“Discovered” During 2) Primary Recovery/Production

Data Constraints

- Wells usually not located to maximize rate or reserves
- Well pattern interventions still possible
- Static data can still be obtained
- Correlation between static and dynamic data still possible

Procedures

- Plan static data collection wells
 - Perform multiple well tests
 - Model fracture system and *in situ* stress and correlate with dynamic data
 - Determine directional permeability vectors
 - Correlate fracture directions, *in situ* stress, and directional permeability
 - Refine reservoir simulations using fractures
-

Table 5–10
Data Constraints and Procedures When a Fractured Reservoir is
“Discovered” During 3) Secondary Recovery/Harvest

Data Constraints

- Few “elective” wells can be drilled
- Cannot gather fracture description or other static data easily or cheaply
- Generally have good dynamic data
- Little remaining flexibility in well locations and well patterns/spacing

Procedures

- Re-evaluate flood patterns
 - Evaluate water production in terms of fractures
 - Model *in situ* stress across the field
 - Infer characteristics of the fracture system from dynamic data
 - Re-evaluate reservoir simulations to include fracture anisotropy
 - Revise predicted recovery factor (down)
-

CORE AND OUTCROP ANALYSIS

Fracture Stratigraphy and the Interrelation of Deformation, Petrology, and Petrophysics

To obtain meaningful fracture data from observation of core or outcrops, it is important to look primarily at the fracture distribution first and not the standard stratigraphic breakdown of the section. Primary evaluation of the fracture system distribution on the basis of character and intensity (or for that matter deformation or physical diagenesis in general) allows for the delineation of a “fracture stratigraphy.” Deformation, in general, and fractures, in particular, are very sensitive to small changes in rock properties. Therefore, we are often able to do fine-scale petrology and petrophysics on the basis of fracture stratigraphy. Once a fracture stratigraphy or layering by fracture distribution is constructed, analysis must proceed for the reasons for, or controls of, this distribution. Some important controls are:

1. Localization of deformation by structural position
2. Bedding thickness
3. Petrology
4. Reservoir properties
5. Strain partitioning (for example, stylolitization versus fracturing versus flow).

Once the structural controls (strain distribution during tectonism) on fracture stratigraphy are determined, rock controls can be related to standard subsurface information sources such as mechanical logs and a measure of predictability gained. This procedure is distinctly different from the standard logging techniques for fracture detection discussed in Chapter 3 and is far superior to them. In the fracture stratigraphy approach, we are relating fracture distribution to rock or petrologic controls (such as composition, grain size, and porosity) and mapping these rock property distributions in the subsurface, a task for which mechanical logs are quite well suited. In fracture detection, mechanical logs are used to detect fracture properties directly, a task for which they are not well suited.

Determining Natural Versus Induced Fractures

Induced Fracture Systems

Many formations contain little or no effective natural fracturing and must be artificially fractured to stimulate production. There are two basic reasons for fracture stimulating a well:

1. To stimulate production by either increasing the effective surface area of the borehole or by increasing the average permeability of the formation.
2. To bypass low or non-permeable zones such as wellbore damage or facies changes.

In general, formations are fracture stimulated because they have adequate porosity or storage capacity and low permeability.

Many formations contain numerous artificially induced fractures that mask the natural fracture system present. This is especially evident in core analysis. It becomes important to know how artificial and stimulation fractures are formed and what their characteristics are in order to recognize them in analysis and evaluation. An excellent discussion on the characteristics of induced versus natural fractures is found in Kulander and others (1990).

There are several ways to form artificially induced or stimulation induced fractures:

1. Explosive fracturing, often called shooting
2. Indention or impact fracturing
3. Thermal fracturing
4. Hydraulic fracturing
5. Unloading
6. Careless core handling
7. Drillstring/rock interaction

Explosive Fracturing

Explosive charges set off within rock characteristically generate a system of fractures radially symmetric about the detonation point. They can be observed in surface rock blasts in mining operations and road construction. Such fractures can be generated in a wellbore to stimulate production (Figures 5-1 and 5-2). This fracture system is dominated by tensile or extension fractures with some minor shear fracturing present. In rock subjected

to a high-velocity explosive charge, the area immediately surrounding the charge is characteristically pulverized and compacted. This can cause substantial wellbore damage in a petroleum reservoir. This pulverized zone appears to be minimized when low-velocity explosives are used. The intensity of fracturing and distance of fracture propagation are related to the total energy of the blast and the subsequent partial velocity. Blast-generated fractures frequently curve into natural fracture systems, when present, just prior to termination as propagation rate decreases.

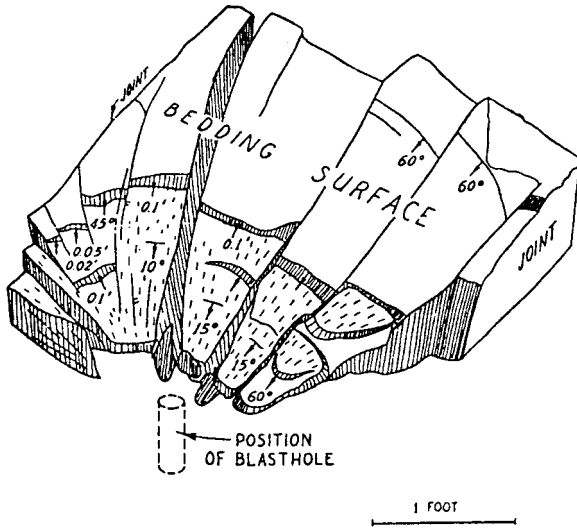


Figure 5-1 Blast-related fractures in Cretaceous Limestone in West Texas showing the arrangement of fracture surfaces to blasthole and natural “joints.” From Birkimer (1970). Courtesy of American Institute of Mining, Metallurgical and Petroleum Engineers.



Figure 5-2 Radial blast or explosive induced fractures in outcrop, southern Oklahoma.

Impact and Indention Fracturing

Included within this very loose classification are all fracture systems related to either impact or indention. Indention is the major rock-breaking process in rock/bit-tooth interaction in rotary or cable tool drilling (Figure 5-3). Impact fracturing results from such excavation processes as high-velocity water jet and spark drilling, and from mishandling of core as it is being hammered out of the core barrel.

Failure under indention or impact is predominantly from shear fracturing. The major distinction between indention and impact deformation is a difference in strain rate. The direction of shear failure is dependent on the state of stress below the indenter and the stress trajectory patterns derived from it (Cheatham and Gnirk, 1967). If the state of stress can be determined, the subsequent fracture patterns can be predicted, and vice versa.

Thermal Fracturing

Thermal fracturing is perhaps the least understood of induced fractures. There are really two different kinds of thermally derived fracturing: those related to a triaxial state of thermal stress and those related to thermal expansion and contraction of rock material due to the creation of thermal gradients. This distinction may be artificial, but is of use in the discussion of fracture patterns derived from temperature effects.

The three-dimensional state of stress derived from temperature is analogous to that derived from pressure; in fact, the two stress states can be superimposed when solving for the total state of stress in a material. Normally, thermal stresses in rock are small. Upon homogeneous heating to high temperatures, however, thermal stresses may cause fracturing. From such heating, either shear or tensile fracturing can take place. The orientation of the fractures generated can be calculated knowing the thermal state

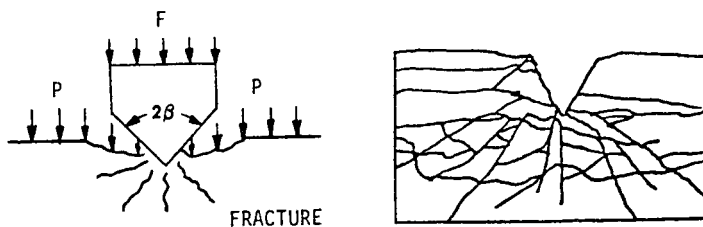


Figure 5-3 Extension and shear fracture network surrounding indention craters in Solenhofen Limestone as obtained with 60 bit-teeth at a confining pressure of 15,000 psi. From Cheatham and Gnirk (1967), courtesy of American Institute of Mining, Metallurgical and Petroleum Engineers.

of stress. It is common to encounter fractures associated with thermal gradients (thermal spalling) during coring and drilling operations (Figure 5–4). Such gradients can be established in the heating and cooling of rock next to drilling and coring bits. The fractures are tensile in nature and are formed perpendicular to the thermal gradient. These fractures are often purposely generated in hard rock mining to excavate rock material. Spalling due to high-energy electrical input could be considered to be a form of thermal fracturing.

Hydraulic Fracturing

In hydraulic fracturing, the wellbore fluid pressure is increased until it exceeds the total of pore pressure of rock plus the tensile strength of the rock plus the *in situ* least-principal rock stress. At this pressure, a fracture is generated on either side of the wellbore and will propagate some distance away from the hole. Due to the low tensile strength of rock, the fracture will generally be oriented perpendicular to the *in situ* least-principal stress (Figure 5–5). As such, the fracture is predominantly vertical at depth, but often horizontal at shallower depths (2000 ft. or less). If the direction of the least-principal stress changes away from the wellbore, so will the orientation of the hydraulic fracture. If the difference between the maximum and



Figure 5–4 Thermal unloading fractures in Tertiary basalt near Great Salt Lake, Utah. Field of view is about 2 ft.

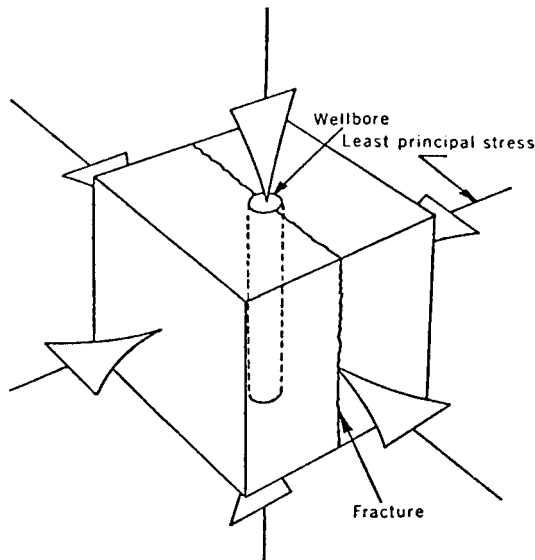


Figure 5-5 Geometry of an induced hydraulic fracture and its relation to the subsurface stress state and the wellbore. From Hubbert and Willis (1972), courtesy of AAPG.

minimum *in situ* principal stresses is low (in one known case less than 200 psi), rock anisotropies (including natural fractures) can control fracture orientation (Komar and Frohme, 1973; Teufel, 1976; and Blanton, 1982).

Hydraulic fractures can sometimes be generated in the wellbore by accident. Overbalanced mud systems often cause failure by hydraulic fracture at the wellbore. Such fractures can propagate uphole behind the casing, causing substantial production problems. These induced fractures follow the same mechanics of formation as fractures generated during stimulation.

Several recent papers discuss natural hydraulic fractures developed from fluid pressure increases resulting from organic maturation in source rocks. The fractures have been documented in thin sections of shale and are often used as an explanation of oil expulsion routes. While these are undoubtedly fluid-pressure related, they do not follow the mechanics of hydraulic fracturing, and they are best described by Coulomb failure (Domenico and Palciauskus, 1979).

Unloading

Many rocks may release locked-in stress or strain when removed from their subsurface environment. Sheeting, spalling, rock bursts, and unloading are all part of this process of induced fracture development. Such fractures generated in outcrop and core form perpendicular to the maximum unloading direction in the rock, which is often dictated by free surface

geometry, including erosion surface, core axis, etc. These fractures are, therefore, easily defined in outcrop.

Often in shale-rich zones in core, we observe shale partings parallel to bedding. When intense they are often called “poker chips.” These are a form of unloading fractures, unloading parallel to *in situ* maximum stress (σ_1) or perpendicular to bedding. Kulander et al. (1990) has documented plumose markings on these shale parting surfaces with an origin within the parting surface indicating that the fractures are induced. However, the markings also point out that the plume axis is oriented and parallels the *in situ* maximum horizontal stress direction (σ_2), making the markings stress indicators in an oriented core.

Careless Core Handling

Careless core handling can cause numerous induced fractures in core material. Removing jammed core from the core barrel with a sledge hammer, causing the core to fall in a heap on the rig floor, causes numerous fractures. Rough transportation and flexing of core boxes can also cause numerous bedding plane breaks within a core, especially in shale cores. Allowing some oil-saturated cores to completely dry out often induces contractional fractures, which look identical in their polygonal pattern to chickenwire fractures. But the polygonal fracture pattern caused by drying dissipates as you cut into the core, and it is often unequally developed on the sides away from, and resting on, the bottom of the core box due to differences in drying rate.

Drill String/Rock Interaction

Several types of induced fractures develop during the drilling or coring process. One is called a centerline fracture. It is an extension fracture propagated in front of the drilling or coring bit due to the weight of the drill string. If core is being cut, the fracture is often cored and occurs exactly in the center of the core (Kulander et al., 1990).

Breakage of core during the coring process sometimes causes a helical or spiral induced fracture to develop. This is due to twisting or torque applied to the core from the core bit and core barrel (Figure 5–6).

Another form of induced fracturing is “chatter” or petal fractures (Kulander et al., 1990). Chatter is a form of fracturing due to unstable frictional stick-slip between the core and core bit. It forms short, well-spaced, periodic fractures on two opposite sides of the core. Infrequently, two will intersect from opposite sides of the core, producing a strange-looking sinusoid-shaped induced fracture. The fractures are generally short and enter the core at the edge, and often propagate down and into the core as a centerline

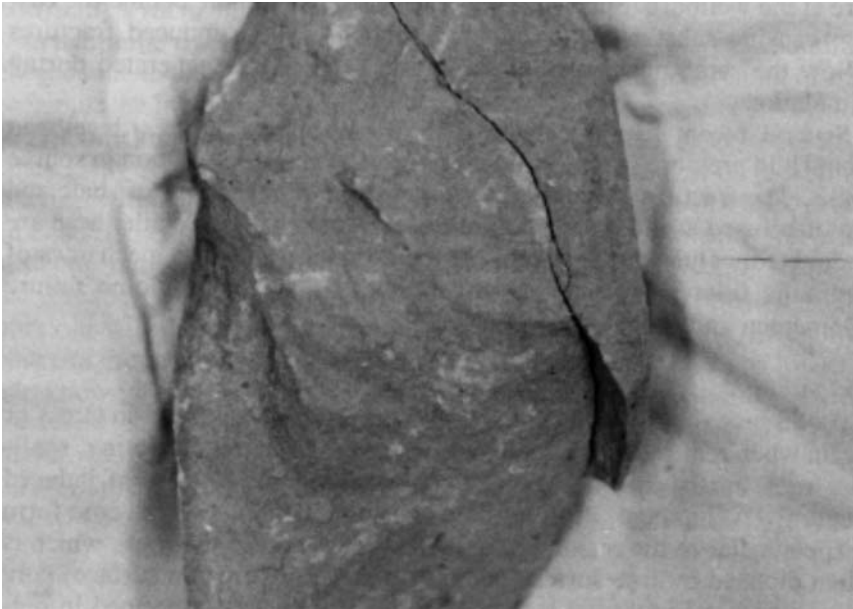


Figure 5–6 Helical, torque-induced fractures in 4-in. diameter Nugget sandstone core.

fracture, cutting the core into two equal halves (Figure 5–7). Long an enigma, centerline fractures and their associated petal fractures are now known to be extension fractures generated in front of the coring bit due to the weight of the drill string (Lorenz and Finley, 1988).

In hard rocks, the driller will often increase weight on drill string to maintain penetration rate. If high enough, this weight drives a propagating extension fracture below the drill string, and the coring bit cores it shortly after it formed. We now know that these can occur below drilling bits as well as coring bits and can occur in the borehole wall as well as in core. When centerline fractures form, the maximum load (σ_1) is parallel to the drillstring, therefore for a vertical well, it is a vertical fracture. Its azimuth is controlled by the *in situ* stress state in the subsurface with the induced fracture parallel to the maximum horizontal stress (σ_2) and perpendicular to the minimum horizontal stress (σ_3). These centerline fractures can be feet in height to hundreds of feet in height. If the core in which they reside is oriented, the azimuth of these fractures can depict the *in situ* stress directions in the subsurface. In addition, numerous centerline fractures are now found in the borehole wall on imaging logs (sonic or electrical). Because the image logs are oriented tools, the strike of these interpreted fractures can be determined and could be confused with accidental hydraulic fractures, which they would parallel.

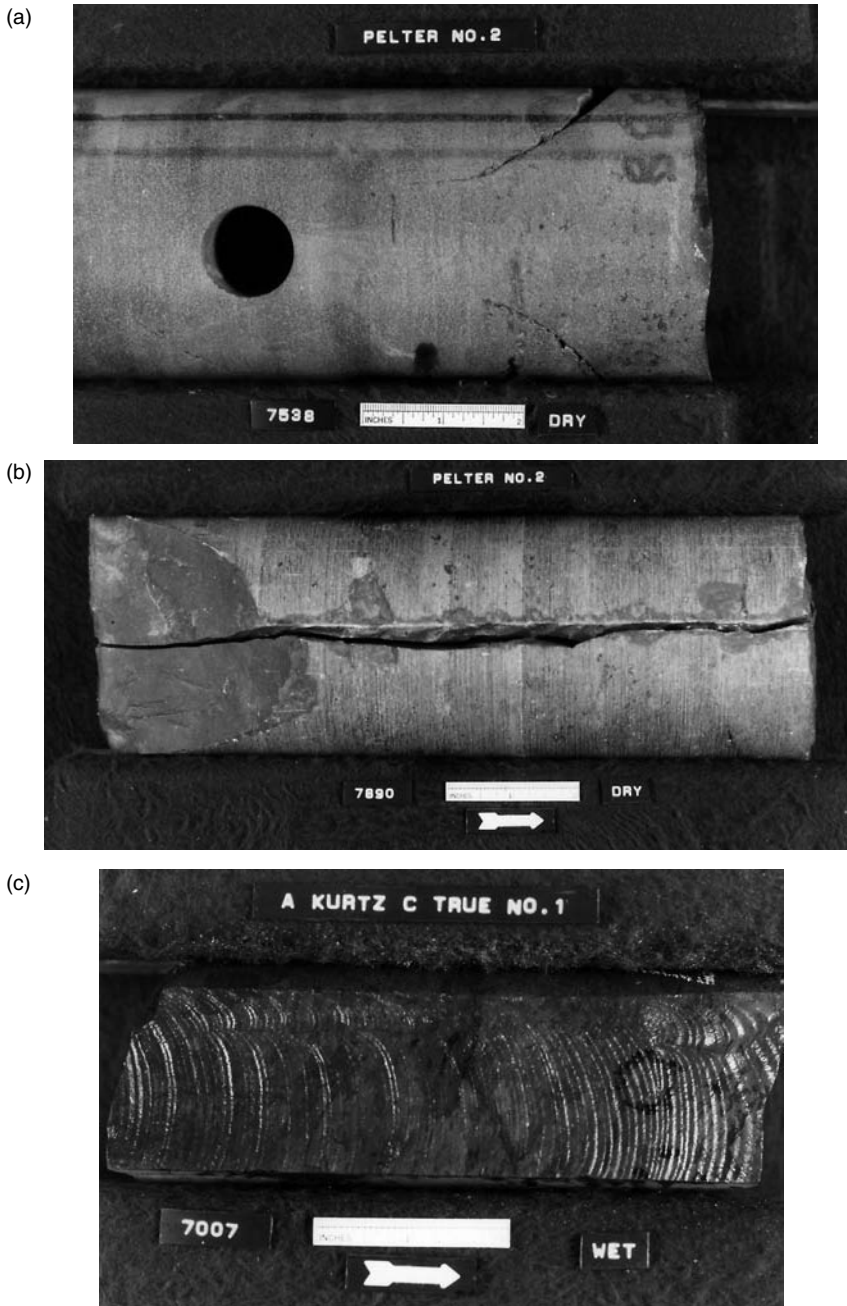


Figure 5-7 Petal and centerline induced fractures in core. (a) A pair of petal fractures on opposite sides of a core sample. (b) Core trace of a centerline fracture cutting the core in two equal halves. (c) Plumose and arrest lines on a centerline induced fracture surface in core showing downward propagation of the mode 1 crack in front of the bit. Photos courtesy of B. Ward and B. Kulander.

Observational Clues

The first step in observing core fracture data is to determine which are natural reservoir fractures and which are induced fractures. Several rules of thumb for this determination are listed below. The reader should also see Sangree (1969), Kulander et al. (1977), and Aguilera and Van Poolen (1977).

The observer should consider fractures to be induced or artificial if the fracture planes:

1. Are very irregular or conchoidal (especially true if the rock is fine-grained).
2. Parallel a scribe or orientation groove for a significant distance.
3. Always parallel the core axis even though bedding dip varies drastically with depth.
4. Are coincident with bedding planes.
5. Are cup-shaped or change strike or dip at the edge of the core. These can be unloading fractures due to removal of overburden pressure.
6. Are spiral or helical in shape. These are due to torque in the core barrel.

The observer should consider the fracture planes real, natural, reservoir fractures if they:

1. Contain cements or minerals not related to the drilling fluid.
2. Are enclosed within the core (both ends terminate within the core and do not intersect the core edge).
3. Form one or more parallel sets.
4. Are slickensided with an inferred movement direction consistent with deduced maximum stress direction during natural fracturing event.
5. Have directions or orientations consistent within the core and correlative with models of fracture distribution discussed in Nelson (1979) and Chapter 2.

The distinction between real and artificial fractures is difficult and inexact. The observer's ability to make such distinctions increases with experience. In some ways, it is more an art than a science. The overriding rule in core fracture work is *consistency of data*. Are the observed orientations consistent? Are the data consistent with models of and hypotheses for fracture distribution?

Data Acquisition

In natural fracture work, problems can range from the very general (e.g., Do natural fractures need to be considered in evaluation of this reservoir?) to the very specific (e.g., What will be the percentage contribution of natural fractures in condensate production from a specific field in the fifth year of production?). The level and importance of the initial problem must dictate the kind and amount of data generated during the study. There are so many aspects of fractured reservoirs that can be quantified and evaluated that no single study will likely incorporate all of them in a reasonable time. For practical reasons, analysis programs must be tailored to the specific questions asked.

Unfortunately, the geologists, engineers, or managers requesting analyses often are not familiar enough with fractured reservoirs or fracture analysis to pose proper or well-defined questions. Therefore, the fracture worker must learn to redirect a task (such as “work up the fractures”) into specific problems and questions (such as: Problem—“Fracture volume may not be sufficient to make the reservoir economic;” and Question—“What is the fracture system spacing, width, and porosity in the subsurface?”). Understanding the type of evaluation necessary is of paramount importance in defining the problems to address, the questions to answer, and subsequently the procedures to follow in analysis.

Levels of Observation

Once the specific problems and questions are structured in a particular evaluation, various observational and numerical data can be generated from relevant cores and/or outcrops. The complexity of these observations and data should be no greater than necessary to answer the questions posed. For example, in ascertaining if fractures will play a role in production from a formation, study of available core material and petrophysical data will be of a qualitative, near-cursory nature. On the other hand, if the object is to determine fracture system permeability in the formation at 10,000 ft., detailed quantitative distribution data and experimental data will be required. The level of observation should be commensurate with the type of question being asked.

Coring in Fractured Reservoirs

Coring in fractured reservoirs is often more difficult than in more normal reservoirs. Poor results are the result of core jamming due to rotation of fractured pieces of rock and subsequent low core recovery. In addition, fractured core is often handled poorly causing additional breakage making natural fracture interpretation more difficult. Some general procedures used in coring fractured formations are:

1. Most use a core barrel liner of either plastic or aluminium. It helps keep the core intact and prevents jamming. Some have used a flexible mesh liner like a Chinese finger puzzle to keep the core from falling out of the barrel on the rig floor, but this is not used very much.
2. Care is often taken not to put too much weight on a bit while coring. If weight on a string is too high, we can generate an induced extension fracture in front of the coring bit. It is then captured in the core as a “centerline fracture.” It will also show up in the borehole wall on image logs (FMI, etc.). These get in the way of interpreting the real fractures, but can be used as a stress direction indicator. The most fractured rocks are usually the hardest most brittle rocks, hence the tendency to weight up on a bit to maintain penetration rate.
3. Special handling of the core is often needed. If we are interested in natural fractures, removing the core from the barrel with a sledge hammer is not a good idea.
4. Care should be taken during twist-off at the bottom of the core. We often generate helical induced fractures in the bottom of the core if we are too aggressive in breaking the core off bottom.
5. Most workers try to core as long a continuous core as possible (often up to 90 ft. at a time). The idea is that once the coring is working, you don’t want to start and stop. That’s where recovery falls off.
6. In some hard rocks, some workers add the Hugel Knives to the mouth of the core barrel. These knives create the orienting scribes on the core when taking an oriented core. The idea is that the knives keep the fractured core from spinning as it enters the barrel and, therefore, prevents jamming.
7. Core is usually taken with a constant weight on a bit. Fluctuations in weight on a string causes problems.
8. Care is often taken in tripping the bit. Drillers should not trip too fast, as this often causes problems and damage in the core.

9. One successful company had success in coring fractured chalk by paying a bonus to the core handlers based on the percentage of core recovery. This was perhaps the thing that influenced the process the best; care!

Core Analysis Methods

Factors to Consider

The following general points should be considered when doing fracture analyses from core.

1. There is no substitute for core observations, especially early in the development of a field.
2. Large-diameter cores are preferred to small-diameter cores. The larger-diameter core depicts more regularly spaced high-angle fractures and, therefore, gives a better representation of fracture spacing and reservoir properties.
3. Whole-core porosity and permeability analyses are preferable in that they sample fracture properties better than plug analyses. Three-dimensional whole-core permeability analyses are the best form of such data.
4. Core observation should be backed up with appropriate logs from the same zone for extrapolation to uncored wells. The acoustic or electrical borehole imagery tools are good for this purpose.
5. Structural and petrological descriptions of the core go hand-in-hand.

Core Procedures

The following procedures have proven useful in fracture analyses in core.

1. Lay out all of the core from a given well at once for observation. This makes descriptions of relative fracture distribution and intensity easier and more consistent.
2. Next, do initial observations while the core is in its whole-core state (unslabbed). In this state, all fractures are present, and their angular relationships retained. The core can be slabbed later, and a finer internal description done at that time.

3. Have the core analyses (porosity and permeability) data in hand while observing the core to determine the relative effect of the features observed. Get 3-D whole-core data, if possible, if from observation the fractures or other anisotropic features are going to be important.
4. Do the fracture stratigraphy (involves procedures 5 through 16).
5. Construct a core/deformation map at a relevant scale, which includes the major lithology and formation breaks, lost core and noncored intervals, and oil/water or gas/water contacts, and if available, fractures, and stylolites. Often hairline fractures in the core will be difficult to see. These can be enhanced by painting the core with a volatile liquid and observing the drying pattern. Overlooked fractures may “jump out” at the observer by persistence of wetting along hairline fractures reaching the core surface.
6. Record fracture distribution with depth.
7. Record fracture distribution with rock type.
8. Record the dip of fractures.
9. Record the strike of fractures if the core is oriented core or locally oriented by an imaging log.
10. Look for intersection angles of fractures as expressed on the outside surface of the core or on the ends of the samples.
11. Determine natural versus induced fractures.
12. Describe stylolite distribution.
13. Determine fracture morphology, paying particular attention to any partial mineralization along the fracture planes that might act as a natural proppant during depletion. If present, determine its mineralogy and strength.
14. Measure the relative size or height of the fractures, paying particular attention to any features that tend to control the vertical extent of the fractures: lithology breaks, bedding planes, stylolites, unconformities, etc.
15. Observe the width and width variation of the fractures.
16. Estimate or measure fracture spacing and its variability with depth.
17. Determine principal stress directions, and the origin and continuity of the fracture system(s).
18. Determine relative timing of deformational events.

19. Relate fracture distribution to rock properties and rock fabric (composition, porosity, preferred grain orientation, bedding, crossbedding, etc.).
20. Select samples for additional petrophysical/petrological determinations (X-ray, thin sections, permeability, etc.).
21. Estimate the permeability of individual fractures from the core analysis.
22. Qualitatively estimate fracture and matrix property interaction or at least determine if there is an evident impedance to cross-flow.
23. Determine the fractured reservoir type.
24. Photograph important relationships shown in the core, for documentation in reports, if needed.
25. Select samples for mechanical testing (if appropriate).
26. If needed, set up a checklist of important parameters and document as many parameters as needed on a foot-by-foot basis (on each whole-core piece is ideal).
27. Write down impressions and conclusions before leaving the core. Include thoughts on the relative importance of fractures to production and flow, the permeability of the fractures present, fracture porosity (qualitative), relative compressibility of the fractures fracture origin and continuity in the reservoir, the percentage of real versus induced fractures, and the fractured reservoir type.

Field Analysis Methods

To date, fracture analysis has remained very nonritualized. Each worker has developed his or her own field methods and parameters of interest. Methods briefly presented here should be altered and tailored to the individual analyst and the problem being addressed. This section has been written in such a manner that a novice investigator could, by recording as many of the noted items as possible, collect all of the field data necessary to quantify the fractured reservoir. Notebook pages should contain forms to be filled out at each station. By correlating these data and laboratory data on the rock of interest, approximations of reservoir fracture porosity and fracture permeability are possible.

Factors to Consider

1. Look for rocks similar to the reservoir rocks of interest on similar outcropping structures. Look at more of the rock section than just the perspective reservoir rock, including potential sealing beds. Look for *relative* deformational response and intensity (fracture versus flow, etc.) in the outcrops.
2. Measure fracture spacing in different layers (in and out of the formation in the same structural position). Relate fracture intensity to bed thickness. If a great difference in fracture intensity exists and is not related to thickness or structural position, take samples for porosity and X-ray mineralogy determinations.
3. Look for fracture orientation changes in different layers (in and out of formation in the same structural position). Look for fracture orientation changes with respect to structure and structural position. Determine principal stress directions from the fracture patterns at each outcrop and relate these directions to models of folding, faulting, etc. Pay particular attention to patterns and principal stress directions that do not fit working models.
4. Record fracture plane morphology (open, deformed, mineralized).
5. Postulate depth at which the fractures formed.
6. Observe fracture patterns in view of making cross predictions of fracture spacing and potential drainage area of wells (including the shape of drainage area).
7. Take representative samples of the formations of interest for possible mechanical testing (about 10" × 6" × 5").

Field Procedures

1. Select an outcrop area having representative fracture patterns for a specific structural position. Record strike and dip data, or at least strike data.
2. For a so-called quantitative measurement station (enough fracture measurements to be statistically meaningful), all fractures in the measurement area should be recorded and should number from 100 to 150 fractures. The actual number should depend on the complexity of the fracture patterns present.

3. For a so-called qualitative measurement station (not enough fracture measurements to be statistically meaningful), only general fracture trends are recorded, along with a judgment of relative abundance of the individual fracture orientations, when spot-checking areas between statistical measurement stations. If no major change in orientation and intensity of fracture patterns is observed away from nearby statistical measurement stations, the use of qualitative stations gives valid intermediate data.
4. At the individual measurement stations the analyst should record as much of the following general data as possible:
 - A locality number corresponding to a location map
 - A brief station location and data
 - The formation(s) and rock type(s) measured at the station
 - Strike and dip of the bed(s)
 - Structural position and attitude of the structure
 - Bed thickness(es)
 - Fracture spacing (number of fractures per foot of outcrop) along lines that are
 - (a) Parallel to the major fracture trend (with strike of line), and
 - (b) Perpendicular fracture to the major trend (with strike of line), *or*
 - (c) Parallel to bedding strike and,
 - (d) Parallel to bedding dip
 - Comments
 - Postulate the maximum stress direction (or,) at fracturing
 - Postulate the origin of fracture sets
5. Each individual fracture measurement should record as much of the following data as possible:
 - A sequential number
 - Fracture strike
 - Fracture dip
 - Fracture morphology (gouge, open, mineralized, slicken-sided, vuggy)
 - Fracture length or length class
 - Comments
6. At convenient times, the fracture data should be plotted in preliminary form on either rose diagrams or pole plots (PI diagrams). Such pre-

liminary plotting is necessary in the field to establish trends and application to simple geological fracture models. In this way, working interpretive models can be created and altered or updated while field data are still being gathered. At all times, the observer should examine fracture patterns in light of their relation to other localities and to local structural configuration.

7. The number and frequency or spacing of quantitative measurement situations are generally high in the early stages of study in a region and decrease in relation to qualitative stations throughout the length of study.
8. When dealing with outcrops containing a predominance of contractional fractures, much of the abovementioned quantitative orientation data will be ill-defined due to their isotropic distribution in orientation. In these outcrops, matrix block size (fracture spacing in 3-D) will be very important as will be lateral distribution and lithology.

Useful Checklists

In doing core and outcrop analyses of fractures to determine reservoir properties and reservoir type, it is often difficult to judge the relative effect of the fracture system. To help alleviate this problem, there are two useful checklists that can be used (Figures 5–8 and 5–9). Plotting the percentage of total reservoir permeability (Figure 5–8) and porosity (Figure 5–9) as a function of fracture width and fracture spacing for three orders of magnitude of matrix values proves helpful. When analyzing a core or outcrop, assumptions can be made for width at depth and matrix properties (determined from core analyses, thin sections, etc.) and the relative contribution of the fracture system for various spacings read off the graph.

For example, if the fracture system accounts for only 10 percent of the total permeability and 1 percent of the total pore volume of the reservoir, the analyst may choose to neglect the system in further study. Conversely, if the fracture system provides 80 percent of the permeability and 50 percent of the total pore volume, an in-depth quantitative study of fractures in the reservoir is indicated.

Checklists such as those presented here are important in early evaluations and in structuring evaluation programs. The reader is encouraged to investigate the use of these and other checklists of their own design.

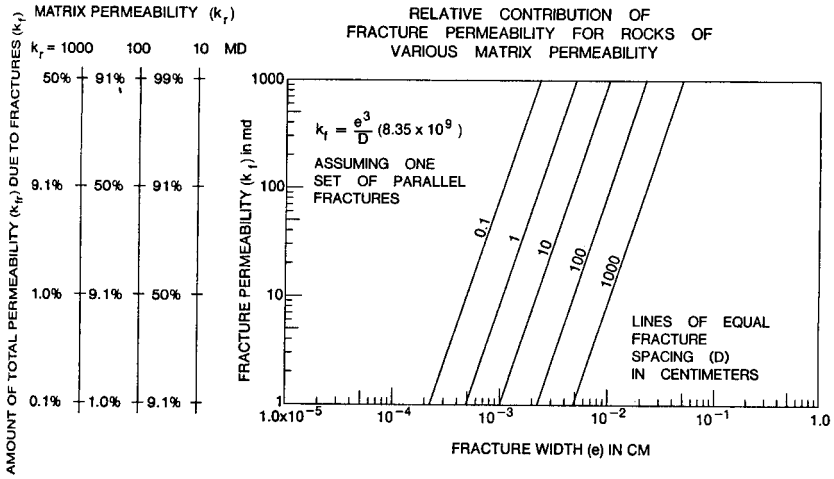


Figure 5-8 Total reservoir permeability due to fractures plotted as a function of fracture width, fracture spacing, and matrix permeability.

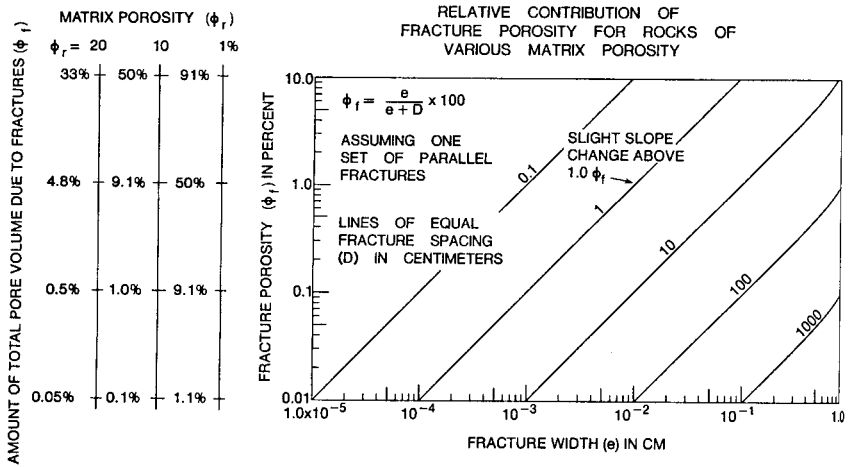


Figure 5-9 Total reservoir volume due to fractures plotted as a function of fracture width, fracture spacing, and matrix porosity.

Data Presentation

Methods of presenting individual station outcrop fracture data depend on the type of data available and may be divided as follows:

1. If only strike data are available, Rose diagrams or Azimuth histograms are used (Figure 5–10). Either can be used with absolute numbers or with percentages of the total population.
2. If only dip data are available, Dip histograms or Dip Quadrant diagrams are used. Either can be used as absolute number or percentage of the total population.
3. If both strike and dip data are available, stereographic projection plots are used (Pi diagrams) (Figure 5–11). These data are often contoured. For a description of how these diagrams are constructed, see Billings (1954).

Individual station fracture intensity data can be plotted on any of the above diagrams by adding the numerical intensity on the azimuth corresponding to the measurement line.

Areal and cross-sectional variations in fracture orientation and intensity data are generally plotted as points on simplified structure maps and structural cross-sections. Orientation maps plot the type of data available (strike data or strike and dip data.) (See Figure 5–12). Fracture dip data alone is plotted as points on structural cross-sections. Fracture intensity data is plotted on either structure maps or structural cross-sections. Fracture spacing data can be contoured for particular fracture sets or for particular compass directions.

Presentation of fracture data in final form is often facilitated by using a schematic format which simplifies the data and makes it easier to present in oral form.

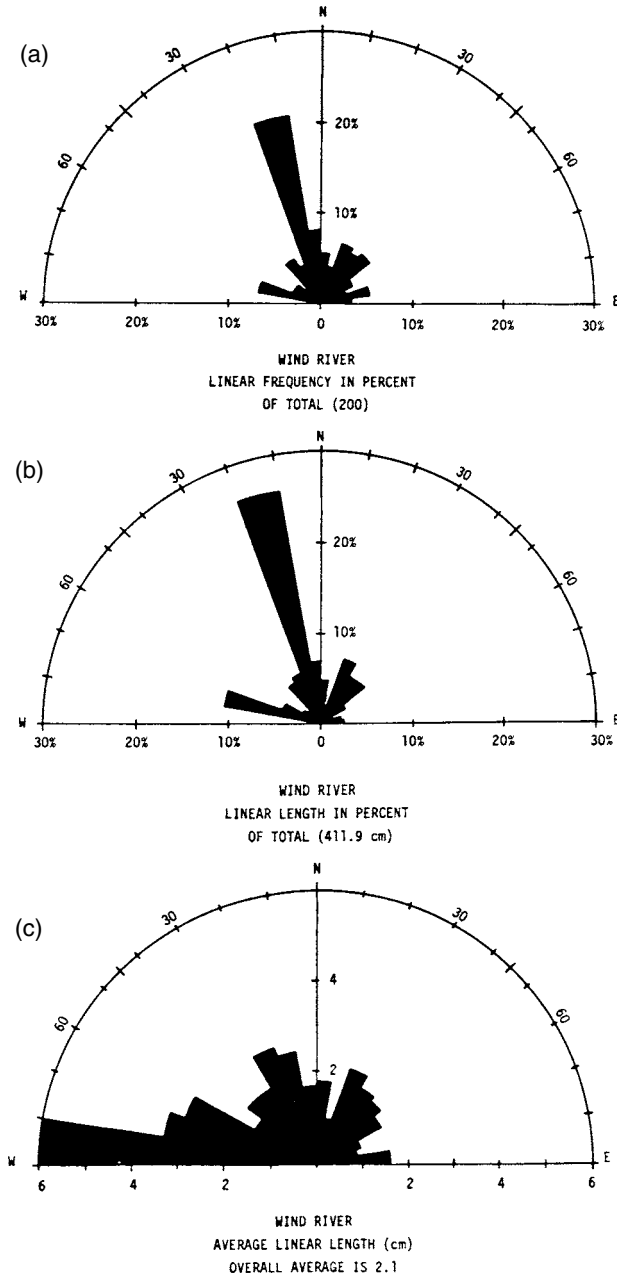
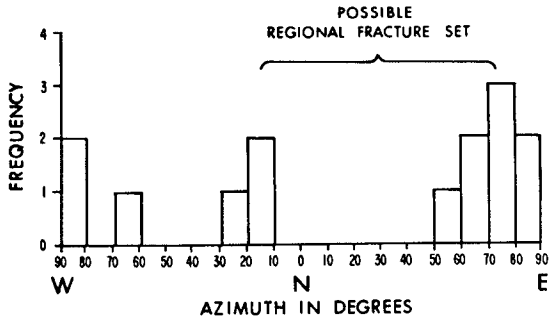


Figure 5-10a-c Polar strike histogram (Rose diagrams) using frequency (top), percent of total length (middle), and average length (bottom) of linears measured on 1:250,000 scale satellite photographs of the Wind River Mountains, Wyoming.

(d) ALL FRACTURES VERTICAL
 TOTAL OF 14 ORIENTED FRACTURES
 FRACTURES MINERALIZED WITH CALCITE



DEVONIAN ANTRIM SHALE
 AMOCO UNION NO. MI-21
 1580'-1846'

Figure 5-10d Cartesian strike histograms using fracture data from core.

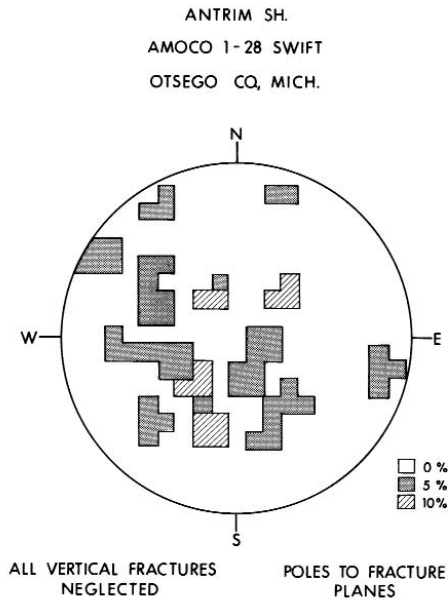


Figure 5-11 Example of strike and dip frequency in the form of a contoured, stereographic projection of poles to fracture plane diagram.

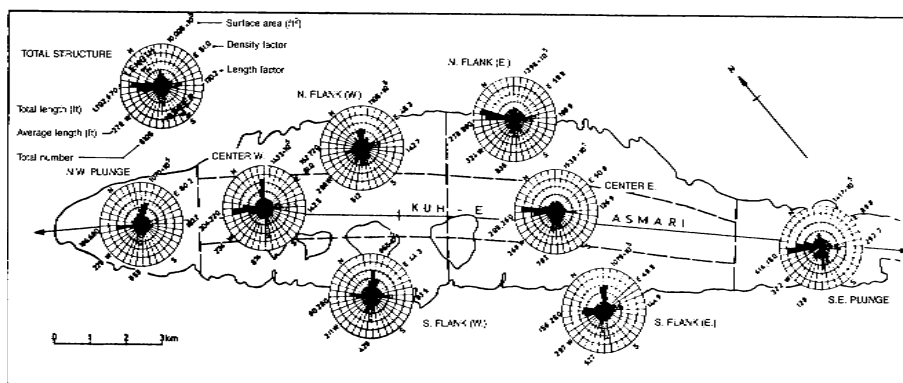


Figure 5-12 Example of how strike-frequency diagrams can be combined in map form to display 2-D distribution or orientation. From McQuillan (1974), courtesy of AAPG.

PRESSURE AND PRODUCTION ANALYSIS FOR QUANTIFYING FRACTURE SYSTEM PROPERTIES

Logging Techniques

Natural fracture systems may be detected in the subsurface by numerous mechanical and computer-assisted logging suites. These tools often do not find fractures and are certainly not of great use in quantifying porosity, permeability, width, spacing, etc. (Hirsch et al., 1981). The tools most useful in this regard are those that measure total porosity (fractures and matrix). If these can be combined with detailed core analysis to determine a statistically significant matrix porosity value, fracture porosity variation (the difference between total and matrix porosity) can be plotted. Such techniques are usually most accurate in reservoirs with moderate to low matrix porosity where fracture volume is significant with respect to total porosity. The borehole gravity meter is one such tool that may eventually have success in finding and quantifying fracture porosity.

Well Testing

Single and multiple well tests can be of great help in quantifying certain parameters in fractured reservoirs. The parameters best described are frac-

ture porosity and overall permeability anisotropy direction or effective open fracture orientation. These and other parameters are obtained effectively by pressure transient analysis, pressure pulse testing, and interference testing, which define fracture properties in short-term response and matrix properties in long-term fluid flow response. These methods are discussed in detail in Aguilera (1980), Reiss (1980), van Golf-Racht (1982), Kamal (1983), and Serra et al. (1983).

NUMERICAL MODELING IN GEOLOGY

In the study of fractured reservoirs, mathematical modeling is useful in predicting rock failure, gross-structural geometry, orientation of fractures, and fracture intensity or spacing. The two basic classes of approaches are analytical, which gives exact solutions to stress-strain boundary value problems, and numerical, which gives approximate solutions to stress-strain boundary value problems.

The analytical approaches can be quite elegant and useful and range from the sophisticated work of Patton (1984) to the simple forms of curvature analysis (Murray, 1968). They are, however, somewhat limited in terms of the complexity of geometry and internal material property variations that can be used. Complex bodies with large variations in physical properties are frequent in geological problems and are best handled by numerical modeling techniques.

The two primary forms of numerical modeling in common use are the finite element and finite difference techniques. In both, the body to be modeled is divided into a number of either elements or nodes, each being assigned a set of physical/mechanical properties. The finite difference technique is best suited for problems where the array of nodal points remains stationary during the model and material moves through the mesh. This makes this class of models ideal for modeling fluid flow in reservoir engineering and sonic wave transmission in seismic studies.

In the finite element technique the elements deform or are carried along with the material as it moves. This makes this class of models ideal for studying structural deformations. In fact, it is this technique that is used most frequently in the petroleum industry for predicting subsurface structural geometry and natural fracturing.

Finite element models have been used to predict the geometry of folds involving rocks of known properties and well-constrained boundary loads or displacements (Stein and Wickham, 1980). Models have also been used

to predict or explain fracturing, fracture orientation, and fracture intensity (Tapp and Wickham, 1978; and Jamison and Stearns, 1982). The finite element techniques are far superior to simple analytical curvature techniques for predicting fracture occurrence because in their best form they model deformational behavior using real rock experimental data. As such, they can predict ductile behavior as well as brittle. They can therefore allow for compressive behavior in zones of high curvature, whereas the curvature approach can predict only dilatancy.

Finite element models can output maps and sections depicting the distribution of various stress and strain parameters (such as stress difference, mean stress, equivalent plastic strain, etc.). Predictions of fracture intensity from the models are probably best done with one of the various strain parameters.

In order to do this, the models must be calibrated to natural fracture intensities. Individual outcropping structures must be modeled with the proper rock properties and loads and/or displacements. The natural fracture distributions in these outcrops must then be meticulously measured to calculate the strain due to fractures. With the fracture strain distribution and a knowledge of strain partitioning (the amount of strain accounted for by each deformational mechanism present), the finite-element-model strain maps or sections can be calibrated and subsequent solutions for analogous rocks and deformations used for fracture intensity predictions. Such calibration to outcrops is tedious and must be done for a variety of rock types and structural situations. However, once done, the strain output of carefully constructed numerical models can be an excellent predictor of natural fracture intensity.

Appendix A

List of Documented Fractured Reservoirs

An excellent compilation of fractured reservoirs in the United States is found in Hubbert and Willis (1955). In the 45 years since publication of that work, many new and more detailed reports of specific fractured reservoirs have been added to the literature. Table A-1 represents a compilation of published data on fractured reservoirs based on Hubbert and Willis (1955), Chilingar et al. (1972), and Daniel (1954) with personal additions through 2000 and Venezuela additions from F. Chartegui. In addition, selected fields have also been included from a 100 field fractured reservoir data compilation by C & C Reservoir Analogs. The 370 or so fields on this list produced from fractures of virtually every mode of origin and rock type. While additions can be made, this list includes a sufficient number of fields and a sufficient amount of reserves to document the impact of naturally occurring fracture systems in the exploration for petroleum reserves.

Table A-2 presents a subset of Table A-1, which has been studied in detail by the author. These fields are listed with greater quantitative detail.

Table A-1
Compilation of Documented Fractured Reservoirs with Selected References

Field	State or Country	Formation	Reference
Rocky Mountains			
Dineh-Bi-Keyah	Arizona	Syenite (T)	McKenny & Masters (1968)
Beaver River	Canada	Nahanni Ls (D)	
Elmworth	Canada	Spirit River Ss (K)	
Midale	Canada	Midale Dolo (Miss)	
Norman Wells	Canada	Kee Scarp Ls (D)	Bacon & Kempthorne (1984)
Pointed Mountain	Canada	Nahanni Ls (D)	
Weyburn	Canada	Midale Dolo (Miss)	
Canon City	Colorado	Pierre Sh (K)	Washburne (1910)
Chromo	Colorado	Mancos Sh (K)	Wengoro & Gill (1952)
Duchesne	Colorado	Green River, Wasatch Sh (E)	Marshall & Saterdal (1952)
Florence	Colorado	Pierre Sh (K)	DeForm (1929)
Iles Dome	Colorado	Mancos Sh (K)	Washburne (1910)
Niobrara Fields	Colorado	Niobrara Sh (K)	Heaten (1929)
(17 in Colorado and 8 in Wyoming)	Wyoming		Harnett (1966)
Rangely	Colorado	Mancos Sh (K) Weber Ss (Penn)	Pickering & Dorn (1949)

Roosevelt	Colorado	Mesa Verde (K)	Larsen (1953)
Rulison	Colorado	Mancos Sh (K)	Heaten (1929)
Two Creek	Colorado	Mancos Sh (K)	Abrassart et al. (1958)
West Puerto Chicquito	Colorado	Amsden Dolo (Penn)	Abrassart et al. (1958)
Big Wall	Montana	Sun River Ls	Abrassart et al. (1958)
Blackfoot	Montana	Dolo (M)	Abrassart et al. (1958)
Black Leaf	Montana	Madison Ls (M)	Abrassart et al. (1958)
Boman's Pocket	Montana	Amsden Dolo (Penn)	Abrassart et al. (1958)
Cabin Creek	Montana	Red River Dolo (0)	Hadley & Smith (1953)
Deer Creek	Montana	Interlake Dolo (S)	Abrassart et al. (1958)
Devil's Basin	Montana	Red River Dolo (0)	Abrassart and others (1958)
East Poplar	Montana	Van Duzen Ls (M)	Cox (1953)
Elk Basin	Montana,	Charles Ls (M),	Wayhan & McCaleb (1969)
	Wyoming	Madison Ls (M)	
Glendive	Montana	Madison Ls (M)	Hadley & Smith (1953)
Gypsy Basin	Montana	Red River Dolo (0)	Abrassart et al. (1958)
Little Beaver	Montana	Madison Ls (M)	Hadley & Smith (1953)
Northwest	Montana	Red River Dolo (0)	Abrassart et al. (1958)
Pine	Montana	Amsden Dolo (Penn)	Smith & Hadley (1954)
Richey	Montana	Red River Dolo (0)	Hadley & Smith (1953)
Sumatra	Montana	Madison Ls (M)	Cox (1953)
West Brady	Montana	Piper Ls (J)	Abrassart et al. (1958)
	Montana	Sun River Dolo (M)	Abrassart et al. (1958)

Field	State or Country	Formation	Reference
Wolf Springs	Montana		
Bravo Dome	New Mexico	Tubb Ss (Pm)	Abrassart et al. (1958)
Cedar Hill	New Mexico	Fruitland Coal (K)	
Crossroads South	New Mexico	Ls, Dolo (S-D)	Kinney & Schatz (1967)
Empire-Abo	New Mexico	Abo Ls (Pm)	
Indian Basin	New Mexico	Dolo (Penn)	Kinney & Schatz (1967)
South & West Bitter Lake	New Mexico	San Andres Dolo (P)	Kinney & Schatz (1967)
Blackburn	Nevada	Basalt (T)	
Eagle Springs	Nevada	Volcanics (T)	
Trap Springs	Nevada	Volcanics (T)	
Antelope (Spanish Peak)	North Dakota	Bakken	Murray (1968)
Beaver Lodge	North Dakota	Madison Ls (M)	
Little Knife	North Dakota	Madison Ls (M)	Cox (1953)
Tioga	North Dakota	Madison Ls (M)	Cox (1953)
Altamont-Bluebell	Utah	Wasatch Ss (T)	Narr & Currie (1982)
Cedar Rim	Utah	Wasatch Ss (T)	
Lisbon	Utah	Leadville Dolo (Miss)	
West Rozel	Utah	Basalt (T)	
Anschutz Ranch East	Wyoming	Nugget Ss (Jr)	White et al. (1990)
Beaver Creek	Wyoming	Tensleep Ss (Penn)	
Cottonwood Creek	Wyoming	Phosphoria Ls (P)	Willingham & McCaleb (1967)
East Painter	Wyoming	Nugget Ss (Jr) Twin Creek Ls (Jr)	

Ferris	Wyoming	Mowry Sh (K)	Irwin (1929)
Jonah	Wyoming	Lance Ss (K)	
Lost Soldier	Wyoming	Mowry Sh(K)	Irwin (1929)
		Madison Ls (M)	Pott & DeVore (1951)
Moxa Arch	Wyoming	Fronteir Ss (K)	
Painter	Wyoming	Nugget Ss (Jr)	
Pineview	Wyoming	Nugget Ss (Jr)	
Ryckman Creed	Wyoming	Nugget Ss (Jr)	
Salt Creek	Wyoming	Niobrara, Carlisle (K)	Beck (1929)
Silo	Wyoming	Niobrara Ls & Sh	
Wamsutter	Wyoming	Mesa Verde (K)	
Wertz Dome	Wyoming	Mowry Sh (K)	Irwin (1929)
Whitney Canyon	Wyoming	Madison Ls (M)	
Yellow Creek	Wyoming	Twin Creek Ls (Jr)	
		Frontier Sh (K)	
Mid-Continent and Gulf Coast			
Gilberttown	Alabama	Selma Ls (K)	Braunstein (1953)
Dupo	Illinois	Kimmiswisch Ls (O)	Miller (1968)
		Dolo (O)	
Waterloo	Illinois	Kimmiswisch Ls (O)	Miller (1968)
Beaver	Kansas	Granite (PC)	Landes et al. (1960)
Bloomer	Kansas	Granite (PC)	Landes et al. (1960)
Eveleigh	Kansas	Granite (PC)	Landes et al. (1960)
Gorhan	Kansas	Granite (PC)	Landes et al. (1960)
Kraft-Prusa	Kansas	Granite (PC)	Landes et al. (1960)
Hall-Gurney	Kansas	Granite (PC)	Landes et al. (1960)

Field	State or Country	Formation	Reference
Hugoton	Kansas	Council Gv. Slt (Pm)	Landes et al. (1960)
Silica	Kansas	Granite (PC)	Landes et al. (1960)
Trapp	Kansas	Granite (PC)	Heithecker (1934)
Blue Lake	Louisiana	Annona Ls (K)	Fletcher (1929)
Caddo	Louisiana	Annona Ls (K)	Fletcher (1929)
Converse	Louisiana	Annona Ls (K)	Fletcher (1929)
Red River - Bull Bayou	Louisiana	Annona Ls (K)	Fletcher (1929)
Zwolle	Louisiana	Annona Ls (K)	Fletcher (1929)
Berlin	Oklahoma	Atoka Dolo (Penn)	
Oklahoma City	Oklahoma	Arbuckle Dolo (C-O)	
Red Oak	Oklahoma	Atoka Ss (Penn)	
Sooner Trend	Oklahoma	Argil. Ls	
West Edmond (Hunton Pool)	Oklahoma	Bois d'Arc Ls (M)	Elkins (1969)
Andector	Texas	Ellenburger Ls	Littlefield, et al. (1947)
		Dolo (0)	Kelton (1950)
			Moore & Truby (1951)
			Atkinson & Johnson (1949)
			Bulnes & Fitting (1945)
Bradford	Texas	Cleveland Ss (Penn)	
Brown	Texas	Glorieta Dolo (P)	West Texas Geol Soc (1966)
Brown-Basset	Texas	Ellenburger	West Texas Geol Soc (1966)
		Dolo (0)	
Chapman	Texas	Serpentine	Sellards (1932)
		Volcanics (K)	Hanna (1953)
			Collingwood & Rettger (1926)

Coyanosa	Texas	Ellenburger Dolo (O)	West Texas Geol Soc (1966)
Dale	Texas	Serpentine Volcanics (K)	Sellards (1932) Hanna (1953) Collingwood & Rettger (1926)
Darst Creek	Texas	Edwards Ls (K)	Hanna (1953)
Dollarhide	Texas	Thirtyone Chert (D)	Ruppel & Barnaby (2000)
Ellis Ranch	Texas	Cleveland Ss (Penn)	
Embar	Texas	Ellenburger Ls Dolo (O)	Buines & Fitting (1945) Bulnes & Fitting (1945)
Giddings	Texas	Austin Ls (K)	Landes et al. (1960)
Granite Wash	Texas	Granite (PC)	Sellards (1932)
Hilbig	Texas	Serpentine Volcanics (K)	Hanna (1953) Collingwood & Rettger (1926)
Lytton Springs	Texas	Serpentine Volcanics (K)	Sellards (1932) Hanna (1953) Collingwood & Rettger (1926)
Martin	Texas	Ellenburger Ls Dolo (O)	
New Hope	Texas	Smackover Ls (J)	
Pearsall (17 fields)	Texas	Austin Ls (K)	
Red Hills	Texas	Bone Spring Ss (Pm)	Hart et al. (2000)
Reeves	Texas	San Andres Dolo Ls (P)	West Texas Geol Soc (1966)
Spraberry Trend	Texas	Spraberry Sit (Penn)	Wilkinson (1953) Lytle & Rieke (1951) Elkins (1953)

Field	State or Country	Formation	Reference
Thralln	Texas	Serpentine Volcanics (K)	McLennan & Bradley (1951) Bartley (1951) Sellards (1932) Hanna (1953) Collingwood & Rettger (1926)
Three Bar TXL	Texas Texas	Thirtyone Chert (D) Ellenburger Ls Dolo (O)	Ruppel & Barnaby (2000) Bulnes & Fitting (1945) West Texas Geol Soc (1966)
University Waddell Wheeler Yellow House	Texas Texas Texas	Thirtyone Chert (D) Ellenburger Ls San Andres Dolo Ls (P)	Ruppel & Barnaby (2000) Bulnes & Fitting (1945) West Texas Geol Soc (1966)
Yost	Texas	Serpentine Volcanics (K)	Sellards (1932) Hanna (1953) Collingwood & Rettger (1926)
small fields	Texas	Serpentine Volcanics (K)	Sellards (1932) Hanna (1953) Collingwood & Rettger (1926)
Appalachians			
Oak Grove Big Sandy	Alabama Kentucky W. Virginia	Pottsville Coal (Penn) Mahogany Sh (D)	Hunter & Young (1953) Thomas (1953) Bagnall & Ryan (1976) Jenkins (1976)
Oriskany Fields	New York	Oriskany Ss(O)	

Antrim Fields	Michigan	Antrim Sh (D)	
Calidonia	Ohio	Knox Dolo (O)	Debrosse, Vohwinkel (1974)
Cardington East	Ohio	Knox Dolo (O)	Debrosse, Vohwinkel (1974)
Cardington South	Ohio	Knox Dolo (O)	Debrosse, Vohwinkel (1974)
Chesterfield NW	Ohio	Knox Dolo (O)	Debrosse, Vohwinkel (1974)
Denmark West	Ohio	Knox Dolo (O)	Debrosse, Vohwinkel (1974)
Denmark	Ohio	Knox Dolo (O)	Debrosse, Vohwinkel (1974)
East Canton	Ohio		Shearow (1968)
Edison	Ohio	Knox Dolo (O)	Debrosse, Vohwinkel (1974)
Edison SW	Ohio	Knox Dolo (O)	Debrosse, Vohwinkel (1974)
Marengo	Ohio	Knox Dolo (O)	Debrosse, Vohwinkel (1974)
Marengo Central	Ohio	Knox Dolo (O)	Debrosse, Vohwinkel (1974)
Marengo East	Ohio	Knox Dolo (O)	Debrosse, Vohwinke (1974)
Mt. Gilead	Ohio	Knox Dolo (O)	Debrosse, Vohwinkel (1974)
Mt. Gilead South	Ohio	Knox Dolo (O)	Debrosse, Vohwinkel (1974)
Woodbury South	Ohio	Knox Dolo (O)	Debrosse, Vohwinkel (1974)
Devil's Elbow	Pennsylvania	Tuscarora Ss (S)	Miller (1948, 1954)
Rose Hill	Virginia	Trenton, Moccasin Ls (O)	Patchen & Larese (1976)
Cottageville	W. Virginia	Sh (D)	Ryan (1976)
Pacific Coast			
Granite Point	Alaska	Tyonek Cong (T)	
Kuparuk	Alaska	Kuparuk Ss (K)	
Lisburne	Alaska	Wahoo Ls (Penn)	
Middle Ground Shoals	Alaska	Tyonek Cong (T)	
Niakuk	Alaska		

Field	State or Country	Formation	Reference
Prudhoe Bay	Alaska	Saddlerochet Ss	McMasters (1943)
Buena Vista Hills	California	McLure, Brown Sh (Mio)	Church (1952) Regan (1953) Porter (1943)
Casmalia	California	Knoxville Ss (J)	
Cato Ridge	California	Monterey Sh (Mio) Knoxville Ss (M)	
Edison	California	Monterey Sh (Mio)	Hubbert & Willis (1955)
Ethel D	California	Schist (J)	McNaughton (1953)
Elk Hills	California	McLure, Brown Sh (Mio)	Conrad (1952)
El Segundo	California	McLure, Brown Sh (Mio)	Wells (1952)
Gato Ridge	California	Schist (J)	Regan (1953)
Gen. Arner.	California	McLure, Brown Sh (Mio)	Reese (1943)
Santa Maria Valley	California	McLure, Brown Sh (Mio)	Hubbert & Willis (1955)
Point Arguello	California	Knoxville Ss (M)	Hubbert & Willis (1955)
Oreutt	California	Monterey Sh (Mio)	Regan & Hughes (1949)
Lompoc	California	Monterey Sh (Mio)	McNaughton (1953)
		Knoxville Ss (J)	Dreyer (1943)
		Monterey Sh (Mio)	Dibblee (1943)
		Knoxville Ss M	Manlove (1943)
		Monterey Sh (Mio)	

Long Beach Unit	California	Schist (J)	Truex (1972)
Lost Cat Canyon	California	Knoxville Ss (J)	Cross (1943)
Lost Hills (Cahn Pool)	California	Monterey Sh (Mio)	Ganong (1952)
Midway-Sunset	California	McLure, Brown Sh (Mio)	Hubbert & Willis (1955)
Mountain View	California	McLure, Brown Sh (Mio)	Hubbert & Willis (1955)
North Belridge	California	Schist (J)	Wharton (1943)
	California	McLure, Brown Sh (Mio)	Dooley (1952)
			Regan (1953)
Oilcity (Coalinga Area)	California	Moreno Sh (K)	Birkhauser (1943)
Pacific Area	California	McLure, Brown Sh (Mio)	Hubbert & Willis (1955)
Playa Del Rey	California	Schist (J)	Metzner (1943)
			White (1946)
South Belridge	California	McLure, Brown Sh (Mio)	Wharton (1943)
			Regan (1953)
			Ritzius (1950)
South Ellwood	California	Monterey Sh (T)	Belfield et al. (1983)
Wilmington	California	Schist (J)	White (1946)
Zaca Creek	California	Knoxville Ss (J)	
		Monterey Sh (Mio)	Ganong (1952)
		McLure Brown Sh (T)	
Foreign			
Hassii-Messaoud	Algeria	Ra SS (C)	Massa, and others (1972)

Field	State or Country	Formation	Reference
Hassi-R'Mel	Algeria	Ra Ss (Cam)	Amrane (1993)
Rhourde el Bague	Algeria	Ss (Camb)	Belfield (1998)
Aguarague	Argentina	Huamampampa Ss (O)	
Ramos	Argentina	Santa Rosa Ss (O)	
		Huamampampa Ss (O)	
San Pedrito	Argentina	Santa Rosa Ss (O)	
		Huamampampa Ss (O)	
		Santa Rosa Ss (O)	
Bowen Basin	Australia	Coal (Pm)	
Lycosa	Australia	Dullingari Slt (O)	Taylor et al. (1991)
Mereenie	Australia	Pacoota Ss (O)	Havord (1990)
		Stairway Ss (O)	
Moolalla	Australia	Dullingari Slt (O)	Taylor et al. (1991)
Palm Valley	Australia	Pacoota Ss (O)	Berry et al. (1996)
		Stairway Ss (O)	Berry et al. (1996)
Tirrawarra	Australia	Tirrawarra Ss (Pm)	
Bulo Bulo	Bolivia	Robere Ss (O)	
Margarite	Bolivia	Huamampampa Ss (O)	
		Santa Rosa Ss (O)	
San Alberto	Bolivia	Huamampampa Ss (O)	
		Santa Rosa Ss (O)	
Badejo	Brazil	Basalt (K)	
Linguado	Brazil	Basalt (K)	
Dongshengpu	China	Anshan Meta (PC)	Xiaoguang & Zuan (1991)
Dujiatai	China	Volcanics	Lee (1989)

Guxinzhuang	China	Ls (O)	Lee (1989)
Jinbei	China	Dahongyu Dolo (PC- Pz)	Xiaoguang & Zuan (1991)
Jinganpu	China	Gaoyuzhuang Qtz (PC-Pz)	Xiaoguang & Zuan (1991)
Liubei	China	Anshan Meta (PC)	Xiaoguang & Zuan (1991)
Liuhua	China	Jixian, Qingbaikou,	
Maozhou	China	Changchen Dolo (PC-O)	
Qijia	China	Karsted Ls	
Renqiu	China	Jixian, Qingbaikou,	
Shijutuo	China	Changchen Dolo (PC-O)	
Shuguang	China	Volcanics	Lee (1989)
Wangzhuang	China	Jixian & younger Ls (Pc-O)	Lee (1989)
Weiyuan	China	Basalt (T)	Lee (1989)
Xinglongtai	China	Volcanics	Lee (1989)
Yaerxia	China	Taishan Gneiss (PC)	
Yanling	China	Dengying Dolo (PC)	
Yihezhuang	China	Volcanics	Lee (1989)
Cupiagua	Colombia	Quannaogou Meta (S)	
		Jixian Dolo (Pc-O)	
		Majiagou (O)	
		Badou Ls (O)	
		Mirador Ss (T)	
		Barco Ss (T)	
		Guadalupe Ss (K)	
		La Luna Ls (K)	
		Cogollo Ls (K)	
		La Paz Ss (T)	
		Granite	
Emerald Mountain	Colombia		
Opon	Colombia		
Zdanive-Krystalinkum	Czech		

Field	State or Country	Formation	Reference
Dan	Denmark	Chalk (T)	
Kraka	Denmark	Chalk (K)	
Skjold	Denmark	Chalk (K-T)	
Zeit Bay	Egypt	Granite	
Lacq	France	Mano Dolo (Jr)	
Meillon	France	Ossun-Meillon Dolo (Jr)	
Nagy Lengyel	Hungary	Main Dolo (Tr)	
Szeghalom	Hungary	Gneiss	
Jatibarang	Indonesia	Jatibarang Volcanics (T)	
Agha Jari	Iran	Asmari Ls (T)	
Bibi Hakimeh	Iran	Asmari Ls (T)	Gholipour (1994)
Darius	Iran	Yamamma Ls (K)	
Haft Ket	Iran	Asmari Ls (T)	
Kuh-e Asmari (Suleyman)	Iran	Asmari Ls (T)	McQuillan (1973, 1974)
Kuh-e Dashtak (Kuzerun)	Iran	Asmari Ls (T)	
Kuh-e Pabdeh- Gurpi (Lali)	Iran		McQuillan (1973, 1974)
Kult-e Pahin (Gachsaran)	Iran	Asmari Ls (T)	McQuillan (1973, 1974)
Paris	Iran	Asmari Ls (T)	
Pazanan	Iran	Asmari Ls (T)	Gholipour (1994)
Ain Zalah	Iraq	Asmari Ls (Olig-Mio)	Daniel (1954)

Kirkuk	Iraq	Asmari Ls (Olig-Mio)	Al-Debouni et al. (1971)
Gela	Italy	Noto Dolo (Tr)	
Malossa	Italy	Zandabbio Dolo (Jr)	
Monte Alpi	Italy	Apulian Ls (K)	
Ragusa	Italy	Noto Dolo (Tr)	
Vega	Italy	Siracusa Dolo (Jr)	
Niigata	Japan	Volcanics (T)	
		Volcaniclastic Ss (T)	
Minagish	Kuwait	Najmah/Sargelu Ls (Jr)	Lardenois et al. (1956)
Umm Gudair	Kuwait	Najmah/Sargelu Ls (Jr)	Lardenois et al. (1956)
Amal	Libya	Amal Ss (C-0)	Lardenois et al. (1956)
Augila-Nafoora	Libya	Granite	Lardenois et al. (1956)
Baton	Morocco	Basement Rocks	
Bled Defaa	Morocco	Basement Rocks	
Bled Eddoum	Morocco	Basement Rocks	
Bled Khatara	Morocco	Basement Rocks	
Cactus	Mexico	Dolo (K)	
Cantarell	Mexico	Dolo (K)	
Mers el Kharez	Morocco	Basement Rocks	Lardenois et al. (1956)
Oure Mellah	Morocco	Basement Rocks	Lardenois et al. (1956)
Sitio Grande	Mexico	Dolo (K)	
Sidi Fili	Morocco	Basement Rocks	Lardenois et al. (1956)
Tisserand	Morocco	Basement Rocks	Lardenois et al. (1956)
Zrar	Morocco	Basement Rocks	Lardenois et al. (1956)
Several Offshore Fields	Norway	Chalk (K)	Byrd (1975)
Alpuf	Venezuela	Cogollo Ls (K)	

Field	State or Country	Formation	Reference
Alturitas	Venezuela	Cogollo Ls (K)	
Ambrosio	Venezuela	Cogollo Ls (K)	
Bloque I	Venezuela	Cogollo Ls (K)	
Centro	Venezuela	Cogollo Ls (K)	
Ensenada	Venezuela	Cogollo Ls (K)	
Garcia	Venezuela	Cogollo Ls (K)	
La Conception	Venezuela	Cogollo Ls (K)	
Lago Sur	Venezuela	Cogollo Ls (K)	
Lama	Venezuela	La Luna Ls (K)	
		Cogollo Ls (K)	
Lamar	Venezuela	Cogollo Ls (K)	
La Paz	Venezuela	La Luna Ls (K)	
		Cogollo Ls (K)	
		Granite (Jr)	
Las Cruces	Venezuela	Cogollo Ls (K)	
Machiques	Venezuela	Cogollo Ls (K)	
Mara	Venezuela	La Luna Ls (K)	
		Cogollo Ls (K)	
		Granite (Jr)	
Rosario	Venezuela	La Luna Ls (K)	Apotria et al. (1996)
		Cogollo Ls (K)	
San Julian	Venezuela	Cogollo Ls (K)	
Sibucara	Venezuela	Cogollo Ls (K)	
Sur Del Lago	Venezuela	Cogollo Ls (K)	
Sur Oeste Lago	Venezuela	Cogollo Ls (K)	

Tia Juana Lago	Venezuela	Cogollo Ls (K)	Brehm (1993)
Totumos	Venezuela	Cogollo Ls (K)	Nelson & Hsu (1993)
Urdaneta Este Lago	Venezuela	Cogollo Ls (K)	Nelson & Hsu (1993)
Urdaneta Oeste Lago	Venezuela	Cogollo Ls (K)	
Urdaneta Tierra	Venezuela	Cogollo Ls (K)	
Belli	Tunisia	Bou Dabbous Ls (T)	
El Franig	Tunisia	Hamra Ss (O)	
Sabria	Tunisia	El Atchane (O)	
Sidi El Itayem	Tunisia	El Atchane (O)	
Sidi Al Kilani	Tunisia	El Gueria Ls (T)	Boubaker (1993)
Zinnia	Tunisia	Abiod Ls (K)	Brahim (1993)
Kahaif	Sharjah	Abiod Ls (K)	Brahim (1993)
Sajaa	Sharjah	Shuaiba Ls (K)	
Rijn	Sharjah	Shuaiba Ls (K)	
Eldfisk	Netherlands	Rijn Ss	
	Norway	Tor Ch (T)	
		Hod Ch (K)	
		Ekofisk Ch (K)	
	Norway	Ekofisk Ch (K)	
	Norway	Tor Ch (T)	
		Hod Ch (K)	
	Norway	Ekofisk Ch (K)	
	Norway	Ekofisk Ch (K)	
	Norway	Tor Ch (T)	
		Hod Ch (K)	
	Oman	Natih Ls (K)	
Fahud			

Field	State or Country	Formation	Reference
Natih	Oman	Natih Ls (K)	
Yibal	Oman	Shuaiba Ls (K)	
Nuryal	Pakistan	Khairabad Ls	Shuaib (1973)
Nido	Phillippines	Nido Ls (T)	
Dukhan	Qatar	Arab Ls (J)	Daniel (1954)
		Khuff Ls (Pm)	
Idd El Shargi	Qatar	Shuaiba Ls (K)	
Ardalin	Russia	Kardsted LS (D)	
Orenburg	Russia	Ls (Carb-Pm)	
Salym	Russia	Bazhenov Sh (Jr-K)	
Sangori	Russia	Volcanics (T)	
Vutkyl	Russia	Ls (Pm)	
Amposta	Spain	Montsia Ls (K)	
Casablanca	Spain	Montsia Ls (K)	
Tarraco	Spain	Montsia Ls (K)	
Bati-Raman	Turkey	Garzan Ls (T)	
Raman	Turkey	Mardi Karababa Ls (K)	
Argyll	UK	Zechstein Dolo (Pm)	
Auk	UK	Zechstein Dolo (Pm)	
Barque	UK	Leman Ss (Pm)	
Clair	UK	Eolian Ss (O)	
Clipper	UK	Leman Ss (Pm)	
Hoton	UK		
Machar	UK	Tor Ch (T)	Nicholson et al. (1999)
		Ekofisk (K)	

Magnus	UK	Kimmeridge Cl (Jr)	Welch (1999)
Ravenspur	UK	Leman Ss (Pm)	
West Sole	UK	Intrusives	
Bach Ho	Vietnam		
Plio —Pliocene	K —Cretaceous	M —Mississippian	PC —Precambrian
Mio —Miocene	J —Jurassic	D —Devonian	Ls —Limestone
Olig —Oligocene	Tr —Triassic	S —Silurian	Ss —Sandstone
E —Eocene	P —Permian	O —Ordovician	Sh —Shale
Paleo —Paleocene	Penn —Pennsylvanian	C —Cambrian	Dolo —Dolomite

Table A-2
Properties of Fractured Reservoirs Studied by the Author

Fields	Location	Age and Formation	Fracture Type	Matrix Por. %	Frac. Por. %	Matrix Perm. md	Frac. Perm. md	Recovery %
Anschutz Ranch East	Wyoming	Jr Nugget Sandstone	Tectonic, fold	10-12	0.05	0.01-100	up to 300	
Beaver Creek	Wyoming	Penn. Tensleep Sandstone	Tectonic, fold	2-10	less than matrix	0.01-10	0.01	
Beaver River	British Columbia	Dev. Nahanni Dolomite	Tectonic, fold	3.5	0.05-5 (diss)	20-00		11
<i>Blackburn</i>	Nevada	Mio. Humbolt Basalt	Contractional, Col. joints		less than 0.05		less than 10	high
		Olig. Indian Well Welded Tuff	Contractional, Tec. fault	17		0.5		
Bravo Dome	New Mexico	Dev. Nevada Dolomite	Tectonic, fault	5		21		20?
Bulo Bulo	Bolivia	Perm. Tubb Sandstone	Regional?	20		42		20-40
Cedar Rim Field	Utah	Dev. Robere & Sara Sandstones	Tectonic, fold	2-6				
Chennyboro	Texas	Tert. Wasatch Sandstone	Regional					
Cottonwood Creek	Wyoming	Tert. Cotton Valley Limestone	Tectonic, fold ?	1		2	10-100	
<i>Darius</i>	Iran	Perm. Phosphoria Ls	Tectonic, fold					
<i>Devil's Elbow</i>	Pennsylvania	Cret. Yammama Limestone	Regional/Diagenetic?					
East Painter	Wyoming	Sil. Tuscarora Quartzite	Tectonic, fold	Less than 0.5	up to 3.5 (diss)	less than 0.05	0.1-18	n/a (high)
<i>El Franig</i>	Tunisia	Jr Nugget Sandstone	Tectonic, fold					
		Ord. Hamra &						
<i>Elk Basin</i>	Wyoming	El Atchane Sandstones	Tectonic, fold	9	0.2	0.4	2.1-5.2	n/a
		Miss. Madison Ls	Tectonic, fold, Karst	10-14		3-73	368	40
		Perm. Phosphoria Ls	Tectonic, fold					
<i>Granite Point</i>	Alaska	Penn. Tensleep Ss	Tectonic, fold			29.8		
Hod	Norway	Tert. Tyonek Conglomerate	Tectonic, fold	14				
Hugoton	Kansas	Mas.-Dan. Hod Chalk	Tectonic, fold/diapir	30-40	0.2	0.1-0.7		medium
		Pm Council Grove Group siltstones						
Jonah	Wyoming	Cret. Lance Sandstone	Contractional, Chickenwire	1-4	0.1-0.3			
Kahaif	Sharjah	Cret. Shuaiba Limestone	Tectonic, fault & Regional					
			Tectonic, fold					

Fields	Location	Age and Formation	Fracture Type	Matrix Por. %	Frac. Por. %	Matrix Perm. md	Frac. Perm. md	Recovery %
<i>Little Knife</i>	North Dakota	Miss. Madison	Tectonic, fold	16		21		50
Lihua	China	Mio. Zhujiang karsted Ls	Tectonic, faulting, Karst	25	1	5	1000	10
Lost Soldier	Wyoming	Miss. Madison Ls	Tectonic, fold	8.5	up to 0.25	2.5	50-3,000	39
		Penn. Tensleep Ss	Tectonic, fold	12	less than matrix	60	0.04	59
<i>Middle Ground Shoals</i>	Alaska	Tert. Tyonek Conglomerate	Tectonic, fold	14		29.8		
<i>Opon</i>	Colombia	Tert. La Paz Sandstone	Tectonic, fold	7-10	0.05	0.1-1		n/a (low)
<i>Pearsall</i>	Texas	Cret. Austin Chalk	Regional	7		0.02		10?
Pineview	Wyoming	Jr Nugget Sandstone	Tectonic, fold	4-14		1-11.6		
<i>Pointed Mountain</i>	Northwest Terr.	Jr Twin Creek Limestone	Tectonic, fold	1-4		less than 0.1	greater than 1,000	
Red Oak	Oklahoma	Dev. Nahaanni Dolomite	Tectonic, fold	3.5	0.05-5 (diss)	20-200		11
Rijn	Netherlands	Penn. Atoka Sandstone	Tectonic, fold	14		0.25	45	85
Ryckman Creek	Wyoming	Rijn Sandstone	Tectonic, fold					
<i>Sabria</i>	Wyoming	Jr Nugget Sandstone	Tectonic, fold	15	-1	30	10	
	Tunisia	Ord. Hamra &						
San Juan Basin Coal	Colo./N. Mex.	El Atchane Sandstones	Tectonic, fold	9	0.2	0.4	2.1-5.2	high
San Pedrito	Argentina	Tert. Fruitland Coal	Regional/Cleat					
		Dev. Huamampampa &						
Sajaa	Sharjah	Santa Rosa Ss	Tectonic, fold	2	0.2		less than 0.1	50
Triassic in BC	British Columbia	Cret. Shuaiba Limestone	Tectonic, fold					
		Tr Baldomel &						
Vålhall	Norway	Pardomel Limestone	Tectonic, fold	4		1		
		Mas. Hod Chalk	Tectonic, fold	20-35	0.2	0.1-0.7		29
Wamsutter	Wyoming	Dan. Tor chalk	Tectonic, fold & slumping	35-55	0.3		66	med. to high
Watts Creek	Mississippi	Cret. Mesa Verde Sandstone	Regional	3-20		less than 1		
Wertz Dome	Wyoming	Cret. Smackover Limestone	Regional					
		Miss. Madison Ls	Tectonic, fold	8.5	up to 0.25	2.5	50-3,000	29
<i>West Rozel</i>	Utah	Penn. Tensleep Ss	Tectonic, fold	12	less than matrix	60	0.04	51
		Tert. Basalt	Tectonic, faulting plus					n/a
			Contractional, col. joints					

Appendix B

Procedures Checklist

Each procedure step is listed by number with data types and tasks listed by letters.

- 1. Document fracture presence**
 - A. Logs
 - B. Cores
 - C. Anomalous flow rates

- 2. Determine if structure is present**
 - A. Seismic, gravity, magnetics
 - B. Structure maps
 - C. Dipmeters

- 3. Determine lithologic control of fracture distribution**
 - A. Logs
 - B. Cores
 - C. Logs and flow tests/DST's

- 4. Document fracture system geometry**
 - A. BHTV
 - B. Cores
 - C. Predictions (including relevant outcrops)

- 5. Document fracture morphology**
 - A. Cores
 - B. BHTV
 - C. Predictions (including relevant outcrops)

- 6. Determine fracture type (origin)**
 - A. Application of observations to empirical models using data from (Procedure Steps 1–5)
- 7. Predict fracture distribution/extent**
 - A. Extrapolation using fracture type and observations
- 8. Estimate fracture spacing and spacing variability**
 - A. Cores
 - B. BHTV
 - C. Predictions (including relevant outcrops)
- 9. Estimate fracture width**
 - A. Laboratory data
 - B. Flow test data
- 10. Estimate reservoir properties at depth**
 - A. ϕ_m, K^m
 - B. ϕ_f, K_f
 - C. Using data from (Procedure Steps 7–9)
- 11. Estimate fracture/matrix interaction**
 - A. ϕ_f/ϕ_m interaction
 - B. K_f/K_m , contrast
- 12. Correlate small-scale petrophysical properties with large-scale reservoir engineering tests**
- 13. Determine fractured reservoir type**

Correlate matrix and fracture properties and their communication to determine relative contribution of the fracture system and potential recovery problems.
- 14. Make conclusions relevant to the type of evaluation**
 - A. Early exploration evaluation
 - B. Estimation of economic potential
 - C. Recovery planning and reservoir modeling

Appendix C

Averaging Techniques

AFTER ROEBUCK (1979)

Arithmetic Average (Parallel Flow)

$$\bar{k}_{\text{arith}} = \frac{\sum(k_i \times h_i)}{h_t} \quad (\text{C-1})$$

Harmonic Average (Series Flow)

$$\bar{k}_{\text{har}} = \frac{h_t}{\sum \frac{h_i}{k_i}} \quad (\text{C-2})$$

Geometric Average (Random Flow)

$$\bar{k}_{\text{geo}} = 1n^{-1} \left(\frac{\sum h_i \times 1nk_i}{t_t} \right) \quad (\text{C-3})$$

where k_i is permeability measurement
 h_i is height of sample measurement (often 1 ft. in whole-core analysis)
 h_t is total height (sum of h_i)
 \bar{k} is average permeability

Glossary

BHTV: Borehole televiewer.

body (internal) forces: Those forces that act on all elements of volume of a continuum. Examples are gravity and inertial forces. Expressed as force per unit mass or force per unit volume.

BOPD: Barrels of oil per day.

brittle behavior: Characterized by predominantly elastic deformation up to the point of fracture; that is, no permanent strain, only small, recoverable elastic strains are present before rupture.

conjugate fractures: The two potential shear fracture orientations in any compressive state of stress formed at identical but opposing angles to the maximum principal stress direction.

contractional fractures: Fractures whose origin is associated with a general bulk volume reduction within the rock mass.

deformation: Any change in the original form or volume of rock masses produced by either surface or body forces.

dessication fractures: Fractures whose origin is associated with shrinkage or bulk volume reduction in clay or shale-rich sediments due to loss of water in subaerial drying.

differential (triaxial) state of stress and strain: The situation where at least two of the three principal stresses or strains are not equal.

dihedral angle: The acute angle formed between the maximum principal stress direction and a potential shear fracture. This angle is dependent on depth of burial, state of stress, and the properties of the material.

DST: Drill stem test.

ductile behavior: Characterized by predominantly permanent strain and drastic changes in shape.

ductility: The ability to deform or flow without visible fracture.

elasticity: An ideal constitutive relationship between stress and strain. Elastic behavior is time independent with all strain instantly recoverable upon release of load. A typical stress-strain curve for an elastic body is an inclined straight line.

EOD: Environment of deposition.

extension fracture: A fracture that has a sense of displacement perpendicular to and away from the fracture plane, and forms parallel to the maximum and intermediate principal stress directions and perpendicular to the minimum principal stress direction. All principal stresses must be compressive.

failure: The yielding of a material either by brittle fracture or ductile flow. A decrease in the ability to sustain load.

faulting: Failure along a plane or restricted zone with displacement parallel to the plane; with or without loss of cohesion, loss of strain energy or ability to sustain load.

flow: Any deformation, not instantly recoverable, without permanent loss of cohesion.

fracture: Verb—Loss of cohesion across a plane. Associated with release of strain energy and at least momentary inability to sustain load. Noun—A surface of discontinuity within a rock mass that has at some time in the past been a plane of no cohesion. It may have been subsequently altered, healed, or mineralized.

fractured reservoir: A reservoir in which naturally occurring reservoir fractures either have or are predicted to have a significant effect on subsurface fluid flow either in the form of increased reservoir permeability and/or porosity or increased permeability anisotropy.

fracture spacing: The average linear distance between parallel fracture planes.

fracture strength: The differential stress at the moment of fracture of the material in a laboratory experiment. This is often smaller than the ultimate strength.

hydrostatic state of stress and strain: The situation where all principal stresses or strains within a body are equal. Often called spherical stress or strain.

ideal plasticity: An ideal constitutive relationship relating stress and strain. Plastic behavior is time dependent with all strain being permanent. Strain is zero until a fixed stress value is reached. Infinite strain will occur at or above this stress value. An ideal stress-strain curve for a plastic body would be a horizontal straight line at some constant stress level.

IP: Initial rate of production (flow rate).

microfaults: Planar zones across which small but discernible shear displacement has occurred.

MMBO: Million barrels of oil.

mode 1, 2, 3: Basic theoretical forms of microcrack propagation to which all fracture is said to conform (extension, shear, twist).

normal stress and strain: Stress and strain components that act perpendicular to a given real or imaginary plane within a body.

orthogonal fracture set: A group or set of two or three mutually perpendicular fractures.

principal stress and strain: The three mutually perpendicular planes in a state of stress or strain at any point in a body along which there are no shear stresses or strains, only normal stresses or strains.

regional fractures: Fractures that are developed over large areas of the earth's crust with relatively little change in orientation, that show no evidence of offset across the fracture plane, and that are always perpendicular to major bedding surfaces. They are commonly developed in orthogonal sets.

reservoir fracture: A naturally occurring macroscopic planar discontinuity in a reservoir rock, which is interpreted to be due to deformation or physical diagenesis. For practical reasons, it is assumed to have been initially open and may have been subsequently deformed or mineralized. It may have either a positive or negative effect on fluid flow within the reservoir.

shear fracture: A fracture that has a sense of displacement parallel to the fracture plane and forms at some acute angle to the maximum principal stress direction. All principal stresses must be compressive.

shear stress and strain: Stress and strain components that act along or parallel to a given real or imaginary plane within a body.

strain: A mathematical description of the deformational response to a state of stress within a body. Changes in size or shape of a body are the result of strain. Strain is a tensor quantity that is dependent on the properties of the material and can be measured or calculated from the stress field using one of the constitutive equations.

stress: A mathematical description of the resultant interaction of all points within a body when forces are applied at its boundaries; that is, how force is distributed throughout a body. This mathematical description is accomplished by the use of tensor mathematics and is independent of the material properties or the coordinate system used to describe it.

stress and strain difference: The difference between the maximum and minimum principal stresses or strains.

surface (external) forces: These forces act on a surface element, whether it is a portion of the bounding surface of the continuum or perhaps an imaginary internal surface. Forces with which neighboring parts of the medium act on each other and which are transmitted across surfaces.

surface-related fractures: Fractures whose origin is associated with the creation of free, unsupported surfaces in rock (unloading, slumping, and spalling).

synaeresis fractures: Fractures whose origin is associated with bulk volume reduction in sediments by subaqueous or subsurface dewatering. This dewatering may be either a physical or chemical process.

TCFG: Trillion cubic feet of gas.

tectonic: Of, pertaining to, or designating the rock structure and external forms resulting from the deformation of the earth's crust.

tectonic fractures: Fractures whose origin can, on the basis of orientation, distribution, and morphology, be attributed to or associated with a local tectonic event such as folding or faulting.

tensile fracture: A fracture that has a sense of displacement perpendicular to and away from the fracture plane, and forms parallel to the maximum and intermediate principal stress directions and perpendicular to the minimum principal stress direction. At least one principal stress (σ_3) must be tensile.

ultimate strength: The maximum differential stress achieved during a laboratory experiment; that is, the maximum ordinate on a stress-strain curve.

viscosity: An ideal constitutive relationship relating stress and strain rates. Viscous behavior is time dependent with all strain being permanent.

σ_1 , σ_2 , σ_3 : The maximum, intermediate, and minimum principal stress directions, respectively.

ϵ_1 , ϵ_2 , ϵ_3 : The maximum, intermediate, and minimum principal strain directions, respectively.

References

- Abrassart, C.P., Nordquist, J.W., and M.C. Johnson, 1958, Montana Oil and Gas Fields Symposium, Billings Geological Society, p. 247.
- Adams, A.R., Ramey, R.J., and R.J. Burgess, "Gas Well Testing of a Fractured Carbonate Reservoir," *Journal of Petroleum Technology*, October 1968, pp. 1187–1194.
- Aguilera, R., 1980, *Naturally Fractured Reservoirs*, 1st ed., PennWell Books, Tulsa, Oklahoma, 703 pp.
- Aguilera, R., 1995, *Naturally Fractured Reservoirs*, 2nd ed., PennWell Books, Tulsa, Oklahoma, 521 pp.
- Aguilera, R., and H.K. Van Poolen, May–June 1977, "Current Status on the Study of Naturally Fractured Reservoirs," *The Log Analyst*, pp. 2–23.
- Akbar, M., Bright, D.J., and R.D. Nurmi, 1995, "Anticlinal Reservoir Characterization and Modeling Using Outcrop, Seismic and Borehole Data," SPE 29800, 10 pp.
- Al-Debouini, R.M., Al-Irhayim, R.A., Al-Naqib, F.M., and D.M. Morris, 1971, "Water Drive Performance of the Kirkuk Field of Northern Iraq," 46th Annual SPE-AIME Fall Preprint no. SPE 3437, 19 pp.
- Amrane, O.B., 1993, "Etued Des Gres Reservoirs Fissures Du Cambrien De Hassi-R'Mel," Proc. Tunisian Fractured Reservoir Symp. (ETAP), Tunis, September 1–2, 1993, pp. 29–39.
- Anderson, J.Q., 1952, "Coalinga oil fields," American Association of Petroleum Geology, Annual Meeting Guidebook, p. 177.
- Antonellini, M.A., and A. Aydin, 1995, "Effect of Faulting on Fluid Flow in Porous Sandstones: Geometry and Spatial Distribution," *American Association of Petroleum Geology Bulletin*, vol. 79, pp. 642–671.
- Antonellini, M.A., Aydin, A., and D.D. Pollard, 1994, "Microstructure of Deformation Bands in Porous Sandstones at Arches National Park, Grand County, Utah," *Journal of Structural Geology*, vol. 16, pp. 941–959.

- Apotria, T.G., Wilkerson, M.S., and S.L. Knewton, 1996, "3D Geometry and Controls on Fracturing in a Natural Fault-Bend Fold: Posario Field, Maracaibo Basin, Venezuela," Abstract, Proc. II American Association of Petroleum Geology, Venezuelan Geological Society and International Congress and Exhibition, Caracas, September 8–11, 1996, p. A2.
- Arndt, H.A., Carter, M.D., and G.H. Wood, Jr., 1969, "Systematic Jointing in the Western Part of the Anthracite Region of Eastern Pennsylvania," *U. S. Geology Survey Bulletin*, no. 1271-D, 18 pp.
- Atkinson, B., and D. Johnston, 1949, "Core Analysis of Fractured Dolomite in the Permian Basin," *Trans. Am. Inst. Mining Met. Eng., Petroleum Branch*, vol. 179, p. 128.
- Atkinson, B.K., 1982, "Subcritical Crack Propagation in Rocks, Experimental Results and Applications," *Journal of Structural Geology*, vol. 4, no. 1, pp. 41–56.
- Aydin, A., 1977, "Small Faults Formed as Deformation Bands in Sandstone," Proc. Conf. H, Exp. Studies Rock Friction with Applications to Earthquake Prediction, Evernden Ed., U.S. Geological Survey, Menlo Park, California, pp. 617–653.
- Aydin, A., and J.M. DeGraff, 1988, "Evolution of Polygonal Fracture Patterns in Lava Flows," *Science*, vol. 239, pp. 441–532.
- Babcock, E.A., 1973, "Regional Jointing in Southern Alberta," *Canadian Journal of Earth Sciences*, vol. 10, no. 12, December 1973, pp.1769–1781.
- Babcock, E.A., 1974a, "Photolineaments and Regional Joints: Lineation Density and Terrain Parameters, South-Central Alberta," *Bulletin of Canadian Petroleum Geology*, vol. 22, no. 2, June 1974, pp. 89–105.
- Babcock, E.A., 1974b, "Jointing in Central Alberta," *Canadian Journal of Earth Science*, vol. 11, no. 8, August 1974, pp. 1181–1186.
- Bacon, J.R., and R.H. Kempthorne, "Waterflood Oil Recovery in Fractured Reservoirs, with Directionally Drilled Wells," *Society of Petroleum Engineering Journal*, August 1984, pp. 375–381.
- Badgley, P.C., 1965, *Structural and Tectonic Principles*, Harper and Row, New York, 521 pp.
- Baecher, G.B., 1983, "Statistical Analysis of Rock Mass Fracturing," *Math. Geol.*, vol. 15, no. 2, pp. 329–348.
- Bagnall, W.D., and W.M. Ryan, "The Geology Reserves and Production Characteristics of the Devonian Shale in Southwestern West Virginia;" Talk

- Presented at the Appalachian Petroleum Geology Symposium, Morgantown, West Virginia, March 1976.
- Bahat, D., 1982, "Extensional Aspects of Earthquake Induced Ruptures Determined by an Analysis of Fracture Bifurcation," *Tectonophysics*, vol. 83, pp. 163–183.
- Bahat, D., and T. Engelder, 1984, "Surface Morphology on Cross-Fold Joints of the Appalachian Plateau, New York and Pennsylvania," *Tectonophysics*, vol. 104, pp. 299–313.
- Barbe, J. A., 1983, "Reservoir Management at Dunlin," *Journal of Petroleum Technology*, vol. 35, no. 1, January 1983, pp. 227–233.
- Barenblatt, G., Zheltov, I., and I. Kochina, 1960, "Basic Concepts in the Theory of Seepage of Homogeneous Liquids in Fissured Rocks," *Prikl. Mat. Mekh.*, vol. 24, 1960, pp. 852–864.
- Bartley, J.H., 1951, "Stratigraphy and Structure of the Spraberry Sand," Proceedings of the 3rd Oil Recovery Conference, Texas Petroleum Committee, Midland, p. 5.
- Barton, N., 1982, "Block Tests for Rockmass Characterization," Proc. Conf. Updating Subsurface Sampling of Soils and Rocks and Their In Situ Testing, Santa Barbara, CA.
- Bastin, E.S., 1940, "A Note on Pressure Stylolites," *Journal Geol.*, vol. 48, pp. 214–216.
- Bathurst, R.G.C., 1976, *Carbonate Sediments and Their Diagenesis*, Develop in Sedimentology Series no. 12, 2nd Edition, Chapter 11, Elsevier Pub., New York, 677 pp.
- Beaudoin, G.J., T.A. Chaimov, Haggard, W.W., Mueller, M.C., and L.A. Thomsen, 1996, "Use of Multicomponent Seismology in Coal Bed Methane Exploration," Abstract, 2nd International. Mining Technology Symposium: Coalbed Methane Development and Application, Xian, China, October 1996, Republished in Eur. Assoc. Geosci. and Eng., Extended Abstracts 59, B009, 1997.
- Beck, Alfred, 1929, "Salt Creek Oil Field, Natrona County, Wyoming," in *Structure of Typical American Fields*, American Association of Petroleum Geologists, Tulsa, Oklahoma, vol. 2, p. 1929.
- Belfield, W., 1998. "Predicting Spatial Distribution of Fracture Permeability: An Example from the Rhourde el Baguel Field, Algeria," Abstract, Proc. Rocky Mountain Association of Geologists, Conf., Fractured Reservoirs: Practical Exploration and Development Strategies, January 19–90, 1998, pp. 337–338.

- Belfield, W., 2000, "Predicting Natural Fracture Distribution in Reservoirs from 3D Seismic Estimates of Structural Curvature," SPE 60298, SPE Rocky Mountain Regional/Low Permeability Reservoirs Symposium, Denver, March 12–15, 2000, 9 pp.
- Billings, M.P., 1954, *Structural Geology*, 2nd ed., Prentice-Hall, Englewood Cliffs, New Jersey, 514 pp.
- Birkhauser, Max, 1943, "Coalinga Oil Field," *California Division of Mines Bulletin*, no. 118, p. 484.
- Birkimer, D.L., 1970, "A Possible Fracture Criterion for the Dynamic Tensile Strength of Rock," Proc. 12th U.S. Symposium on Rock Mech., pp. 573–593.
- Blake, D.B. and C.J. Roy, 1949, "Unusual Stylolites," *American Journal of Science*, vol. 247, pp. 779–790.
- Blanchet, P.H., 1957, "Development of Fracture Analysis as Exploration Method," *American Association of Petroleum Geology Bulletin*, vol. 41, no. 8, pp. 1748–1759.
- Blanton, T.L., 1982, "An Experimental Study of Interaction Between Induced and Pre-Existing Fractures," SPE/DOE Unconventional Gas Recovery Symposium, Pittsburgh, May 16–18, 1982, Preprint SPE/DOE 10847, pp. 559–562.
- Bles, J.L., and B. Feuga, *Fracture of Rocks*, Elsevier, New York, 131 pp.
- Bogdanov, A.A., 1947, "The Intensity of Cleavage as Related to the Thickness of the Bed (Russian Text)," *Sov. Geol.*, vol. 16, pp. 147.
- Brace, W.F., 1961, "Dependence of Fracture Strength of Rocks on Grain Size," *Penn State Univ. Min. Export Sta. Bulletin*, vol. 79, pp. 99–103.
- Brace, W.F., and D.K. Riley, 1972, "Static Uniaxial Deformation of 15 Rocks to 30 Kb," *International Journal Rock Mech. Min. Sci.*, vol. 9, pp. 271–288.
- Brahim, A.B., 1993, "Upper Cretaceous Abiod Formation Carbonates as a Fractured Reservoir in Sidi El Kilani Field," Proc. Tunisian Fractured Reservoir Symposium (ETAP), Tunis, September 1–2, 1993, pp. 57–77.
- Braunstein, J., 1953, "Fracture-Controlled Production in Gilbertown Field, Alabama," *American Association of Petroleum Geology Bulletin*, vol. 37.
- Bredehoeft, J.D., Wolff, R.G., Keys, W.S., and E. Shuter, 1976, "Hydraulic Fracturing to Determine the Regional In Situ Stress Field, Piceance Basin, Colorado," *Geological Society of America Bulletin*, vol. 87, February 1976, pp. 250–258.

- Brehm, J.A., 1993, "Reservoir Geology of the Belli Field," Proc. Tunisian Fractured Reservoir Symposium (ETAP), Tunis, September 1–2, 1993, pp. 19–28.
- Brock, W.G., 1973, "Characterization of the Muddy Mountain-Keystone Thrust and Related Deformation," MS Thesis, Texas A&M University, College Station, Texas.
- Bulnes, A.C., and R.V. Fitting, 1945, "An Introductory Discussion of the Reservoir Performance of Limestone Formations," *Trans. Am. Inst. Mining Met. Eng.*, Petroleum Division, vol. 160, p. 179.
- Burger, H.R., III, and M.D. Thompson, 1969, "Petrofabric Investigation of Fractures Associated with Folding," Geological Society of America, Annual Meeting, Program Pt. 7, pp. 25–26.
- Burger, H.R., III, and M.D. Thompson, 1970, "Fracture Analysis of the Carmichael Peak Anticline, Madison County, Montana," *Geological Society of America Bulletin*, vol. 81, pp. 1831–1836.
- Burst, J. F., "Subaqueously Formed Shrinkage Cracks in Clay," *Journal of Sedimentary Petrology*, vol. 35, no. 2, pp. 348–353, June, 1965.
- Butters, S.W., Nielson, R.R., Jones, A.H., and S.J. Green, 1974, "Material Properties of Grouts and of Tuffs from Selected Drill Holes," Terra Tek Report no. DNA3383F, Salt Lake City, Utah, July 10, 1974, 161 pp.
- Byars, E.F., and R.D. Snyder, 1966, *Engineering Mechanics of Deformable Bodies*, International Textbook Co., Scranton, Pennsylvania, 400 pp.
- Byrd, W.D., 1975, "Geology of the Ekofisk Field, Offshore Norway," *Petroleum and the Continental Shelf of Northwest Europe*, vol. 1, *Geology*, A.W. Woodland, Ed., John Wiley and Sons, New York, pp. 439–445.
- Canfield, C.R., 1943, "Santa Maria Valley Oil Field," *California Division of Mines Bulletin*, no. 118, p. 440.
- Case, LE., and H.R. Joesting, 1972, "Regional Geophysical Investigations in the Central Colorado Plateau," U.S. Geological Survey Prof. Paper, no. 736.
- Charlesworth, H.A.K., 1968, "Some Observations on the Age of Jointing in Macroscopically Folded Rocks," in *Kink Bands and Brittle Deformation*, A.J. Baer and D.K. Norris, eds., *Geol. Surv. Can.*, Paper 68-52, pp. 125–135.
- Cheatham, J. B., and P.F. Gnirk, 1967, "The Mechanics of Rock Failure Associated with Drilling at Depth," Proc. 8th Symposium on Rock Mech., University of Minnesota, *Failure and Breakage of Rock*, Fairhurst Editor, Chapter 17, pp. 410–439.

- Chilingar, R.V., Mannon, R.W., and H.H. Rieke, 1972, *Oil and Gas Production from Carbonate Rocks*, Elsevier, New York, 408 pp.
- Cleary, J.M., 1959, "Hydraulic Fracture Theory, Part III-Elastic Properties of Sandstones," Illinois State Geological Survey, Circular 182, 44 pp.
- Choukroune, R., 1969, "An Example of Mesoscopic Analysis of Concentric Folding in Limestone Series," *Tectonophysics*, vol. 7, no. 1, pp. 57–70.
- Church, V., 1952, "Buena Vista Hills," American Association of Petroleum Geology, Annual Meeting Guidebook, p. 245.
- Coates, J.M., 1995, "Integrated Approach to Fracture Characterization: Niobrara Formation, Silo Field Area, Laramie County, Wyoming," Abstract, American Association of Petroleum Geology, Annual Meeting, 4 pp.
- Collingwood, D.M., and R.E. Rettger, 1926, "The Lytton Springs Oil Field, Caldwell County, Texas," *American Association of Petroleum Geology Bulletin*, vol. 10, p. 953.
- Collins, J.A., and L. Smith, 1975, "Zinc Deposits Related to Diagenesis and Intrakarstic Sedimentation in the Lower Ordovician St. George Formation, Western New Foundland," *Bulletin of Canadian Petroleum Geology*, vol. 23, no. 3, pp. 393–427.
- Committee on Fracture Characterization and Fluid Flow, 1996, "Rock Fractures and Fluid Flow: Contemporary Understanding and Applications," National Research Committee, National Academy Press, Washington D.C., 551 pp.
- Conrad, R.E., III, "Microscopic Feather Fractures in the Faulting Process," MS Thesis, Texas A&M University, College Station, Texas, August 1974.
- Conrad, S.D., 1952, "Maricopa Flats-Thirty-Five Anticline Area," American Association of Petroleum Geology, Annual Meeting Guidebook, p. 263.
- Corbett, K.P., "Structural Stratigraphy of the Austin Chalk," MS Thesis, Department of Geology, Texas A&M University, College Station, Texas, December 1982, 111 pp.
- Cox, H.M., 1953, "Williston Basin: Mississippian Reservoir Characteristics and Proved Reserves," *American Association of Petroleum Geology Bulletin*, vol. 37, p. 2294.
- Crampin, S., Lynn, H.B., and D.C. Booth, "Shear Wave VSP's: A Powerful New Tool for Fracture and Reservoir Description," *Journal of Petroleum Technology*, March 1989, pp. 283–288.
- Cross, R.K., 1943, "Gato Ridge Area of the Cat Canyon Oil Field," *California Division of Mines Bulletin*, no. 118, p. 438.

- Currie, J.B., "Study Examines Fracture Porosity and Permeability in Stratigraphic Traps," *Oil and Gas Journal*, June 24, 1974, pp. 178–181.
- Currie, J.B., and C.A. Reik, 1977, "A Method of Distinguishing Regional Directions of Jointing and of Identifying Joint Sets Associated with Individual Geological Structures," *Canadian Journal of Earth Science*, vol. 14, pp. 1211–1228.
- Daniel, E.J., 1954, "Fractured Reservoirs of the Middle East," *American Association of Petroleum Geology Bulletin*, vol. 38, no. 5, pp. 774–815.
- Darcy, H., 1856, *Les Fontaines Publiques de La Ville de Dijon*, Paris, V. Dalmont.
- Das Gupta, U., and J.B. Currie, 1983, "An Application of Photoelastic Models to Explain Microfractures and Joints in Carbonate Strata," *Canadian Journal of Earth Science*, vol. 20, pp. 1682–1693.
- Davis, G.H., 1999, "Structural Geology of the Colorado Plateau Region of Southern Utah, with Special Emphasis on Deformation Bands," *Geological Society of America, Special Paper 342*, 157 pp.
- Daw, G.P., Howell, F.T., and F.A. Woodhead, 1974, "The Effect of Applied Stress Upon the Permeability of Some Permian and Triassic Sandstones of Northern England," in *Advances in Rock Mechanics*, Proc. of 3rd International Symposium Rock Mech., Denver, 1974, pp. 537–542.
- deBoer, R.B., 1977a, "On the Thermodynamics of Pressure Solution-Interaction Between Chemical and Mechanical Forces," *Geochemica et Cosmochimica Acta*, vol. 41, pp. 246–256.
- deBoer, R.B., 1977b, "Pressure Solution: Theory and Experiments," *Tectonophysics*, vol. 39, pp. 287–301.
- deBoer, R.B., Nagtegaal, P.J.C., and E.M. Duyvis, 1977, "Pressure Solution: Experiments on Quartz Sand," *Geochemica et Cosmochimica Acta*, vol. 41, pp. 257–264.
- Debrosse, T.A., and J.C. Vohwinkel, 1974, Oil and Gas Fields of Ohio, *Ohio Geol. Surv. Publication*.
- DeFord, R.K., 1929, "Surface Structure, Florence Oil Field, Fremont County, Colorado," in *Structure of Typical American Oil Fields*, American Association of Petroleum Geology, Tulsa, vol. 2, p. 75.
- DeGraff, J.M., and A. Aydin, 1987, "Surface Morphology of Columnar Joints and Its Significance to Mechanics and Direction of Joint Growth," *Geological Society of America Bulletin*, vol. 99, pp. 605–617.

- Dennis, J.G., 1967, *International Tectonic Dictionary*, American Association of Petroleum Geology, Memoir 7, 196 pp.
- Dibblee, R.W., Jr., 1943, "Lampoc Oil Field," *California Division of Mines Bulletin*, no. 118, p. 427.
- Dobrynin, V.M., 1962, "Effect of Overburden Pressure on Some Properties of Sandstone," *Society of Petroleum Engineers Journal*, no. 12, pp. 360–366.
- Domenico, P.A., and V.V. Palciauskus, 1979, "Thermal Expansion of Fluids and Fracture Initiation in Compacting Sediments," *Geological Society of America, Bulletin*, vol. 90, no. 6, part 2, pp. 953–979.
- Donovan, R.N., and R.J. Foster, 1972, "Subaqueous Shrinkage Cracks from the Caithness Flagstone Series (Middle Devonian) of Northeast Scotland," *Journal of Sedimentary Petrology*, vol. 42, no. 2, pp. 309–317.
- Dooley, A.B., 1952, "North Belridge Oil Field," American Association of Petroleum Geology, Annual Meeting Guidebook, p. 203.
- Dreyer, F.E., 1943, "Santa Maria (Orcutt) Oil Field," *California Division of Mines Bulletin*, no. 118, p. 431.
- Duguid, J.O., Jr., 1973, "Flow in Porous Media," Ph.D. Thesis, Princeton University, 123 pp.; and P.C.Y. Lee, 1977, "Flow in Fractured Porous Media," *Water Resources Research*, vol. 13, no. 3, pp. 558–566.
- Dunn, D.E., LaFountain, L.J., and R.E. Jackson, 1973, "Porosity Dependence and Mechanism of Brittle Fracture in Sandstones," *Journal Geop. Res.*, vol. 78, p. 2403.
- Dunnington, H.V., 1967, "Aspects of Diagenesis and Shape Change in Stylolitic Limestone Reservoirs," 7th World Petrol. Congr., Paper PD-3 (4).
- Durney, D.W., 1972, "Solution-Transfer, An Important Geological Deformation Mechanism," *Nature*, vol. 235, pp. 315–317.
- Dyes, A.B., and O.C. Johnston, 1953, "Spraberry Permeability from Buildup Curves," *Trans. AIME*, vol. 198, p. 135.
- Elkins, L.F., 1953, "Reservoir Performance and Well Spacing, Spraberry Trend Area Field of West Texas," *Trans. AIME*, vol. 198, pp. 177–196.
- Elkins, L.F., 1969, "Internal Anatomy of a Tight, Fractured Hunton Lime Reservoir Revealed by Performance-West Edmond Field," *Journal of Petroleum Technology*, pp. 221–232.

- Engelder, J.T., 1973, "Quartz Fault-Gouge: Its Generation and Effect on the Frictional Properties of Sandstone," Ph.D. Dissertation, Texas A&M University, College Station, Texas, 267 pp.
- Evans, R.D., 1982, "A Proposed Model for Multiphase Flow Through Naturally Fractured Reservoirs," *Society of Petroleum Engineers Journal*, pp. 669–680.
- Fatt, I., and D.H. Davies, 1952, "Reduction in Permeability with Confining Pressure," *American Society of Mechanical Engineers Transactions*, vol. 195, pp. 329–330.
- Feder, J., 1988, *Fractals*, Plenum Press, New York, 283 pp.
- Fletcher, C.D., 1929, "Structure of Caddo Field, Caddo Parish, Louisiana," in *Structure of Typical American Oil Fields*, vol. 2, American Association of Petroleum Geology, Tulsa, Oklahoma, p. 183.
- Fletcher, R.L., and D.D. Pollard, 1981, "Anticrack Model for Pressure Solution Surfaces," *Geology*, vol. 9, pp. 419–424.
- Fons, L.C., 1960, "Downhole Camera Helps Solve Production Problems," *World Oil*, vol. 252, no. 5, pp. 150–152.
- Frank, J. R., Cluff, S., and J.M. Bauman, 1982, "Painter Reservoir, East Painter Reservoir, and Clear Creek Fields," Uinta County, Wyoming, Rocky Mountain Association of Geologists Studies, Cordilleran Thrust Belt Field Conference, Denver, Colorado, Guidebook, vol. 2, pp. 601–611.
- Freund, R., 1974, "Kinematics of Transform and Transcurrent Faults," *Tectonophysics*, vol. 21, pp. 93–134.
- Friedman, M., 1969, "Structural Analysis of Fractures in Cores from the Saticoy Field, Ventura County, California," *American Association of Petroleum Geology Bulletin*, vol. 53, no. 2, pp. 367–389.
- Friedman, M., 1975, "Fracture in Rock," *Reviews of Geophysics and Space Physics*, vol. 13, no. 3, U.S. National Report 1971–1974, 16th General Assembly International Union of Geodesy and Geophysics, Grenoble, France, August 24–September 6, Peter M. Bell, Ed., pp. 352–358.
- Friedman, M., and H.C. Heard, 1974, "Principal Stress Ratios in Cretaceous Limestones from Texas Gulf Coast," *American Association of Petroleum Geology*, vol. 58, no. 1, pp. 71–78.

- Friedman, M., and J.M. Logan, 1970, "Microscopic Feather Fractures," *Geological Society of America, Bulletin*, vol. 81, pp. 3417–3420.
- Friedman, M., and D.W. Stearns, 1971, "Relations Between Stresses Inferred from Calcite Twin Lamellae and Macrofractures, Teton Anticline, Montana," *Geological Society of America, Bulletin*, vol. 82, no. 11, pp. 3151–3162.
- Fritz, R.D., Horn, M.K., and S.D. Joshi, 1991, "Geological Aspects of Horizontal Drilling," American Association of Petroleum Geology, Cont. Educ. Course Note Series, no. 33, 563 pp.
- Fung, Y.C., 1969, *First Course in Continuum Mechanics*, Prentice-Hall, Englewood Cliffs, New Jersey, 301 pp.
- Gale, L.E., 1982, "Assessing the Permeability Characteristics of Fractured Rock," Geological Society of America, Special Paper 189, pp. 163–181.
- Gallagher, J.J., "Fracturing of Quartz Sand Grains," Proc. 17th U.S. Symposium of Rock Mech., Site Characterization, Snowbird, Utah, August 25–27, 1976, pp. 2A41–2A48.
- Gangi, A.F., 1978, "Variation of Whole and Fractured Porous Rock Permeability with Confining Pressure," *International Journal Rock Mechanics and Mining Sciences*, vol. 15, no. 5, pp. 249–257.
- Ganong, R.A., 1952, "Cahn Pool of Lost Hills Oil Field," American Association of Petroleum Geology, 1952 Annual Meeting Guidebook, p. 167.
- Gay, S.P., Jr., 1973, *Pervasive Orthogonal Fracturing in Earth's Continental Crust*, American Stereo Map Co., Salt Lake City, 1973, 124 pp.
- Geiser, P., 1980, "On the Use of Regional Joint Sets as Trajectories of Paleostress Fields During the Development of the Appalachian Plateau, New York," *Journal Geop. Res.*, vol. 85, no. BI I, pp. 6319–6341.
- Geiser, P., and C.H. Scholtz, 1981, "Fluid Flow Along Very Smooth Joints at Effective Pressures up to 200 Megapascals," in *Mechanical Behavior of Crustal Rocks*, Amer. Geop. Union, Monograph 24, 1981, pp. 147–183, in preparation.
- Ghez, F., and R. Janot, 1972, "Statistical Calculation of Elementary Matrix Blocks in Fractured Reservoirs," 47th Annual SPE of AIME Fall Meeting, Preprint SPE 4047, 1972, 10 pp.
- Gholipour, A.M., 1994, "Patterns and Structural Positions of Productive Fractures in the Asmari Reservoirs," Southwest Iran, Proc., Canadian

- SPE/CIM/CANMET Conference, Recent Advances in Horizontal Well Applications, Calgary, Paper HWC94-43, 10 pp.
- Gray, D.M., Fatt, I., and G. Berganini, 1963a, "The Effect of Stress on Permeability of Sandstone Cores," *Society of Petroleum Engineers Journal*, vol. 2, p. 203.
- Gray, D.M., Fatt, I., and G. Berganini, 1963b, "The Effect of Stress on Permeability of Sandstone Cores," *Society of Petroleum Engineers Journal*, vol. 3, pp. 95–100.
- Griffith, A.A., 1921, "The Phenomena of Rupture and Flow in Solids," *Phil. Trans. Roy. Soc. London*, A221, pp. 163–198.
- Groshong, R.H., Jr., 1975, "Strain, Fractures, and Pressure Solution in Natural Single Layer Folds," *Geological Society of America, Bulletin*, vol. 86, no. 10, pp. 1363–1376.
- Gussow, W.C., 1968, "Salt Diapirism: Importance of Temperature, and Energy Source of Emplacement," *American Association of Petroleum Geology Memoir 8, Diapirism and Diapirs*, pp. 16–52.
- Hadley, H.D., and G.W. Smith, 1953, "Developments in Montana, North Dakota, and South Dakota in 1952," *American Association of Petroleum Geology Bulletin*, vol. 37, p. 1233.
- Hafner, W., 1951, "Stress Distributions and Faulting," *Geological Society of America, Bulletin*, vol. 62, no. 4, pp. 373–393.
- Haimson, B.C., "The State of Stress of the Earth's Crust," *Rev. Geophysics and Space Physics*, vol. 13, no. 3, July 1975, pp. 350–352.
- Hallbauer, D.K., Wagner, H., and N.G.W. Cook, 1973, "Some Observations Concerning the Microscopic and Mechanical Behavior of Quartzite Specimens in Stiff, Triaxial Compression Tests," *International Journal of Rock Mechanics and Mining Sciences*, vol. 10, pp. 713–726.
- Hancock, P.L., "Brittle Microtectonics: Principles and Practice," *Journal of Structural Geology*, vol. 7, nos. 3 and 4, pp. 437–457.
- Hancock, P.L., and T. Engelder, 1989, "Neotectonic Joints," *Geological Society of America, Bulletin*, vol. 101, pp. 1197–1208.
- Handin, J.W., Friedman, M., Logan, J.M., Pattison, L.J., and H.S. Swolfs, 1972, "Experimental Folding in Rocks Under Confining Pressure, Part 1: Buckling of Single Layer Rock Beams," in *Flow and Fracture of Rocks*, Geophysical Monograph Series, vol. 16, Heard, H., Borg, L., Carter, N., Eds., American Geophysical Union, Washington, D.C., pp. 1–28.

- Handin, J., Friedman, M., Min, K.D., and L.J. Pattison, 1976, "Experimental Folding of Rocks Under Confining Pressure, Part 11: Buckling of Multilayered Rock Beams," *Geological Society of America, Bulletin*, vol. 87, pp. 1035–1048.
- Handin, J., and R.V. Hager, 1957, "Experimental Deformation of Sedimentary Rocks Under Confining Pressure: Tests at Room Temperature on Dry Samples," *American Association of Petroleum Geology Bulletin*, vol. 41, pp. 1–50.
- Handin, J., Hager, R.V., Jr., Friedman, M., and J.N. Feather, 1963, "Experimental Deformation of Sedimentary Rocks Under Confining Pressure: Pore Pressure Tests," *American Association of Petroleum Geology, Bulletin*, vol. 47, no. 5, pp. 717–755.
- Hanna, M.A., 1953, "Fracture Porosity in Gulf Coast," *American Association of Petroleum Geology Bulletin*, vol. 37, p. 266.
- Harnett, R.A., 1968, "Niobrara Oil Potential," *Earth Science Bulletin*, vol. 1, no. 1968, pp. 37–48.
- Harper, M.L., 1966, "Joints and Microfractures in Glenwood Canyon, Colorado," *Mountain Geologist*, vol. 3, no. 4, pp. 185–192.
- Harris, J.F., Taylor, G.L., and J.L. Walper, 1960, "Relations of Deformational Fractures of Sedimentary Rocks to Regional and Local Structure," *American Association of Petroleum Geology Bulletin*, vol. 44, pp. 1853–1873.
- Hart, B.S., Pearson, R.A., Smith, R., Leiphart, D.J., and R. Robinson, 2000, "Bone Spring Formation, Delaware Basin: Progress and Potential," Abstract, American Association of Petroleum Geology. SW Section Meeting, Midland, Geo2000: Into the Future.
- Havord, P.J., 1987, "Mereenie Oil and Gas Field, Amadeus Basin, Northern Territory," *Australian Petroleum Exploration Association Journal*, pp. 493–510.
- Heald, M.T., 1955, "Stylolites in Sandstones," *Journal Geol.*, vol. 63, no. 2, pp. 101–114.
- Heald, M.T., 1959, "Significance of Stylolites in Permeable Sandstones," *Journal Sed. Petrol.*, vol. 29, no. 2, pp. 251–253.
- Heaton, R.L., 1929, "Relation of Accumulation to Structure in Northwestern Colorado," in *Structure of Typical American Oil Fields*, American Association of Petroleum Geology, Tulsa, Oklahoma, vol. 2, p. 93.
- Heithecker, R.E., 1934, "Studies and Results of Acid Treatment of Wells, Dwolle Oil Field, Sabine Parish, Louisiana," U.S. Bur. Mines Repts. Invest. no. 3251.

- Higgs, N.G., 1981, "Mechanical Properties of Ultrafine Quartz, Chlorite and Bentonite in Environments Appropriate to Upper-Crustal Earthquakes," Ph.D. Dissertation, Texas A&M University, College Station, Texas, 267 pp.
- Hirsch, J.M., Cisar, M.T., Glass, S.W., and D.A. Romanoski, 1981, "Recent Experience with Wireline Fracture Detection Logs," 56th Annual Fall Meeting SPE of AIME, San Antonio, Texas, Preprint no. SPE 10333, 10 pp.
- Hobbs, D.W., 1967, "Formation of Tension Joints in Sedimentary Rocks: An Explanation," *Geological Magazine*, vol. 104, pp. 550–556.
- Hodgson, R.A., 1961a, "Regional Study of Jointing in Comb Ridge-Navajo Mountain Area, Arizona and Utah," *American Association of Petroleum Geology Bulletin*, vol. 45, no. 1, pp. 1–38.
- Hodgson, R.A., 1961b, "Reconnaissance of Jointing in Bright Angle Area, Grand Canyon, Arizona," *American Association of Petroleum Geology Bulletin*, vol. 45, no. 1, pp. 95–97.
- Holst, T.B., "Regional Jointing in the Michigan Basin," *Geology*, vol. 10, May 1982, pp. 273–277.
- Holst, T.B., and G.R. Foote, 1981, "Joint Orientation in Devonian Rocks in the Northern Portion of the Lower Peninsula of Michigan," *Geological Society of America, Bulletin*, vol. 92, no. 1, pp. 85–93.
- Hoshino, K., 1974, "Effect of Porosity on the Strength of the Clastic Sedimentary Rocks," in *Advances in Rock Mechanics*, Proc. 3rd Int. Soc. Rock Mech., Denver, Colorado, vol. 11, Part A, pp. 511–516.
- Howard, G.C. and C.R. Fast, 1970, *Hydraulic Fracturing*, Society of Petroleum Engineering, AIME, Monograph no. 2, 210 pp.
- Hubbert, M.K., 1940, "The Theory of Ground-Water Motion," *Journal Geol.*, vol. 48, pp. 785–944; and 1951, "Mechanical Basis for Certain Familiar Geological Structures," *Geological Society of America, Bulletin*, vol. 62, no. 4, pp. 355–372.
- Hubbert, M.K., and D.G. Willis, 1955, "Important Fractured Reservoirs in the United States," 45th World Pet. Cong. Proc., Section I/A-1, pp. 58–81.
- Hubbert, M.K., and D.G. Willis, 1972, *Mechanics of Hydraulic Fracturing*, American Association of Petroleum Geology Memoir 18, Underground Waste Management and Environmental Implications, pp. 239–257, Reprinted from Society of Petroleum Engineering of AIME, 1959, vol. 2 10, pp. 153–168.
- Hudson, J.A., and S.D. Priest, 1983, "Discontinuity Frequency in Rock Masses," *International Journal Rock Mechanics and Mining Sciences*, vol. 20, no. 2, pp. 73–89.

- Huitt, J.L., 1955, "Fluid Flow in Simulated Fractures," *Amer. Inst. Chem. Eng. Journal*, vol. 2, pp. 259–264.
- Hugman, R.H.H., III, and M. Friedman, 1979, "Effects of Texture and Composition on Mechanical Behavior of Experimentally Deformed Carbonate Rock," *American Association of Petroleum Geology Bulletin*, vol. 63, no. 9, pp. 1478–1489.
- Hunter, C.D., and D.M. Young, 1953, "Relationships of Natural Gas Occurrence and Production in Eastern Kentucky (Big Sandy Gas Field) to Joints and Fractures in Devonian Bituminous Shale," *American Association of Petroleum Geology Bulletin*, vol. 37, pp. 282–299.
- Irwin, J.S., 1929, "Oil and Gas Fields of the Lost Soldier District, Wyoming; in Structure of Typical American Oil Fields," *American Association of Petroleum Geology*, Tulsa, Oklahoma, vol. 2, p. 636.
- Jaeger, J.C., and N.G.W. Cook, 1969, *Fundamentals of Rock Mechanics*, Methuen and Co., London, 513 pp.
- Jamison, W.R., and D.W. Stearns, 1982, "Tectonic Deformation of Wingate Sandstone, Colorado National Monument," *American Association of Petroleum Geology Bulletin*, vol. 66, no. 12, pp. 2584–2608.
- Jenkins, E.B., 1976, "Devonian Shale Gas Production in Eastern Kentucky and Virginia," Talk Presented at the 7th Annual Appal. Petrol. Geol. Symp., Morgantown, West Virginia.
- Johnson, J.N., Swolfs, H.S., Simonson, E.R., Lingle, R., Jones, A.H., Green, S.J., and H.R. Pratt, 1974, "Anisotropic Mechanical Properties of Kayenta Sandstone (mixed company site) for Ground Motion Calculations," Terra Tek Report no. TR 74-61, Salt Lake City, Utah, 96 pp.
- Jones, F.O., 1975, "A Laboratory Study of the Effect of Confining Pressure on Fracture Flow and Storage Capacity in Carbonate Rocks," Society of Petroleum Engineers 48th Annual Fall Meeting, Las Vegas, Paper no. 4569, 8 pp.
- Joubert, T.G., 1998, "Optimal Drilling Direction in Folded Fractured Triassic Carbonates in Northeastern British Columbia Determined by Applying Fracture Occurrence to Frequency Intercept and Flow Diagrams," MS Thesis, Department of Geology and Geophysics, University of Calgary, 148 pp.

- Kahle, C.F., and J.C. Floyd, 1971, "Stratigraphic and Environmental Significance of Sedimentary Structures in Cayugan (Silurian) Tidal Flat Carbonates, Northwestern Ohio," *Geological Society of America, Bulletin*, vol. 82, pp. 2071–2098.
- Kamal, M.M., 1983, "Interference and Pulse Testing: A Review," *Journal of Petroleum Technology*, pp. 2257–2270.
- Kamath, J., Lee, S.H., Jensen, C.L., Narr, W., and H. Wu, 1998, "Modeling Fluid Flow in Complex Naturally Fractured Reservoirs," SPE 39547, Society of Petroleum Engineering India Oil and Gas Conference and Ex., 6 pp.
- Katterfield, G.N., 1976, "Global and Regional Systems of Lineaments on the Earth, Mars and the Moon," Proc. 1st International Conference New Basement Tectonics, pp. 369–378.
- Kelly, V.C., and N.J. Clinton, 1960, "Fracture Systems and Tectonic Elements of the Colorado Plateau," *University of New Mexico Publication in Geology*, no. 6, 104 pp.
- Kelton, F.C., 1950, "Analysis of Fractured Limestone Cores," *Journal of Petroleum Technology*, vol. 2, no. 8, p. 225.
- Kinney, E.E., and F.L. Schatz, 1967, *The Oil and Gas Fields of Southeastern New Mexico*, Roswell Geol. Soc., Roswell, New Mexico, p. 185.
- Klopp, H.C., 1975, "Petrographic Analysis of the Sunnily Formation, An Oil Producing Formation in South Florida," Brigham Young Univ. Geol. Studies, vol. 22, Part 1, pp. 3–27.
- Knutson, C.F., and B.F. Bohor, B.F., 1962, "Reservoir Rock Behavior Under Moderate Confining Pressure," Proc. 5th Symposium of Rock Mech., University of Minnesota, pp. 627–658.
- Komar, C.A., and K.H. Frohme, 1973, "Factors Controlling Fracture Orientations in Sandstone," 48th Annual SPE-AIME, Fall, Preprint no. SPE-4567, 8 pp.
- Kulander, B.R., Dean, S.L., and C.C. Barton, 1977, "Fractographic Logging of Determination of Pre-Core and Core-Induced Fractures-Nicholas Combs no. 7239 Well, Hazard, Kentucky," Energy Research and Development Administration, Morgantown, West Virginia, Eastern Gas Shales Project, MERC/CR-77/3, p. 44.
- Kulander, B.R., Dean, S.L., and B.J. Ward, Jr., 1990, "Fractured Core Analysis: Interpretation, Logging, and Use of Natural and Induced Fractures in Core," *Methods in Exploration Series*, American Association of Petroleum Geology, Tulsa, Oklahoma, no. 8, Tulsa, 88 pp.

- Ladiera, F.L., and N.J. Price, 1981, "Relationship Between Fracture Spacing and Bed Thickness," *Journal of Structural Geology*, vol. 3, no. 2, pp. 179–183.
- Lamb, H., 1957, *Hydrodynamics*, 6th Edition, Cambridge University Press, Cambridge, England.
- Landes, K.K., Amdruso, J.J., Charlsworth, L.J., Heany, F., and P.J. Lesperance, 1960, "Petroleum Resources in Basement Rocks," *American Association of Petroleum Geology Bulletin*, vol. 44, no. 10, pp. 1682–1691.
- Lang, H.B., 1964, "Dolomit und Zuckerkorniger Kalk in Weiben Jurader Mittleren Schwabischen Alb (Wurttemberg)," *N. Jb. Geol. Palaont. AbH.*, vol. 120, no. 3, pp. 253–299.
- La Pointe, P.R., and J.A. Hudson, 1985, "Characterization and Interpretation of Rock Mass Joint Patterns," *Geological Society of America, Special Paper*, no. 199, 37 pp.
- Lardenois, J.M., Levy, R.G., and C.J. Ramette, 1956, "Gisements de Petrole du Maroc," *Int. Geol. Cong.*, 20th, Petroleum Gas, Symp. T. 1, pp. 191–212.
- Larson, T.C., "Geological Considerations of the Weber Sandstone Reservoir, Rangley Field, Colorado," Rocky Mountain Association of Geology 1975 Symposium on Deep Drilling Frontiers in the Central Rocky Mountains, pp. 275–279.
- Laubach, S.E., 1989, "Paleostress Directions from the Preferred Orientations of Closed Microfractures (Fluid-Inclusion Planes) in Sandstone, East Texas Basin, U.S.A.," *Journal of Structural Geology*, vol. 11, no. 5, pp. 603–611.
- Lawn, B.R., and T.R. Wilshaw, 1975, *Fracture of Brittle Solids*, Cambridge University Press, Cambridge, England, 240 pp.
- Lee, K.Y., 1989, "Geology of Petroleum and Coal Deposits in the North China Basin, Eastern China," *U. S. Geol. Survey Bulletin*, vol. 1871, 36 pp.
- Lelek, J.J., 1983, "Geologic Factors Affecting Reservoir Analysis, Anschutz Ranch East Field, Utah and Wyoming," *Journal of Petroleum Technology*, pp. 1539–1545.
- Linscott, J.P., 1985, "Laboratory Study of the Effects of Shear Stress on Fracture Permeability," MS Thesis, Department of Geology and Geophysics, University of Oklahoma, Norman, Oklahoma.
- Littlefield, M., Gray, L.L., and A.C. Godbold, 1948, "A Reservoir Study of the West Edmond Hutton Pool, Oklahoma," *Pet. Trans. AIME*, Reprint Series 4, pp. 89–107.

- Lockner, D., and J. Byerlee, 1977, "Acoustic Emission and Creep in Rock at High Confining Pressure and Differential Stress," *Seismological Society of America Bulletin*, vol. 67, pp. 247–258.
- Logan, J.M., 1983, "Rock Fabric and Hydraulic Fracturing: The Implications for In-Situ Stress Measurements and Permeability Enhancement," Proceedings 24th U.S. Symposium Rock Mech., College Station, Texas, pp. 751–760.
- Logan, J.M., Iwasaki, T., Friedman, M., and S.A. Kling, 1972, "Experimental Investigation of Sliding Friction in Multilithologic Specimens," in *Geological Factors in Rapid Excavation*, Geological Society of America, Eng. Geol. Case History, no. 9, pp. 55–67.
- Long, J.C.S., 1983, "Investigation of Equivalent Porous Medium Permeability in Networks of Discontinuous Fractures," Ph.D. Thesis, University of California at Berkeley, Lawrence Berkeley Lab, LBL-14975, 277 pp.
- Long, J.C.S., Remer, J.S., Wilson, C.R., and P.A. Witherspoon, 1982, "Porous Media Equivalents for Networks of Discontinuous Fractures," *Water Resources Research*, vol. 18, no. 3, pp. 645–658.
- Lorenz, J.C., and S.J. Finley, 1988, "Significance of Drilling and Coring Induced Fractures in Mesaverde Core, Northwestern, Colorado," Sandia National Labs, Report SAND88-1623-UC-92, 36 pp.
- Lorenz, J.C., S.J. Finley, and N.R. Warpinski, 1990, "Significance of Coring Induced Fractures in Mesaverde core, NW Colorado," *American Association of Petroleum Geology*, v. 74, pp. 1017–1029.
- Lorenz, J.C., N. R. Warpinski, and L.W. Teufel, 1993, "Rationale for Finding and Exploiting Fractured Reservoirs, Based on the MWX/SHCT-Pieance Basin Experience," Sandia Report SAND93-1342, 147 pp.
- Lutton, R.J., 1970, "Tensile Fracture Mechanics from Fracture Surface Morphology," Proceedings 12th U.S. Symposium on Rock Mech., pp. 561–571.
- Lytle, W.J., and R.R. Rieke, 1951, "Well Logging in the Spraberry," in Proceedings of the 3rd Oil Recovery Conference, Texas Petroleum Research Committee, Midland, pp. 43.
- Macdonald, K., Sempere, J.C., and P.J. Fox, 1984, "East Pacific Rise from Siqueiros to Orozco Fracture Zones: Along Strike Continuity of Axial Neovolcanic Zone and Structure and Evolution of Overlapping Spreading Centers," *Journal Geop. Res.*, vol 89, no. B7, pp. 6049–6069.

- Manlove, C., 1943, "West Cat Canyon Area of the Cat Canyon Oil Fields," *California Division of Mines Bulletin*, no. 118, p. 432.
- Manten, A.A., 1966, "Note on the Formation of Stylolites," *Geologic en Mijnbouw*, vol. 45, no. 8, pp. 269–274.
- Mapstone, N.B., 1975, "Diagenetic History of a North Sea Chalk," *Sedimentology*, vol. 22, no. 4, pp. 601–613.
- Marin, J., 1935, "Failure Theories of Materials Subjected to Combined Stresses," *Proceedings Am. Soc. Civil Eng.*, vol. 61, pp. 851–867.
- Marshall, J., and A. Saterdal, 1952, "Developments in Colorado, Nebraska, and Utah in 1951," *American Association of Petroleum Geology Bulletin*, vol. 36, pp. 1033.
- Martin, G.H., 1963, "Petrofabric Studies May Find Fracture Porosity Reservoirs," *World Oil*, vol. 156, pp. 52–54.
- Mase, G.E., 1970, *Theory and Problems of Continuum Mechanics*, Schaum's Outline Series, McGraw-Hill, New York, p. 45, 221 pp.
- Massa, D., Ruhland, M., and J. Thouvenin, 1972, "Structure and Natural Fractures in the Hassi-Mossaoud Oil Field (Algeria), Part 1, Observations of Tectonic Phenomena in the Tassili Najjers," *Rev. Inst. Franc. Petrol. Combust. Liquids*, vol. 27, no. 4, pp. 489–534.
- Maurer, W.C., 1967, "The State of Rock Mechanics Knowledge in Drilling," *Proceedings 8th Symp. Rock Mech., Failure and Breakage of Rock*, University of Minnesota, Fairhurst, Ed., pp. 355–395.
- McCaleb, J.A., and D.A. Wayhan, 1969, "Elk Basin Madison Heterogeneity: Its Influence on Performance," *Journal Petroleum Technology*, pp. 153–159.
- McCaleb, J.A., and R.W. Willingham, 1967, "Influence of Geologic Heterogeneities on Secondary Recovery from Permian Phosphoria Reservoir, Cottonwood Creek Field, Wyoming," *American Association of Petroleum Geology Bulletin*, vol. 51, pp. 2122–2132.
- McColloch, C.M., Deul, M., and P.W. Jeran, 1974, "Cleat in Bituminous Coalbeds," U.S. Geological Survey Bur. Mines Rpt. of Invest., #7910, 25 pp.
- McGarr, A., and N.C. Gay, 1978, "State of Stress in the Earth's Crust," in *Ann. Rev. Earth Planet. Sci.*, vol. 6, F.A. Donath, Ed., pp. 405–436.
- McKenny, J.W., and J.A. Masters, 1968, "Dineh-Bi-Keyah Field, Arizona," *American Association of Petroleum Geology Bulletin*, vol. 52, pp. 2045–2057.

- McLatchie, A.S., Hemstock, R.A., and J.W. Young, 1958, "The Effective Compressibility of Reservoir Rock and its Effect on Permeability," *American Society of Mechanical Engineers Transactions*, vol. 213, pp. 386–388.
- McLennan, L., Jr., and H. Bradley, 1951, "Spraberry and Dean Sandstones of West Texas," *American Association of Petroleum Geology Bulletin*, vol. 35, p. 899.
- McMasters, J.H., 1943, "Buena Vista Hills Area of the Midway-Sunset Oil Field," *California Division of Mines Bulletin*, no. 118, p. 517.
- McNaughton, D.A., 1953, "Dilatancy in Migration and Accumulation of Oil in Metamorphic Rocks," *American Association of Petroleum Geology Bulletin*, vol. 37, no. 2, pp. 217–231.
- McQuillan, H., 1973, "Small-Scale Fracture Density in Asmari Formation of Southwest Iran and Its Relation to Bed Thickness and Structural Setting," *American Association of Petroleum Geology Bulletin*, vol. 47, no. 12, pp. 2367–2385.
- McQuillan, H., 1974, "Fracture Patterns on Kuh-e Asmari Anticline, Southwest Iran," *American Association of Petroleum Geology Bulletin*, vol. 58, no. 2, pp. 236–246.
- Means, W.D., 1976, *Stress and Strain: Basic Concepts of Continuum Mechanics for Geologists*, Springer-Verlag, New York, NY, 339 pp.
- Metzner, L.H., 1943, "Playa del Ray Oil Field," *California Division of Mines Bulletin*, no. 118, p. 292.
- Miller, D.N., Jr., 1968, *Geology and Petroleum Production of the Illinois Basin*, Illinois and Indiana-Kentucky Geol. Socs., 301 pp.
- Miller, R.L., 1948, "Rose Hill Oil Field, Lee County, Virginia," in *Structure of Typical American Oil Fields*, American Association of Petroleum Geology, Tulsa, Oklahoma, vol. 3, p. 452.
- Miller, R. L., 1954, "Rose Hill Field. Unique Oil Occurrence," *Oil and Gas Journal*, vol. 53, no. 13, p. 138.
- Mollema, P.N., and M.A. Antonellini, 1996, "Compaction Bands: a Structural Analog for Anti-Mode I Cracks in Aeolian Sandstone," *Tectonophysics*, vol. 267, pp. 267–228.
- Moore, W.D., and L.G. Truby, Jr., 1952, "The Pressure Performance of Five Fields Completed in a Common Aquifer," *Trans. Am. Inst. Mining Met. Eng. Petroleum Branch*, vol. 195, p. 297.

- Mordecai, M., and L.N. Morris, 1971, "An Investigation into Changes of Permeability Occurring in Sandstones When Failed Under Triaxial Stress Conditions," 12th Symposium on Rock Mech., Rolla Proc., Am. Inst. Mech. Eng. Trans., pp. 221–239.
- Morris, R.L., Grine, D.R., and T.E. Arkfeld, 1964, "The Use of Compressional and Shear Acoustic Amplitudes for the Location of Fractures," *Journal of Petroleum Technology*, June 1964.
- Mossop, G.D., 1972, "Origin of the Peripheral Rim, Redwater Reef, Alberta," *Bull. Can. Petrol. Geol.*, vol. 20, no. 2, pp. 238–280,
- Muecke, C.K., and H.A.K. Charlesworth, 1966, "Jointing in Folded Cardium Sandstone Along the Bow River, Alberta," *Canadian Journal of Earth Science*, vol. 3, no. 5, pp. 579–596.
- Murray, G.H., Jr., 1968, "Quantitative Fracture Study-Sanish Pool, McKenzie Co., North Dakota," *American Association of Petroleum Geology Bulletin*, vol. 52, pp. 57–65.
- Nakagawa, K., 1971, "A Fracture System Accompanied with Dome Structure," *Journal Geol. Soc. Japan.*, vol. 77, no. 11, pp. 687–700.
- Narr, W., and J.B. Currie, 1982, "Origin of Fracture Porosity-Example from Altamont Field, Utah," *American Association of Petroleum Geology Bulletin*, vol. 66, no. 9, pp. 1231–1247.
- Narr, W., and I. Lerche, 1984, "A Method for Estimating Subsurface Fracture Density in Core," *American Association of Petroleum Geology Bulletin*, vol. 68, no. 5, pp. 637–648.
- Nelson, R.A., 1975, "Fracture Permeability in Porous Reservoirs, An Experimental and Field Approach," Ph.D. Dissertation, Texas A&M University, 171 pp.
- Nelson, R.A., 1976, "An Experimental Study of Fracture Permeability in Porous Rock," Proc. 17th Symp. Rock Mechanics, Snowbird, Utah, 8 pp.
- Nelson, R.A., 1979, "Natural Fracture Systems, Description and Classification," *American Association of Petroleum Geology Bulletin*, vol. 63, no. 12, pp. 2214–2221
- Nelson, R.A., 1981a, "Significance of Fracture Sets Associated with Stylolite Zones," *American Association of Petroleum Geology Bulletin*, vol. 65, no. 11, pp. 2417–2425.
- Nelson, R.A., 1981b, "A Discussion of the Approximation of Subsurface (Burial) Stress Conditions in Laboratory Experiments," in *Mechanical*

- Behavior of Crustal Rocks*, Amer. Geop. Union, Monograph 24, pp. 311–321.
- Nelson, R.A., 1982, “An Approach to Evaluating Fractured Reservoirs,” *Journal of Petroleum Geology*, September 1982, pp. 2167–2170.
- Nelson, R.A., 1983a, “Geological Implications of Lineaments, Glen Canyon Area, Utah and Arizona-Structural Analysis,” Proc. 4th Intl. Conf. New Basement Tectonics, Oslo, Norway, August 10–14, 1981.
- Nelson, R.A., 1983b, “Localization of Aggregate Stylolites by Rock Properties,” *American Association of Petroleum Geology Bulletin*, vol. 67, no. 2, pp. 313–322.
- Nelson, R. A., 1985, *Geologic Analysis of Naturally Fractured Reservoirs*, Gulf Publishing, Houston, Texas, Contr. in Petrol. Geology and Eng., no. 1, 320 pp.
- Nelson, R.A., 1986, “Fractured Reservoir Analysis,” American Association of Petroleum Geology Annual Meeting Short Course, Atlanta, GA, with course notes, 120 pp.
- Nelson, R. A., 1987, “Fractured Reservoirs: Turning Knowledge into Practice,” *Journal of Petroleum Technology*, Distinguished Author Series, SPE 16470, pp. 407–414; reprinted in *AI-Petrol*, Cairo, 1988.
- Nelson, R. A., 1987, “Distribution and Character of Fractures in Sedimentary Basins, and Their Importance for Hydrocarbon Reservoirs,” Abstract, Soc. Expl. Geop., Workshop on Fractures, Anisotropy, and Birefringence, 57th Annual International Meeting, New Orleans, Louisiana, p. 854.
- Nelson, R.A., 1987, “Oriented Core: Its Use, Error, and Uncertainty,” *American Association of Petroleum Geology Bulletin*, vol. 71, no. 4, pp. 357–367.
- Nelson, R. A., 1988, “Do Workers and Managers View Fractured Reservoirs Differently?” Abstract, American Association of Petroleum Geology 1988 Annual Mtg., Houston, Texas, Abstract published in *American Association of Petroleum Geology Bulletin*, vol. 72, no. 2, p. 227.
- Nelson, R. A., 1990, “Multi-Scale Natural Fracture Development and Its Effect on Reservoir Modeling,” Abstract, Amer. Assoc. Petrol. Geol., 1990 Ann. Mtg., Dallas, TX, Abstract published in *American Association of Petroleum Geology Bulletin*, vol. 75, no. 3, p. 645.
- Nelson, R. A., 1992, “Evaluating Fractured Reservoirs,” in *Development Geology Reference Manual*, R.M. Slatt, Ed., American Association of Petroleum Geology.

- Nelson, R. A., 1998, "Integrated Structural Geology Techniques and How They Constrain Exploration Risk," Amer. Assoc. Petrol. Geol., Distinguished Lecture Abstract, SE Asia Tour.
- Nelson, R.A., 1998, "Modern Approaches to Exploration in Fractured Reservoirs," American Association of Petroleum Geologists, Distinguished Lecture Abstract, SE Asia Tour.
- Nelson, R.A., 1998, "Modern Approaches to Reservoir Characterization in Fractured Reservoirs," Abstract, PETEX conf., Keynote address, Dec. 1998, London.
- Nelson, R.A., 1998, "Overview of Research Applications to Fractured Reservoirs," Abstract Proc. vol., Rocky Mnt. Assoc. Geologists, Fractured Reservoir Symp., January 19–20, 1998, Denver.
- Nelson, R.A., Chaboudy, L.R. Jr., and McGuire, D. J., 1998, "Las Ventanas Fractured Reservoir Play: A La Paz Field Look-Alike in the Catatumbo Basin of Colombia," Abstract of Poster, Fracture and In Situ Stress Characterization of Hydrocarbon Reservoirs Symposium, Geol. Soc. London, June 28–29, 1999, London.
- Nelson, R.A., and Chacartegui, F., 1994, "Fractured Reservoir Analysis with Examples from the Cretaceous Carbonates of Lake Maracaibo, Venezuela," Abstract, Proc. vol. 1st Joint AAPG/AMPG Reservoir Conference on Geological Aspects of Petroleum Systems, Oct 2–6, 1994, Mexico City.
- Nelson, R.A., and J.W. Handin, 1977, "Experimental Study of Fracture Permeability in Porous Rocks," *American Association of Petroleum Geology Bulletin*, vol. 61, no. 2, pp. 227–236.
- Nelson, R.A., and M.Y. Hsu, 1993, "Fractures in the Ordovician Sandstones of the Sabria and El Franig Structures, Tunisia," Proc. Tunisian Fractured Reservoir Symposium (ETAP), Tunis, pp. 113–119.
- Nelson, R.A., Moldovanyi, E.P., Matcek, C.C., Azpirixaga, I. and E. Bueno, 1996, "Structurally Controlled Porosity Evolution and Production, La Paz Field, Maracaibo Basin, Venezuela," Abstract 1996 AAPG International Convention, Caracas, Invited Presentation.
- Nelson, R.A., Moldovanyi, E.P., Matcek, C.C., Azpirixaga, I. and E. Bueno, "Structurally Controlled Porosity Evolution and Production, La Paz Field, Maracaibo Basin, Venezuela," *AAPG Bulletin*, November 2000, vol. 84, No. 11, pp. 1791-1809.
- Nelson, R.A., Patton, T.L., and S. Serra, 1999, "Exploring for Structural Traps," Invited Manuscript, American Association of Petroleum Geology,

- Treatise of Petroleum Geology, Handbook of Petroleum Geology, Exploring for Oil and Gas Traps, Beaumont, E.A. and N.H. Foster, eds., 70 pp.
- Nelson, R.A., Serra, S., Brock, W.G., and B.J. Ward, Jr., 1993, "Vertical and lateral variations in fracture spacing in several carbonate sections," in Proc. Tunisian Fractured Reservoir Seminar (ETAP), Tunis, pp. 79–89.
- Nelson, R.A., and D.W. Stearns, 1977, "Interformational Control of Regional Fracture Orientations," in Rocky Mtn. Assoc. Geol., 1977 Field Trip Guidebook, Exploration Frontiers, Central and Southern Rockies, pp. 95–101.
- Netoff, D.I., 1971, "Polygonal Jointing in Sandstone Near Boulder, Colorado," *Mountain Geologist*, vol. 8, no. 1, pp. 17–24.
- Nicholson, H., Davies, M., and A. Brown, 1999, "Fracture Prediction: Field Development Optimisation of the Machar Chalk Reservoirs," Central North Sea, Abstract, Proc. Geol. Soc. London Conf. Fracture and In Situ Stress Characterisation of Hydrocarbon Reservoirs, London, 1 p.
- Nickelsen, R.R., and V.N.D. Hough, 1967, "Jointing in the Appalachian Plateau of Pennsylvania," *Geological Society of America, Bulletin*, vol. 78, no. 5, pp. 609–629.
- Nickelsen, R.R., and V.N.D. Hough, 1969, "Jointing in South-Central New York: Reply," *Geological Society of America, Bulletin*, vol. 80, no. 5, pp. 923–926.
- Nolen-Hoeksema, R. C., and J.H. Howard, 1987, "Estimating Drilling Direction for Optimum Production in a Fractured Reservoir," *American Association of Petroleum Geology Bulletin*, vol. 71, no. 8, pp. 958–966.
- Noorfishad, J., Witherspoon, P.A., and T.L. Brekke, 1971, "A Method for Coupled Stress and Flow Analysis of Fractured Rock Masses," University of California, Geotechnical Eng. Pub. 71-76, 128 pp.
- Norman, J.W., and T.C. Partridge, 1978, "Fracture Analysis in the Determination of Sub-Unconformity Structure: A Photogeological Study," *Journal of Petroleum Geology*, vol. 1, no. 1, pp. 43–63.
- Norris, D.K., 1966, "Structural Analysis of the Queensway Folds, Ottawa, Canada," 47th Annual Amer. Geop. Union Meeting, Paper T-85.
- Nur, A., 1978, "The Tensile Origin of Fracture-Controlled Lineaments," Proc. 3rd Intl. Conf. on Basement Tectonics, Durango, May 15–19, 1978, Basement Tectonics Comm. Pub. no. 3, D.W. O'Leary and J.L. Earle, Eds., pp. 155–167.

- Nye, J.F., 1957, *Physical Properties of Crystals*, Oxford University Press, Amen House, London EC4, 322 pp.
- Odé, H., 1957, "Mechanical Analysis of the Dike Pattern of the Spanish Peaks Area, Colorado," *Geological Society of America, Bulletin*, vol. 68, p. 567.
- Odeh, A.S., 1965, "Unsteady State Behavior of Naturally Fractured Reservoirs," *Society of Petroleum Engineers Journal*, p. 60.
- Ogden, V., and J. Locke, 1952, "What Are the Facts and Figures for Spraberry Trend Core Analyses?," *Oil and Gas Journal*, vol. 50, no. 36, pp. 94–97.
- Ohnishi, Y., and R.E. Goodman, 1974, "Results of Laboratory Tests on Water Pressure and Flow in Joints," Proc. 3rd Cong. Intl. Soc. Rock Mech., IIA, pp. 660–666.
- Overby, W.K., and R.L. Rough, 1968, "Surface-Joint Fractures Predict Wellbore Fracture Orientation," *Oil and Gas Journal*, pp. 84–86.
- Overby, W.K., and R.L. Rough, 1971, "Prediction of Oil and Gas-Bearing Rock Fractures from Surface Structural Features," U.S. Bur. Mines, Rpt. Investigations no. 7500, 14 pp.
- Paillet, F.L., 1991, "Comparison of Fracture Characterization Techniques Applied to Near-Vertical Fractures in a Limestone Reservoir," Paper XX, Proc. 22nd Ann. SPHILA Logging Symp., June 23–26, 1981.
- Park, W.C., and E.H. Schot, E.H., 1968, "Stylolites: Their Nature and Origin," *Journal of Sedimentary Petrology*, vol. 38, no. 1, pp. 175–191.
- Parker, J.M., 1942, "Regional Systematic Jointing in Slightly Deformed Sedimentary Rocks," *Geological Society of America, Bulletin*, vol. 53, pp. 381–408.
- Parker, J.M., 1969, "Jointing in South-Central New York: Discussion," *Geological Society of America, Bulletin*, vol. 80, no. 5, pp. 919–922.
- Parsons, R.W., 1966, "Permeability of Idealized Fractured Rock," *Society of Petroleum Engineering Journal*, pp. 126–136.
- Patchen, D.G., and R.E. Larese, 1976, "Stratigraphy and Petrology of the Devonian Brown Shale in West Virginia," presented at Appalachian Petroleum Geology Symposium, Morgantown, West Virginia.
- Patrick, D.J., Kirkman, A.C., and R.J. Greenwood, 1972, "The Distribution and Relationships of Stylolites, Fractures, Shale Laminae, Clay, and Calcium,

- Magnesium and Iron Carbonates,” in the Amoco Norway 2/5-1, 2/5-2 and 2/5-3 Well vol. 1, Robertson Research International Oil Fields Report no. 713, p. 20.
- Patton, T.L., III, 1984, “Normal Fault and Fold Development in Sedimentary Rocks Above a Pre-Existing Basement Normal Fault,” Ph.D. Dissertation, Texas A&M University, Geology Department, 164 pp.
- Pauken, R.S., Griffith, J.H., and J.H. Halsey, 1986, “Fracture Patterns and Production Trends, Big Sandy Field, Eastern Kentucky,” 5th Thematic Conference On Remote Sensing for Exploration Geology, Reno, Nevada, 24 pp.
- Peck, D.L., and T. Minakami, 1968, “The Formation of Columnar Joints in the Upper Part of Kilauean Lava Lakes, Hawaii,” *Geological Society of America, Bulletin*, vol. 79, no. 9, pp. 1151–1166.
- Picard, M.D., 1966, “Oriented Linear-Shrinkage Cracks in Green River Formation (Eocene), Raven Ridge Area, Uinta Basin, Utah,” *Journal of Sedimentary Petrology*, vol. 36, no. 4, pp. 1050–1057; and 1969, “Oriented Linear-Shrinkage Cracks in Alcova Limestone Member (Triassic), Southeastern Wyoming,” *Contrib. Geol.*, vol. 8, no. 1, pp. 1–7.
- Pickering, W. Y., and C.L. Dorn, 1948, “Rangley Oil Field, Rio Blanco County, Colorado,” in *Structure of Typical American Oil Fields*, American Association of Petroleum Geology, Tulsa, Oklahoma, vol. 2, p. 132.
- Piske, J., 1981, “Fracture Investigations as a Contribution to Representation of Trap Models for Zechstein Carbonates,” *Z. Geol. Wiss. Berlin* 9, no. 9, pp. 965–982.
- Pittman, E. D., 1981, “Effect of Fault-Related Granulation on Porosity and Permeability of Quartz Sandstones, Simpson Group (Ordovician), Oklahoma,” *American Association of Petroleum Geology Bulletin*, vol. 65, no. 11, pp. 2381–2387.
- Plumb, R.A., and J.W. Cox, 1987, “Stress Directions in Eastern North America Determined to 4.5 km from Borehole Elongation Measurements,” *Journal Geop. Res.*, vol. 92, no. B6, pp. 4805–5816.
- Plumb, R.A., and S.H. Hickman, 1985, “Stress Induced Borehole Elongation: Comparison Between the Four-Arm Dipmeter and the Borehole Televiewer in the Auburn Geotherman Well,” *Journal Geop. Res.*, vol. 90, no. B7, pp. 5513–5521.
- Plumb, R.A., and S.M. Luthi, 1986, “Application of Borehole Images to Geologic Modeling for an Eolian Reservoir,” 61st Ann. Tech. Conf. of Soc. Petrol. Eng., New Orleans, Louisiana, SPE 15487, 11pp.

- Pohn, H.A., 1981, "Joint Spacing as a Method of Locating Faults," *Geology*, vol. 9, pp. 258–261.
- Pollard, D.D., and A. Aydin, 1984, "Propagation and Linkage of Oceanic Ridge Segments," *Journal Geop. Res.*, vol. 89, no. B12, pp. 10017–10028.
- Pollard, D.D., and A. Aydin, 1988, "Progress in Understanding Jointing Over the Past Century," *Geological Society of America, Bulletin*, vol. 100, pp. 1181–1204.
- Poole, R., 1962, "Wind Directions in Late Paleozoic to Middle Mesozoic Time on the Colorado Plateau," U.S. Geol. Survey Prof. Paper 450-D, pp. 147–151.
- Porter, W.W., 1943, "The Casmalia Oil Field," *California Division of Mines Bulletin*, no. 118, p. 430.
- Pott, R.L., and S.F. De-Vore, 1951, "The Lost Soldier Field, Sweetwater County, Wyoming," Wyoming Geol. Assoc., 6th Annual Field Conference Guidebook, p. 103.
- Potter, P.E., and F.J. Pettijohn, 1963, *Paleocurrents and Basin Analysis*, Springer-Verlag, Berlin, 296 pp.
- Price, N.J., 1959, "Mechanics of Jointing in Rocks," *Geological Magazine*, vol. 46, no. 2, pp. 149–167.
- Price, N.J., 1966, *Fault and Joint Development in Brittle and Semi-Brittle Rock*, Pergamon Press, London, 176 p.
- Price, N.J., 1974, "The Development of Stress Systems and Fracture Patterns in Undeformed Sediments," Proc. 3rd Cong. Intern. Rock Mech., TA 487-496.
- Price, N.J., and Hancock, P.L., 1972, "Development of Fracture Cleavage and Kindred Structures," *24th Int. Geol. Cong. Session Proc.*, Sect. 3, pp. 584–592.
- Price, R.A., 1967, "The Tectonic Significance of Mesoscopic Subfacies in the Southern Rocky Mountains of Alberta and British Columbia," *Canadian Journal of Earth Science*, vol. 4, no. 1, pp. 39–70.
- Prost, G.L., 1994, "Remote Sensing for Geologists, a Guide to Image Interpretation," *Gordon and Breach Science Pub.*, Amsterdam, 326 pp.
- Queen, J.H., and Rizer, W.D., 1990, "Geophysical and Geological Characterization of a Shallow Fractured Reservoir," *Journal Geop. Res.*, vol. 95, no. B7, pp. 11255–11273.

- Quillin, M.E., 1983, "Statistical Study of Fracture Orientation and Spacing on the East Kaibab Monocline, Arizona," MS Thesis, Department of Geology, University of Oklahoma, Norman, Oklahoma.
- Ramez, M.R.H., and Mosalamy, F.H., 1969, "The Deformed Nature of Various Size Fractions of Some Clastic Sands," *Journal of Sedimentary Petrology*, vol. 39, no. 3, pp. 1181–1197.
- Ranalli, G., and A.D. Gale, 1976, "Lectures on the Rheology of the Earth, Part I: Basic Concepts," Carleton University, Department of Geology, Geological Paper 76-1, Ottawa, Canada, 157 pp.
- Ray, E.O., 1976, "Devonian Shale Development in Eastern Kentucky," in *Natural Gas from Unconventional Geological Sources*, National Academy of Sciences, Comm. on Nat. Resources, Board on Min. Resources, Washington, D.C., 1976, pp. 100–112.
- Reese, R.G., 1943, "El Segundo Oil Field," *California Division of Mines Bulletin*, no. 118, pp. 295.
- Regan, L.J., 1953, "Fractured Shale Reservoirs of Santa Maria District, California," *American Association of Petroleum Geology Bulletin*, vol. 33, pp. 32–51.
- Regan, L.J., and A.W. Hughes, 1949, "Fractured Reservoirs of Santa Maria District, California," *American Association of Petroleum Geology Bulletin*, vol. 33, p. 32.
- Reik, G.A., and J.B. Currie, 1974, "A Study of Relations Between Rock Fabric and Joints in Sandstone," *Canadian Journal of Earth Science*, vol. 11, no. 9, pp. 1253–1268.
- Reiss, L. H., 1980, *The Reservoir Engineering Aspects of Fractured Formations*, Gulf Publishing, Houston, Texas, 108 pp.
- Reynolds, S.M., 1986, "Identifying Fractured Fields with Photogeology," *Oil and Gas Journal*, Sept. 29, 1986, pp. 70–73.
- Rigert, J.A., 1980, "Uniaxial and Controlled-Lateral Strain Tests on Selected Sedimentary Rocks," Ph.D. Dissertation, Texas A&M University.
- Ritzius, D.E., 1950, "South Belridge Oil Field, Summary of Operations," *California Oil Fields, Division of Oil and Gas, Oil Field Summaries*, vol. 36, no. 118.
- Roberts, J.C., 1966, "A Study of the Relation Between Jointing and Structural Evolution," *Geological Journal*, vol. 5, Part 1, pp. 157–172.

- Roberts, J.C., 1976, "The Joint and Fault Patterns of the North Coast of Counties Antrim and Londonderry Between Murlough Bay and Castlerock," *Proc. Royal Irish Acad.*, vol. 76, Sect. B, pp. 619–628.
- Robertson, E.C., 1955, "Experimental Study of the Strength of Rocks," *Geological Society of America, Bulletin*, vol. 6, pp. 1275–1314.
- Roebuck, I.F., Jr., 1979, *Applied Petroleum Reservoir Technology*, Inst. Energy Development, Course Notes, Tulsa, Oklahoma, 1979, 469 pp.
- Rose, W., 1983, "A Note on the Role Played by Sediment Bedding in Causing Permeability Anisotropy," *Journal of Petroleum Technology*, pp. 330–332.
- Ruf, J.C., Rust, K.A., and T. Engelder, 1998, "Investigating the Effect of Mechanical Discontinuities on Joint Spacing," *Tectonophysics*, vol. 295, nos. 1–2, pp. 245–257.
- Ruppel, S.C., and R.J. Barnaby, 2000, "Contrasting styles of Reservoir Development in Proximal and Distal Thirtyone Chert Reservoirs: Permian Basin," Abstract, American Association of Petroleum Geology, SW Section Meeting, Midland, Geo2000: Into the Future.
- Russell, D.G., and N.E. Truitt, 1964, "Transient Pressure Behavior of Vertically Fractured Reservoirs," *Journal of Petroleum Technology*, pp. 1159–1170.
- Ryan, W.M., 1976, "Remote Sensing Fracture Study, Western Virginia and Southeastern Kentucky," Presented at the Appalachian Petroleum Geology Symposium, Morgantown, West Virginia.
- Sangree, J.B., 1969, "What You Should Know to Analyze Core Fractures," *World Oil*, vol. 168, no. 5, pp. 69–72.
- Schock, R.N., Heard, H.C., and D.R. Stephens, 1973, "Stress-Strain Behavior of a Granodiorite and Two Graywakes on Compression to 20 Kilobars," *Journal Geop. Res.*, vol. 78, no. 26, September 10, 1973, pp. 5922–5941.
- Schmoker, J.W., Coalson, E.B., and C.A. Brown, eds., 1992, *Geological Studies Relevant to Horizontal Drilling: Examples from Western North America*, Rocky Mountain Association of Geologists, Denver, 284 pp.
- Sellards, E.H., 1932, "Oil Fields in Igneous Rocks in Coastal Plain of Texas," *American Association of Petroleum Geology Bulletin*, vol. 16, p. 741.
- Sempere, J.C., and K.C. Macdonald, 1986, "Overlapping Spreading Centers: Implications from Crack Growth Simulation by the Displacement discontinuity Method," *Tectonics*, vol. 5, no. 1, pp. 151–163.

- Serra, K., Reynolds, A.C., and R. Raghavan, 1983, "New Pressure Transient Analysis Methods for Naturally Fractured Reservoirs," *Journal of Petroleum Technology*, pp. 2271–2283.
- Sharp, J.S., Maini, Y.N.T., and T. Brekke, 1972, "Evaluation of Hydraulic Properties of Rock Masses," 14th U.S. Symp. on Rock Mech., Pennsylvania, pp. 481–500.
- Shearrow, G.G., 1968, "The Story of Ohio's Southeastern Sleeper," *Oil and Gas Journal*, pp. 210–212.
- Shepherd, J., Creasey, J.W., and L.K. Rixon, 1982, "Comment on 'Joint Spacing as a Method of Locating Faults,'" *Geology*, vol. 10, p. 282.
- Shimamoto, T., and I. Hara, 1976, "Geometry and Strain Distribution of Single Layer Folds," *Tectonophysics*, vol. 30, no. 1 and 2, pp. 1–34.
- Shuaib, S.M., 1973, "Subsurface Petrographic Study of Joints in Variegated Siltstone-Sandstone and Khairabal Limestone, Pakistan," *American Association of Petroleum Geology Bulletin*, vol. 57, no. 9, pp. 1775–1778.
- Sieverding, J. L., and F. Royse, Jr., 1990, "Whitney Canyon-Carter Creek Field," AAPG Treatise of Petroleum Geology, Atlas of Oil and Gas Fields, Structural Traps III, pp. 1–29.
- Sinclair, S.W., 1980, "Analysis of Macroscopic Fractures on Teton Anticline, Northwestern Montana," M.S. Thesis, Dept. of Geology, Texas A&M University, College Station, Texas, 102 pp.
- Skehan, J.W., 1968, "Recognition of Faults of Regional Importance by Mapping Joints," 3rd Annual Geological Society of America, Northeastern Sect. Meeting, 2/15-17/68, Program, pp. 56–57.
- Slater, J.C., and N.H. Frank, 1947, *Mechanics*, McGraw-Hill Book Co. Inc., New York, 297 pp.
- Smith, G.W., and H.D. Hadley, 1954, "Developments in Montana, North Dakota, and South Dakota in 1953," *American Association of Petroleum Geology Bulletin*, vol. 38, p. 1011.
- Smith, M.B., Holman, G.B., Fast, C.R., and R.J. Colvin, 1978, "The Azimuth of Deep, Penetrating Fractures in the Wattenberg Field," *Journal of Petroleum Technology*, pp. 185–193.
- Snow, D.T., 1965, "A Parallel Plate Model of Fractured Permeable Media," Ph.D. Dissertation, University of California.
- Snow, D.T., 1968a, "Rock Fracture Spacings, Openings, and Porosities," *American Society of Civil Engineers Journal*, Soil Mech. and Foundation Division, vol. 94, SMI.

- Snow, D.T., 1968b, "Fracture Deformation and Change of Permeability and Storage upon Changes of Fluid Pressure," *Colorado School of Mines Quart.*, vol. 63.
- Sowers, G.M., 1970, Private report, 1972, "Theory of Spacing of Extension Fractures," in *Geologic Fractures of Rapid Excavation*, Geological Society of American Engineers, Geol. Case History no. 9, pp. 27–53.
- Spooner, J. A., 1984, "Field and Laboratory Study of Fracture Characteristics as a Function of Bed Curvature in Folded Dolomites, Sawtooth Mountains, Montana," M.S. Thesis, University of Oklahoma, Norman, Oklahoma.
- Stearns, D.W., 1964, "Macrofracture Patterns on Teton Anticline, Northwest Montana," *Amer. Geophys. Union Trans.*, vol. 45, pp. 107–108.
- Stearns, D.W., 1968a, "Fracture as a Mechanism of Flow in Naturally Deformed Layered Rock," in *Kink Bands and Brittle Deformation*, A.J. Baer and D.K. Norris, Eds., Geol. Surv. Can., Paper 68-52, pp. 79–95.
- Stearns, D.W., 1968b, "Certain Aspects of Fracture in Naturally Deformed Rocks," in *NSF Advanced Science Seminar in Rock Mechanics*, R. E. Rieker, Ed., Special Report, Air Force Cambridge Research Laboratories, Bedford, Massachusetts, AD 6693751, pp. 97–118.
- Stearns, D.W., 1971, "Mechanisms of Drape Folding in the Wyoming Province," Guidebook 23rd Annual Field Conference, Wyoming Geol. Assoc., pp. 125–143.
- Stearns, D.W., 1972, "Structural Interpretation of the Fractures Associated with the Bonita Fault," Guidebook 23rd Field Conf., New Mexico Geol. Soc., East Central New Mexico, pp. 161–164.
- Stearns, D.W., and M. Friedman, 1972, "Reservoirs in Fractured Rock," *American Association of Petroleum Geology*, Memoir 16, pp. 82–100.
- Stein, R., and J. Wickham, 1980, "Viscosity-Based Numerical Modeling for Fault Zone Development in Drape Folding," *Tectonophysics*, vol. 6, no. 1–3, 225–251.
- Stiteler, T.C., Nelson, R.A., and F.J. Chacartegui, 1994, "Fractured Reservoir Analysis with Examples from the Cretaceous Reservoirs of Lake Maracaibo, Venezuela," Abstract, 64th SEG Annual Meeting Post-Convention Workshop #4, Char. and Mapping for Field Exploration and Development of Naturally Fractured Reservoirs, Los Angeles, California.
- Stockdale, P.B., 1922, *Stylolites: Their Nature and Origin*, Indiana University Studies, vol. 9, pp. 1–97.

- Stockdale, P.B., 1926, "The Stratigraphic Significance of Solution in Rocks," *Journal Geol.*, vol. 34, no. 5, pp. 399–414.
- Stockdale, P.B., 1936, "Rare Stylolites," *Am. Journal Sci.*, vol. 32, pp. 129–133.
- Stockdale, P.B., 1943, "Stylolites: Primary or Secondary?" *Journal of Sedimentary Petrology*, vol. 13, pp. 3–12.
- Stockdale, P.B., 1945, "Stylolites with Films of Coal," *Journal Geol.*, vol. 53, pp. 133–136.
- Summers, R., Winkler, K., and J. Byerlee, 1978, "Permeability Changes During the Flow of Water Through Westerly Granite at Temperatures of 100°–400°C," *Journal Geop. Res.*, vol. 83, Series no. B1, pp. 339–344.
- Swain, M.W., and J.T. Hagan, 1978, "Some Observations of Overlapping Interacting Cracks," *Eng. Fracture Mech.*, vol. 10, pp. 299–304.
- Swolfs, H.S., Brechtel, C.E., Brace, W.F., and H.R. Pratt, 1981, "Field Mechanical Properties of Jointed Sandstone," in *Mechanical Behavior of Crustal Rocks*, Amer. Geop. Union, Monograph 24, pp. 161–172.
- Szwilski, A.B., 1984, "Determination of the Anisotropic Elastic Moduli of Coal," *International Journal Rock Mech. and Mining Sci.*, vol. 21, no. 1, pp. 3–12.
- Tapp, G., and J. Wickham, 1978, "Fracture Predictions Using Finite Element Computer Models," Abstract, *Geological Society of America Abstr. Pgms.*, vol. 10, no. 1, p. 26.
- Taylor, S., Solomon, G., Tupper, N., Evanochko, J., Horton, G., Waldeck, R., and S. Phillips, 1991, "Flank Plays and Faulted Basement: New Directions for the Cooper Basin," *Australian Petroleum Exploration Association Journal*, pp. 56–72.
- Tchalenko, J.S., and N.N. Ambraseys, 1970, "Structural Analysis of the Dashte Bayaz (Iran) Earthquake Fractures," *Geological Society of America, Bulletin*, vol. 81, pp. 41–60.
- Teeuw, D., 1971, "Predictions of Formation Compaction from Laboratory Compressibility Data," *Society of Petroleum Engineers Journal*, SPE Paper 2973, pp. 263–271.
- Teufel, L.W., 1976, "An Experimental Study of Hydraulic Fractures Propagation in Layered Rock," Ph.D. Dissertation, Texas A & M University, 99 pp.

- Thirumalai, K., 1970, "Process of Thermal Spalling Behavior in Rocks-An Exploratory Study," 11th Symp. on Rock Mech., Berkeley Proc., June 16-19, 1969, pp. 705-727.
- Thomas, R.N., 1951, "Devonian Shale Gas Production in Central Appalachian Area," *American Association of Petroleum Geology Bulletin*, vol. 35, p. 2249.
- Tillman, J.E., 1983, "Exploration for Reservoirs with Fracture-Enhanced Permeability," *Oil and Gas Journal*, February 21, 1983.
- Trémoilières, R., 1981, "Mécanismes de la Déformation en Zones de Plate-Formis Méthodes et Application Au Bassin de Paris," *Revue de l'Institut Français du Pétrole*, vol. 36, no. 4, Juillet-Aout, pp. 395-428.
- Trice, R., 1999a, "Methodology for Applying a Non-Unique, Morphological Classification to Sine Wave Events Picked from Borehole Image Log Data," in *Borehole Imaging: Applications and Case Histories*, Lovell, M.A., Williamson, G., and P.K. Harvey, eds., Geol. Soc. London, Special Publication 159, 77-90.
- Trice, R., 1999b, "Application of Borehole Image Logs in Constructing 3-D Static Models of Productive Fracture Networks in the Apulian Platform, Southern Appennines, in *Borehole Imaging: Applications and Case Histories*, Lovell, M.A., Williamson, G., and P.K. Harvey, eds., Geol. Soc. London, Special Pub. 159, pp. 155-176.
- Trowbridge, A.C., Ed., 1962, *Dictionary of Geological Terms*, Amer. Geol. Inst., Dolphin Reference Book, Doubleday, Garden City, New York, 545 pp.
- Truex, J.N., 1972, "Fractured Shale and Basement Reservoirs, Long Beach Unit, California," *American Association of Petroleum Geology Bulletin*, vol. 56, pp. 1931-1938.
- Trurnit, P., 1968, "Pressure Solution Phenomena in Detrital Rock," *Sedimentary Geology*, vol. 2, no. 2, pp. 89-114.
- Turcotte, D.L., 1986a, "Fractals and Fragmentation," *Journal Geop. Res.*, vol. 91, no. B2, pp. 1921-1926.
- Turcotte D.L., 1986b, "Fractal Model of Crustal Deformation," *Tectonophysics*, vol. 132, pp. 261-269.
- U.S. Bureau of Reclamation, Department of the Interior, 1957, "Technical Data Report for the Use of the Consultants, Glen Canyon Dam, Colorado River Storage Project," prepared by the Office of the Assistant Commissioner and Chief Engineer.

- van Golf-Racht, T. D., 1982, "Fundamentals of Fractured Reservoir Engineering," *Developments in Petroleum Science*, no. 12, Elsevier Scientific Pub. Co., Amsterdam, 710 pp.
- Verbeek, E.R., and Grout, M.A., 1984, "Fracture Studies in Cretaceous and Paleocene Strata in and Around the Piceance Basin Colorado, Preliminary Results and Their Bearing on a Fracture-Controlled Natural Gas Reservoir at the MWX Site," *U.S. Geological Survey Open File Report*, no. 84-156, 30 pp.
- Walsh, J.B., 1981, "Effect of Pore Pressure and Confining Pressure on Fracture Permeability," *International Journal of Rock Mechanics and Mining Sciences*, vol. 18, pp. 429-435.
- Walters, R.E. 1953, "Oil Production from Fractured Precambrian Basement Rocks in Central Kansas," *American Association of Petroleum Geology Bulletin*, vol. 37, no. 2, pp. 300-313.
- Walton, R., 1970, *Groundwater Resource Evaluation*, McGraw-Hill, New York, 664 pp.
- Wanless, H., 1979, "Pervasive Pressure Solution and Associated Dolomitization, Paleozoic Limestones," Talk Presented at the 1st American Association of Petroleum Geology Conference on Deep Burial Diagenesis in Limestones, Tulsa, Oklahoma.
- Warren, J.E., and Price, H.S., 1961, "Flow in Heterogeneous Porous Media," *Society of Petroleum Engineers Journal*, pp. 153-169.
- Washburn, C.W., 1910, "The Florence Oil Field, Colorado," *U.S. Geological Survey Bulletin*, no. 381, p. 517.
- Wayhan, D.A., and J.A. McCaleb, 1969, "Elk Basin Madison Heterogeneity: Its Influence on Performance," *Journal of Petroleum Technology*, pp. 153-159.
- Weber, K.J., and M. Bakker, 1981, "Fracture and Vuggy Porosity," 56th Annual Meeting SPE of AIME, San Antonio, Preprint SPE 10332, 11 pp.
- Wei, L. and A. Pringle, 1998, "Can Fracture Network Models be Constrained for Fractured Reservoirs?" *Bulletin of the London Petroleum Society*, vol. 6, no. 6, pp. 6-9.
- Welch, M., 1999, "Determining the Impact of Fractures on Reservoir Productivity Using Image Logs: An Example From the Magnus Field, UKCS," Abstract, Proc. Geol. Soc. London Conference Fracture and In Situ Stress Characterisation of Hydrocarbon Reservoirs, London, 1 p.

- Wells, John C., 1952, "Elk Hills Field," American Association of Petroleum Geology, 1952 Annual Meeting Guidebook, p. 241.
- Wengerd, S.A., and Gill, J.J., "Geology of the Chromo Oil Field, Archuleta County, Colorado," Four Corners Geol. Soc., Geological Symposium of the Four Corners Regions, p. 107, 1952.
- West Texas Geological Society, 1966, *Oil and Gas Fields in West Texas*, West Texas Geol. Soc., Midland, Texas, 398 pp.
- Weyl, R.K., 1959, "Pressure Solution and the Force of Crystallization a Phenomenological Theory," *Journal Geop. Res.*, vol. 64, pp. 2001–2025,
- Wharton, J. B., 1953, "Belridge Oil Field," *California Division of Mines Bulletin*, no. 118, p. 502.
- Wheeler, R.L., 1980, "Cross-Strike Structural Discontinuities: Possible Exploration Tool for Natural Gas in Appalachian Overthrust Belt," *American Association of Petroleum Geology Bulletin*, vol. 64, no. 12, pp. 2166–2178.
- Whitcombe, P.J., 1970, "Diagenesis of Carbonate Rocks of the Lower Limestone Shale Group (Carboniferous) of South Wales," *Journal of Sedimentary Petrology*, vol. 40, no. 1, pp. 334–338.
- White, J. Lloyd, 1946, "The Schist Surface of the Western Los Angeles Basin, Summary of Operations," *California Oil Fields*, California Division of Oil and Gas, p. 32.
- White, R.R., Alcock, T.J., and R.A. Nelson, 1990, "Anschutz Ranch East Field," in *Treatise of Petroleum Geology, Atlas of Giant Fields: Structural Traps III, Tectonic Fold and Fault Traps*, American Association of Petroleum Geology, Tulsa, Oklahoma, pp. 31–55.
- White, W.A., 1961, "Colloid Phenomena in Sedimentation of Argillaceous Rocks," *Journal of Sedimentary Petrology*, vol. 31, no. 4, pp. 560–570.
- Wiley, R., 1980, "Borehole Televiewer- Revisited," Paper HH, Proc. 21st Annual SPKLA Logging Symposium.
- Wilhelmi, B., and W.H. Somerton, 1967, "Simultaneous Measurement of Pore and Elastic Properties of Rocks Under Triaxial Stress Conditions," *Society of Petroleum Engineers Journal*, vol. 7, pp. 283–294.
- Wilkinson, W.M., 1953, "Fracturing in Spraberry Reservoir, West Texas," *American Association of Petroleum Geology Bulletin*, vol. 37, no. 2, pp. 250–265.
- Willingham, R.W., and J.A. McCaleb, 1967, "The Influence of Geologic Heterogeneities on Secondary Recovery from the Permian Phosphoria

- Reservoir, Cottonwood Creek, Wyoming,” SPE Paper 1770, presented at SPE Rocky Mountain Regional Meeting, Casper, Wyoming.
- Wilson, C.R., and P.A. Witherspoon, 1970, “An Investigation of Laminar Flow in Fractured Rocks,” *Geotechnical Report 70-6*, University of California, Berkeley, 178 pp.
- Winsor, C.N., 1979, “The Correlation of Fracture Directions with Sediment Anisotropy in Folded Rocks of the Delamerian Fold Belt at Port Germein Gorge, South Australia,” *Journal Struc. Geol.*, vol. 1, no. 3, pp. 245–254.
- Witherspoon, P.A., and J.E. Gale, 1976, *Mechanical and Hydraulic Properties of Rocks Related to Induced Seismicity*, University of California at Berkeley, Lawrence Livermore Laboratory, Report LBL-4455, 48 pp.
- Wood, G.V., and M.J. Wolfe, 1969, “Sabkha Cycles in the Arab/Drab Formation of the Trucial Coast of Arabia,” *Sedimentology*, vol. 12, no. 3 and 4, pp. 165–191.
- XiaoGuang, T., and H. Zuan, 1991, “Buried-Hill Discoveries of the Damintun Depression in North China,” *American Association of Petroleum Geology Bulletin*, vol. 75, no. 4, pp. 780–794.
- Yaalon, D.H., and Singer, S., 1974, “Vertical Variation in Strength and Porosity of Calcrete (Nari) on Chalk, Shefela, Israel and Interpretation of its Origin,” *Journal of Sedimentary Petrology*, vol. 44, no. 4, pp. 1016–1023.
- Yamaguchi, T., 1965, “Tectonic Study of Rock Fractures,” *Journal Geol. Soc. Japan*, vol. 71, no. 837, p. 257–275.
- Ziony, J.I., 1966, “Analysis of Systematic Jointing in Part of the Monument Upward, Southeastern Utah,” Ph.D. Dissertation, University of California, Los Angeles, California, 152 pp.

Index

A

- Acoustic borehole imaging logs, 5, 128–129
- Analysis procedures
 - core and outcrop analysis
 - core handling and, 235
 - data acquisition and, 239
 - data consistency and, 238
 - data presentation and, 247–251
 - drill string/rock interaction, 235–237
 - evaluation checklists, 246–247
 - fractured formations, coring of, 240–246
 - fracturing, centerline, 235
 - fracturing, chatter/petal, 235–236
 - fracturing, explosive, 230–231
 - fracturing, extension, 232–233
 - fracturing, hydraulic, 233–234
 - fracturing, impact and indentation, 232
 - fracturing, shear, 232–233
 - fracturing, thermal, 232–233
 - introduction to, 220–230
 - methods, core analysis, 241–246.
See also Core and outcrop analysis
 - methods, field analysis, 241–243
 - natural vs. induced fractures, determination of, 229–237
 - observational clues, 238
 - permeability matrix, 247
 - porosity matrix, 247
 - rock bursts and, 234–235
 - sheeting and, 234–235
 - spalling and, 233–235
 - stratigraphy vs. deformation, petrology, and petrophysics, 229
 - unloading, 234–235
 - data acquisition
 - introduction to, 239
 - levels of observation, 239
 - discovery and
 - data constraints, 227–228
 - data types, 226
 - exploration/access phase and, 226–227
 - introduction to, 226–227
 - recovery/harvest phase and, 226, 228
 - recovery/production phase and, 226, 228
 - timing of, 226–228
 - work procedures for, 226
 - evaluation checklists, 246–247, 277–278
 - fracture system properties
 - introduction to, 251
 - pressure and production analysis of, 251–252
 - introduction to, 223
 - logging techniques and, 251. *See also* Logs and logging tools
 - modeling, numerical, 113–123, 252–253
 - observational clues
 - introduction to, 238
 - real vs. artificial fractures, 238
 - screening tools and checklists
 - basic, 223
 - discipline-based, 224–226
 - drilling data-based, 225
 - engineering data-based, 226
 - evaluation checklists, 246–247
 - flow behavior-based, 223
 - geological data-based, 224
 - geophysical data-based, 225
 - introduction to, 223
 - well testing and, 251–252

Anisotropic reservoirs

- definition of, 3–4
- introduction to, 163
- modeling and statistical data
 - averaging techniques, 212–215, 279–280
 - block sizes, characterization of, 217
 - correlations of properties, three-dimensional, 215–216
 - introduction to, 207
 - research methods, types of, 212
 - reservoir domains and compartments, 207–212

- permeability tensors, development of
 - cementation size and, 194
 - combined tensors, 206–207
 - continuity of reservoir features and, 203–204
 - crossbedding and, 186–189, 198–202
 - data types, 204
 - fractures, effect on, 189–193, 198–202
 - grain size and, 193
 - introduction to, 185–186
 - random plugs, 194–196, 201
 - rock parameters, effect of, 202
 - scaling and, 194–198
 - stylolites and, 204–206

- stimulation in fractured reservoirs, 217–222

stylolites

- as indicator of mechanical properties, 173–174
- contribution to reservoir anisotropy, 165
- definition of, 163
- deformation and, 169–172
- discontinuities and, 176
- fractures associated with, 166–168
- introduction to, 163–165
- lithologic boundaries, 174–176
- locations of initiation, 174–176
- low-porosity zones, 176
- permeability tensors and, 204–206
- porosity vs. permeability and, 172–173, 176
- stress concentration localization, 176–185
- stylolite columns, 169
- tension gashes, 166–167

- unloading fractures, 166–168. *See also* Unloading

- Averaging techniques, 212–215, 279–280. *See also* Modeling

B

- Blast-related fracturing. *See* Explosive fracturing

Boreholes

- gravity meters, 131
- imaging logs, 5, 128–129

C

- Caliper logs, 128

- Cameras, downhole, 126

- Centerline fracturing, 235

- Chatter/petal fracturing, 235–236

- Checklists and screening tools. *See* Screening tools and checklists

- Chicken-wire fractures, 28–30

Classification of fractured reservoirs

- contrasting histories and, 103–108
- introduction to, 101
- reservoir listings and examples, 103–108. *See also* Example fractures, reservoirs, and fields
- reservoir management and. *See* Management of fractured reservoirs
- reservoir types
 - introduction to, 101–103
 - type 1, 101–105, 108–109, 116–119, 122
 - type 2, 101–102, 105–106, 108–109, 118–119, 122
 - type 3, 101–102, 108, 110, 118–119, 122

Classification of fractures

- experimental classification
 - extension fractures, 8, 10
 - introduction to, 8–9
 - shear fractures, 8–9
 - tension fractures, 8, 10
- geologic classification, 10–12
- introduction to, 7–8
- naturally-occurring classification
 - contractional fractures, 27–31
 - desiccation fractures (mud cracks), 27
 - fault-related fracture systems, 13–16
 - fold-related fracture systems, 16–20

- impact fractures, 20–21
 - introduction to, 8
 - piercement and, 20–21
 - regional fractures, 20–28
 - surface-related fractures, 31–32
 - syneresis fractures, 27–28
 - tectonic fractures, 8, 13–21
 - thermal contractional fractures, 28–31
 - Columns, stylonite, 169
 - Combined gouge-filled and slickensided fractures, 55–58
 - Contractional fractures, 27–31
 - Conversation factors, 285–286
 - Core and outcrop analysis
 - analysis procedures. *See* Analysis procedures
 - checklists for
 - introduction to, 246
 - permeability matrix, 247
 - porosity matrix, 247
 - coring and
 - analysis methods, core, 241–246
 - analysis methods, field, 243–246
 - introduction to, 240–241
 - data
 - acquisition and, 239
 - consistency and, 238
 - levels of observation and, 239
 - presentation and, 247–251
 - introduction to, 5, 90, 229–230
 - natural vs. induced fractures, determination of
 - core handling and, 235
 - drill string/rock interaction, 235–237
 - fracturing, centerline, 235
 - fracturing, chatter/petal, 235–237
 - fracturing, explosive, 230–231
 - fracturing, hydraulic, 233–234
 - fracturing, impact and indentation, 232
 - fracturing, shear, 232–235
 - fracturing, thermal, 232–233
 - induced fracture systems, 230–237
 - introduction to, 230
 - rock bursts and, 234–235
 - sheeting and, 234–235
 - spalling and, 234–235
 - unloading, 234–235
 - observational clues, 238
 - stratigraphy vs. deformation, petrology, and petrophysics, 229
 - Core handling, 235
 - Cross-flow
 - deformation and, 100
 - inhibited, 96
 - introduction to, 95–96
 - mineralization and, 96–99
 - porosity interaction and, 100
 - uninhibited, 96
 - Crossbedding, 186–189, 198–202
- ## D
- Darcy flow, 66–67
 - Definition of terms, 3–4, 281–284
 - Deformation bands (gouge-filled fractures), 37, 39–47, 55–58
 - Deformed fractures, 37, 39–60
 - Denial of fractures, problems associated with, 1–4
 - Density log compensation curves, 131
 - Desiccation fractures (mud cracks), 27
 - Detection (fracture occurrence and intensity)
 - application of techniques, 135
 - direct detection
 - core analysis, 5, 126
 - downhole cameras, 126
 - impression packers, 126–127
 - introduction to, 125
 - observation, direct, 126
 - indirect detection
 - flow test evaluation, 132
 - introduction to, 127
 - log evaluation, 127–132. *See also* Logs and logging tools
 - remote sensing, 134–135
 - reservoir rock property data, manipulation of, 132–134
 - well test evaluation, 132
 - introduction to, 125
 - prediction and. *See* Prediction (fracture occurrence and intensity)
 - techniques of, 125, 135
 - Devonian shale, 63–64
 - Dipmeter logs, 131
 - Dipole sonic logs, 130
 - Direct detection (fracture occurrence and intensity)
 - application of techniques, 135
 - core analysis, 5, 126. *See also* Core and outcrop analysis

downhole cameras, 126
 impression packers, 126–127
 introduction to, 125
 observation, direct, 126
 Discipline-based screening tools, 224–226
 Discontinuities and stylolites, 176
 Discovery of fractured reservoirs
 data
 constraints of, 227–228
 types of, 226
 introduction to, 226–227
 phases of
 exploration/access phase, 226–227
 recovery/harvest phase, 226, 228
 recovery/production phase, 226, 228
 timing of, 226–228
 Downhole cameras, 126
 Drill string/rock interaction, 235–237
 Drilling data-based screening tools, 5, 225
 Ductility and rock strength, 61–64

E

Electrical borehole imaging logs, 5, 128–129
 Engineering data-based screening tools, 226
 Evaluation of fractured reservoirs
 classification of fractures
 contractional fractures, 8, 12, 27–31
 experimental classification, 8–10
 experimental vs. naturally-occurring classification, 8
 extension fractures, 8, 10
 geologic classification, 10–12
 introduction to, 8
 naturally-occurring classification, 8, 13–32
 regional fractures, 8, 12, 21–26
 shear fractures, 8–9
 surface-related fractures, 8, 12, 31–32
 tectonic fractures, 8, 12–21
 tension fractures, 8, 10
 core analysis, 90–92, 90. *See also* Core and outcrop analysis
 cross-flow
 deformation and, 100
 inhibited, 96
 introduction to, 95–96
 mineralization and, 96–99
 porosity interaction and, 100
 uninhibited, 96
 definition of terms, 3–4, 281–284
 fracture denial, problems associated with, 1–4
 introduction to, xiii–xv, xvii, 1–2
 logs and log suites, 92–95. *See also* Logs and logging tools
 multiple well tests, 95
 order of investigation
 introduction to, 4–7
 phases of, 7
 origins of fracture systems
 introduction to, 7–8
 types of fractures and, 8–32
 properties affecting performance
 combined gouge-filled and slickensided fractures, 55–58
 deformed fractures, 37, 39–58
 fracture morphology, 37–64
 fracture porosity vs. fracture permeability, 61–78, 90–100
 fracture porosity vs. fracture volume, 88
 fracture porosity vs. matrix porosity, 83–100
 fracture spacing, 79–82. *See also* Fracture spacing
 fracture width, 64–78
 gouge-filled fractures, 37, 39–48, 55–58
 introduction to, 32–36
 mineral-filled fractures, 58–60
 open fractures, 37–38
 rock strength and ductility, 61–64
 slickensided fractures, 37, 48–58
 vuggy fractures, 60
 study sequences of, 4–7
 types of
 early exploration evaluations, 4–5
 economic potential evaluations, 4–6
 introduction to, 4
 recovery planning and modeling evaluations, 4, 6–7
 Example fractures, reservoirs, and fields
 Agha Jari (Iran), 105
 Altamont-Blue Bell, 26–27, 105–106
 Amal Field (Libya), 5, 103

- American Quasar 301 (Wyoming), 169
 Amoco Amos 32-12 (Alabama), 168–170, 176
 Amoco Myler Gas Unit No. 2 (Kansas), 29
 Amoco No. 1, Texas-Gulf Well (Pennsylvania), 56
 Amoco Norway 2/5-1 Well (North Sea), 164
 Anshultz Ranch East Field, 208
 Big Elk Anticline (Wyoming), 49, 154
 Big Sandy, 26–27, 103–104
 Bighorn Basin (Wyoming), 157
 Black Anticline (Rocky Mountains Foreland), 18
 Champlin Wells (Wyoming), 50–51, 62, 72, 97–98, 208
 Colorado Plateau, 22–27, 141
 Cottonwood Creek (Wyoming), 106–107
 Darius Field (Persian Gulf), 33, 167–168, 175, 183
 Deer Creek Thrust (Nevada), 47–48, 52–53
 Dine-Bi-Keyah, 117
 Dukhan (Qatar), 106
 East Anschutz, 117
 Edison (California), 103–104
 Ellenburger Fields (Texas), 103
 Florence, 117
 Gaschsharan (Iran), 106
 Granite Point, 117
 Great Salt Lake (Utah), 30
 Gulf of Suez, 15
 Haft Kel (Iran), 105
 Hassi Messaoud (Algeria), 106
 Kirkuk (Iraq), 106–107
 La Paz/Mara (Venezuela), 105, 115–117
 Lacq (France), 106
 Lake Powell (Utah), 23, 34, 39
 Little Elk Creek (Wyoming), 152
 Littleknife Field (North Dakota), 178
 Lost Soldier Field (Wyoming), 115, 149, 162
 Michigan Basin, 21
 Middle Ground Shoals, 117
 Nahanni Butte (N.W.T., Canada), 59
 Otsego County (Michigan), 139
 Page (Arizona), 142
 Painter, 117
 Panoma Field (Kansas and Oklahoma), 27, 181
 PC Fields (Kansas), 103
 Piceance Basin (Rocky Mountains), 23
 Pineview, 117
 Point Arguello, 117
 Pointed Field (N.W.T., Canada), 144
 Rangely (Colorado), 105, 117
 Rose Well (Kansas), 179
 Ryckman Creek Field, 62, 117, 185, 203–204
 Sawtooth Mountains (Montana), 140, 151, 159
 Sheep Mountain Anticline (Wyoming), 138, 142–143, 159, 162
 Simpson Group (Oklahoma), 42
 Sinai (Egypt), 24–25
 Sooner Trend (Oklahoma), 105
 Spraberry (Texas), 105–106
 Summit County (Utah), 43
 Trap Spring, 117
 Tuscarora Amoco No. 1 Texas-Gulf, 91, 99
 Upper Valley, 117
 Vahall Field (Norwegian North Sea), 70, 75–77, 90–91, 164, 177
 Valley of Fire State Park (Nevada), 38
 Walker Creek, 117
 Wertz Dome, 117
 Western Canadian Thrust Belt, 18, 158
 Western Wyoming Thrust Belt, 12, 42, 55–56, 94, 153–155, 159, 162, 185, 203–204, 207
 Whitney Canyon, 117
 Wolf Springs (Montana), 103
 Experimental classification of fractures, 8–10
 Experimental vs. naturally-occurring classification of fractures, 8
 Exploration/access phase (discovery), 226–227
 Explosive fracturing, 230–231
 Extension fractures, 8, 10
 Extension fracturing, 232–233
 Extension vs. shear, 3
- F**
 Fault-related fracture systems, 13–16

- Field analysis methods, 241–243
- Fields, examples of. *See* Example fractures, reservoirs, and fields
- Fixed hinges, 160–162
- Flow behavior-based screening tools, 223
- Flow test evaluation, 132
- Fold-related fracture systems, 16–20
- Folded fractured reservoirs, 152
- Fracture and matrix porosity
 - compressibility differences, 86
 - core analysis and, 90
 - cross-flow and, 95–100
 - deformation and, 100
 - estimations and calculations of, 89–90, 100
 - field-lab determination, 91–92
 - fractured volume vs. fractured porosity, 88
 - introduction to, 82–84
 - logs and log suites, 92–95
 - magnitude differences, 86–87
 - multiple well tests, 95
 - porosity-permeability relationships, 84–86, 90–91
 - scale vs. non-scale dependency, 84
 - significance of, 89
- Fracture denial, problems associated with, 1–4
- Fracture occurrence and intensity
 - detection of
 - application of techniques, 135
 - core analysis, 126
 - direct detection techniques, 125–127
 - downhole cameras, 126
 - flow test evaluations, 132
 - impression packers, 126–127
 - indirect detection techniques, 127–135
 - introduction to, 125
 - log evaluations, 127–132. *See also* Logs and logging tools
 - observations, direct, 126
 - remote sensing, 134–135
 - rock property data, manipulation of, 132–135
 - well test evaluations, 132
 - examples of, 153–160
 - folded fractured reservoirs and, 152–153
 - introduction to, 125
 - prediction of
 - application of techniques, 135
 - bed-thickness and, 141–146
 - composition and, 137
 - fracture spacing, parameters of, 79–82, 137–149
 - grain size and, 141
 - introduction to, 135–137
 - Parson’s equation and, 136
 - porosity and, 137–140
 - structural position and, 146–149
 - reservoir rock, strength and ductability and, 150–152
 - wall trajectory and, 160–162
 - well locations and paths, selection of, 152–153
- Fracture spacing, 79–82, 135–149
- Fracture width and permeability
 - distributions
 - experimental fracture widths, 78–79
 - introduction to, 77–78
 - natural fracture widths, 78–79
 - fluid flow
 - effect of fractures on, 70–73
 - equations, 64–70
 - fracture width vs. confining pressure, 75–77
 - introduction to, 64
 - permeability vs. confining pressure, 73–75
 - fracture spacing and
 - introduction to, 79–80
 - techniques for calculating, 80–82
 - variation in, effect of, 80
 - introduction to, 64
- Fracture, definition of, 3–4
- Fractured reservoirs
 - analysis procedures for, 223–253. *See also* Analysis procedures
 - anisotropic reservoirs, 163–222. *See also* Anisotropic reservoirs
 - classification of, 101–122. *See also* Classification of fractured reservoirs
 - classification of fractures, 7–32. *See also* Classification of fractures
 - definition of, 3–4, 223–226
 - evaluation of, 1–100. *See also* Evaluation of fractured reservoirs

fracture occurrence and intensity, detection and prediction of, 125–162
 introduction to, 1–4
 management of, 101–124. *See also* Management of fractured reservoirs
 morphology of fractures, 37–64. *See also* Morphology of fractures
 Fractured reservoirs, examples of. *See* Example fractures, reservoirs, and fields
 Fractured volume vs. fractured porosity, 88
 Fractures, examples of. *See* Example fractures, reservoirs, and fields

G

Geologic numerical modeling, 252–253.
See also Modeling
 Geological data-based screening tools, 224
 Geophysical data-based screening tools, 225
 Glossary and definition of terms, 3–4, 281–284
 Gouge-filled fractures (deformation bands), 37, 39–47, 55–58
 Grain size and permeability tensors, 193

H

Hinges (fixed and migrating), 160–162
 Hydraulic fracturing, 233–234

I

Imaging logs, 5, 128–129
 Impact and indentation fracturing, 232
 Impact fractures, 20–21
 Impression packers, 126–127
In situ stress data, 5, 131–133, 152, 234–237
 Indirect detection (fracture occurrence and intensity)
 application of techniques, 135
 flow test evaluation, 132
 introduction to, 127
 log evaluation, 127–132. *See also* Logs and logging tools
 remote sensing, 134–135
 reservoir rock property data, manipulation of, 132–134
 well test evaluation, 132
 Induction logs, 130

Inhibited cross-flow, 96
 Intensity of fractures, 125–162. *See also* Fracture occurrence and intensity

L

Lithologic boundaries (stylolites), 174–176
 Log suites, 92–95
 Logs and logging tools
 evaluation logs and log suites, 92–95
 introduction to, 127, 251
 types of
 acoustic borehole imaging logs, 5, 128–129
 borehole gravity meters, 131
 caliper logs, 128
 density log compensation curves, 131
 dipmeter logs, 131
 dipole sonic logs, 130
 electrical borehole imaging logs, 5, 128–129
 induction logs, 130
 microlaterologs, 131
 sonic amplitude logs, 127
 Low-porosity zones (stylolites), 176

M

Management of fractured reservoirs
 classification of reservoirs
 contrasting histories and, 103–108
 introduction to, 101
 reservoir listings and examples, 103–108. *See also* Examples fractures, reservoirs, and fields
 reservoir types, 101–122
 type 1, 101–105, 108–109, 116–119, 122
 type 2, 101–102, 105–106, 108–109, 118–119, 122
 type 3, 101–102, 108, 110, 118–119, 122
 type 4, 101–102, 110, 118–119, 122
 introduction to, 101
 positive attributes and, 107–108
 production problems and
 as predictors, 110
 introduction to, 109
 reservoir types and, 109–110

- risk analysis and, 123–124
 - strategies of
 - descriptions of, 110–112
 - historic production distributions, 115–123
 - iteration and, 114–115
 - modeling and, 114–115
 - production history and, 113–114
 - reservoir description, 113–123
 - technology, impact of, 112
 - Mathematical modeling. *See* Modeling
 - Microfault vs. fracture, 3
 - Microlaterologs, 131
 - Migrating hinges, 160–162
 - Mineral-filled fractures, 37, 58–60
 - Mode 1 vs. mode 2, 3
 - Modeling
 - anisotropic reservoirs, statistical data and
 - averaging techniques, 212–215, 279–280
 - block sizes, characterization of, 217
 - correlation of reservoir properties, three-dimensional, 215–216
 - introduction to, 207–208
 - research requirements, 212
 - reservoir domains and compartments and, 207–212
 - conversion factors, 285–286
 - evaluations (recovery planning and modeling), 4, 6–7
 - geologic numerical modeling, 252–253
 - notation, xix–xx
 - reservoir management and, 113–123
 - Morphology of fractures
 - deformed fractures
 - combined gouge-filled and slickensided fractures, 55–58
 - gouge-filled fractures (deformation bands), 37, 39–47, 55–58
 - introduction to, 39
 - mineral-filled fractures, 37, 58–60
 - slickensided fractures, 37, 48–58
 - vuggy fractures, 37, 60
 - introduction to, 37
 - open fractures, 37–38
 - rock strength and ductility and
 - Devonian shale, 63–64
 - introduction to, 61–62
 - Nugget sandstone, 62–63
 - Mud cracks (desiccation fractures), 27
 - Multiple well tests, 95
- N**
- Naturally-occurring classification, 8, 13–32
 - Notation, xix–xx
 - Nugget sandstone, 62–63
 - Numerical modeling. *See* Modeling
- O**
- Occurrence of fractures, 125–162. *See also* Fracture occurrence and intensity
 - Open fractures, 37–38
 - Origins of fracture systems
 - introduction to, 7–8
 - types of fractures and, 8–32
 - Outcrop analysis. *See* Core and outcrop analysis
- P**
- Packers, impression, 126–127
 - Parson's equation, 136
 - Permeability
 - analysis procedures and, 223–253
 - anisotropic reservoirs and, 163–222
 - fracture occurrence and intensity and, 125–162
 - fracture width and, 64–82
 - permeability matrix, 247
 - porosity vs. permeability, 61–78, 90–100, 172–173, 176
 - porosity-permeability relationships, 84–86, 90–91
 - reservoir evaluation and, 1–100
 - reservoir management and, 101–124
 - tensors. *See* Permeability tensors
 - Permeability tensors
 - anisotropic reservoirs and. *See* Anisotropic reservoirs
 - cementation size and, 194
 - combined tensors, 206–207
 - continuity of reservoir features and, 203–204
 - crossbedding and, 186–189, 198–202
 - data types, 204
 - fractures, effect on, 189–193, 198–202
 - grain size and, 193
 - introduction to, 185–186

- random plugs and, 194–196, 201
 - rock parameters, effect of, 202
 - scaling and, 194–198
 - stylolites and, 204–206. *See also* Stylolites
 - Petal/chatter fracturing, 235–236
 - Petrology and petrophysics, 229
 - Piercement and fracture classification, 20–21
 - Porosity
 - analysis procedures and, 223–253
 - cross-flow and, 95–100
 - fracture and matrix porosity, 82–100
 - fracture evaluation and, 1–100
 - fracture occurrence and intensity and, 125–162
 - fracture porosity *vs.* matrix porosity, 83–100
 - low-porosity zones, 176
 - low-porosity zones (stylolites), 176
 - porosity matrix, 247
 - porosity *vs.* permeability, 61–78, 90–100, 172–173, 176
 - porosity *vs.* volume, 88
 - reservoir management and, 101–124
 - Potential fracture planes, 9
 - Prediction (fracture occurrence and intensity)
 - application of techniques, 135
 - bed-thickness and, 141–146
 - composition and, 137
 - fracture spacing, parameters of, 79–82, 137–149
 - grain size and, 141
 - introduction to, 135–137
 - Parson's equation and, 136
 - porosity and, 137–140
 - structural position and, 146–149
 - Pressure and production analysis, 251–252
 - Procedures checklists, 246–247, 277–278
 - Properties affecting reservoir performance, 32–36
- R**
- Random plugs and permeability tensors, 194–196, 201
 - Recovery/harvest phase (discovery), 226, 228
 - Recovery/production phase (discovery), 226, 228
 - Regional fractures, 20–28
 - Reservoir fractures, definition of, 3–4
 - Reservoir management. *See* Management of fractured reservoirs
 - Reservoir quality, definition of, 185
 - Reservoirs, examples of. *See* Example fractures, reservoirs, and fields
 - Risk analysis, 123–124
 - Rock bursts, 234–235
 - Rock property data, manipulation of, 132–134
 - Rock strength and ductility, 61–64
 - Rock/drill string interaction, 235–237
 - Rose diagram (shear fractures), 14
- S**
- Scale *vs.* non-scale dependency, 84
 - Scaling, permeability tensors and, 194–198
 - Screening tools and checklists
 - basic
 - flow behavior-based, 223
 - introduction to, 223
 - discipline-based, 224–226
 - drilling data-based, 225
 - engineering data-based, 226
 - geophysical data-based, 225
 - introduction to, 223–224
 - evaluation checklists, 246–247
 - Shear fractures, 8–9, 232–233
 - Sheeting, 234–235
 - Slickensided fractures, 37, 48–58
 - Sonic amplitude logs, 127
 - Spacing. *See* Fracture spacing
 - Spalling, 233–235
 - Statistical data and modeling. *See* Modeling
 - Stratigraphy *vs.* deformation, petrology, and petrophysics, 229
 - Stylolites
 - anisotropic reservoirs and. *See* Anisotropic reservoirs
 - as indicator of mechanical properties, 173–174
 - contribution to reservoir anisotropy, 165
 - definition of, 163
 - deformation and, 169–172
 - fractures associated with
 - introduction to, 166
 - stylolite columns, 169

tension gashes, 166
unloading fractures, 166–168. *See also* Unloading
introduction to, 163–165
lithologic boundaries, 174–176
locations of initiation
 discontinuities, 176
 introduction to, 174
 lithologic boundaries, 174–176
 low-porosity zones, 176
permeability tensors and, 204–206. *See also* Permeability tensors
porosity vs. permeability and, 172–173, 176
Subsurface fracture spacing, 135–149. *See also* Fracture spacing
Surface-related fractures, 31–32
Syneresis fractures, 27–28

T

Tectonic fractures, 8, 13–21
Tension fractures, 8, 10
Tension gashes (stylolites), 166
Tensors, permeability. *See* Permeability tensors
Thermal contractional fractures, 28–31
Thermal fracturing, 232–233
Three-dimensional variable intensity logs, 128
Tools, screening. *See* Screening tools
Types of fractured reservoirs

classification and. *See* Classification of fractured reservoirs
introduction to, 101–103
type 1, 101–105, 108–109, 116–119, 122
type 2, 101–102, 105–106, 108–109, 118–119, 122
type 3, 101–102, 108, 110, 118–119, 122
type 4, 101–102, 110, 118–119, 122

U

Uninhibited cross-flow, 96
Unloading
 analysis procedures and, 234–235
 stylolites, 166–168. *See also* Stylolites

V

Variable intensity three-dimensional logs, 128
Vuggy fractures, 37, 60

W

Wall trajectory, 160–162
Weathering fractures, 32
Well testing, 95, 132, 251–252
Width, fracture. *See* Fracture width and permeability

Z

Zones, stylolite. *See* Stylolites